

**COMPARATIVE PROTEOMIC ANALYSIS APPLIED FOR STUDY OF
MORPHOGENIC COMPETENCE DURING SOMATIC
EMBRYOGENESIS IN SUGARCANE**

ANGELO SCHUABB HERINGER

**UNIVERSIDADE ESTADUAL DO NORTE FLUMINENSE
DARCY RIBEIRO – UENF**

**CAMPOS DOS GOYTACAZES - RJ
OUTUBRO – 2016**

**COMPARATIVE PROTEOMIC ANALYSIS APPLIED FOR STUDY OF
MORPHOGENIC COMPETENCE DURING SOMATIC
EMBRYOGENESIS IN SUGARCANE**

ANGELO SCHUABB HERINGER

“Tese apresentada ao Centro de Ciências e Tecnologias Agropecuárias da Universidade Estadual do Norte Fluminense Darcy Ribeiro, como parte das exigências para obtenção do título de Doutor em Genética e Melhoramento de Plantas.”

Orientador: Prof. Dr. Vanildo Silveira

CAMPOS DOS GOYTACAZES - RJ
OUTUBRO – 2016

**COMPARATIVE PROTEOMIC ANALYSIS APPLIED FOR STUDY OF
MORPHOGENIC COMPETENCE DURING SOMATIC
EMBRYOGENESIS IN SUGARCANE**

ANGELO SCHUABB HERINGER

“Tese apresentada ao Centro de Ciências e Tecnologias Agropecuárias da Universidade Estadual do Norte Fluminense Darcy Ribeiro, como parte das exigências para obtenção do título de Doutor em Genética e Melhoramento de Plantas.”

Aprovada em 25 de outubro de 2016.

Comissão Examinadora:

Prof. (D.Sc., Fitotecnia) Virginia Silva Carvalho – UENF

Prof. (D.Sc., Ciências Biológicas) Valdirene Moreira Gomes – UENF

Prof. (D.Sc., Ciências Biológicas) Miguel Pedro Guerra – UFSC

Prof. Vanildo Silveira (D.Sc., Biotecnologia) – UENF
(Orientador)

ACKNOWLEDGMENTS

I would like to thank the Universidade Estadual do Norte Fluminense Darcy Ribeiro for the quality of education

I would like to thank the Genetic and Plant Breeding Graduate Program for the quality of education and for all the support given when I was abroad.

I would like to thank my advisor, Professor Ph.D. Vanildo Silveira, which allowed laboratory structure and education to complete my entire PhD project, and also encouraged me to stay abroad, for one year, as a visiting scholar in University of California Davis.

I would like to thank my counselors Professor Ph.D. Gonçalo Apolinário de Souza Filho and Professor Ph.D Virginia Silva Carvalho for education and all suggestions given to my Ph.D project.

I would like to thank the Laboratório de Biotecnologia (LBT) and the Unidade de Biologia Integrativa UENF for the laboratory structure that allowed the development of my entire Ph.D. project.

I would like to thank the Grupo de Pesquisa em Biotecnologia Vegetal UENF for the scientific collaborations and friendship.

I would like to thank the research funding and scholarships were supported by the Carlos Chagas Filho Foundation for Research Support in the State of Rio de Janeiro (FAPERJ), the Coordination for the Improvement of Higher Education

Personnel (CAPES), and the National Council for Scientific and Technological Development (CNPq).

I would like to thank my family for all care and incentives to keep up this research career.

I would like to thank all my friends for the familiarity and laughs time.

SUMMARY

RESUMO	vii
ABSTRACT.....	ix
1. INTRODUCTION.....	1
2. OBJECTIVES	4
2.1 General objective	4
2.2 Specific objectives.....	4
3. CHAPTERS.....	5
3.1 LABEL-FREE QUANTITATIVE PROTEOMICS OF EMBRYOGENIC AND NON-EMBRYOGENIC CALLUS DURING SUGARCANE SOMATIC EMBRYOGENESIS	5
3.1.1 INTRODUCTION	5
3.1.2 REVIEW	9
3.1.2.1 Sugarcane	9
3.1.2.2 Somatic embryogenesis in sugarcane	10
3.1.3 MATERIALS AND METHODS	11
3.1.3.1 Plant material.....	11
3.1.3.2 Maturation treatment.....	12
3.1.3.3 Total protein extraction	13
3.1.3.4 Protein digestion.....	13
3.1.3.5 Mass spectrometry analysis	14
3.1.3.6. Histological analysis	15

3.1.4 RESULTS	16
3.1.4.1 Maturation and morphogenetic changes.....	16
3.1.4.2 Protein identification during maturation treatment	20
3.1.4.3 Protein functional classification during maturation treatment	27
3.1.5 DISCUSSION	29
3.1.5.1 Maturation and morphogenetic changes.....	29
3.1.5.2 Unique proteins that are abundant in embryogenic (E-0) callus	31
3.1.5.3 Unique proteins that are abundant in matured embryogenic (E-21) callus	35
3.1.5.4 Unique proteins abundant in non-embryogenic (NE-0) and matured non-embryogenic (NE-21) callus	36
3.1.5.5 Common proteins in embryogenic and non-embryogenic callus	37
3.1.6 CONCLUSION.....	38
3.2 COMPARATIVE PROTEOMICS ANALYSIS OF THE EFFECT OF COMBINED RED AND BLUE LIGHTS ON SUGARCANE SOMATIC EMBRYOGENESIS	40
3.2.1 INTRODUCTION	40
3.2.2.1 Somatic embryos maturation	42
3.2.2.2 Temporary immersion system (TIS).....	43
3.2.2.3 Light emitting diode (LED)	46
3.2.2.4 Proteomics in sugarcane somatic embryogenesis.....	47
3.2.3 MATERIAL AND METHODS	48
3.2.3.1 Plant Material.....	48
3.2.3.2 Maturation treatment with combinations of red and blue wavelengths	49
3.2.3.3 Somatic embryo conversion with a RITA temporary immersion system combining red and blue wavelengths	50
3.2.3.4 Plantlet elongation and acclimatization.....	50
3.2.3.5 Protein extraction.....	51
3.2.3.6 Protein digestion.....	51
3.2.3.7 Mass spectrometry analysis	52
3.2.4 RESULTS AND DISCUSSION	54
3.2.4.1 Maturation and conversion of somatic embryos with different combinations of red and blue wavelengths.....	54

3.2.4.2 Proteomic analysis of maturation callus subjected to different combinations of red and blue wavelengths.....	60
3.2.5 CONCLUSION.....	72
REFERENCES.....	74
APPENDICES	93
APPENDICE A.....	93
APPENDICE B.....	130

RESUMO

HERINGER, Angelo Schuabb; D.Sc.; Universidade Estadual do Norte Fluminense Darcy Ribeiro; Setembro, 2016; Comparative proteomic analysis applied for study of morphogenic competence during somatic embryogenesis in sugarcane Orientador: Prof. Dr. Vanildo Silveira; Conselheiros: Prof. Dr. Gonçalo Apolinário de Souza Filho e Profa. Dra. Virginia Silva Carvalho.

O desenvolvimento de células embriogênicas a partir de células somáticas depende de várias fases que culminam na formação de embriões somáticos, e a maioria destas alterações bioquímicas e moleculares ainda não foram bem esclarecidas. A embriogênese somática juntamente com a transformação genética pode vir a ser uma ferramenta biotecnológica para melhorar o rendimento das colheitas em cultivares potenciais de cana-de-açúcar. O objetivo deste estudo foi observar o desenvolvimento de embriões somáticos e identificar proteínas diferencialmente abundantes em calos embriogênicos e não-embriogênicos durante um tratamento de maturação, e avaliar a influência de combinações de comprimentos de onda vermelho e azul de lâmpadas LED na maturação de embriões somáticos de cana-de-açúcar para identificar proteínas que possam estar associados com a resposta morfogenética. Calos embriogênicos e não-embriogênicos foram cultivados em meio de cultura de maturação MS suplementado com diferentes concentrações (0,0, 0,75, 1,5 e 2,0 g L⁻¹) de carvão activado (AC). A formação de embriões somáticos e a abundância diferencial de proteínas foram avaliados nos dias 0 e 21. No outro experimento, calos embriogênicos foram submetidos a tratamentos de maturação com várias

combinações de comprimentos de onda vermelho e azul, sendo a lâmpada fluorescente utilizada como um controle. O tratamento com 1,5 g L⁻¹ AC resultou em taxas mais elevadas de maturação de embriões somáticos em calos embriogênicos (158 embriões somáticos em 14 dias), mas não teve efeito em calos não-embriogênicos. Foi identificado um total de 752 proteínas comuns em todos os tratamentos. O calo embriogênico apresentou 65 proteínas exclusivas no dia 0, incluindo a desidrogenases, proteína relacionada com a dessecação, calose e uma óxido nítrico sintase. Após 21 dias no tratamento de maturação, 14 proteínas exclusivas foram identificadas em calos embriogênicos, incluindo a catalase. Calos não-embriogênicos apresentaram 23 proteínas exclusivas no dia 0 e 10 proteínas exclusivas após 21 dias no tratamento de maturação, incluindo muitas proteínas relacionadas com a degradação protéica. No experimento de maturação, o tratamento W_mB_dR_fR (450/530/660/735 nm) durante 28 dias produziu 58 embriões somáticos por calo, enquanto que o controle produziu 23 embriões somáticos por calo. A análise proteômica apresentou 1.171 proteínas comuns ao controle com luz fluorescente e ao tratamento W_mB_dR_fR, e destes, 39 e 38 proteínas foram up e down reguladas, respectivamente. O tratamento W_mB_dR_fR induziu uma maior abundância de metiltransferases e clatrina cadeia pesada 1, que estão relacionadas com os processos de diferenciação e desdiferenciação e podem ser marcadores candidatos à embriogênese somática em cana-de-açúcar. Em conclusão, a indução de maturação levou ao desenvolvimento de embriões somáticos, o que possivelmente pode ser dependente da abundância diferencial de proteínas específicas ao longo do processo, como pode ser visto em calos embriogênicos sob um tratamento de maturação. Por outro lado, algumas proteínas exclusivas também podem inibir o desenvolvimento de embriões somáticos, como pode ser visto nos calos não-embriogênicos. Além disso, os LEDs podem ser substitutos vantajosos para lâmpadas fluorescentes, e uma combinação de luzes vermelhas e azuis podem melhorar a maturação e conversão de embriões somáticos em cana-de-açúcar.

ABSTRACT

HERINGER, Angelo Schuabb; D.Sc.; Universidade Estadual do Norte Fluminense Darcy Ribeiro; Setembro, 2016; Comparative proteomic analysis applied for study of morphogenic competence during somatic embryogenesis in sugarcane. Advisor: Ph. D. Vanildo Silveira; Counselors: Ph. D. Gonçalo Apolinário de Souza Filho e Ph. D. Virginia Silva Carvalho.

The development of somatic cells into embryogenic cells occurs in several stages and ends in somatic embryo formation, though most of these biochemical and molecular changes have not been yet to be elucidated. Somatic embryogenesis coupled with genetic transformation could be a biotechnological tool to improve potential crop yields potential in sugarcane cultivars. The objective of this study was to observe somatic embryo development and to identify differentially abundant proteins in embryogenic and non-embryogenic callus during maturation treatment, and beyond that, evaluate the influence of combinations of red and blue wavelengths from LED lamps on the maturation of somatic embryos of sugarcane and to identify proteins that might be associated with the morphogenetic response. Embryogenic and non-embryogenic callus were cultured on maturation culture medium supplemented with different concentrations (0.0, 0.75, 1.5 and 2.0 g L⁻¹) of activated charcoal (AC). Somatic embryo formation and differential protein expression were evaluated at days 0 and 21. In the other experiment, embryogenic callus were subjected to maturation treatments with various combinations of red and blue wavelengths, and a fluorescent lamp was used as a control. Treatment with 1.5 g L⁻¹ AC resulted in higher somatic embryo

maturity rates (158 somatic embryos in 14 days) in embryogenic callus but has no effect in non-embryogenic callus. A total of 752 common proteins were identified. embryogenic callus showed 65 exclusive proteins on day 0, including dehydrogenase, desiccation-related protein, callose synthase 1 and nitric oxide synthase. After 21 days on maturation treatment, 14 exclusive proteins were identified in embryogenic callus, including catalase and secreted protein. Non-embryogenic callus showed 23 exclusive proteins on day 0 and 10 exclusive proteins after 21 days on maturation treatment, including many proteins related to protein degradation. In the other experiment, the W_mB_dR_fR (450/530/660/735 nm) treatment for 28 days yielded 58 somatic embryos per callus, whereas the control yielded 23 somatic embryos per callus. The quantitative shotgun proteomics analysis identified 1,171 proteins common to the fluorescent and WmBdRfR treatments, and of these, 39 and 38 proteins were up-regulated and down-regulated, respectively, in the W_mB_dR_fR compared with the fluorescent treatment. The W_mB_dR_fR treatment induced a higher abundance of methyltransferases and clathrin heavy chain 1, which are related to differentiation and dedifferentiation processes and might be candidate markers for sugarcane somatic embryogenesis. In conclusion, the induction of maturation leads to somatic embryo development, which likely depends on the expression of specific proteins throughout the process, as seen in embryogenic callus under maturation treatment. On the other hand, some exclusive proteins can also specifically prevent of somatic embryos development, as seen in the non-embryogenic callus. Further, LEDs can be advantageous substitutes for fluorescent lamps and that a combination of red and blue lights can enhance somatic embryo maturation and conversion in sugarcane.

1. INTRODUCTION

Classified as one of the most important crops for biofuel production and an important bioenergetic source, sugarcane (*Saccharum* spp.) is an allogamous plant belonging to Poaceae family, and also a significant component of the economy in more than 100 countries in tropical and subtropical regions (de Souza et al. 2014; Waclawovsky et al. 2010).

The species has a limited genetic diversity because most modern hybrids are derived from interspecific hybridization *Saccharum officinarum* x *Saccharum spontaneum* (Butterfield et al. 2001; Snyman et al. 2011). The adoption of biotechnologies, such as clonal propagation and genetic transformation, aiming the development and acceleration of gains made by plant breeding programs, may represent in the near future, increased competitiveness and productive elite cultivars (Arencibia et al. 1998; Joyce et al. 2014). One important requirement to develop a suitable genetic transformation protocol is an efficient regeneration protocol for genetically modified plant tissue. Therefore, somatic embryogenesis is more effective for the regeneration of plants derived from both transformation techniques, particle bombardment and Agrobacterium -mediated transformation (Arruda 2012).

Somatic embryogenesis is a process close to zygotic embryogenesis, wherein one or more somatic cells in optimal conditions culminate in the development of bipolar structures without vascular connections to the mother tissue (Guerra et al. 1999; Tautorus et al. 1991). Among the various plant tissue

culture techniques, somatic embryogenesis offers the advantages of production on a large automated scale, the genetic stability of the regenerated plants, and important in breeding programs, allowing the attachment of genetic gain, capturing additive and non-additive components of genetic variability (Guerra et al. 1999; Steinmacher et al. 2007). Furthermore, somatic embryogenesis enables cultivation of cyclic cultures by using cell suspensions, or by secondary somatic embryogenesis, which allows plant production as large commercial scale (Steinmacher et al. 2007). However, despite these advantages, the maturation and conversion phases of somatic embryos still are considered as a bottleneck to achieve a high efficiency plant regeneration protocol. In order to optimize the protocols related to the plant morphogenesis, temporary immersion system (TIS) has been used for several species, including sugarcane (Mordocco et al. 2009). This culture system can be combined with LED lighting to optimize the maturation and conversion phase of sugarcane somatic embryo. The LED lighting (Light Emitting Diode) is seen as a revolution in world horticulture, due to its small size, long life, low heat emission and option to select different wavelengths (Massa et al. 2008).

During the development of somatic embryos several biochemical and molecular processes occur and are important for the understanding this morphogenetic route; several of these processes being not fully elucidated (Mordhorst et al. 1997). The study of the physiological, biochemical and molecular aspects associated with competence and determination of callus of sugarcane has a high potential for the identification of biomarkers for monitoring the development of somatic embryos.

In recent years, some works have been published with a study of the physiological and molecular basis of somatic embryogenesis in sugarcane. Histomorphological characterization of sugarcane callus evidenced that embryogenic callus are formed by round cells, prominent nuclei, small vacuoles and globular structures organized (pre- somatic embryos) (Silveira et al. 2013). Meanwhile, the non-embryogenic callus showed elongated cells, with a low nucleus:cytoplasm ratio and no organized globular structures. In this work it was also observed that the contents of the endogenous polyamine, spermidine, was higher in embryogenic callus as compared to non-embryogenic callus, which may be related to the callus embryogenic capacity. Thus, further studies, including

proteomics allow a better understanding of somatic embryogenesis and culminate in the development of strategies for the in vitro propagation and genetic manipulation of this plant (Marsoni et al. 2008). The use of proteomic techniques allows identification and quantification of proteins during somatic embryogenesis experiments in sugarcane to elucidate some of this biochemical and molecular processes. Two recent studies shows the potential of proteomics in this context, such as proteome differences in embryogenic and non-emбриogenic sugarcane callus (Heringer et al. 2015) and understanding of different cultures responses to polyamines (Reis et al. 2016).

The proteomics is presented as an alternative for elucidate biochemical and molecular processes important for the understanding this morphogenetic route, focusing in the identification and quantitation of proteins with different abundance. Thus, providing advances in knowledge with high potential for generating innovative results and on the border of science and help to understand the physiological and molecular bases associated with morphogenetic competence during somatic embryogenesis.

2. OBJECTIVES

2.1 General objective

Improve the maturation and conversion steps of sugarcane somatic embryos with temporary immersion system combined with different LED wavelengths and identify and quantified proteins differentially abundant associated with morphogenic competence and the somatic embryos development

2.2 Specific objectives

- Analysis of different proteins abundance, through shotgun proteomics, in embryogenic and non-embryogenic callus, to identify differentially proteins associated with embryogenic competence;
- Establish efficient induction and maturation and conversion protocols for sugarcane embryogenic callus coupled with temporary immersion system and LED lamps;
- Analysis of different proteins abundance through shotgun proteomics, in embryogenic callus during maturation treatments, in different wavelengths provided by the LED lamp.

3. CHAPTERS

3.1 LABEL-FREE QUANTITATIVE PROTEOMICS OF EMBRYOGENIC AND NON-EMBRYOGENIC CALLUS DURING SUGARCANE SOMATIC EMBRYOGENESIS

3.1.1 INTRODUCTION

Sugarcane (*Saccharum* spp.) is an allogamous plant belonging to the Poaceae family and is the main source of sugar worldwide. Sugarcane is a significant component of the economy in more than 100 countries in tropical and subtropical regions (Arruda 2011). Brazil plays an important role in the sugar industry being both the largest producer of this species (FAO 2014) and the largest producer of sugar derived from sugarcane worldwide (USDA 2012). In addition, sugarcane has become an important bioenergy source and is classified among the most important energy crops for bioethanol production. Given its high potential to accumulate biomass, sugarcane lignocellulosic materials are candidates for the production of second-generation ethanol from cell wall hydrolysis (Ragauskas et al. 2006). Even though it has not yet proven economically viable, second-generation ethanol is highly desirable because it

would enable to use of crop biomass fractions that are not animal feed or food for humans, for biofuel generation (Waclawovsky et al. 2010).

Sugarcane displays limited genetic diversity because most cultivated hybrids are derived from the interspecific hybridization of *Saccharum officinarum* and *Saccharum spontaneum* (Butterfield et al. 2001; Snyman et al. 2011). Crop yield improvement is highly dependent on the incorporation of superior features, and with conventional breeding, this process occurs very slowly, taking 10-14 years to release a new variety (Butterfield and Thomas 1996). Modern sugarcane breeding programs include biotechnological approaches, such as marker-assisted breeding, DNA mapping and genetic transformation (Lakshmanan et al. 2005). Genetic transformation, which can introduce genes that encode desirable traits into elite sugarcane cultivars, provides an alternative method to improve pest and disease resistance, as well as yield. This method has already generated positive results, not only in terms of increased sugar content but also improved crop performance (Arruda 2012). Improving sugarcane will require the development of an optimized tissue culture and plant regeneration system as a prerequisite for the production of genetically modified sugarcane plants. *In vitro* techniques for the mass propagation of sugarcane plantlets via somatic embryogenesis pathways are well established, but the production of highly nodular embryogenic callus is a critical step in many ongoing efforts to improve the sugarcane germplasm through genetic transformation (Lakshmanan et al. 2005). This pathway is preferred for the regeneration of plants that have been obtained from the genetic transformation of sugarcane using either particle bombardment or *Agrobacterium*-mediated transformation (Arruda 2012).

Somatic embryogenesis is analogous to zygotic embryogenesis, wherein a single cell or a small number of somatic cells are precursors to the formation of a somatic embryo (Tautorus et al. 1991). This process is only possible with totipotent plant cells, which can undergo genetic reprogramming to differentiate into any cell type, thereby leading to the creation of an entire embryo from a group of cells or even a single somatic cell (Verdeil et al. 2007). Sugarcane presents 2 types of callus: embryogenic callus is smooth and compact, with the potential for somatic embryo formation, whereas non-embryogenic callus is friable or soft and translucent and lacks the potential for somatic embryos formation (Silveira et al. 2013). Microscopically, the embryogenic callus contains cells with embryogenic

characteristics, such as a rounded shape, prominent nuclei, high nucleoplasmatic ratio, small vacuoles, and organized globular structures. However, non-embryogenic callus presents dispersed, elongated and vacuolated cells with a low nucleoplasmatic ratio and does not permit the development of somatic embryos even upon exposure to a maturation stimulus (Silveira et al. 2013). Compared with others tissue culture techniques, somatic embryogenesis offers advantages such as automated large-scale production and genetically stable regenerated plantlets, which are important in breeding programs, permitting the fixation of genetic gain by the capture of the additive and non-additive components of genetic variability (Guerra et al. 1999; Steinmacher et al. 2007). In addition, somatic embryogenesis permits the creation of cycling cultures through the use of cell suspensions or through secondary somatic embryogenesis, thereby permitting the large-scale commercial production of elite plants (Steinmacher et al. 2007). However, in spite of such advantages, the maturation and conversion phases for sugarcane somatic embryos still present a bottleneck against reaching the high-efficiency regenerative protocol.

Several biochemical and molecular processes occurring in somatic embryo development have not been fully elucidated (Mahdavi-Darvari et al. 2014; Mordhorst et al. 1997). The study of the physiological, biochemical and molecular aspects associated with the competence and determination of the embryogenic callus in sugarcane have the potential to identify specific markers (such as proteins), that could be used to monitor the development of somatic embryos in embryogenic and non-embryogenic callus and/or genetically modified embryos. These studies could help in understanding induction and the acquisition of competence in embryogenic and non-embryogenic callus to develop somatic embryos in this species. A better understanding of the phenomena related to somatic embryogenesis will permit the development of strategies for *in vitro* culture propagation and the genetic manipulation of plants (Marsoni et al. 2008).

Proteomic techniques can be used to develop specific proteomic maps for each stage of the somatic embryogenesis protocol, permitting the identification of specific differentially abundance of proteins to serve as molecular markers for the acquisition of embryogenic competence and somatic embryo evolution during *in vitro* sugarcane morphogenesis. Through these proteomic maps, along with transgenesis technology, these markers can be extrapolated and translated into

practical applications in the field, which is a growing area known as translational plant proteomics (Agrawal et al. 2012). The multidimensional protein identification technology “MudPIT” has become a popular approach for performing shotgun proteomics with high resolution orthogonal separation coupled to tandem mass spectrometry (2D-nanoLC-MS/MS) (Chen et al. 2006). This technology has enabled the identification of low-abundant proteins (Washburn et al. 2001), which are often missed when using two-dimensional electrophoresis (Washburn et al. 2001). Therefore, proteomics has evolved to focus on the functionality of the huge datasets that are acquired through a vast number of analytical technologies. The quality of the procedures, the orthogonality that is provided by MudPIT and the ion mobility (Lalli et al. 2013; Ruotolo et al. 2005; Wu et al. 2000) with increased selectivity and specificity have recently received great attention with regard to untargeted proteomics samples. Thus, modern acquisition techniques, such as a multiplex high-resolution format MS^E (multiplexed DIA – data-independent acquisition) (Silva et al. 2005) and high-definition HDMS^E (DIA with ion mobility) are valuable acquisitions that are required for shotgun proteomics and complex samples due to the overlapping chimeric peptide resolving power (Chakraborty et al. 2007; Geromanos et al. 2009). This work is the first study to compare of embryogenic and non-embryogenic callus under maturation treatment using 2D-nanoESI-HDMS^E technologies in sugarcane.

The present study determined the effects of maturation treatments on morphology and proteomics, as well as the relationship between maturation treatment and somatic embryogenesis competence and evolution in sugarcane cv. SP80-3280. In this sense, proteomics analyses were used to investigate differences in the acquisition of competence and somatic embryo development between embryogenic and non-embryogenic sugarcane callus. In this work proteins were identified using the HDMSE (data independent acquisition with ion mobility) technique, which permits the identification of large number of protein in complex samples, being a qualitative and quantitative analysis.

3.1.2 REVIEW

3.1.2.1 Sugarcane

Sugarcane (*Saccharum* spp.) is an allogamous plant belonging to Poaceae family. This plant displays limited genetic diversity because most cultivated hybrids are derived from the interspecific hybridization of *Saccharum officinarum* and *Saccharum spontaneum* (Butterfield et al. 2001; Snyman et al. 2011). This cross show a hybrid plant more complex than the parental genomes, featuring a chromosome constitution of $2n=100-130$, where 60-70% of the chromosomes have been inherited from *S. officinarum* (Arruda 2012), which has the characteristic of accumulates high sugar content.

Main source of sugar in the world, the cane has been cultivated on an industrial scale for the production of sugar in more than 100 countries around the world for about a hundred years (Arruda, 2011). Brazil has a prominent position in the sugar cane sector is the largest producer of this species (FAO 2014). The sugarcane crop continues to expand in Brazil, the production estimated to 2016/17 is 684.77 million tonnes, increase of 2.9% in relation to the previous harvest. The area to be harvested was estimated at 8,973,200 hectares, increase of 3.7% compared to the harvest 2015/16. According to the latest survey by the National Supply Company (CONAB 2016), 43,7% of sugarcane crop will be used for sugar production, while the remaining 56,3% will go to ethanol production.

Sugarcane has been seen as one of the most promising sources of renewable energy on the planet, much for bioethanol production (Griffin and Scandiffio 2009). This biofuel is the major currently in use in the world (Tatsis and O'Connor 2016). Moreover, given its high performance to accumulate biomass, lignocellulosic materials are candidates for the production of second-generation ethanol from cell wall hydrolysis (Ragauskas et al. 2006). In this context, genetic manipulation of plants, including sugarcane, to increase biomass production for biofuels will necessitate the development of genetic tools and resources (Lao et al. 2015).

The adoption of biotechnologies, such as micropropagation and genetic transformation, increase the development and acceleration of gains made by breeding programs, and its may come to represent in the near future, increased

competitiveness and productive elite cultivars potential (Arencibia et al. 1998; Joyce et al 2014). One important requirement to have a suitable genetic transformation protocol is the existence of an efficient regeneration protocol for genetically modified plant tissue. Therefore, somatic embryogenesis is more effective for the regeneration of plants derived from both transformation techniques, particle bombardment and Agrobacterium-mediated transformation (Arruda 2012).

3.1.2.2 Somatic embryogenesis in sugarcane

Somatic embryogenesis is analogous to zygotic embryogenesis, in which a single cell or a small number of somatic cells are the precursors to the formation of a somatic embryo (Tautorus et al. 1991). The induction of somatic embryogenesis is only possible using totipotent plant cells, which may be genetically reprogrammed to differentiate into any cell type, thereby leading to the creation of an entire embryo from a group of cells or even a single somatic cell (Verdeil et al. 2007). This reprogramming is only possible if the cells are both competent and able to receive the appropriate inductor stimuli.

Among the various plant tissue culture techniques, somatic embryogenesis offers the advantages of production on a large automated scale, the genetic stability of the regenerated plants, and important in breeding programs, allowing the attachment of genetic gain, capturing additive and non-additive components of genetic variance (Guerra et al. 1999; Steinmacher et al. 2007).

The first evidence of obtaining somatic embryos from sugarcane callus occurred in the 1980s (Ahloowalia and Maretzki 1983; Ho and Vasil 1983a; Ho and Vasil 1983b). From these studies, several other works with somatic embryogenesis in sugarcane were conducted to different applications such as micropropagation, plant breeding, germplasm conservation and genetic engineering (Lakshmanan et al. 2005).

During the induction of sugarcane somatic embryogenesis, both embryogenic and non-embryogenic callus can be obtained. These types of callus differ in their growth and can be visually differentiated by their morphology; however, little is known about the biochemical and molecular events that take place when somatic cells become competent to produce somatic embryos (Nieves et al. 2003; Silveira et al. 2013).

Our research group has achieved important results related to the topic, with the histomorphological characterization and quantification of endogenous and exogenous polyamines in embryogenic and non-embryogenic callus of sugarcane (Silveira et al. 2013), identification of unique proteins by comparative proteomics of embryogenic and non-embryogenic callus (Heringer et al. 2015), and the action of exogenous polyamines as maturation agent, such as putrescine, in embryogenic callus, and comparative proteomics associated with the action of polyamines on somatic embryos maturation (Reis et al. 2016).

Furthermore, somatic embryogenesis enables cultivation of cyclic cultures by using cell suspensions, or by secondary somatic embryogenesis, which allows large commercial scale plant production (Steinmacher et al. 2007). However, despite these advantages, the maturation and conversion step of somatic embryos still presented as a bottleneck to achieve a high efficiency plant regeneration protocol.

3.1.3 MATERIALS AND METHODS

3.1.3.1 Plant material

Embryogenic and non-embryogenic callus from the sugarcane cv. SP80-3280 were induced as previously described (Silveira et al. 2013). Briefly, immature nodal segments with axillary buds were collected at Universidade Federal Rural do Rio de Janeiro (UFRRJ), located at Campos dos Goytacazes, Rio de Janeiro, Brazil, with previous permission from the researcher Dr. Carlos Frederico de Menezes Veiga. The nodal segments were then planted in plastic trays containing the commercial substrate PlantMax (DDL Agroindustria, Paulínia, São Paulo, Brazil). The trays were maintained under ambient conditions for approximately 3 months. During this time, new plants originated from sprouting axillary buds and grew approximately 45 cm. After removal of the mature leaves, the apical bud were used as explants for callus induction. The shoot apical bud were surface sterilized in 70% ethanol for 1 min, immersed in 50% commercial bleach (hypochlorite from 1 to 1.25%) for 30 min and subsequently washed 3 times with

sterilized water in a laminar flow chamber. Subsequently, explants were transversely sectioned into 2-mm-thick slices and inoculated in assay tubes (150 × 25 mm) containing 10 mL of MS (Murashige and Skoog 1962) (Phytotechnology Lab, Overland Park, KS, USA) culture medium supplemented with 20 g.L⁻¹ sucrose, 2 g.L⁻¹ Phytagel (Sigma-Aldrich, St. Louis, MO, USA) and 10 µM 2,4-dichlorophenoxyacetic acid (2,4-D) (Sigma-Aldrich). The culture medium pH was adjusted to 5.8 prior to autoclaving for 15 min at 1.5 atm and 121 °C. The explants were maintained in a growth room at 25 °C ± 2 °C in the dark.

After approximately 45 days, the induced callus were transferred to Petri dishes (90 × 15 mm) containing 20 mL of the same culture medium. The callus was subcultured every 21 days and separated into 2 types, embryogenic and non-embryogenic, as previously described (Silveira et al. 2013). Smooth and compact callus were classified as embryogenic, whereas friable and soft callus were classified as non-embryogenic.

3.1.3.2 Maturation treatment

For the maturation treatment, three colonies containing 200 mg of fresh mass (FM) obtained from embryogenic and non-embryogenic callus were inoculated in Petri dishes containing 20 mL of MS culture medium supplemented with 20 g.L⁻¹ sucrose, 2 g.L⁻¹ Phytagel, and varying concentrations of activated charcoal (AC; Sigma-Aldrich; 0.0, 0.75, 1.5 and 3.0 g.L⁻¹). The pH of the culture medium was adjusted to 5.8 prior to the addition of Phytagel (Sigma-Aldrich) was added. The culture medium was sterilized by autoclaving at 121 °C for 15 min. After inoculation, the callus were maintained in a growth chamber at 25 ± 1 °C under dark conditions for the first 7 days. Thereafter, photoperiods of 16 h light (60 µmol.m².s⁻¹) were used for up to 28 days of culture.

Embryogenic callus competence was analyzed at 0 (before incubation on maturation treatment), 7, 14, 21 and 28 days of incubation by monitoring the FM (the initial FM was 200 mg FM per colony) and the number of somatic embryos produced.

For both types of callus, three separate Petri dishes, containing three colonies each, were examined per treatment at each sampling time.

Samples of both callus types were collected at 0 and 21 days and stored at -20 °C for later proteomic analysis.

3.1.3.3 Total protein extraction

Only the treatment yielding the greatest number of somatic embryos (MS medium supplemented with 1.5 g.L⁻¹ AC) was used for proteomic analysis. Embryogenic and non-embryogenic callus at the beginning of the experiment (day 0, before incubation with the maturation treatments) and after 21 days of culture were selected for analysis and marked as E-0, E-21, NE-0, and NE-21. These time points were chosen because day 0 corresponds to callus that are still in the dark, whereas day 21 corresponds to one week prior to the end of the maturation treatment in the light, thus yielding embryos at advanced stages of development, since on day 28 somatic embryos were already converting to plantlets.

Protein extracts were prepared in biological triplicate (500 mg FM) that as previously described (Balbuena et al. 2009). The samples were ground and transferred to clear, 2-mL microtubes containing 1.5 mL of extraction buffer containing 7 M urea (GE Healthcare, Freiburg, Germany), 2 M thiourea (GE Healthcare), 1% DTT (GE Healthcare), 2% triton X-100 (GE Healthcare), 0.5% pharmalyte (GE Healthcare), 1 mM PMSF (Sigma-Aldrich), and 5 µM pepstatin (Sigma-Aldrich). The extracts were briefly vortexed and kept in extraction buffer on ice for 30 min followed by centrifugation at 12,000 g for 5 min at 4 °C. The supernatants were transferred to clear microtubes, and the proteins were precipitated on ice for 30 min in 10% trichloroacetic acid (Sigma-Aldrich) and washed three times with cold acetone (Merck, Darmstadt, Germany). Finally, the proteins were re-suspended and concentrated in 0.5 mL of the same extraction buffer. The protein concentration was estimated using the 2-D Quant Kit (GE Healthcare) using bovine serum albumin (BSA, GE Healthcare) as a standard, and the samples were stored at -20 °C until proteomic analyses.

3.1.3.4 Protein digestion

The three resulting protein extracts from each treatment were pooled according to Luge et al. (2014) (Luge et al. 2014), totaling 1000 µg, in order to evaluate the biological variance between treatments in the discovery proteomics

approach. This pool was solubilized in 50 mM NH₄HCO₃ pH 8.5 and then centrifuged at 4000 g for 5 min at 8 °C. Then, 50 µL (100 µg) of the supernatant was pipetted onto a VivaSpin membrane (GE Healthcare), to which 400 µL of 50 mM NH₄HCO₃, pH 8.5, was added and followed by centrifugation at 4000 g for 10 min. at 8 °C. This last step was repeated at least 2 more times for protein concentration and clean-up. Finally, 50 µL was left on the membrane, collected and used for digestion (Murad et al. 2011).

For trypsin digestion, a 2 µg.µL⁻¹ solution of 50 µL of the previous sample plus 25 µL of 0.2% v/v *RapiGEST* (Waters, USA) (Yu et al. 2003) was added to a 1.5-mL microfuge tube, vortexed for 5 sec and heated in an Eppendorf Thermomixer Comfort device at 80 °C for 15 min. Then, 2.5 µL of 100 mM dithiothreitol (DTT) was added and placed in the thermomixer at 60 °C for 30 min. The tubes were placed on ice (30 sec), and 2.5 µL of 300 mM iodoacetamide (IAA) was added, followed by vortexing for 5 sec and incubation in the dark for 30 min at room temperature. Then, 20 µL of trypsin (50 ng.µL⁻¹) solution that was prepared with 50 mM NH₄HCO₃ pH 8.5 was added (Promega USA) and placed in a thermomixer at 37 °C overnight, after which 10 µL of trifluoroacetic acid (TFA) 5% v/v was added to precipitate the surfactant *RapiGEST* SF, vortexed for 5 sec, incubated at 37 °C for 90 min (without shaking) and centrifuged at 4000 × g for 30 min at 8 °C. Then, 100 µL of the supernatant was collected and transferred to the Total Recovery Vial (Waters, USA) for further shotgun mobility-DIA proteomics analysis.

3.1.3.5 Mass spectrometry analysis

Qualitative and quantitative bidimensional nanoUPLC tandem nanoESI-HDMS^E (multiplexed DIA – data-independent acquisition) experiments were conducted using both a 1-h reverse-phase gradient from 7% to 40% (v/v) acetonitrile (0.1% v/v formic acid) and a 500 nL·min⁻¹ nanoACQUITY UPLC 2D Technology system. A nanoACQUITY UPLC HSS T3 1.8 µm, 75 µm × 15 cm column (pH 3) was used in conjunction with a reverses-phase (RP) XBridge BEH130 C18 5 µm, 300 µm × 50 mm nanoflow column (pH 10). Typical on-column sample loads were 500 ng of total protein digests for each of the 5 fractions (500 ng per fraction/load). For every measurement, the mass spectrometer was operated in resolution mode with a typical *m/z* resolving power of at least 35000

FWHM and an ion mobility cell that was filled with nitrogen gas and a cross-section resolving power at least $40 \Omega/\Delta\Omega$. The effective resolution with the conjoined ion mobility was 1,800,000 FWHM. Analyses were performed using nano-electrospray ionization in positive ion mode nanoESI (+) and a NanoLockSpray (Waters, Manchester, UK) ionization source. The lock mass channel was sampled every 30 sec. The mass spectrometer was calibrated with an MS/MS spectrum of [Glu1]-Fibrinopeptide B human (Glu-Fib) solution ($100 \text{ fmol}.\mu\text{L}^{-1}$) that was delivered through the reference sprayer of the NanoLockSpray source. $[\text{M} + 2\text{H}]^{2+} = 785.8426$ was used for initial single-point calibration, and MS/MS fragment ions of Glu-Fib were used to obtain the final instrument calibration. DIA scanning with added specificity and selectivity of a non-linear ‘T-wave’ ion mobility (HDMS^E) device (Giles et al. 2011) was performed with a SYNAPT G2-S HDMS mass spectrometer (Waters, Manchester, UK), which was automatically planned to switch between standard MS (3 eV) and elevated collision energies HDMS^E (19–45 eV) applied to the transfer ‘T-wave’ CID (collision-induced dissociation) cell with argon gas; the trap collision cell was adjusted to 1 eV, using a millisecond scan time that was previously adjusted based on the linear velocity of the chromatographic peak that was delivered through nanoACQUITY UPLC to generate a minimum of 20 scan points for each single peak, both in low-energy and high-energy transmission at an orthogonal acceleration time-of-flight (oa-TOF) and a mass range from *m/z* 50 to 2000. The RF offset (MS profile) was adjusted such that the nanoESI-HDMS^E data were effectively acquired from *m/z* 400 to 2000, ensuring that any masses that were observed in the high-energy spectra with less than *m/z* 400 arose from dissociations in the collision cell. The samples and conditions were injected with the same amount on the column. Stoichiometric measurements based on scouting runs of the integrated total ion account (TIC) prior to analysis were performed to ensure standardized molar values across all conditions.

3.1.3.6. Histological analysis

Samples from embryogenic and non-embryogenic callus at day 0 were used for histological analysis, in order to demonstrate the histomorphological differences between these two types of sugarcane cell cultures. Samples were fixed with 2.5 % glutaraldehyde (Merck, Darmstadt, Germany) and 4 % p-

formaldehyde (Merck) in 100 mM sodium cacodylate (pH 7.2) (Merck) for 24 h, followed by dehydration with an increasing series of aqueous ethanol solutions. After dehydration, the samples were infiltrated with HistoResin (Leica® HistoResin, Heidelberg, Germany). Sections (approximately 5 µm thick) were cut and stained with a 1 % toluidine blue solution (Sigma-Aldrich). After water evaporation, sections were stained with a 1 % toluidine blue solution (Sigma-Aldrich). The sample sections were observed under an Axioplan light microscope (Carl Zeiss, Jena, Germany) equipped with an Axiocam MRC5 digital camera (Carl Zeiss), and the images were analyzed using AxioVisionLE version 4.8 software (Carl Zeiss).

3.1.4 RESULTS

3.1.4.1 Maturation and morphogenetic changes

Embryogenic callus containing a pro-embryogenic masses (Figure 1) were removed from the growth regulators and supplemented with AC, they were able to develop somatic embryos in advanced developmental stages during the 28 days in culture, generating large numbers of healthy plantlets at the end of the process (Figure 2). In contrast, maturation treatment were unable to promote somatic embryo differentiation in the non-embryogenic callus at the end of 28 days of culture (Figure 2). Comparing the treatments, the response were observed on MS culture medium supplemented with 1.5 g.L^{-1} AC , with a high number of somatic embryos (158) already reached on the 14th day of culture, and a total of 160 somatic embryos at the end of 28 days of culture (Table 1 and Figure 3). The treatment with 0.75 g.L^{-1} AC also showed a large number of somatic embryos at the end of the process (181 somatic embryos), but this treatment proved to be slightly delayed compared with the best treatment, generating a smaller number of somatic embryos (114) at 14 days (Table 1 and Figure 3). MS culture medium without AC (control) also produced somatic embryos but to a significantly lower degree than the other two treatments described above (Table 1 and Figure 3). Activated charcoal cleary increased maturation and the number of somatic

embryos. However, providing this compound in excess can also be harmful to somatic embryo formation, as observed with 3 g.L⁻¹ AC, which led to a low number of somatic embryos (74) at the end of the process (Table 1 and Figure 3).

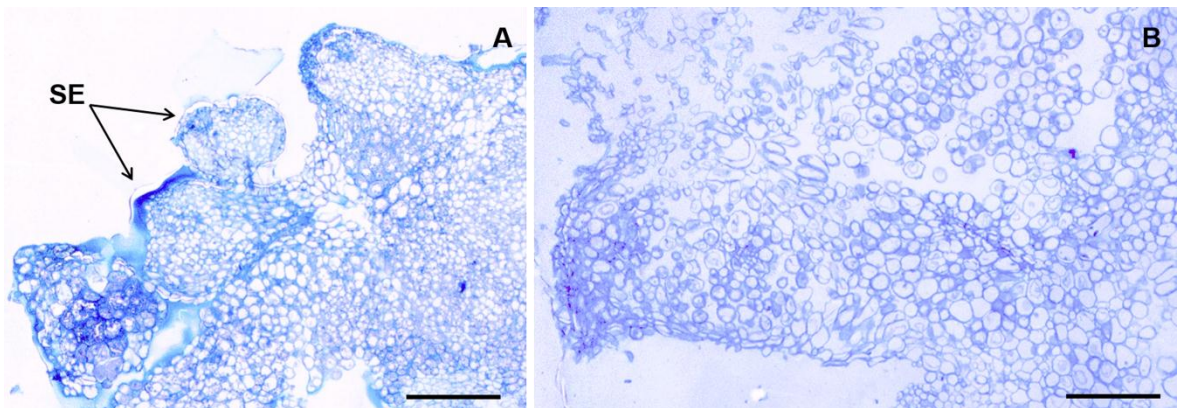


Figure 1. Histomorphological aspects of embryogenic and non-embryogenic callus. Embryogenic (A) and non-embryogenic (B) callus of sugarcane var. SP80-3280 on day 0 of maturation treatment submitted to histomorphological analyses. SE: somatic embryos; bars: A 500 µm; B 200 µm

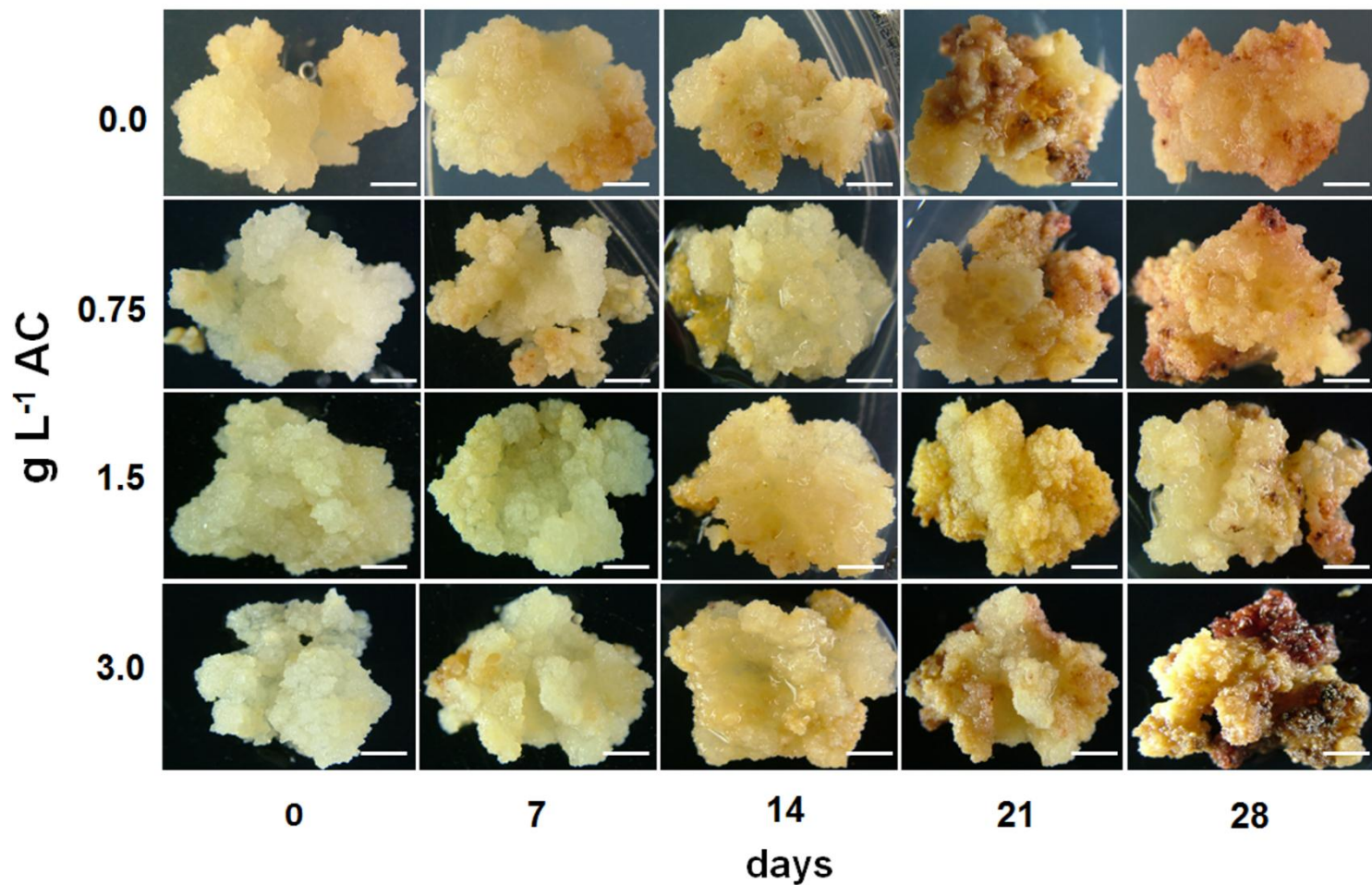


Figure 2. Morphological response of sugarcane non-embryogenic callus during maturation treatment. Non-embryogenic (NE) callus subjected to maturation treatment in the presence of different concentrations (0.0; 0.75; 1.5 and 3 g L⁻¹) of activated charcoal (AC).

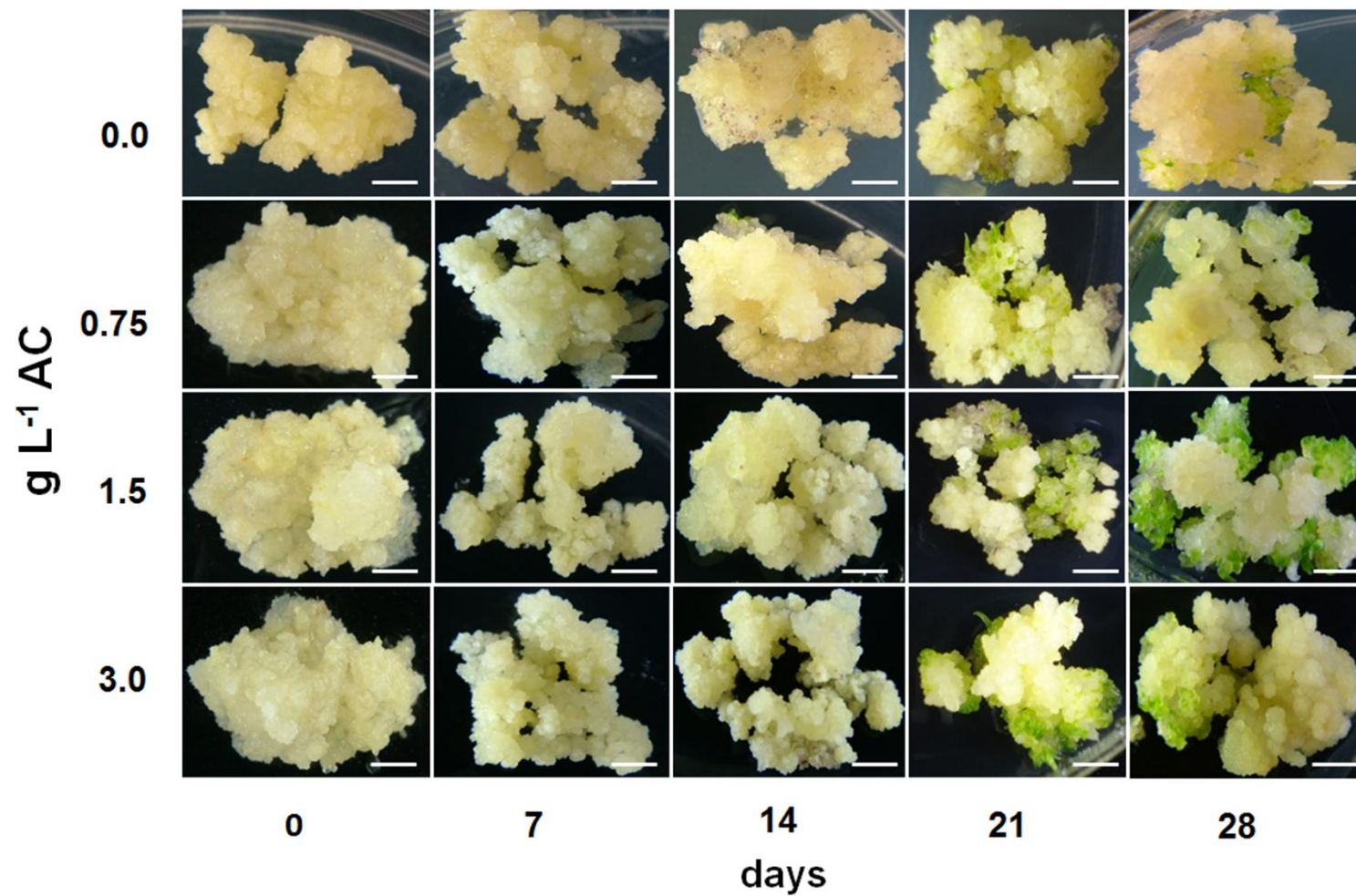


Figure 3. Morphological response of sugarcane embryogenic callus during maturation treatment. Embryogenic (E) callus were subjected to maturation treatment in the presence of different concentrations (0.0; 0.75; 1.5 and 3 g L^{-1}) of activated charcoal (AC). Bars = 5 mm.

Table 1. Effect of activated charcoal (AC) on the number of somatic embryos that formed in sugarcane embryogenic (E) callus (200 mg FM) under different maturation treatments.

Time of culture (days)	AC (g L ⁻¹)			
	0.0	0.75	1.5	3.0
0	0*	0	0	0
7	0	0	0	0
14	12 ± 3.61 ^a	114 ± 3.61	158 ± 11.93	29 ± 1.53
21	97 ± 7.94	120 ± 15.72	120 ± 11.59	129 ± 15.31
28	110 ± 15.70	181 ± 17.50	160 ± 11.68	74 ± 11.68

^a*Mean ± standard deviation, n= 4.

3.1.4.2 Protein identification during maturation treatment

The protein identification and quantitative data processing were performed using dedicated algorithms (Silva et al. 2005) and by searching against a database using the default parameters for ion accounting and quantitation (Li et al. 2009; Silva et al. 2006). The databases utilized were reversed “on-the fly” during the database queries and appended to the original database to assess the false-positive identification rate. For proper spectra processing and database searching conditions, the ProteinLynx Global Server (PLGS) v2.5.2 software package with Apex3D, Peptide 3D, and Ion Accounting informatics (Waters, UK) was used. The SUCEST protein databank (<http://sucest-fun.org/>) containing specific annotations for sugar cane was utilized. The search conditions were based on taxonomy (*Saccharum spp.*); up to 1 maximum missed cleavages by trypsin allowed; variable modifications by carbamidomethyl (C), acetyl N-terminal, and oxidation (M); and a default maximum false discovery rate (FDR) value of 4%. The obtained proteins were organized by the software algorithm into a statistically significant list corresponding to increased and decreased regulation ratios between the different groups. Normalizations were performed automatically by Expression^E software which was included inside PLGS informatics (Waters, UK) using the recommended default parameters. Common proteins were filtered based on a fold change of log₂ 1.2, as determined by the overall coefficient of variance for all

quantified proteins across all replicates, and classified as up-regulated when \log_2 is 1.2 or greater and as down regulated when \log_2 is -1.2 or less.

After searching the SUCEST project database (<http://sucest-fun.org/>), 1267 proteins were identified with an average of 15 peptides per protein and were filtered only when found across all replicates. From these proteins, 752 were present in all four samples (S1 Table), and 403 were common across all of the conditions, as identified in two of three type of samples (S2 Table). From the total identified proteins, 65 were unique to the embryogenic callus at the beginning (E-0), with 14 proteins that were unique at 21 days of maturation treatment (E-21) (Table 2). The non-embryogenic callus showed 23 unique proteins at the beginning (NE-0) and 10 unique proteins at 21 days of the maturation treatment (NE-21) (Table 2).

Table 2. Unique proteins identified in embryogenic (E) or non-embryogenic (NE) sugarcane callus under maturation treatment.

SUCEST accession	Description	Peptide count	Confidence score	Counts
Unique E-0 Proteins				
SCVPCL6041D12	udp-sugar pyrophosphorylase-like	14	74.88	507.73
SCJFRZ2009B04	s-adenosylmethionine:2-demethylmenaquinone...	12	74.35	1252.10
SCRFLB1054G06	charged multivesicular body protein 5	10	63.70	3159.40
SCRLSB1041H10	chorion family 2 expressed	9	52.40	46.50
SCEZLB1007H06	meiotic nuclear division protein 1 homolog	8	43.04	495.37
SCBFAD1089G07	akin gamma	7	41.21	1282.14
SCACAM1071C11	coiled-coil protein	8	39.56	1466.22
SCQSR1T035C03	peptidylprolyl cis-trans isomerase	7	39.09	736.50
SCCCRZ1001D08	tubulin--tyrosine ligase-like protein 12	7	36.03	328.78
SCQSAM1033A03	u4 tri-snrrnp-associated 65 kda protein	7	34.98	579.64
SCCCCL3120E07	mtn19-like protein	5	34.31	5131.92
SCBGLR1098A04	Ism sm-like protein family member	3	28.31	1286.06
SCQQLB1030C05	phosphoprotein phosphatase pp7	5	25.56	39.68
SCEQRT1027A06	3-deoxy-d-arabino heptulosonate-7-phosphate synthase	5	24.48	78.72
SCEPLR1051B05	chromdomain-containing protein crd101	5	24.40	450.84
SCQQLR1062D09	methylosome subunit picln-like	4	22.27	1118.28
SCQGSB1143E08	polyphosphoinositide phosphatase-like isoform 1	3	21.48	1624.85
SCCCCL4002E09	monosaccharide transport protein mst1	2	20.80	9.31
SCCCLB1025C07	deoxyribonuclease tadt	4	20.63	94.61
SCQGRT1042A06	amp binding protein	4	19.80	89.38
SCJLLR1054E12	ncase_orysj ame: full=neutral ceramidase short=n-cdase...	3	19.17	556.98

Table 2 cont.

SUCEST accession	Description	Peptide count	Confidence score	Counts
SCCCLR1001H11	cosa_orysj ame: full=costars family protein	3	18.77	3920.17
SCCCLR2002H10	ring-box protein	2	17.69	3728.50
SCEPLR1008D03	had-superfamily subfamily iia	3	17.34	102.14
SCRFLR2038B03	gata transcription factor 25	3	16.94	1444.23
SCCCST2003E11	pheophorbide a oxygenase	2	14.51	1202.84
SCACLR1036F06	hydroxymethylbutenyl 4-diphosphate synthase	3	14.14	249.50
SCSFRT2070B09	carbohydrate transporter sugar porter transporter	3	13.68	14.26
SCCCLR1068F03	ru1c1_sorbi ame: full=u1 small nuclear ribonucleoprotein...	1	13.24	80.59
SCBGLR1047G06	cation transport protein chac	3	12.99	298.91
SCCCLB2005F01	long form-like	2	11.23	260.34
SCEZST3147G06	bcplh protein	2	10.84	776.66
SCRULB1060G07	prli-interacting factor I-like	2	10.83	2170.47
SCQGHR1012E03	nitric oxide synthase interacting protein	2	10.80	425.00
SCSBHR1051A12	burp domain-containing protein	2	10.79	813.98
SCCCCL4006E10	glycerophosphoryl diester phosphodiesterase-like	2	10.65	679.69
SCBGSB1025C10	2 coiled coil domains of eukaryotic origin (kd)-like protein	2	10.55	1808.32
SCUTRZ3073E01	carboxylic ester hydrolase	2	10.44	821.02
SCSFAD1108H10	callose synthase 1 catalytic subunit	2	10.16	265.93
SCAGLR1021B10	phosphoribosylanthranilate transferase	2	9.81	156.17
SCAGLR2033F09	folylpolyglutamate synthase	2	9.77	158.84
SCQSST3116H01	drought-inducible protein 1os	2	9.71	155.50
SCCCCL4007E09	brca1 c terminus domain containing expressed	2	9.34	844.00
SCQSST1036B01	adenylyl-sulfate kinase	2	8.92	64.13
SCRFAM1026C02	dehydrogenase-like protein	2	8.68	129.72

Table 2 cont.

SUCEST accession	Description	Peptide count	Confidence score	Counts
SCBFSD2038B09	gibberellin-regulated protein 2 precursor	1	8.27	570.52
SCVPLR1028B03	hua enhancer 2	1	6.71	1482.94
SCEQLB1068H03	methylglutaconyl- methylglutaconyl- hydratase	1	6.41	81.74
SCEPCL6019C12	transferring glycosyl groups	1	5.83	27.80
SCQSFL3032A08	Os03g0157700 [Oryza sativa Japonica Group]	1	5.60	72.20
SCEPCL6029B05	af466199_12gb protein	1	5.60	208.87
SCSBFL5016D03	sec14-like protein 1	1	5.26	25.97
SCRLRZ3115E11	thimet oligopeptidase-like	1	5.17	422.23
SCCCLB1C03F07	cslc7_orysj ame: full=probable xyloglucan glycosyltransferase...	1	5.11	757.22
SCSGRZ3061F09	upf0414 transmembrane protein c20orf30 homolog	1	5.07	316.79
SCCCRT1004A07	root-specific protein rcc3	1	5.03	350.96
SCRLFL3005C03	speckle-type poz protein	1	4.90	679.77
SCBFSD1037G05	desiccation-related protein pcc13-62 expressed	1	4.84	499.12
SCJFRT2059A12	hipl1 protein expressed	1	4.49	124.63
SCCCLB1023H09	200 kda antigen p200 -like protein	1	4.21	283.81
SCCCCL1002F10.b	cmp-kdo synthetase	1	4.16	482.69
SCJFLR1013D06	zn -- containing protein	1	3.99	344.94
SCJLLR1104A12	abivp1 transcription factor	1	3.99	631.91
SCVPRZ2044C07	copper-transporting p-type atpase	1	3.73	24.30
SCQSHR1020G11	lecithine-cholesterol acyltransferase-like 4-like	1	3.72	254.95
Unique E-21 Proteins				
SCCCCL3120D10.b	catalase- expressed	5	46.01	247.02
SCQSAM1033H01	disulfide oxidoreductase electron carrier oxidoreductase	7	40.30	176.62
SCSGRZ3060B04	b-keto acyl reductase	3	23.03	401.66

Table 2 cont.

SUCEST accession	Description	Peptide count	Confidence score	Counts
SCSGST1070D03	putative kinesin [<i>Oryza sativa</i> Japonica Group]	4	22.74	35.63
SCSBSD2032F10	secreted protein	2	20.51	2497.09
SCAGLR1064D03	wd40 repeat-containing protein smu1-like	3	15.79	592.08
SCQGRT1045A06	tho complex subunit 4	3	14.61	526.94
SCEQAM2038G11	craniofacial development protein	2	9.73	122.92
SCCCRZ1002A07	transformation transcription domain-associated protein	2	9.70	301.41
SCAGLB1071A03	ac079853_1 myosin heavy chain-like	2	8.66	220.75
SCCCCL3080D01	arp9_orysi ame: full=actin-related protein 9	1	5.20	145.22
SCJFSB1010B12	tgacg-sequence-specific dna-binding protein tga- -like	1	4.97	651.41
SCSBFL4011C12	Os07g0646200 [<i>Oryza sativa</i> Japonica Group]	1	4.32	299.86
SCRFAM1027C11	ac079874_16 dna binding protein	1	4.04	346.24
Unique NE-0 Proteins				
SCJFRZ2028D05	esterase d	6	38.40	202.16
SCCCRZ3001A02	smc n terminal domain containing expressed	4	23.50	985.08
SCVPRT2075D04	af061282_24 patatin-like protein	3	20.92	1306.42
SCBFRT1071A02	4cll4_orysj ame: full=4-coumarate-- ligase-like 4	4	20.43	144.22
SCBGR1T046F12	pleckstrin homology domain-containing protein 1	4	20.32	199.51
SCJLFL1047A09	hox1b protein	3	19.41	4845.25
SCQGST1032A06	myb-like dna-binding domain containing protein	2	18.26	324.54
SCEPRZ1010A01	fasciclin domain	2	18.11	194.33
SCCCRZ2C04F12	L-allo-threonine aldolase	3	15.03	205.83
SCQGLR1041H02	primary amine oxidase-like	3	14.38	78.77
SCBGST3106D08	isoflavone reductase irl	3	13.67	204.58
SCRUSB1078F12	cmv 1a interacting protein 1	1	11.01	6097.33

Table 2 cont.

SUCEST accession	Description	Peptide count	Confidence score	Counts
SCAGLB1069B07	helix-loop-helix dna-binding domain containing expressed	2	10.54	1992.79
SCRFLB1053G11	mgdg synthase type a	2	10.14	5580.03
SCAGLR2011C06	ring zinc finger protein	2	10.00	2380.70
SCCCCL4001E08	pyridoxal biosynthesis protein pdx2-like	1	9.53	63.64
SCCCCL4007B04	Os04g0129900 [Oryza sativa Japonica Group]	2	8.88	341.06
SCMCRT2103F09	hmngt_sorbi ame: full=cyanohydrin beta-glucosyltransferase...	1	6.01	1475.92
SCMCST1053E03	af114171_7tnp2-like protein	1	5.44	2735.70
SCCCCL1001D11.b	oxoglutarate dehydrogenase (succinyl-transferring) e1...	1	5.43	521.40
SCCCCL3005D09.b	tyrosine specific protein phosphatase family protein	1	5.19	50.02
SCSGAD1006E05	cyt-p450 monooxygenase	1	4.72	392.38
SCACLR1130H08	dl related protein	1	4.66	68.53
Unique NE-21 Proteins				
SCRLLV1026A01.b	polyubiquitin-like protein	14	141.40	247.11
SCEQLB1063H08	nicotinate-nucleotide pyrophosphorylase family protein	7	40.67	13721.30
SCJLRT1018B07	nicotianamine aminotransferase a-like	4	21.43	1618.19
SCEQRT1024G07	alkaline neutral invertase	3	18.70	154.00
SCVPLR2027H10	pleckstrin domain-containing expressed	3	13.35	2332.11
SCBFLR1083H12	bacterial-induced peroxidase precursor	1	12.70	713.41
>SCQSFL3038G02.b	Os12g0534000 [Oryza sativa Japonica Group]	2	9.44	2677.01
>SCCCCL4005F07	mitosis protein dim1	1	5.40	5183.42
>SCJFRT1012E10	loc100136880 isoform 1	1	5.34	8092.31
>SCSGRZ3062C02	af466200_17 galactosyltransferase Family	1	4.60	5144.71

^a Confidence scores were calculated by ProteinLynx Global Server (PLGS).

3.1.4.3 Protein functional classification during maturation treatment

Functional classifications based on protein gene ontology were performed using the program Blast2GO (www.blast2go.com).

When the functional classifications were performed on the four samples, approximately 23% of the 65 unique E-0 proteins were observed to possess hydrolase activity compared with 7% in the 14 unique E-21 proteins, 18% had heterocyclic compound binding activity, versus 25% in E-21, and 18% showed organic cyclic compound binding, versus 25% in E-21 (Figure 4). Lipid binding activity, which appeared in approximately 3% of the unique E-0 proteins, did not appear in E-21 (Figure 4). Of the 23 unique NE-0 proteins, approximately 6% had chromatin binding activity, which did not appear in the unique E-0 and E-21 proteins (Figure 4). In the NE-21 callus 50% of the unique proteins had transferase activity (Figure 4).

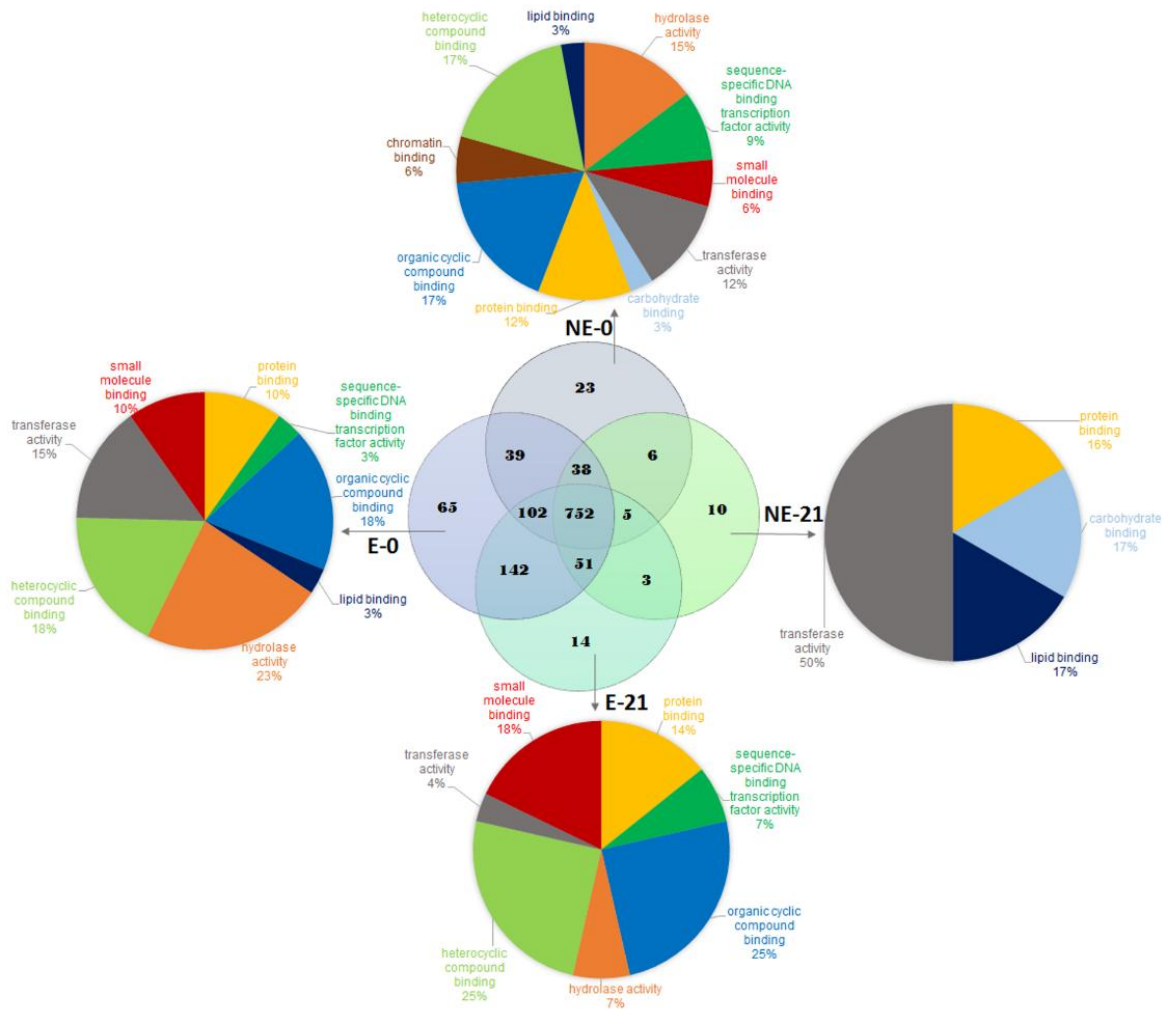


Figure 4. Venn diagram and pie charts displaying the numbers and functions of unique and common proteins. The number of unique and common proteins from embryogenic(E) and non-embryogenic (NE) callus during maturation treatment and the functional classification of unique proteins from embryogenic (E) and non-embryogenic (NE) callus at 0 and 21 days of maturation treatment (E-0, E-21, NE-0 and NE-21).

When we analyzed the 752 proteins that were common in all callus samples, we observed that these proteins were categorized according to 3 main biological functions: 22% showed organic cyclic compound binding activity, 22% showed chromatin binding activity and 17% showed small molecule binding activity (Figure 5). E-0 callus had 163 proteins that were up-regulated and 129 that were down-regulated compared with NE-0 callus (S1 Table). When comparing callus between E-0 and E-21, 68 proteins were up-regulated, and 57 were down-regulated (S1 Table). The NE-0 callus had 107 proteins that were up-regulated compared with NE-21 callus and 111 that were down-regulated (S1 Table).

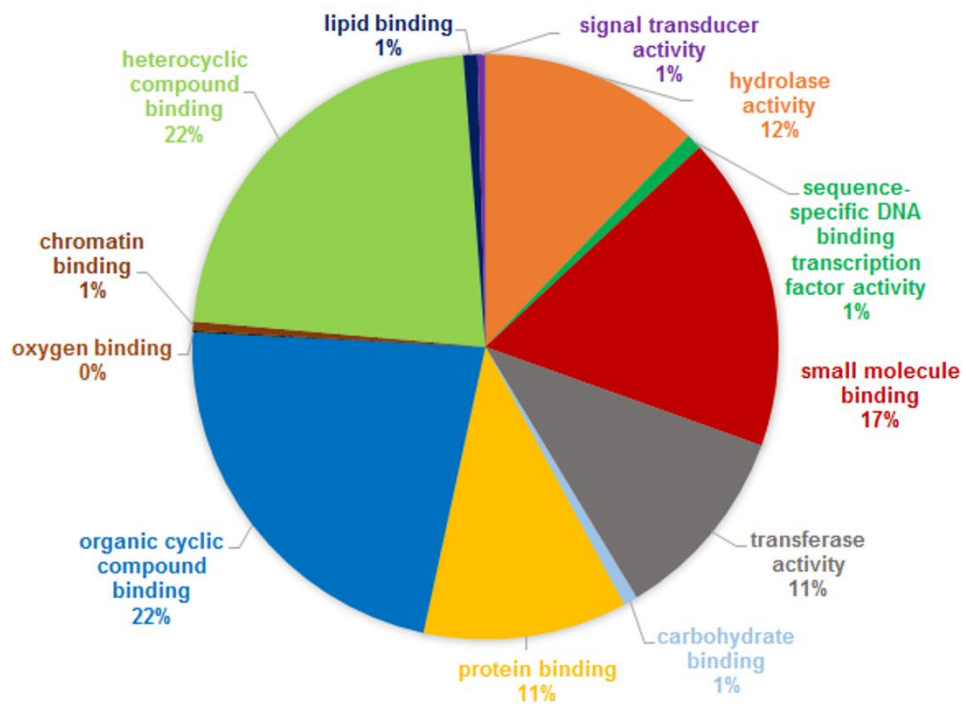


Figure 5. Pie charts showing the functional classification of the common proteins. Functional classification of the common proteins from sugarcane embryogenic (E) and non-embryogenic (NE) callus before (0) and after 21 days of maturation treatment (E-0, E-21, NE-0 and NE-21).

3.1.5 DISCUSSION

3.1.5.1 Maturation and morphogenetic changes

Somatic embryo maturation and the progression to somatic seedling development represent bottlenecks in many species-specific somatic embryogenesis protocols. In the present work, supplementation with specific concentrations AC (0.75 and 1.5 g L⁻¹) was essential for somatic embryogenesis in sugarcane cv. SP80-3280 (Figure 3 and Table 1). The addition of 2,4-D into the culture medium is also necessary for induction and maintenance of sugarcane callus; this plant growth regulator (PGR) inhibits somatic embryo formation, whereas removing 2,4-D from the culture medium is necessary for somatic embryogenesis evolution (Silveira et al. 2013). Furthermore, the addition of AC to

the culture media caused a drastic decrease in endogenous levels of PGR and other organic supplements through the adsorption of these components (Thomas 2008), thereby promoting a decrease in the endogenous contents of 2,4-D content in sugarcane callus. A likely explanation is that during the switch from auxin-containing to auxin-free culture medium, a residual amount of auxin travels with the callus, which can delay the evolution of somatic embryo development. Furthermore, in the AC addition, this auxin residue is rapidly adsorbed, thus preventing this PGR from inhibiting cell differentiation and permitting faster somatic embryo progression (Figure 3). However, the addition of AC to the culture medium will adsorb unwanted substances but may also adsorb some needed substances, such as macro- and micro-nutrients, vitamins and sucrose, which are important for somatic embryo development (Thomas 2008). In this sense, the addition of high AC concentrations (3.0 g L^{-1}) can disturb the formation of somatic embryos, as observed in this study (Figure 3 and Table 1). During maturation treatment, the culture medium supplemented with 3.0 g L^{-1} AC produced five times fewer somatic embryos (29) than did the treatment with the best AC concentration (1.5 g L^{-1}), which promoted the formation of 158 somatic embryos at 14 days in culture (Figure 3 and Table 1). The excess AC may also have adsorbed essential substances for somatic embryo differentiation, such as macronutrients, micronutrients, vitamins, and sucrose, rendering them unavailable to the callus and preventing the formation of somatic embryos in sugarcane.

Some somatic cells, especially those of embryonic origin, possess embryogenic potential during their cell cycle. However this potential can diminish with the time, and one way to regain it is through an intermediary callus phase (Mahdavi-Darvari et al. 2014). The transition from an embryonic cell to a somatic embryo depends on the embryogenic potential of these somatic cells. During this process, specific proteins may be abundant, that permit the resumption of embryogenic potential, culminating in the emergence of a totipotent cell that can give rise to a somatic embryo.

3.1.5.2 Unique proteins that are abundant in embryogenic (E-0) callus

There are certain limitations to the identification of sugarcane proteins. First, because the sugarcane genome has not been sequenced. However, protein identification has been carried out using the sugarcane SUCEST EST database. Additionally, sugarcane possesses a polyploid genome (Ming et al. 1998), and several cases have arisen in which different ESTs matched, causing redundancy in the identification of some proteins. Despite these difficulties, 2D-nanoESI-HDMS^E technology proved to be a good alternative in the identification of sugarcane proteins.

In shotgun proteomics analyses, 65 unique proteins were identified in E-0 callus (Table 2) and can be grouped into broad functional groups, such as high metabolic activity (Figure 4). These characteristic are common in the embryogenic callus of various species and are associated with the acquisition of competence (Fehér 2014; Ikeda-Iwai et al. 2003; Vale et al. 2014).

Some proteins are highly related to intense cellular metabolic activity, a remarkable characteristic of embryogenic callus (Baba et al. 2008; Zhang et al. 2009). Embryogenic callus are formed by cells with prominent nuclei, culminating with a high nucleus:cytoplasm ratio (Silveira et al. 2013; Verdeil et al. 2007). This high ratio translates to the high expression of proteins that follow these cells to receive external signals and express their inherent potential in highlighting somatic embryo formation as the greatest essential characteristic of a totipotent cell (Verdeil et al. 2007). Among these are the lsrn sm-like protein (SCBGLR1098A04) (Table 2) which functions in mRNA metabolism in plants (He and Parker 2000), peptidylprolyl cis-trans isomerase (SCQSRT1035C03) (Table 2), which has catalytic activity; coiled-coil protein (SCACAM1071C11) (Table 2), which functions in function of organizational and regulatory processes (Rose and Meier 2004); and sec14-like protein 1 (SCSBFL5016D03) (Table 2), which has transporter activity (Peterman et al. 2004).

Another group of proteins is highly related to stress, which is an important factor in achieving embryogenic competence in plant cells. Stress induced by culture medium supplements, such as PGR, sucrose and AC, leads to changes the genetic reprogramming, which must take place at the chromatin level (Fehér

2014; Smulders and Klerk 2011), and consequently causes the expression of stress proteins, which leads to somatic embryo development. One of these proteins, the cation transport protein chac (SCBGLR1047G06) (Table 2), is associated with a general defensive response to various environmental stresses in plants (Qi et al. 2005). Similarly, the protein polyphosphoinositide phosphatase-like isoform 1 (SCQGSB1143E08) (Table 2) is also associated with vesicular trafficking events and plant stress responses (Gillaspy 2010). Another protein, copper-transporting p-type ATPase (SCVPRZ2044C07) (Table 2), is abundant in response to oxidative stress and hormone signaling (Shikanai et al. 2003). The expression of the proteins drought-inducible protein 1os (SCQSST3116H01) (Table 2) (Sugiharto et al. 2002) and S-adenosylmethionine:2-demethylmenaquinone methyltransferase-like (SCJFRZ2009B04) (Table 2) is also related to plant adaptation to drought stress (Zhang et al. 2011). The expression of these proteins suggests that the callus are experiencing some type of stress and which may be responsible for the physiological modulation of the cells, thereby allowing the embryogenic competence (Moon et al. 2015).

In addition to these proteins, some of the unique E-0 callus proteins are closely related to embryogenic callus and somatic embryo characteristics (Table 2). Among these proteins, BURP domain-containing protein (SCSBHR1051A12) (Table 2) has been reported in plant microspores, and in somatic and zygotic embryogenesis, but its action in embryogenesis is not fully understood (Malik et al. 2007; Tsuwamoto et al. 2007) (Table 2). The BURP domain is conserved in diverse plant proteins, being found with divergent expression profiles and most likely divergent functions, suggesting that this protein is important and has a fundamental functional role (Hattori et al. 1998). Another protein closely related to somatic embryo formation is the dehydrogenase-like protein (SCRFAM1026C02) (Table 2), which is an enzyme that oxidizes a substrate through a reduction reaction in which one or more hydrides (H^-) is transferred to an electron acceptor. Plants express many dehydrogenases, but we can highlight alcohol dehydrogenase 3 (ADH3). ADH3 represents a class of enzymes that may be related to a specific stage of embryonic development in *Vitis rupestris* (Martinelli et al. 1993), *Daucus carota* (Kessell and Carr 1972) and *Bactris gasipaes* Kunth (Heringer et al. 2014) somatic embryos. Therefore, the function of this enzyme is important, among many other functions as the possible association of this protein

with embryogenic competence for somatic embryo formation. In addition, hua enhancer 2 (HEN2) (SCVPLR1028B03) (Table 2) is a nuclear localized DExH helicase that plays a role in determining cell fate during late stages of floral development (Linder and Owttrim 2009). SKI2, an *Arabidopsis thaliana* DExH RNA helicase related to HEN2, is also associated with cell fate, affecting development during embryogenesis (Kobayashi et al. 2007), which indicate that HEN2 may also be related to the somatic embryo development.

Some proteins were related to cell defences against biotic or abiotic stress, which can serve as a stimulus for the modulation of somatic embryogenesis, as a survival mechanism. In this context, nitric oxide synthase (NOS) interacting protein (SCQGHR1012E03) (Table 2), which synthesizes nitric oxide (NO), is unique in E-0 callus. In plants, NO serves as a signal in hormonal and defense response being a key signaling molecule in different intracellular processes (Guo et al. 2003). NO can stimulate the activation of cell division and embryogenic cell formation in *Medicago sativa* (Otvos et al. 2005), in addition to showing synergism with polyamines (PAs) in *Araucaria angustifolia* somatic embryogenesis (Silveira et al. 2006). Another stress response protein was the callose synthase 1 catalytic subunit (SCSFAD1108H10) (Table 2), a part of callose synthase, which is produced in response to wounding and pathogen attack (Jacobs et al. 2003) as well as during cell wall development (Hong et al. 2001) (Table 2). This enzyme is also abundant in *Arabidopsis* callus that are exposed to hyper-gravity (Martzivanou and Hampp 2003) and in tomato seedlings that are exposed to salt stress (Zhou et al. 2007). In *Cichorium*, callose deposition seems to be an early marker in somatic embryogenesis (Dubois et al. 1990). Additional proteins were identified that are abundant in response to abiotic stress such as desiccation-related protein pcc13-62 expressed (SCBFSD1037G05) (Table 2) which is a protein that is up-regulated under desiccation or osmotic stress conditions or under the effect of abscisic acid (ABA) and does not depend on light for its expression (Bartels et al. 1992; Wise 2003). This protein is usually related to seeds whose embryos from undergo ABA signaling during desiccation and accumulate late embryogenesis-abundant (LEA) proteins, which are involved in desiccation resistance (Alamillo et al. 1994; Bartels et al. 1992; Wise 2003). Such proteins are highly related to embryo formation and are present in embryogenic

callus of sugarcane but not in non-embryogenic callus, which have no potential for somatic embryo formation.

Other proteins were involved in metabolic pathways that may be able the embryogenic potential of the cells. UDP-sugar pyrophosphorylase-like (SCVPCL6041D12) (Table 2) catalyzes the conversion of various monosaccharide 1-phosphates to the corresponding UDP-sugars, indicating a housekeeping function in plant (Kotake et al. 2007). One type of this enzyme, UDP-glucuronic acid, was also related to zygotic embryo development in *Glycine max* L., exhibiting a linear increase during this process (Litterer et al. 2006). In plants, saccharides act as carbon and energy sources, as well as osmotic agents and signal molecules (Smeekens et al. 2010). Sucrose and hexoses exhibit similar endogenous saccharide patterns, regulating carbohydrate metabolism and being important for structural somatic embryo development (Kubeš et al. 2014). In addition to sugar metabolism, vitamins may be involved in embryogenic competence. Folylpolyglutamate synthase (SCAGLR2033F09) (Table 2) catalyzes glutamylation following the initial glutamylation catalyzed by dihydrofolate synthase during plant folate synthesis (Basset et al. 2005; Ravanel et al. 2001) (Table 2). The role of the vitamins biotin and folate are not fully known, but when combined with proline perhaps synergistically, these compounds permit high levels of somatic embryogenesis in hybrid onions (*Allium fistulosum* × *A. cepa* F1) (Lu et al. 1989).

Certain metabolic pathways, such as the tryptophan (Trp) pathway, may be highly related to embryonic competence. The protein 3-deoxy-D-arabino-heptulosonate-7-phosphate synthase (SCEQRT1027A06) (Table 2) is the first enzyme of the shikimate pathway, which converts phosphoenolpyruvate (PEP) and erythrose 4-phosphate (E-4P) into 3-deoxy-D-arabino-heptulosonate 7-phosphate (DAHP) (Herrmann 1995). The shikimate pathway of plants mediates the conversion of primary carbon metabolites into phenylalanine (Phe), tyrosine (Tyr) and tryptophan (Trp), and numerous secondary metabolites that are derived from these metabolites (Tzin et al. 2012) may be important for the acquisition of cell competence to develop somatic embryos in sugarcane callus. Along these same lines is phosphoribosylanthranilate transferase (SCAGLR1021B10) (Table 2). It is an enzyme that converts anthranilate and phosphoribosylpyrophosphate (PRPP) into phosphoribosylanthranilate (PR-anthraniate) and inorganic

pyrophosphate in the Trp biosynthetic pathway (Rose et al. 1992). Trp is the substrate for the synthesis of indoleacetic acid (IAA) (Cohen et al. 2003), an important auxin for embryogenic callus induction. The expression of this protein in E-0 callus of sugarcane could be associated with the competence of these callus to develop somatic embryos during maturation treatments.

The balance of endogenous plant hormones plays a key role in somatic embryogenesis (Jimenez 2005). In this context along with the participation of other proteins in the formation of IAA as seen above, adenylyl-sulfate kinase (SCQSST1036B01) (Table 2) participates in the brassinosteroids biosynthesis pathway, where it catalyzes the ATP-dependent synthesis of adenosine 3'-phosphate 5'-phosphosulfate (PAPS), which is an essential metabolite for sulfur assimilation in plants (Ravilious and Jez 2012). PAPS serves as the sulfate donor for the sulfonation of brassinosteroids and peptide hormones (Klein and Papenbrock 2004). Brassinosteroids are a class of plant steroid hormones whose functions are the promotion of cell elongation, cell division, and dedifferentiation (Müssig 2005). A family of somatic embryogenesis receptor kinases (SERKs) has been genetically implicated in mediating early brassinosteroid signaling events (Santiago et al. 2013), highlighting the importance of this PGR in somatic embryo development.

3.1.5.3 Unique proteins that are abundant in matured embryogenic (E-21) callus

When embryogenic callus are transferred to maturation culture medium supplemented with AC and are exposed to light for 21 days, their protein expression changes, leading to the identification of 14 unique proteins (Figure 4 and Table 2). Of these proteins, we can mention some that are related to embryogenic callus maturation.

Metabolic processes produce active oxygen species that are highly destructive to cellular components such as proteins, membrane lipids and nucleic acids (Mhamdi et al. 2010). Upon entering the maturation protocol, callus are exposed to intense light, which is a form of oxidative injury (Heyneke et al. 2013). To minimize this effect, some proteins are differentially abundant in these callus, such as catalase-expressed (SCCCCL3120D10) (Table 2) and ac079853_1

myosin heavy chain-like (SCAGLB1071A03) (Table 2), representing one of the primary enzymatic defenses against oxidative stress (Ahsan et al. 2007; Matsumura et al. 2002). The TGACG-sequence-specific DNA-binding protein TGA-like (TGA) (SCJFSB1010B12) (Table 2) is involved in defense responses in Arabidopsis, but this function remains unknown (Shimizu et al. 2008).

Secreted proteins (SCSBSD2032F10) (Table 2) are of great importance for somatic embryogenesis because some of them have the ability to convert non-embryogenic to embryogenic callus when added to the culture medium, such as like arabinogalactan proteins (Poon et al. 2012). These proteins are likely to be used to enhance somatic embryogenesis protocols, to increase induction in non-responsive or low-embryogenic genotypes and to improve regeneration rates (de Carvalho Silva et al. 2014; Steinmacher et al. 2012). In these present study, the expression of this protein leads us to believe that this protein is also important in the maturation phase, during which we observed somatic embryo development in sugarcane. The maturation and conversion phases for sugarcane somatic embryos still present a bottleneck against generating a high-efficiency regenerative protocol, and these proteins could help to improve these rates.

3.1.5.4 Unique proteins abundant in non-embryogenic (NE-0) and matured non-embryogenic (NE-21) callus

Embryogenic and non-embryogenic callus have different phenotypes and hence, different proteomes. However, NE-0 callus abundant proteins with similar functions to those abundant in E-0 and E-21 callus, save for proteins with lipid binding and chromatin binding activities (Figure 4). These may represent differentially abundant proteins, that provided the characteristics that are unique to non-embryogenic callus. Among the proteins with lipid binding activity, pleckstrin homology domain-containing protein 1 (SCBGRT1046F12) (Table 2) interacts with the important, second messenger phosphatidylinositol 3,4,5-trisphosphate and may regulate specific cellular processes (Dowler et al. 2000). This binding can block external signals prevent response to these stimuli, in contrast to embryogenic callus, in which the cells would respond. Chromatin binding activity is found in the MYB-like DNA-binding domain containing protein (SCQGST1032A06) (Table 2), which is a transcription factor that is found in almost all eukaryotes

(Prouse and Campbell 2012). In plants, MYB proteins regulate a vast array of metabolic, cellular and developmental processes and can act as transcriptional activators, repressors, or both (Dubos et al. 2010). Thus, this transcription factor may act on the differential expression of specific proteins in non-embryogenic callus or may block the transcription of proteins that are essential in embryogenic callus, causing non-embryogenic callus to lose the capacity to differentiate into somatic embryos. A few unique proteins (10) appeared in the NE-21 callus. One of these proteins was differentially, polyubiquitin-like protein (SCRLLV1026A01) (Table 2), which participates in the ubiquitin-dependent proteolytic pathway in which ubiquitin covalently attaches to proteins to be degraded (Vierstra 1993). The close relationship of protein to the proteolytic pathway may explain the low number of unique proteins in NE-21 callus, as many of these proteins may have been degraded. These 10 unique proteins seem to indicate that the lack of-embryogenic induction in the NE callus is largely determined by the absence of proteins that are present in the embryogenic callus, rather vice versa.

3.1.5.5 Common proteins in embryogenic and non-embryogenic callus

The common proteins in all four types of callus predominantly consist of housekeeping proteins or proteins that are essential for the maintenance of basal cellular metabolism, such as chaperones, which promote correct protein folding (Figure 5 and S1 Table). These housekeeping proteins have been identified in several studies and are considered Déjà vu proteomics (Petrak et al. 2008). With this, it is worth mentioning only a few up-regulated proteins that are directly related to the development of somatic embryos.

Because these proteins appear in all callus, one would think that none of these proteins would play a key role in somatic embryogenesis and the development/conversion of somatic embryos. However, these proteins do not appear at the same concentration in all callus and may be up-regulated or down-regulated in relation to one another. Comparing the E-0 and NE-0 callus, the embryo-specific protein (SCCCCL3005C05.b) (S1 Table) appears up-regulated more than 15 times in E-0 callus, indicating that this callus is competent to develop somatic embryos (S1 Table). The late-embryogenesis-abundant group 3 protein variant 2 (SCQSRT2031H06) (S1 Table) and late-embryogenesis-abundant

protein (SCJLLR1107G02) (S1 Table), an important class of proteins that are well known as markers of somatic embryos maturity, are also up-regulated more than 5 times in the E-0 callus (S1 Table). Proteins that are up-regulated in sugarcane E-0 callus may be associated with the acquisition of competence to develop somatic embryos, and the higher metabolism of embryogenic cells in E-0 could induce these changes in protein expression.

In E-21 callus, germin protein-like protein subfamily 1 member 17 precursor (SCCCCL7037E09) was identified (S1 Table), which is up-regulated almost 12 times compared E-0 callus (Table 2). Germins are thought to play a significant role during zygotic and somatic embryogenesis (Patnaik and Khurana 2001), indicating that the maturation treatment of E-21 callus led to an increase in the expression of this protein, thereby resulting in the development of somatic embryos in sugarcane. The embryo-specific protein (SCCCCL3005C05.b) (S1 Table) also appears up-regulated more than 35 times in E-21 compared with E-0, suggesting that this protein as an excellent marker of embryogenesis. The kinase interacting protein 1 (CIPK) (SCBFFL5072F08) up-regulated more than 119 times in E-21 compared with E-0. This protein is a target of Ca^{2+} sensors (calcineurin B-likeproteins [CBLs]) (Luan 2009). Ca^{2+} is a important second messenger, and the CBL-CIPK signaling network translates Ca^{2+} signals them into the correct cellular responses (Luan 2009). CBL and CIPK proteins are important components of abiotic stress responses, hormone reactions and ion transport processes in plants (Batistić and Kudla 2009), indicating that all of these processes can be crucial for the development of sugarcane somatic embryos.

3.1.6 CONCLUSION

The best treatment to promote somatic embryo maturation in sugarcane cv. SP80-3280 was MS culture medium supplemented with AC 1.5 g L⁻¹, which led to the highest number of somatic embryos in E callus. In non-embryogenic callus the formation of somatic embryos was not observed with any of the applied treatments.

The unique proteins found in the embryogenic callus, including dehydrogenase-like protein, desiccation-related protein-62 pcc13, callose synthase 1 catalytic subunit and NOS-interacting protein could play an important role in sugarcane morphogenesis and embryogenic competence, permitting the formation of somatic embryos. The non-embryogenic callus exhibited more unique proteins that were related to protein degradation, which is indicative of callus with low metabolic activity and, consequently, a low level of cell differentiation, which therefore do not form somatic embryos. The unique proteins in E-21 callus, such as catalase-expressed and secreted protein could play an important role in the maturation of sugarcane somatic embryos. These proteins could be potential candidates for use in enhancing somatic embryogenesis protocols, potentially by increasing induction in non-responsive or low-embryogenic genotypes and improving regeneration rates. The common proteins were presented at high levels, and a crude analysis revealed that many of these proteins were involved in housekeeping functions. However, the expression levels of these proteins, whether down- or up-regulated, may indicate a role in certain important morphogenetic pathways, such as the embryo-specific protein in E-0 and E-21 callus and germin protein-like protein subfamily 1 member 17 precursor and kinase interacting protein 1 in E-21 callus. Thus, these proteins may also represent candidate biochemical markers for different stages of sugarcane somatic embryogenesis.

3.2 COMPARATIVE PROTEOMICS ANALYSIS OF THE EFFECT OF COMBINED RED AND BLUE LIGHTS ON SUGARCANE SOMATIC EMBRYOGENESIS

3.2.1 INTRODUCTION

Several plant biotechnology techniques have been used as alternatives to the conventional propagation of sugarcane (*Saccharum spp.*), and somatic embryogenesis stands out among these tools as a method for improving sugarcane productivity rates worldwide. Analogous to zygotic embryogenesis, somatic embryogenesis is a process through which a single cell or a small number of somatic cells serve as precursors for the formation of a somatic embryo (Tautorus et al. 1991). The somatic embryo maturation and conversion phases for sugarcane somatic embryos still present a bottleneck in the development of a high-efficiency regenerative protocol. Thus, new technologies are necessary to increase the conversion rate of somatic embryos into somatic plantlets.

The modern sugarcane breeding programs include biotechnological approaches, such as genetic transformation and mass propagation (Lakshmanan et al. 2005), which can introduce genes encoding desirable traits into elite sugarcane cultivars. In this context, somatic embryogenesis is preferred for the regeneration of plants that have been obtained from the genetic transformation of sugarcane through either particle bombardment or *Agrobacterium*-mediated transformation (Arruda 2012).

An alternative to optimizing the somatic embryogenesis protocols might be the use of light-emitting diode (LED) lamps. LED lamps are a new form of lighting that presents numerous advantages over traditional lighting and is gaining interest worldwide in horticulture (Gupta and Jatohu 2013). Their small size, long life, and low heat emission, as well as the ability to select different wavelengths, make LED lamps revolutionary in plant lighting (Gupta and Jatohu 2013; Massa et al. 2008). Such lighting systems have been used in several somatic embryogenesis protocols, such as those for *Pinus taeda*, *Pinus elliottii* and *Pinus palustris* (Merkle et al. 2006), *Pinus densiflora* (Kim and Moon 2014), *Oncidium* (Mengxi et al. 2011), and *Phalaenopsis* (Park et al. 2010), and these systems were found to be efficient for somatic embryo formation and conversion in these different species.

Plant development and physiology are strongly influenced by the light spectrum; for example, a particular wavelength can promote the induction of physiological processes and thereby change gene expression and developmental programs in plants (Liu et al. 2011; Shimizu-Sato et al. 2002). In traditional photomorphogenesis, light signals are perceived by multiple photoreceptors and interpreted by a series of intermediate signaling factors for downstream transduction (Huang et al. 2014). Photoreceptors sense far-red and red light through phytochromes (phyA and phyB) and blue/UV-A light through cryptochromes (cry1 and cry2) (Huang et al. 2014; Liu et al. 2011). Additionally, the wavelength may influence the accumulation or depletion of certain pigments; for example, blue LEDs accumulate the highest contents of leaf chlorophylls, and red LEDs inhibit chlorophyll accumulation (Hung et al. 2016).

In addition to the direct genetic alterations in plant physiology and development caused by light, light influences plant epigenetics and might consequently induce phenotypic modifications through the regulation of gene expression (Barneche et al. 2014; Li et al. 2013; Tatra et al. 2000). In brown cotton (*Gossypium hirsutum*), differences in the patterns of DNA methylation have found among samples treated with different light wavelengths (blue, white + ultraviolet-B, red, white, and yellow) (Li et al. 2013). Tatra et al. (2000) showed that in *Stellaria longipes*, low red/far-red light ratios, which mimic greater shade, promote lower methylation levels and consequently produce taller plants compared with high red/far-red light ratios. Light might also control seed germination by regulating phytochrome B (phyB) and downstream genes, such as *JMJ20/JMJ22*, which

encode redundant histone arginine demethylases, and *GA3ox1/GA3ox2*, which are gibberellic acid anabolic genes. The light-dependent activation of *phyB* modulates the repression of histone arginine demethylase genes, which remove the repressive histone arginine methylations at *GA3ox1/GA3ox2*, and thereby promotes seed germination (Cho et al. 2012).

In this context, similarly to proteomics, studying the functional genome is an alternative approach for evaluating the impacts of light intensity and light source on photosynthetic metabolism and other physiological processes (Muneer et al. 2014). Thus far, few studies have reported the effects of different wavelengths on the cellular and molecular alterations of plants and their influence on the embryogenic capacity of callus to develop plantlets. A better understanding of this process will allow the development of strategies for the *in vitro* culture, propagation and genetic manipulation of plants (Marsoni et al. 2008). Proteomics analysis has been used to identify the specific and differential abundance of proteins that might be associated with somatic embryo development (Heringer et al. 2015; Lippert et al. 2005; Marsoni et al. 2008). Modern proteomic acquisition techniques with increased selectivity and specificity, such as multiplex high-resolution format MS^E [multiplexed data-independent acquisition (DIA)] (Silva et al. 2005) and high-definition HDMS^E (DIA with ion mobility) (Lalli et al. 2013; Ruotolo et al. 2005; Wu et al. 2000), are required for shotgun proteomics and other complex samples due to their resolving power for overlapping chimeric peptides (Chakraborty et al. 2007; Geromanos et al. 2009).

The aim of the present work was to study the influence of various combinations of red and blue wavelengths on the somatic embryo maturation and conversion, allies to RITA temporary immersin system, of sugarcane cv. SP80-3280 and on the abundances of differentially abundant proteins associated with different morphogenetic responses.

3.2.2 REVIEW

3.2.2.1 Somatic embryos maturation

During the maturation step, somatic embryos undergo morphological and biochemical changes. The cotyledons expand concomitantly with the accumulation of storage substances such as proteins, lipids and amino acids, which are useful in the conversion of somatic embryos into plantlets (Businge et al. 2013; Thomas 1993). These compounds are known to be involved in the acquisition of desiccation tolerance during seed development and maturation (Businge et al. 2013). However, the storage may vary from somatic embryos and zygotic.

The main effort to optimize the somatic embryogenesis system in many species mainly concentrated in the somatic embryos maturation and conversion steps, and normally the culture media is supplement with specific concentration of growth regulators, especially abscisic acid (ABA) (Sghaier-Hammami et al. 2010) and polyamines (Reis et al. 2016). In some cases, the somatic embryos needs a osmotic adjustment, which is usually done with suplementation by not plasmolyzing, as polyethylene glycol (PEG) (Heringer et al. 2013), or lasmolyzing agents, as carbohydrates and hexitols, (Krajňáková et al. 2009; Lakshmanan et al. 2006). In sugarcane somatic embryos maturation, the ative charcoal is the best maturation agent promoter (Silveira et al. 2013).

However, despite these advantages about the supplementation with different compunds, the somatic embryo maturation and conversion steps in sugarcane still presented as a bottleneck to achieve a high efficiency plant regeneration protocol. In order to optimize the protocols related to the plant morphogenesis, temporary immersion system (TIS) and LED lighting can be useful to optimize the maturation and conversion step of sugarcane somatic embryos.

3.2.2.2 Temporary immersion system (TIS)

Bioreactor is an automated cell culture system, which its main function is to provide a controlled environment in order to achieve the essential conditions for cell growth. Their use may be linked to various utilities such as the cultivation of plant cells to obtain biomass or secondary metabolites, culture automation, and control of the culture internal parameters.

These bioreactors are also classified into two types, continue immersion system where the culture remains continuously immersed in the culture medium. This continuous dipping causes overhydration problem in tissues, organs and

plants. Depending on the species and the type of medium culture used, overhydration of tissue may cause serious physiological disorders, which will affect the growth and development of the material. The second type is the temporary immersion system (TIS) (Alvard et al. 1993). In this type of bioreactor culture the culture medium remains in contact with the explant for a predetermined period. Then, the culture medium is drained and the explant leaves to stay in direct contact with the culture medium. TIS combines the advantages of semi-solid and liquid culture medium. These may be associated with better supply of nutrients and therefore have an absence of nutrient gradients, common in semi-solid medium. Another advantage is the absence of anoxia in the explants and the lowest rates of hyperhydricity usually observed in liquid culture medium (Etienne and Berthouly 2002; Murch et al. 2004).

There are different temporary immersion system models already developed: RITA system (Figure 1A), and Twin Flasks (BIT) (Figure 1B-C).

The RITA system (Figure 1A) is a temporary immersion bioreactor with airflit type system, and is widely used for plant cell cultures. Its working principle (Figure 4D) is based on the air pump at the bottom compartment, where this culture medium is forcing thereby flooding the upper compartment, where cell cultures are located. These two compartments are separated by a sieve, which holds the plant cells. Thus cultures are nourished and aerated throughout this process. Exhausted time, the air pump turn off and the air exits the lower chamber and makes the medium culture return by gravity, leaving the cell cultures without contact with culture medium for a further time. Air pump time can be adjusted according to each type of culture.

Since the Twin flaks system (Figure 1A) also uses the temporary immersion system, with a difference: the twin flaks are connected with a silicon tube. In one flask, the cultures are inoculated, and in the other the medium culture. The principle operation (Figure 1B) is based on air pumping into the culture medium flask, causing it to go through the silicone tube until the culture flask. Thus cultures are nourished and aereted throughout this process. Exhausted time, the air pump turn on in the opposite direction, causing the culture medium back to its compartment. As in RITA system, air pump time can be adjusted according to each type of culture.

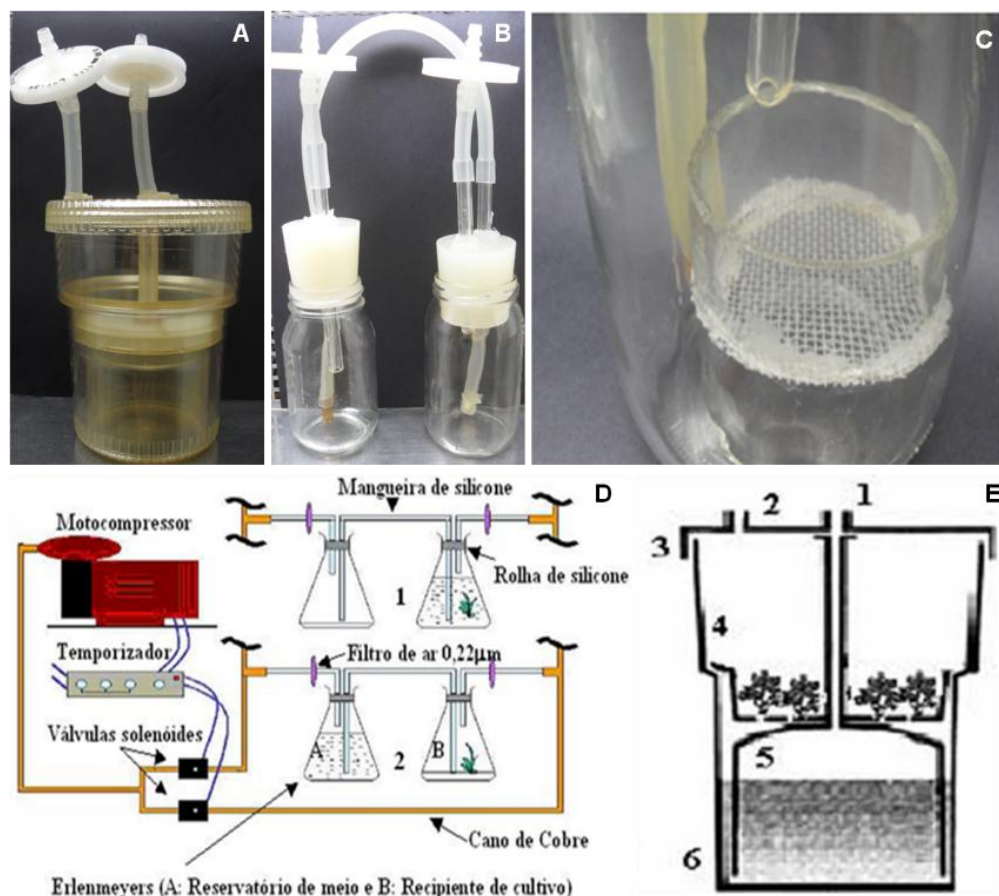


Figure 1. Temporary immersion system. A) RITA system. B) Twin flasks system; C) Twin flasks system modified D) Principle operating of Twin flasks system; E) Principle operating of RITA system (Legend: 1 air inlet 2 air outlet, 3 sealing cap, 4 growth compartment , 5 medium culture compartment, 6 main flask)

RITA system has been used in several different species and its allows to optimize plant morphogenesis protocols, such as maturation and conversion of peach palm somatic embryos (Heringer et al. 2014), multiplication of apple buds (Zhu et al. 2005), the production of eucalyptus plantlets for commercial purposes (Mc Alister et al. 2005), regeneration of strawberry shoots (Hanhineva et al. 2005), mass propagation of sugarcane (Mordocco et al. 2009) and multiplying coffee somatic embryos (Etienne-Barry et al. 1999). Therefore, we can make use of this technology to optimize the maturation and conversion step of sugarcane somatic embryos.

There are also ways to adapt these systems according to the culture type. As an example, the modified twin flasks system (MFT) (Heringer et al. 2014) which was placed a support with a sieve in the culture flask, and the cultures are

maintained inside this support. Thus, the cultures stay away from the remaining culture medium in the flask, similar to RITA system.

3.2.2.3 Light emitting diode (LED)

Light emitting diode (LED) are a new form of lighting that is gaining ground in world horticulture, with numerous advantages over traditional lighting. Its small size, long life, low heat emission and option to select different wave lengths make this technology is seen as a revolution in the lighting of the current horticulture (Massa et al. 2008). The reduction in illumination cost with this technology can be found in different aspects, such as the low heat emission, thereby facilitating the temperature control of a growth chamber at high energy conversion into light, so that there is a reduction in spending energy of a plant production unit and its long durability, avoid costly repairs. Additionally the option of selecting lengths of different wavelengths can contribute to the improvement of plant response in relation to the used culture system, increasing the regenerative rate and may also help in the maturation and conversion step of sugarcane somatic embryogenesis coupled with the temporary immersion system.

LED system has been used in several somatic embryogenesis protocols, such as those for *Pinus taeda*, *Pinus elliottii* and *Pinus palustris* (Merkle et al. 2006), *Pinus densiflora* (Kim and Moon 2014), *Oncidium* (Mengxi et al. 2011), *Phalaenopsis* (Park et al. 2010), *Dendrobium officinale* (Lin et al. 2011), *Panax vietnamensis* (Nhut et al. 2015), and these systems were found to be efficient for somatic embryo formation and conversion in these different species.

The combination of wavelengths of LEDs influence plant morphogenesis and results in improved responses (Gupta and Jatothu 2013; Massa et al. 2008). However, the role of light quality in in vitro morphogenesis is still with poor information, since this effect depends on the plant species, developmental stage of the plant and environmental conditions. Thus, a study of different wavelengths in somatic embryogenesis of sugarcane contributes to elucidate morphogenetic responses of plants in relation to light quality.

3.2.2.4 Proteomics in sugarcane somatic embryogenesis

The use of proteins as candidate biomarker for monitoring and understanding the different biological responses is presented as a potential strategy to study the development of the sugarcane tissue culture. Three proteomic approaches are among the most used (Schluter et al. 2009) (Figure 2). The first is the two-dimensional electrophoresis (2-DE), which initially separates proteins on two-dimensional electrophoresis followed by enzymatic digestion and identification of proteins by mass spectrometry. The second approach is the 'bottom-up' or 'shotgun', which begins with the digestion of proteins in a complex sample followed by separation of peptides by liquid chromatography and mass spectrometry for identification. The third approach is the 'top-down' that starts with the separation of proteins by chromatographic methods followed by the identification of these by mass spectrometry. Although the two-dimensional electrophoresis remains a technology widely used in proteomics, especially for new sequencing species with genome not sequenced, the shotgun is gaining more space (Rogowska-Wrzesinska et al. 2013).

The shotgun allows evaluating differentially abundant proteins, either in the induction phase of embryogenic callus (Heringer et al. 2015) and in the maturation of somatic embryos (Reis et al. 2016). These may lead to the identification of some of these regulatory little abundant proteins, and thus help in the improvement of somatic embryogenesis protocol for this specie. The identified proteins contribute to the understanding of embryo development in this species, and may be used as a biochemical marker for monitoring somatic embryogenesis or genetically modified embryos.

Proteomic studies associated with somatic embryogenesis in sugarcane have addressed aspects of development during the process of somatic embryogenesis related polyamines (Reis et al. 2016), dehydrins accumulation during somatic embryos formation (Burrieza et al. 2012) and comparative studies between embryogenic and non-emбриogenic callus (Heringer et al. 2015).

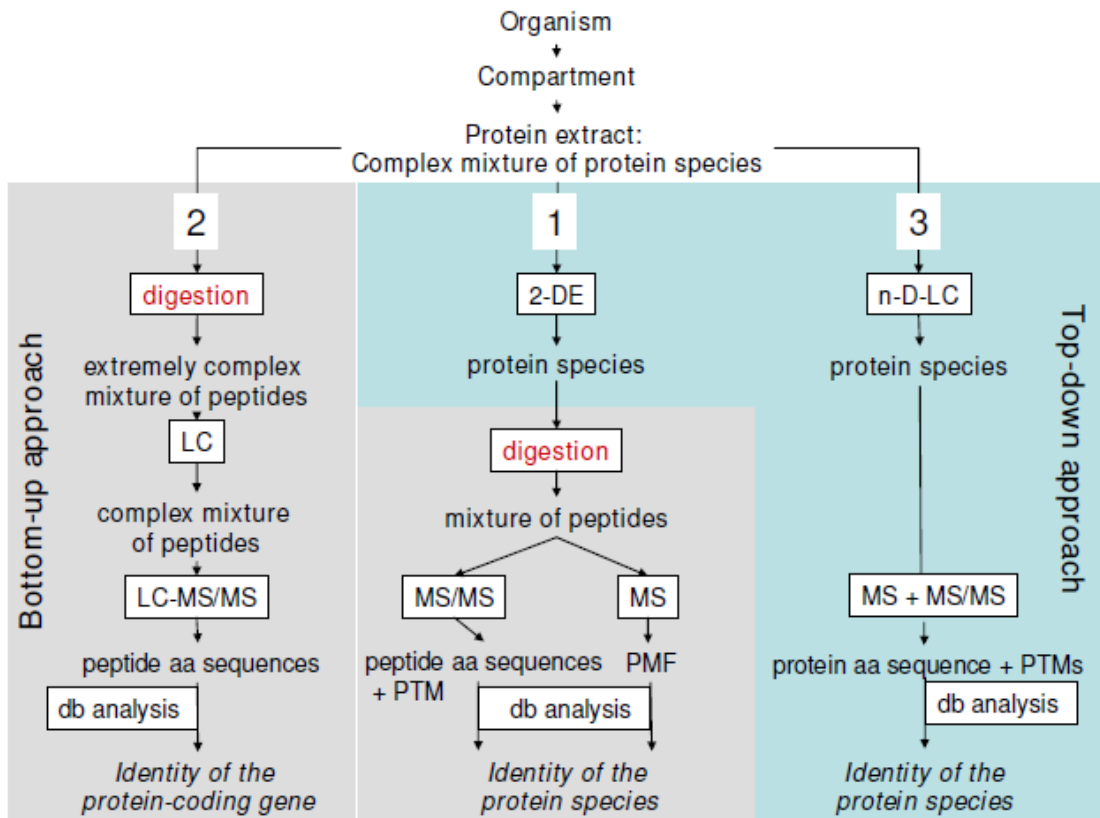


Figure 2. Scheme of three approaches most used in proteomic analysis (Schluter et al. 2009)

3.2.3 MATERIAL AND METHODS

3.2.3.1 Plant Material

Embryogenic callus from sugarcane cv. SP80-3280 were induced as previously described by Silveira et al. (2013). The nodal segments with axillary buds were then planted in the commercial substrate PlantMax (DDL Agroindustria, Paulínia, São Paulo, Brazil) and maintained in a greenhouse for approximately 45 days. The shoot apical meristems were surface sterilized in 70% ethanol for 1 min, immersed in 30% commercial bleach (1 to 1.25% sodium hypochlorite) for 15 min and subsequently washed three times with sterilized water in a laminar flow chamber. The explants were then transversely sectioned into 2-mm-thick slices and inoculated into test tubes (150 × 25 mm) containing 10 mL of MS (Murashige

and Skoog 1962) (PhytoTechnology Lab, Overland Park, KS, USA) culture medium supplemented with 20 g.L⁻¹ sucrose, 2 g.L⁻¹ Phytagel (Sigma-Aldrich, St. Louis, MO, USA) and 10 µM 2,4-dichlorophenoxyacetic acid (2,4-D) (Sigma-Aldrich). The pH of the culture medium was adjusted to 5.8, and the culture medium was then autoclaved for 15 min at 1.5 atm and 121 °C. The explants were maintained at 25 ± 2 °C in the dark.

After 45 days, the induced callus were transferred to Petri dishes (90 × 15 mm) containing 20 mL of the same culture medium. Each callus was subcultured every 21 days and separated into two types: embryogenic and non-embryogenic (Silveira et al. 2013). Only embryogenic callus (Figure 1A) were used in the study.

3.2.3.2 Maturation treatment with combinations of red and blue wavelengths

For the maturation treatment, three colonies containing 200 mg of fresh matter (FM) of embryogenic callus (Figure 1a) were inoculated into Petri dishes (fifteen per treatment) containing 20 mL of MS culture medium supplemented with 20 g.L⁻¹ sucrose, 2 g.L⁻¹ Phytagel, and 1.5 g.L⁻¹ activated charcoal (AC; Sigma-Aldrich) according to Heringer et al. (2015). After inoculation, the cultures were maintained in a growth chamber at 25 ± 1 °C in the dark for seven days.

After the first seven days, the callus were subjected to photoperiods consisting of 16 h of light at 25 ± 1 °C with six different GreenPower TLED (Koninklijke Philips Electronics NV, Netherlands) wavelengths (Table 1) for 28 days of culture, and a fluorescent lamp was used as the control treatment. After 28 days, the number of somatic embryos was evaluated, and a USB 2000 spectrometer (Ocean Optics, Dunedin, FL, USA) was used to measure the peak wavelength of each LED and the fluorescent lamp used in the experiment (Table 1).

Samples from all of the treatments were collected after 28 days and stored at -20 °C for subsequent (after conversion treatment) selection of the contrasting treatments for shotgun proteomics analysis.

Table 1. Characteristics of the different wavelengths used in sugarcane somatic embryo maturation and conversion treatments.

Treatment	Lamp wavelength	$\mu\text{mol. m}^{-2} \text{s}^{-1}$	Peak (nm)	wavelength
Control	Tubular fluorescent	55	435 / 545 / 580	
W _m B	W/MB	55	450 / 530	
W _h B	W/HB	55	450 / 530	
W _l B _d R	W/LB/DR	45	450 / 530 / 660	
W _m B _d R	W/MB/DR	45	450 / 530 / 660	
W _l B _d R _f R	W/LB/DR/FR	40	450 / 530 / 660 / 735	
W _m B _d R _f R	W/MB/DR/FR	40	450 / 530 / 660 / 735	

White (W); Low Blue (LB) = 8-10% blue; Medium Blue (MB) = 12-14% blue; High Blue (HB) = 16-18% blue; Deep Red (DR) = 30-50% deep red; Far Red (FR) = 12% far red.

3.2.3.3 Somatic embryo conversion with a RITA temporary immersion system combining red and blue wavelengths

For the conversion of somatic embryos, 3.0 g of matured callus, which were derived from the earlier maturation experiment, was inoculated into each RITA temporary immersion system (Vitropic, Saint-Mathieu-de-Tréviers, France) containing MS medium supplemented with 20 g.L⁻¹ sucrose. Each treatment consisted of three repetitions, and each RITA was considered one sampling unit. The callus inoculated into RITA were maintained at 25 ± 1 °C under the conditions described in Table 1. After 28 days, the number of plantlets and the FM were evaluated. After 56 days, the number of plantlets and the FM in the two best treatments were determined.

The best treatment in terms of the production and conversion of somatic embryos, as well as the control treatment, were utilized for the subsequent proteomic analyses.

3.2.3.4 Plantlet elongation and acclimatization

The plantlets obtained from RITA, which were approximately 15-20 mm in height, were grown in flasks containing 20 mL of MS culture medium supplemented with 20 g.L⁻¹ sucrose and 2 g.L⁻¹ Phytagel. The plantlets were

maintained at 25 ± 2 °C under the same GreenPower TLED (Koninklijke Philips Electronics) wavelengths until they reached a height of 110-130 mm.

Acclimatization was performed according to Heringer et al. (2014). Briefly, the plantlets were transferred to 50-mL plastic cups containing commercial substrate (PlantMax) and vermiculite (1:1). The cups were placed in a plastic box covered with transparent plastic to allow light entry and high humidity. The plants were maintained at 25 °C ± 2 °C with a 16-h photoperiod, and plant survival was evaluated after one month.

3.2.3.5 Protein extraction

Proteomics analyses were performed during the 28-day maturation of embryogenic callus collected from the control (fluorescent lamp) and WmBdRfR (the best treatment for somatic embryo production and conversion) treatments.

Protein extraction was performed using five biological replicates (500 mg FM) according to Heringer et al. (2015) and Reis et al. (2016). The samples were pulverized using a mortar and pestle in liquid nitrogen on ice and macerated with extraction buffer containing 7 M urea (GE Healthcare, Freiburg, Germany), 2 M thiourea (GE Healthcare), 1% dithiothreitol (DTT - GE Healthcare), 2% Triton X-100 (GE Healthcare), 0.5% Pharmalyte (GE Healthcare), and 1 mM phenylmethanesulfonyl fluoride (PMSF-Sigma-Aldrich). Subsequently, the samples were centrifuged at 12,000 g and 4 °C for 20 min. The supernatants were collected, and the protein concentration was measured using a 2-D Quant Kit (GE Healthcare, Piscataway, NJ, USA). The five protein extracts resulting from each treatment were pooled, totaling 100 µg of protein (Heringer et al. 2015; Luge et al. 2014; Reis et al. 2016).

3.2.3.6 Protein digestion

The pooled samples (100 µg of protein) were desalted on 5000 MWCO Vivaspin 500 membranes (GE Healthcare, UK) using 50 mM ammonium bicarbonate (NH_4HCO_3 , Sigma-Aldrich), pH 8.5, as the buffer. The samples were washed by the addition of 400 µL of buffer to the membrane followed by

centrifugation at 15,000 g and 8 °C for 20 min. This procedure was repeated at least three times, retaining approximately 50 µL of sample.

For trypsin digestion, a 2 µg.µL⁻¹ solution consisting of 50 µL of the previous sample plus 25 µL of 0.2% v/v *RapiGEST* (Waters, USA) was vortexed for 5 s and heated in an Eppendorf Thermomixer® Comfort device at 80 °C for 15 min. Then, 2.5 µL of 100 mM DTT was added, and the mixture was placed in the thermomixer at 60 °C for 30 min. The tubes were placed on ice (30 s), and 2.5 µL of 300 mM iodoacetamide (IAA) was added. After vortexing for 5 s and incubation in the dark for 30 min at room temperature, 20 µL of trypsin (50 ng.µL⁻¹) solution prepared with 50 mM NH₄HCO₃, pH 8.5, was added (Promega USA), and the mixture was placed in a thermomixer at 37 °C overnight. Then, 10 µL of 5% v/v trifluoroacetic acid (TFA) was added to precipitate the surfactant *RapiGEST* SF. The samples were then vortexed for 5 s, incubated at 37 °C for 90 min (without shaking) and centrifuged at 14,000 × g and 8 °C for 30 min. Then, 100 µL of the supernatant was collected and transferred to a Total Recovery Vial (Waters, USA) for proteomics analysis.

3.2.3.7 Mass spectrometry analysis

The ESI-QTOF HDMS^E analyses were conducted in a nanoAcquity UPLC connected to a Synapt G2-Si HDMS mass spectrometer (Waters) according to Reis et al. (2016). The peptide mixture was first loaded into a nanoAcquity UPLC 5-µm C18 trap column (180 µm x 20 mm) and then into a nanoAcquity HSS T3 1.8-µm analytical reversed-phase column (100 µm x 100 mm). For all measurements, the mass spectrometer was operated in the resolution mode (35,000 FWHM) with an ion mobility cell filled with nitrogen gas. The effective resolution with conjoined ion mobility was >1,800,000 FWHM. All analyses were performed using nano-electrospray ionization in the positive ion mode [nanoESI (+)] and a NanoLockSpray (Waters, Manchester, UK) ionization source. The lock mass channel was sampled every 30 s. The mass spectrometer was calibrated with the MS/MS spectrum of [Glu1]-fibrinopeptide B human (Glu-Fib) solution (100 fmol.µL⁻¹) delivered through the reference sprayer of the NanoLockSpray source. The formula [M + 2H]2+ = 785.8426 was used for the initial single-point calibration, and MS/MS fragment ions of Glu-Fib were used to obtain the final instrument

calibration. Multiplexed data-independent (DIA) scanning with the added specificity and selectivity of a non-linear ‘T-wave’ ion mobility (HDMS^E) device (Giles et al. 2011) was performed using a Synapt G2-Si HDMS mass spectrometer (Waters, Manchester, UK), which was automatically programmed to switch between standard MS (3 eV) and elevated collision energies HDMS^E (19–45 eV) applied to the transfer ‘T-wave’ CID (collision-induced dissociation) cell with argon gas; the trap collision cell was adjusted to 1 eV and generated a minimum of 20 scan points for each peak with both low-energy and high-energy transmission at an orthogonal acceleration time-of-flight (oa-TOF) and a mass range from m/z 50 to 2000. The same amount of each of the samples from the different conditions was injected on the column. Stoichiometric measurements based on scouting runs of the integrated total ion account (TIC) prior to the analysis were performed to ensure standardized molar values across all conditions.

3.2.3.8 Proteomics data analysis

Progenesis QI for Proteomics Software V.2.0 (Nonlinear Dynamics, Newcastle, UK) was used to process the MS^E data. The analysis used the following parameters: one missed cleavage, minimum fragment ion per peptide equal to 1, minimum fragment ion per protein equal to three, minimum peptide per protein equal to 1, fixed modifications of carbamidomethyl C, variable modifications of oxidation M and phosphoryl STY, and a default false discovery rate (FDR) maximum of 4%. The SUCEST database (<http://sucest-fun.org>) was used for protein identification. Proteins common to all treatments were filtered based on a fold change of log₂ 1.2, which was determined by the overall coefficient of variance for all quantified proteins across all replicates. Proteins with differential abundances were considered up-regulated when log₂ was 1.2 or greater and down-regulated when log₂ was -1.2 or less.

Functional annotation was performed using the Blast2Go software v3.0 PRO (Conesa et al. 2005) and UniProtKB (www.uniprot.org) information. The subcellular localization of the proteins was predicted through TargetP (<http://www.cbs.dtu.dk/services/TargetP/>) based on UniProtKB site information.

3.2.4 RESULTS AND DISCUSSION

3.2.4.1 Maturation and conversion of somatic embryos with different combinations of red and blue wavelengths

The effects of light quality on somatic embryogenesis have been poorly investigated in comparison to those of various biochemical compounds, such as plant growth regulators, osmotic regulators, and inhibitors (Hoshino and Cuello 2006). However, the development of LED technology and its use in the lighting of plants (Morrow et al. 1989) broadened these studies because LED lamps, unlike fluorescent lamps, allow the emission of different wavelengths.

In our study, various combinations of red and blue wavelengths were used to improve somatic embryogenesis responses in sugarcane. No significant differences in FM between the different treatments were observed during the first 28 days of treatment (data not shown). Morphologically, embryogenic callus maintained under fluorescent light exhibited reduced amount of green tissue (Figure 1). The treatments with different combinations of red and blue wavelengths that resulted in a higher number of somatic embryos showed higher amounts of green tissue (Figs. 1c-1h). However, among all the treatments, the fewest number of somatic embryos (i.e., 23) was obtained with the control treatment (fluorescent lamp; Table 2 and Figure 1).

Since the control treatment resulted in a low number of somatic embryos, it was not continued to the next somatic embryo conversion step. After 28 days of culture, an average of 58 somatic embryos was obtained with the W_mB_dR_fR treatment (Table 2 and Figure 1), which involves a light composition comprising white, blue, deep red, and far red wavelengths (Table 1).

Regarding the general influence of light, many studies have shown that red light promotes and blue light inhibits the induction of somatic embryos (Hoshino and Cuello 2006). However, after induction, blue light generally promotes the development of somatic embryos in *Hyacinthus orientalis* and *Daucus carota L.* (Bach and Krol 2001; Michler and Lineberger 1987). In this context, the combination of red and blue wavelengths appears to be ideal for somatic embryo formation and development (Mengxi et al. 2011). In the present work, the presence of blue light (medium blue light – _mB) was found to be essential for

somatic embryo maturation in sugarcane because the W_mB , W_mB_dR and $W_mB_dR_fR$ treatments resulted in the highest numbers of somatic embryos reaching the maturation phase (Table 2). However, the conversion of somatic embryos into plantlets appears to require a combination of medium blue ($_mB$) and deep red ($_dR$) light because the highest somatic embryo conversion into plantlets (Table 3) was observed with the $W_mB_dR_fR$ followed by the W_mB_dR treatments, both of which included medium blue ($_mB$) and deep red ($_dR$) light.

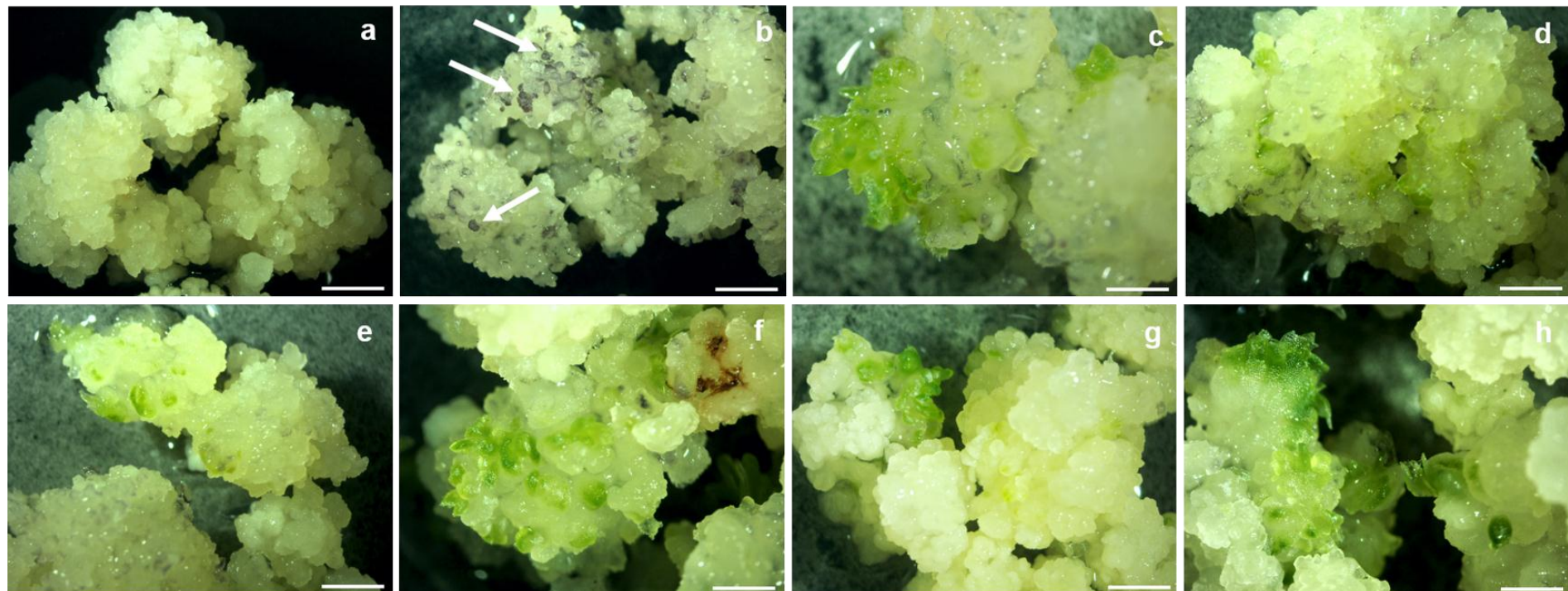


Figure 1. Sugarcane embryogenic callus on day 0 (a) and day 28 exposed to maturation treatments consisting of different wavelengths: Control (b), W_mB (c), W_hB (d), W_lB_dR (e), W_mB_dR (f), $W_lB_dR_fR$ (g) and $W_mB_dR_fR$ (h). Bar a = 10 mm; Bars b, c, d, e, f, g, h = 15 mm; white arrow = pigments. Treatments: Control = fluorescent lamp; the other treatments consisted of various mixtures of LED lamps of W = white; lB = low blue; _mB = medium blue; _hB = high blue; _dR = deep red; and _fR = far red.

Table 2. Number of somatic embryos (per callus) of sugarcane during maturation treatment with different light wavelengths.

Treatments	Day 14		Day 21		Day 28	
Control	7.40	b	13.50	c	23.00	c
W _m B	10.6	b	38.80	a	56.33	a
W _h B	13.5	ab	17.90	c	34.00	bc
W _l B _d R	17.5	a	22.70	bc	24.47	c
W _m B _d R	10.4	b	22.20	bc	44.07	ab
W _l B _d R _f R	7.60	b	18.70	c	38.27	bc
W _m B _d R _f R	12.6	ab	31.90	ab	58.67	a

Values followed by the same letter in the same column are not significantly different according to the Student-Newmann Keuls test ($p < 0.05$) ($n = 15$). Treatments: Control = Fluorescent lamp; LED lamps mixture of W= White; lB= Low Blue; _mB= Medium Blue; _hB= High Blue; _dR= Deep Red; _fR= Far Red.

In a previous study in *Phalaenopsis*, far-red wavelengths produced the highest number of somatic embryos as compared to other light treatments that were tested (Park et al. 2010). In the present work, far-red light was not found to be essential because the W_lB_dR_fR treatment did not induce significant somatic embryo formation (Table 2). Our results show that the use of a combination of red and blue wavelengths, as in the W_mB_dR and W_mB_dR_fR treatments, might be a feasible approach for obtaining improved somatic embryo maturation protocols for sugarcane.

In this study, after maturation of the embryogenic callus in semi-solid culture medium, somatic embryo conversion was held in a RITA temporary immersion system. After 28 days under the W_mB_dR_fR treatment, an average of 3,906 converted plantlets were obtained with 31.5 g of FM (Table 3 and Figure 2a), and after 56 days, the number of plantlets was further increased, reaching a mean of 18,964 plantlets (Figure 2b and Table 4). The FM and plantlet numbers for 56 days were obtained only for the two best treatments, W_mB_dR and W_mB_dR_fR (Table 4). During this phase, far-red light was found to have a strong influence on the conversion of somatic embryos. The comparison of the W_mB_dR and W_mB_dR_fR treatment revealed that these resulted in the conversion of 3,305.5 and 3,906.4 plantlets, respectively (Table 3). The only difference between these treatments was the addition of the far-red wavelength in the W_mB_dR_fR treatment (Table 1), which provided an increase of more than 18% in the number of somatic embryos converted.



Figure 2. Sugarcane somatic embryo conversion in a RITA temporary immersion system on days 28 (a) and 56 (b) under the $W_mB_dR_fR$ treatment. Converted plantlets at 15-20 mm (c) and plantlets at 110-130 mm (d) after the elongation step. Plantlets were acclimatized in plastic cups inside a plastic box covered with transparent plastic (e) and were then maintained in the greenhouse after acclimatization (f). Bars a, b and c = 16 mm; d = 23 mm; e = 45 mm; f = 140 mm. The $W_mB_dR_fR$ treatment consisted of a mixture of LED lamps of W = white; $_mB$ = medium blue; $_dR$ = deep red; and $_fR$ = far red.

Table 3. Sugarcane fresh mater (FM) and plantlet numbers after 28 days in a RITA temporary immersion system, under different wavelength treatments.

Treatments	FM (g)	plantlets (nº)
W _m B	22.8	b 2468.1 c
W _h B	16.8	c 1158.8 d
W _l B _d R	13.2	d 824.2 d
W _m B _d R	22.0	b 3305.5 b
W _l B _d R _f R	10.4	e 327.9 e
W _m B _d R _f R	31.5	a 3906.4 a

Values followed by the same letter in the same column are not significantly different according to the Student-Newmann Keuls test ($p < 0.05$) ($n = 3$). Control = Fluorescent lamp; LED lamps mixture of W= White; _lB= Low Blue; _mB= Medium Blue; _hB= High Blue; _dR= Deep Red; _fR= Far Red.

Table 4. Sugarcane fresh mater (FM) and plantlet numbers after 56 days in a RITA temporary immersion system under different wavelength treatments.

Treatments	FM (g)	plantlets (nº)
W _m B _d R	81.8	b 14,485.4 b
W _m B _d R _f R	107.0	a 18,964.8 a

Values in the same column followed by the same letter are not significantly different according to the Student-Newman-Keuls test ($p < 0.05$) ($n = 3$). The treatments consisted of various mixture of LED lamps of W = white; _mB = medium blue; _dR = deep red; and _fR = far red.

However, the W_lB_dR and W_lB_dR_fR treatments, both of which include the low-blue wavelength, resulted in the lowest average plantlet conversion (824 and 327, respectively) and FM (13.2 and 10.4 g, respectively) (Table 3). The blue light also exerted effects on the process, and the low-blue treatments (W_lB_dR and W_lB_dR_fR) produced lower numbers of converted plantlets. These findings are in agreement with the results obtained by Latkowska et al. (2000) with Norway spruce somatic embryos, who found that blue light inhibited 50% of the conversion of somatic embryos. In contrast, the combination of the blue, deep-red, and far-red wavelengths yielded enhanced leaf and root expansion, higher leaf numbers, and greater chlorophyll contents in *Oncidium* plantlets (Chung et al. 2010). Combination with LEDs, the RITA temporary immersion system was used in this study to facilitate the conversion of somatic embryos with the aim of obtaining a higher number of plantlets in a shorter time, as was previously shown with *Coffea*

arabica (Etienne-Barry et al. 1999), *Musa* spp. (Kosky et al. 2002), *Quercus robur* (Mallón et al. 2012), and *Bactris gasipaes* Kunth (Heringer et al. 2014).

Plantlets of 15-20 mm (Figure 2c) were grown in semi-solid culture medium to a size of 110-130 mm (Figure 2d) and then acclimatized (Figs. 2e-2f). All the acclimatized plantlets survived.

Taken together, the results suggest that LEDs can be potentially advantageous substitutes for fluorescent lamps in sugarcane somatic embryogenesis protocols. In addition, the use of a temporary immersion system in the conversion phase of sugarcane somatic embryos can be combined with a semi-solid system to increase the number of plantlets obtained at the end of the process.

3.2.4.2 Proteomic analysis of maturation callus subjected to different combinations of red and blue wavelengths

The proteomics analysis of samples collected during the maturation of embryogenic callus identified 1,171 proteins common to the control and W_mB_dR_fR treatments (Tables 5 and S1) with an average of 11 peptides per protein. No unique proteins were identified. Among the identified proteins, 1094 were considered unchanged between the treatments, whereas 39 and 38 were considered up-regulated and down-regulated in the W_mB_dR_fR treatment, respectively.

Table 5. Up and down regulated proteins identified in the embryogenic sugarcane callus submitted to W_mB_dR_fR (LED lamps mixture of W= White; _mB= Medium Blue; _dR= Deep Red; _fR= Far Red) relative to fluorescent lamp (control) treatment on day 28 of maturation treatment. Proteins with differential abundance were considered up-regulated when the log₂ of the fold change was greater than 1.2 and down-regulated when the log₂ of the fold change was less than -1.2.

Accession	Description	Peptide count	Confidence score	Log ₂ of fold change	Total Ion Counts - Control	Total Ion Counts – W _m B _d R _f R	Subcellular Localization	Biological Function
UP								
SCAGLR1064E01	protein usf transcription factor	10	107.3236	1.4646	27730.48	76530.99	M	transferase activity nucleotide binding
SCAGLR2011E07	btf3 peptidyl-prolyl cis-trans isomerase	8	91.7917	1.2398	39823.08	94047.87	-	
SCCCAD1003D12	cyp40-like heat shock cognate 70 kda protein 4-like isoform 1	7	60.3982	2.2264	816.0797	3819.052	Cy	post-embryonic development
SCCCCL3120G07	adenylosuccinate lyase	37	411.4297	1.3915	27588.87	72377.92	-	nucleotide binding
SCCCCL4007F09	pyruvate decarboxylase	13	80.6426	1.2014	5834.581	13417.36		catalytic activity carbohydrate metabolic process
SCCCCL4011D12	clathrin heavy chain 1 40s ribosomal protein sa	28	265.0548	2.2472	23611.29	112100.9	C	structural molecule activity
SCCCLR1001D03	stem-specific protein expressed	5	44.4072	4.0186	2355.977	38184.59	G	structural molecule activity
SCCCLR1024E09		15	138.5072	1.4966	7411.807	20914.36	R	
		9	74.9381	2.1784	3662.391	16577.65	C	-

Table 5 cont.

Accession	Description	Peptide count	Confidence score	Log ₂ of fold change	Total Ion Counts - Control	Total Ion Counts – W _m B _d R _f R	Subcellular Localization	Biological Function
SCCCLR1048F06	phospholipid transfer protein 1 nadp-specific isocitrate	8	72.7343	3.0619	5929.854	49518.56	-	lipid binding
SCCCLR1C04G09	dehydrogenase eukaryotic initiation factor 4a	26	214.2853	1.3768	27392.7	71136.08	-	nucleotide binding
SCCCLR1C07G11	transposon protein 60s ribosomal protein l23	40	415.7629	1.8661	20646.86	75269.03	R	hydrolase activity
SCCCLR2003E04	40s ribosomal protein s15	6	34.5736	2.4177	812.1053	4339.179	M	-
SCCCLR2004E03	annexin p33 hypothetical protein SORBIDRAFT_05g0	7	52.4258	1.4124	18066.48	48088.97	M	structural molecule activity
SCCCLR2C02A08	23700	7	51.6361	1.7813	2236.735	7688.291	R	structural molecule activity
SCCCLR2C03F11	glyoxylate reductase bifunctional aspartokinase homoserine dehydrogenase	15	115.1521	3.3018	3198.752	31544.3	-	lipid binding
SCCCRT1004D11	hypothetical protein SORBIDRAFT_02g0	2	21.304	1.3414	13266.56	33616.01	S	hydrolase activity
SCCCST1C06G09	SCCCST2003F12	4	31.1426	1.2254	6526.657	15260.92	-	nucleotide binding
SCEQRT2095C10	30240	7	45.5937	1.5953	6142.363	18559.16	M	kinase activity
		1	5.7647	2.7580	6679.271	45183.47	M	-

Table 5 cont.

Accession	Description	Peptide count	Confidence score	Log ₂ of fold change	Total Ion Counts - Control	Total Ion Counts – W _m B _d R _f R	Subcellular Localization	Biological Function
SCEZRZ1012F05	methylenetetrahydrofolate expressed	13	77.8655	1.2503	21144.36	50299.38	-	catalytic activity
SCEZRZ1015F10	qltg3-1	5	57.6076	2.2338	44010.67	207020.2	S	-
SCJFRT1008G05	lichenase-2 precursor	3	20.5209	2.2895	662.621	3239.356	S	hydrolase activity
SCJFRZ2010B03	histone h1	9	78.0088	1.2717	2549.279	6155.079	-	nucleotide binding
SCJFRZ2026E06	pura1_sorbi	8	48.51	1.5991	14542.11	44055.86	P	nucleotide binding
SCMCRT2103A12	lipid transfer protein	4	28.8562	1.4648	56645.32	156356.6	S	lipid binding
SCMCST1058E10	40s ribosomal protein s15a	12	103.4207	1.5585	64287.03	189355.2	R	structural molecule activity
SCQGAD1066A05	cytosolic factor-like protein	4	22.188	1.2052	2584.649	5959.567	M	-
SCQGLR1086B07	selenium binding protein	12	77.5916	1.5375	91.87424	266.7075	M	protein binding
SCQSAM1032A01	macrophage migration inhibitory factor	5	49.142	1.3214	14730.43	36812.04	Pe	biosynthetic process
SCQLSR1040E09	6-phosphogluconate dehydrogenase2	25	182.9948	1.2357	34833.79	82030.92	S	response to stress
SCQSST1036H09	probable methyltransferase							
SCQSST1036H09	pmt19-like membrane-associated	4	36.5639	4.5648	3717.306	87975.19	ER	transferase activity
SCQSST1039D10	salt-inducible	2	10.867	1.7900	1545.878	5345.691	M	catalytic activity

Table 5 cont.

Accession	Description	Peptide count	Confidence score	Log ₂ of fold change	Total Ion Counts - Control	Total Ion Counts – W _m B _d R _f R	Subcellular Localization	Biological Function
SCRURT2012C09	zeamatin-like protein	2	13.4343	1.9709	216.8431	850.0301	S	response to stress carbohydrate metabolic process
SCSBAD1085A06	xylose isomerase nadp-dependent oxidoreductase p2	11	88.3728	1.8307	4074.014	14491.83	RE	catalytic activity embryo development
SCFSB1106D06	sumo-activating enzyme subunit 2-like hypothetical protein SORBIDRAFT_01g02	6	37.3217	1.2761	9026.491	21861.1	-	
SCSGHR1071C01		17	114.5367	3.8446	69821.45	1003044	S	
SCUTLR1058D06	8650 aspartic proteinase nepenthesin-1 precursor	3	18.2568	1.3376	4143.553	10471.87	Cy	cellular process
SCVPLR2012E01		4	36.6414	2.2275	2396.59	11223.61	S	hydrolase activity
DOWN								
SCACAM1072H07	gcn5-related n-expressed uncharacterized protein	1	5.3669	-2.0213	2847.165	701.3743	-	transferase activity
SCACRZ3110B01	LOC100279462 ubiquitin-conjugating enzyme e2-17 kda hypothetical protein SORBIDRAFT_03g03	6	36.5361	-2.2511	1598.423	335.7789	C	protein binding
SCBFRZ2048H03		2	13.6117	-1.5613	3411.144	1155.891	-	catalytic activity
SCBFSB1049D06	5360	3	17.4523	-1.4198	1705.965	637.6366	M	-

Table 5 cont.

Accession	Description	Peptide count	Confidence score	Log ₂ of fold change	Total Ion Counts - Control	Total Ion Counts – W _m B _d R _f R	Subcellular Localization	Biological Function
SCBGFL4055E08	wall-associated receptor kinase-like 17-like	2	12.0654	-1.6016	4237.022	1396.187	-	kinase activity
SCBGLR1114E02	vacuolar atp synthase subunit g	9	63.7146	-1.4562	8356.548	3045.494	M	hydrolase activity response to stress
SCCCCL3005C05.b	embryo-specific protein	8	69.7682	-1.8011	32089.04	9208.026	M	
SCCCCL6002E05	late embryogenesis abundant domain-containing protein	9	59.217	-1.3158	52365.35	21034.98	-	
SCCCLB1002A04	bet v i allergen cosa_orysj ame: full=costars family	12	88.8076	-1.5429	4190.332	1438.132	-	response to stress
SCCCLR1001H11	protein cytosolic factor-like	4	22.7827	-1.2214	4609.492	1976.806	C	-
SCCCLR1072H04	protein brassinosteroid biosynthesis-like	4	25.8129	-1.7127	4992.841	1523.272	Me	-
SCCCLR1076E03	protein ras-related protein	6	33.1722	-1.3286	1289.024	513.2287	ER	protein binding
SCCCRT1001E12	rab11d hypothetical protein SORBIDRAFT_02g	5	31.9129	-1.3862	895.6048	342.6258	S	hydrolase activity
SCCCRT2001F09	024000	1	5.3202	-2.0113	1817.992	450.9546	M	-
SCCCRZ1001H04	histone h2b	14	171.045	-3.1517	4274.762	481.0156	Nu	protein binding

Table 5 cont.

Accession	Description	Peptide count	Confidence score	Log ₂ of fold change	Total Ion Counts - Control	Total Ion Counts – W _m B _d R _f R	Subcellular Localization	Biological Function
SCCCRZ1004C09	26s proteasome non- atpase regulatory subunit 13	19	132.8374	-1.2205	418274.3	179501.9	-	protein binding nucleotide binding
SCCCRZ2001A11	arginine serine-rich splicing factor	7	41.23	-1.3351	14393.63	5705.274	-	transferase
SCCCRZ2002G02	ornithine--oxo-acid aminotransferase	3	16.08	-2.8080	3509.999	501.2053	M	activity
SCCCSD1089G05	early light-induced protein	3	17.1112	-1.3294	27807.1	11065.04	C	-
SCEQLR1029H08	glycine-rich rna- binding protein 2	7	54.5536	-1.4769	1813.847	651.6203	-	nucleotide binding
SCEQLR1092H02	oleosin 18 kda flowering time control	6	49.4996	-1.4875	12452.06	4440.908	Me	lipid binding embryo
SCEQRT2098H07	protein fpa-like bromodomain protein	3	18.1384	-2.8488	1103.063	153.1215	Nu	development
SCEQSB1015B08	103	1	6.4026	-1.2308	20347.29	8669.525	-	hydrolase activity carbohydrate metabolic
SCJFRT1005D04	pyruvate decarboxylase	16	137.3942	-2.8746	6950.727	947.7397	S	process
SCJLRT1015H07	protein z peroxidase 24	2	10.4748	-1.8985	3355.217	899.9534	M	-
SCJLRT1019B02	precursor	3	24.9787	-2.0639	10879.8	2602.072	C	response to stress
SCQGRT1042A09	protein chloroplast expressed	3	27.2802	-2.5402	2014.193	346.2791	P	post-embryonic development
SCQSAD1057C09	receptor-like protein kinase	1	5.2122	-1.5301	513.2691	177.7167	M	kinase activity

Table 5 cont.

Accession	Description	Peptide count	Confidence score	Log ₂ of fold change	Total Ion Counts - Control	Total Ion Counts – W _m B _d R _f R	Subcellular Localization	Biological Function
SCQSAM2100C08	protein mago nashi ran gtpase activating protein	5	32.6694	-1.7367	4855.788	1456.986	Nu	embryo development
SCRFAM1026D04	isopentenyl pyrophosphate	2	11.0267	-6.9627	868.9878	6.966771	M	-
SCRFLR1012E03	oleosin 18 kda	5	29.108	-1.2835	1531.017	628.9572	R	hydrolase activity
SCSBSD1031A09	50s ribosomal protein I12-1	6	37.0171	-1.2870	1606.462	658.322	-	lipid binding structural molecule activity
SCSBSD1058H12	riboflavin biosynthesis protein	1	5.4853	-2.9675	845.285	108.0704	R	-
SCSFST3078D11	ribd uncharacterized protein	2	10.9791	-2.5001	234.6181	41.47331	M	hydrolase activity
SCSGRT2061F06	LOC100277064 pyruvate kinase isozyme	1	6.1995	-1.3708	4177.092	1615.145	C	protein binding
SCVPCL6040C10	chloroplastic-like seed maturation protein pm41	5	28.1418	-3.5928	3044.87	252.3652	C	post-embryonic development
SCVPLR2012E08	glutamine synthetase	4	25.1237	-1.9054	13822.06	3689.576	-	- nucleotide binding
SCVPRT2075G12		10	108.3859	-3.4824	723.4603	64.73046	Cy	

^a Confidence scores were calculated by Progenesis QI for proteomics.

^b C: chloroplast; Cy: cytosol; G: golgi; M: mitochondria; Me: membrane; Nu: nucleus; P: plastid; Pe: peroxisome; R: ribosome; RE: endoplasmic reticulum; S: secretory pathway.

Our analysis of the biological function of the proteins that were up- and down-regulated in the $W_mB_dR_fR$ treatment revealed that the up-regulated proteins showed a predominance of nucleotide binding (6) and structural molecular activity (5) functions (Figure 3 and Table 5). In contrast, the down-regulated proteins showed a predominance of protein binding (5) and hydrolase activity (5) functions (Figure 3 and Table 5).

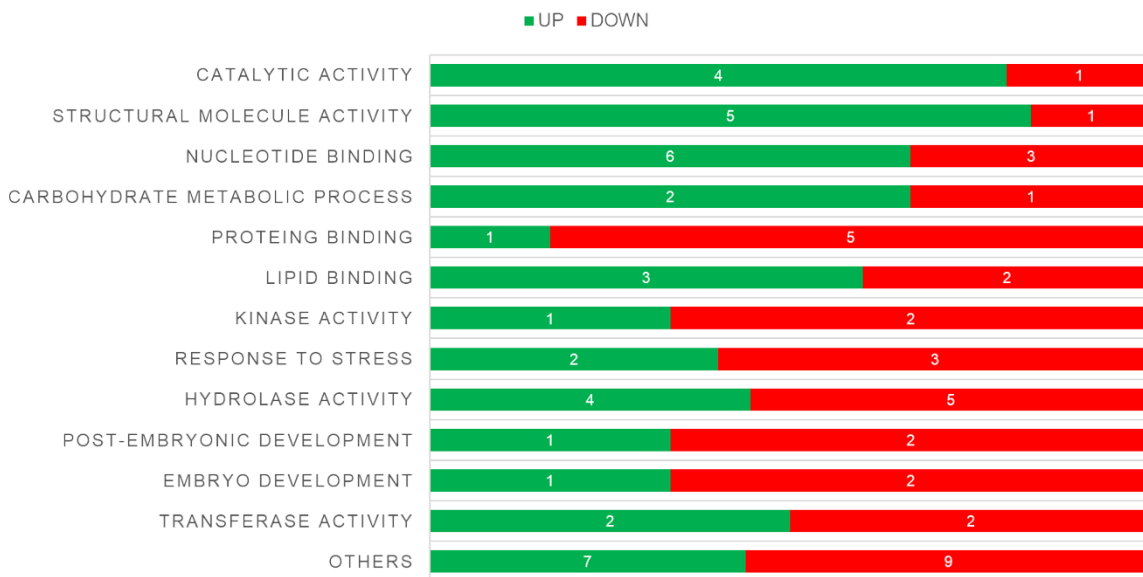


Figure 3. Biological function classification graphic showing the up- and down-regulated sugarcane proteins in the $W_mB_dR_fR$ compared with the fluorescent light (control) treatment. Colors: green = up-regulated proteins; red = down-regulated proteins; blue = unchanged proteins. The $W_mB_dR_fR$ treatment consisted of a mixture of LED lamps of W = white; $_mB$ = medium blue; $_dR$ = deep red; $_fR$ = far red.

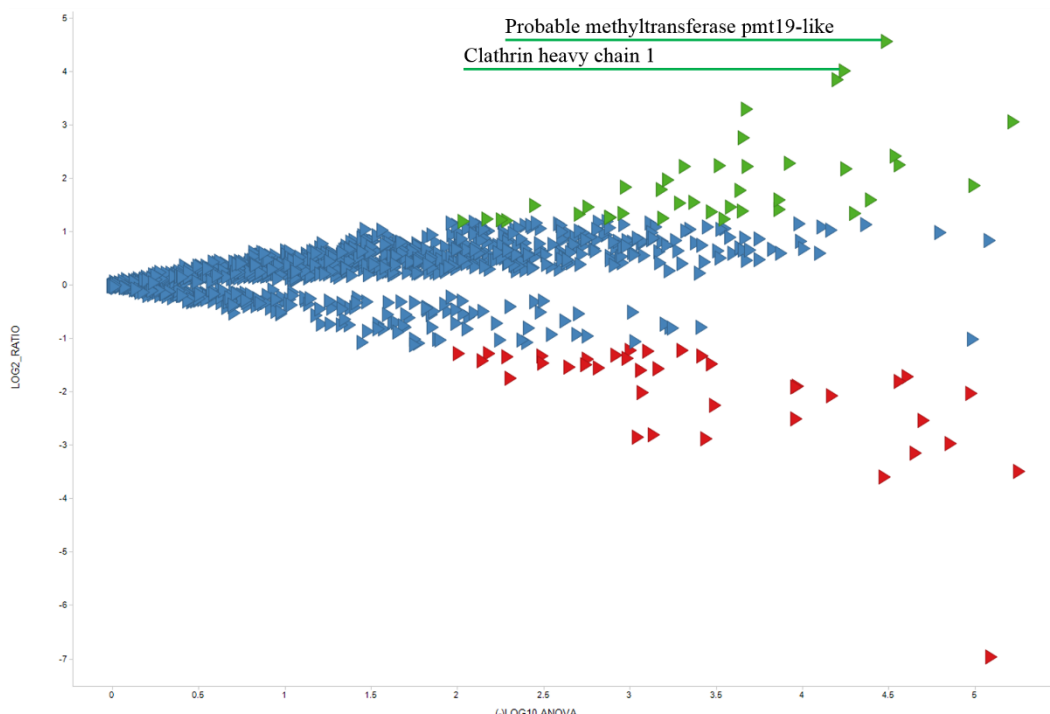


Figure 4. Volcano plot graphic showing the up- and down-regulated sugarcane proteins in the $W_mB_dR_fR$ compared with the fluorescent light (control) treatment. Colors: green = up-regulated proteins; red = down-regulated proteins; blue = unchanged proteins. The $W_mB_dR_fR$ treatment consisted of a mixture of LED lamps of W = white; mB = medium blue; dR = deep red; and fR = far red.

The callus cultured in the $W_mB_dR_fR$ treatment, which promoted the highest number of somatic embryos, showed 39 up-regulated proteins (Figure 4) relative to those matured under the control treatment (fluorescent light). The highest max-fold change was presented by the probable pmt19-like methyltransferase (PMT19 MET; SCQSST1036H09), which was 23-fold more abundant (Table 5). The methyltransferase (MET) family catalyzes the addition of a methyl group to the cytosine nucleotide in DNA at the CpG, CpHpG and CpHpH sites (Mahdavi-Darvari et al. 2015), and this methyl group can be transferred to the other strand during DNA replication (Saze et al. 2012), mediating global DNA methylation. In plant cell tissue culture, the differentiation and dedifferentiation processes are followed by methylation and demethylation events in tissue-specific genomic DNA (Smulders and de Klerk 2010). This process has also been identified in epigenetic mechanisms that regulate the induction of somatic embryogenesis (Santos and Fevereiro 2002). Our study showed that the high abundance of MET family proteins culminated in a greater development of somatic embryos. Furthermore, progressive DNA methylation is closely related to the presence of 2,4-

dichlorophenoxyacetic acid (2,4-D), a methylating agent, and this process occurs concomitantly with somatic embryo development (Fraga et al. 2012). 2,4-D acts by promoting cell expansion and divisions, which normally occur in young tissues of the explants as the procambial cells (Raghavan 2004). Briefly, during exposure to 2,4-D, the explants initiate cell divisions that will give rise to callus formation. After removal of 2,4-D by transferring the callus to somatic embryo-inducing medium containing or not containing maturation agents, the callus will form bipolar structures (somatic embryos) that can be converted into a whole plant. (Silveira et al. 2013; Tautorus et al. 1991)

In this context, clathrin heavy chain 1 (CHC1; SCCCL4014A03), one of the up-regulated proteins, was 16-fold more abundant in the plantlets subjected to the W_mB_dR_fR treatment (Table 5). This protein is required for the correct polar distribution of PIN auxin transporters (Kitakura et al. 2011). PIN auxin transporters are responsible for the establishment of auxin gradients, which determine the cell polarity in the pro-embryo and define the main axis of early embryogenesis (Su et al. 2013). Therefore, in the present study, the W_mB_dR_fR treatment promoted an increased expression of CHC1 protein, which assists in the correct distribution of the PIN transporters. This treatment might have influenced the formation of the auxin gradients and polarity of the cells, resulting in the differentiation of a higher number of somatic embryos

The DNA global methylation pattern, which is affected by MET, can either activate or inhibit the expression of certain genes (Jones 2012), which, as a consequence, will affect the pool of proteins. In our study, we observed many up-regulated proteins that are directly related to protein synthesis, including proteins that contribute to the structural integrity of the ribosome, 60S ribosomal protein I23 (SCCCLR2004E03) (Table 5), 40S ribosomal protein SA (SCCCLR1001D03) (Table 5), 40S ribosomal protein S15A (SCMCST1058E10) (Table 4), and 40S ribosomal protein s15 (SCCCLR2C02A08) (Table 4).

Another related protein was eukaryotic initiation factor 4a (SCCCLR1C07G11) (Table 4), an ATP-dependent RNA helicase that is involved in the cap recognition required for ribosome binding to mRNA (Metz et al. 1992). In addition, we identified a protein of the chaperone family, heat shock cognate 70-kDa protein 4 isoform-like 1 (SCCCCL3120G07) (Table 5), which stabilizes preexisting proteins against aggregation and mediates the folding of newly

translated polypeptides (Lin et al. 2001). The high abundance of this protein indicates that this machinery is highly active, which is characteristic of cells in the full differentiation stage and, in this case, of cells that will form somatic embryos.

Furthermore, plant cell tissue culture and morphogenetic responses are often motivated by stress (Smulders and de Klerk 2010). Our work also identified up-regulated proteins related to stress, such as NADP-specific isocitrate dehydrogenase (SCCCLR1C04G09) (Table 5), which may be involved in the response to oxidative stress (Leterrier et al. 2012). In this context, the stress caused by low gas exchange might have led to a high abundance of pyruvate decarboxylase (SCCCCL4011D12) (Table 5), which is involved in ethanolic fermentation during anoxia (Kürsteiner et al. 2003).

Callus matured in the W_mB_dR_fR treatment showed 38 down-regulated proteins (Figure 3) compared with those subjected to the control treatment. The most strongly down-regulated protein was GTPase activating protein (SCRFAM1026D04) (Table 5), which was 124-fold more abundant in the control callus. This protein is involved in nucleocytoplasmic transport, chromatin condensation and the control of the cell cycle (Matunis et al. 1996). Chromatin condensation most often leads to gene silencing and therefore lower protein abundance (Bannister and Kouzarides 2011). This protein, which is down-regulated in the W_mB_dR_fR treatment, might have resulted in chromatin decondensation and the translation of proteins that play important roles in somatic embryo formation, such as those that were discussed in the above paragraphs. In this context, chromatin condensation might prevent the translation of proteins that are important for somatic embryo formation because the control treatment showed the lowest number of somatic embryos.

In addition, the control treatment showed a high abundance of proteins related to the degradation process, such as ubiquitin-conjugating enzyme e2-17-kDa (SCBFRZ2048H03) (Table 5) and 26S proteasome non-ATPase regulatory subunit 13 (SCCCRZ1004C09) (Table 5). Thus, proteins translated by acetylated DNA regions and that are important for somatic embryo formation might be degraded through this process.

The peroxidase 24 precursor (SCJLRT1019B02) (Table 5) might be closely related to the high levels of pigments visible on the surface of the control treatment (Figure 1b) because this protein may play a role in the degradation of excess

antioxidant pigments (Zhang et al. 2005) that might be toxic to the cells. This protein also has the function of removing toxic oxidative compounds. For example, anthocyanin pigments can help protect cells from oxidative DNA damage caused mainly by light (Winkel-Shirley 2002). However, excessive production of anthocyanin might also be harmful to cells, which might explain the high abundance of peroxidase and the concomitant low level of somatic embryo formation.

The control treatment showed the highest abundance of embryo-related proteins, including late embryogenesis-abundant domain-containing protein (LEA; SCCCCL6002E05) (Table 5), embryo-specific protein (SCCCCL3005C05.b) (Table 4), pyruvate kinase isozyme chloroplastic-like (SCVPCL6040C10) (Table 5) and the protein mago nashi (SCQSAM2100C08) (Table 5). Although these proteins are down-regulated in the $W_mB_dR_fR$ treatment, this treatment formed more somatic embryos compared with the control. Thus, we cannot rule out the importance of these proteins in this morphogenetic pathway, but the up-regulation of the MET family and CHC1 protein might exert greater importance in increasing the number of somatic embryos formed. Although the testing of LEDs for plant growth began in the late 1980s and early 1990s (Bula et al. 1991; Morrow et al. 1989), most of the work on plant cell tissue culture still involve the use of fluorescent lamps. Thus, the protein abundance in callus exposed to fluorescent lamps is more frequently reported in the literature. However, in our work, embryos subjected to combinations of red and blue wavelengths presented a differential profile of up-regulated proteins, and this information, coupled with the number of somatic embryos formed, demonstrates the importance of these differential abundances.

3.2.5 CONCLUSION

The maturation of embryogenic callus differed in the presence of different light wavelengths, and medium blue light was found to be essential for somatic embryo maturation in sugarcane. Additionally, the W_mB , W_mB_dR and $W_mB_dR_fR$ treatments induced the greatest numbers of somatic embryos in the maturation

phase. The analysis of somatic embryo conversion revealed that the $W_mB_dR_fR$ treatment coupled with the RITA temporary immersion system exhibited the best performance compared with the other wavelength combinations, with 3,906 plantlets after 28 days of culture and 18,964 plantlets/RITA at the end of the 56-day conversion treatment. Thus, the conversion of somatic embryos into plantlets appears to require a combination of medium-blue, deep-red and far-red light because higher somatic embryo conversion into plantlets was obtained with the $W_mB_dR_fR$ treatment.

The $W_mB_dR_fR$ treatment up-regulated proteins related to differentiation and dedifferentiation processes, such as MET and CHC1, and these proteins might be related to the fact that a higher number of somatic embryos were obtained with this treatment. Accordingly, the substitution of LED lamps for fluorescent lamps might result in improved maturation protocols for sugarcane embryogenic callus. In addition, the MET and CHC1 proteins are candidate protein markers for sugarcane somatic embryogenesis and could be used in transgenic tissue regeneration processes to improve modern sugarcane breeding programs.

REFERENCES

- Agrawal GK et al. (2012) Translational plant proteomics: a perspective Journal of Proteomics 75:4588-4601 doi:10.1016/j.jprot.2012.03.055
- Ahsan N, Lee S-H, Lee D-G, Lee H, Lee SW, Bahk JD, Lee B-H (2007) Physiological and protein profiles alternation of germinating rice seedlings exposed to acute cadmium toxicity C R Biol 330:735-746
- Alamillo J et al. (1994) Molecular analysis of desiccation tolerance in barley embryos and in the resurrection plant *Craterostigma plantagineum* Agronomie 14:161-167
- Alvard D, Cote F, Teisson C (1993) Comparison of methods of liquid medium culture for banana micropropagation Plant Cell Tiss Org Cult 32:55-60
- Arencibia AD, Carmona ER, Tellez P, Chan MT, Yu SM, Trujillo LE, Oramas P (1998) An efficient protocol for sugarcane (*Saccharum* spp. L.) transformation mediated by *Agrobacterium tumefaciens* Transgenic Res 7:213-222 doi:10.1023/a:1008845114531
- Arruda P (2011) Perspective of the sugarcane industry in Brazil Tropical Plant Biology 4:3-8
- Arruda P (2012) Genetically modified sugarcane for bioenergy generation Curr Opin Biotechnol 23:315-322 doi:10.1016/j.copbio.2011.10.012

- Baba AI et al. (2008) Proteome analysis of secondary somatic embryogenesis in cassava (*Manihot esculenta*) Plant Sci 175:717-723
- Bach A, Krol A (2001) Effect of light quality on somatic embryogenesis in *Hyacinthus orientalis* L. Delft's Blue Biol Bull Poznań 1:103-107
- Balbuena TS, Silveira V, Junqueira M, Dias LLC, Santa-Catarina C, Shevchenko A, Floh EIS (2009) Changes in the 2-DE protein profile during zygotic embryogenesis in the Brazilian Pine (*Araucaria angustifolia*) Journal of Proteomics 72:337-352 doi:10.1016/j.jprot.2009.01.011
- Bannister AJ, Kouzarides T (2011) Regulation of chromatin by histone modifications Cell Res 21:381-395 doi:10.1038/cr.2011.22
- Barneche F, Malapeira J, Mas P (2014) The impact of chromatin dynamics on plant light responses and circadian clock function J Exp Bot 65:2895–2913
- Bartels D, Hanke C, Schneider K, Michel D, Salamini F (1992) A desiccation-related Elip-like gene from the resurrection plant *Craterostigma plantagineum* is regulated by light and ABA The EMBO journal 11:2771
- Basset GJ, Quinlivan EP, Gregory JF, Hanson AD (2005) Folate synthesis and metabolism in plants and prospects for biofortification Crop Sci 45:449-453
- Batistič O, Kudla J (2009) Plant calcineurin B-like proteins and their interacting protein kinases Biochimica et Biophysica Acta (BBA)-Molecular Cell Research 1793:985-992
- Bula R, Morrow R, Tibbitts T, Barta D, Ignatius R, Martin T (1991) Light-emitting diodes as a radiation source for plants HortScience 26:203-205
- Burrieza HP, Lopez-Fernandez MP, Chiquieri TB, Silveira V, Maldonado S (2012) Accumulation pattern of dehydrins during sugarcane (var. SP80.3280) somatic embryogenesis Plant Cell Rep 31:2139-2149 doi:10.1007/s00299-012-1323-z
- Businge E, Bygdell J, Wingsle G, Moritz T, Egertsdotter U (2013) The effect of carbohydrates and osmoticum on storage reserve accumulation and

germination of Norway spruce somatic embryos Physiol Plant 149:273-285
doi:10.1111/ppl.12039

Butterfield M, D'Hont A, Berding N The sugarcane genome: a synthesis of current understanding, and lessons for breeding and biotechnology. In: Proceedings of African Sugarcane Technology Association, 2001. pp 1-5

Butterfield M, Thomas D Sucrose, yield and disease resistance characteristics of sugarcane varieties under test in the SASEX selection programme. In: Proceedings of African Sugarcane Technology Association, 1996. pp 103-105

Chakraborty AB, Berger SJ, Gebler JC (2007) Use of an integrated MS-multiplexed MS/MS data acquisition strategy for high-coverage peptide mapping studies Rapid communications in mass spectrometry 21:730-744

Chen EI, Hewel J, Felding-Habermann B, Yates JR (2006) Large scale protein profiling by combination of protein fractionation and multidimensional protein identification technology (MudPIT) Molecular & Cellular Proteomics 5:53-56

Cho J-N et al. (2012) Control of seed germination by light-induced histone arginine demethylation activity Dev Cell 22:736-748

Chung J-P, Huang C-Y, Dai T-E (2010) Spectral effects on embryogenesis and plantlet growth of Oncidium 'Gower Ramsey' Sci Hortic 124:511-516

Cohen JD, Slovin JP, Hendrickson AM (2003) Two genetically discrete pathways convert tryptophan to auxin: more redundancy in auxin biosynthesis Trends Plant Sci 8:197-199

CONAB (2016) 2º Levantamento cana-de-açucar safra 2016/2017 - ago/2016. Companhia Nacional de Abastecimento (CONAB). <http://www.conab.gov.br/>. Accessed 02/09/2016

Conesa A, Gotz S, Garcia-Gomez JM, Terol J, Talon M, Robles M (2005) Blast2GO: a universal tool for annotation, visualization and analysis in functional genomics research Bioinformatics 21:3674-3676
doi:10.1093/bioinformatics/bti610

- de Carvalho Silva R, Carmo LST, Luis ZG, Silva LP, Scherwinski-Pereira JE, Mehta A (2014) Proteomic identification of differentially expressed proteins during the acquisition of somatic embryogenesis in oil palm (*Elaeis guineensis* Jacq.) Journal of Proteomics 104:112-127
- de Souza AP, Grandis A, Leite DC, Buckeridge MS (2014) Sugarcane as a bioenergy source: history, performance, and perspectives for second-generation bioethanol BioEnergy Research 7:24-35
- Dowler S, Deak M, Kular G, Downes C (2000) Identification of pleckstrin-homology-domain-containing proteins with novel phosphoinositide-binding specificities Biochem J 351:19-31
- Dubois T, Guedira M, Dubois J, Vasseur J (1990) Direct somatic embryogenesis in roots of *Cichorium*: is callose an early marker? Ann Bot 65:539-545
- Dubos C, Stracke R, Grotewold E, Weisshaar B, Martin C, Lepiniec L (2010) MYB transcription factors in *Arabidopsis* Trends Plant Sci 15:573-581
- Etienne-Barry D, Bertrand B, Vasquez N, Etienne H (1999) Direct sowing of *Coffea arabica* somatic embryos mass-produced in a bioreactor and regeneration of plants Plant Cell Rep 19:111-117
- Etienne H, Berthouly M (2002) Temporary immersion systems in plant micropropagation Plant Cell Tiss Org Cult 69:215-231
- FAO (2014) FAOSTAT - Crop production. Food and Agriculture Organization of the United Nations - Statistics Division (FAOSTAT). http://faostat3.fao.org/browse/Q/*/E. Accessed 12-03-2014 2014
- Fehér A (2014) Somatic embryogenesis–stress-induced remodeling of plant cell fate Biochimica et Biophysica Acta (BBA)-Gene Regulatory Mechanisms
- Fraga HP et al. (2012) 5-Azacytidine combined with 2,4-D improves somatic embryogenesis of *Acca sellowiana* (O. Berg) Burret by means of changes in global DNA methylation levels Plant Cell Rep 31:2165-2176 doi:10.1007/s00299-012-1327-8

- Geromanos SJ et al. (2009) The detection, correlation, and comparison of peptide precursor and product ions from data independent LC-MS with data dependant LC-MS/MS Proteomics 9:1683-1695
- Giles K, Williams JP, Campuzano I (2011) Enhancements in travelling wave ion mobility resolution Rapid Communications in Mass Spectrometry 25:1559-1566
- Gillaspy GE (2010) Signaling and the polyphosphoinositide phosphatases from plants. In: Lipid signaling in plants. Springer, pp 117-130
- Griffin WM, Scandiffio MIG (2009) Can Brazil replace 5% of the 2025 gasoline world demand with ethanol? Energy 34:655-661
- Guerra M, Torres A, Teixeira J, Torres A, Caldas L, Buso J (1999) Embriogênese somática e sementes sintéticas Cultura de tecidos e transformação genética de plantas
- Guo F-Q, Okamoto M, Crawford NM (2003) Identification of a plant nitric oxide synthase gene involved in hormonal signaling Science 302:100-103
- Gupta SD, Jatotu B (2013) Fundamentals and applications of light-emitting diodes (LEDs) in in vitro plant growth and morphogenesis Plant Biotechnology Reports:1-10
- Hanhineva K, Kokko H, Kärenlampi S (2005) Shoot regeneration from leaf explants of five strawberry (*Fragaria × ananassa*) cultivars in temporary immersion bioreactor system In Vitro Cellular & Developmental Biology-Plant 41:826-831
- Hattori J, Boutilier K, Campagne ML, Miki B (1998) A conserved BURP domain defines a novel group of plant proteins with unusual primary structures Molecular and General Genetics MGG 259:424-428
- He W, Parker R (2000) Functions of Lsm proteins in mRNA degradation and splicing Curr Opin Cell Biol 12:346-350

Heringer AS et al. (2015) Label-free quantitative proteomics of embryogenic and non-embryogenic callus during sugarcane somatic embryogenesis PLoS One 10:e0127803 doi:10.1371/journal.pone.0127803

Heringer AS et al. (2014) Improved high-efficiency protocol for somatic embryogenesis in Peach Palm (*Bactris gasipaes* Kunth) using RITA® temporary immersion system Scientia Horticulturae 179:284-292

Heringer AS, Vale EM, Barroso T, Santa-Catarina C, Silveira V (2013) Polyethylene glycol effects in Somatic embryogenesis of papaya hybrid UENF/CALIMAN01 seeds Theoretical and Experimental Plant Physiology 25:116-124

Herrmann KM (1995) The shikimate pathway: early steps in the biosynthesis of aromatic compounds The Plant Cell 7:907

Heyneke E, Luschin-Ebengreuth N, Krajcer I, Wolking V, Müller M, Zechmann B (2013) Dynamic compartment specific changes in glutathione and ascorbate levels in *Arabidopsis* plants exposed to different light intensities BMC Plant Biol 13:104

Hong Z, Delauney AJ, Verma DPS (2001) A cell plate-specific callose synthase and its interaction with phragmoplastin The Plant Cell Online 13:755-768

Hoshino T, Cuello JL (2006) Environmental design considerations for somatic embryogenesis. In: Mujib A, Samaj J (eds) Somatic embryogenesis. Springer, Berlin, pp 25-34

Huang X, Ouyang X, Deng XW (2014) Beyond repression of photomorphogenesis: role switching of COP/DET/FUS in light signaling Curr Opin Plant Biol 21:96-103 doi:10.1016/j.pbi.2014.07.003

Hung CD et al. (2016) LED light for in vitro and ex vitro efficient growth of economically important highbush blueberry (*Vaccinium corymbosum* L.) Acta Physiol Plant 38:1-9

- Ikeda-Iwai M, Umehara M, Satoh S, Kamada H (2003) Stress-induced somatic embryogenesis in vegetative tissues of *Arabidopsis thaliana* The Plant Journal 34:107-114
- Jacobs AK, Lipka V, Burton RA, Panstruga R, Strizhov N, Schulze-Lefert P, Fincher GB (2003) An *Arabidopsis* callose synthase, GSL5, is required for wound and papillary callose formation The Plant Cell Online 15:2503-2513
- Jimenez VM (2005) Involvement of plant hormones and plant growth regulators on *in vitro* somatic embryogenesis Plant Growth Regulation 47:91-110 doi:10.1007/s10725-005-3478-x
- Jones PA (2012) Functions of DNA methylation: islands, start sites, gene bodies and beyond Nat Rev Genet 13:484-492 doi:10.1038/nrg3230
- Joyce P, Hermann S, O'Connell A, Dinh Q, Shumbe L, Lakshmanan P (2014) Field performance of transgenic sugarcane produced using Agrobacterium and biolistics methods Plant Biotechnol J 12:411-424
- Kessell R, Carr A (1972) The effect of dissolved oxygen concentration on growth and differentiation of carrot (*Daucus carota*) tissue J Exp Bot 23:996-1007
- Kim YW, Moon HK (2014) Enhancement of somatic embryogenesis and plant regeneration in Japanese red pine (*Pinus densiflora*) Plant Biotechnol Rep 8:259-266
- Kitakura S, Vanneste S, Robert S, Lofke C, Teichmann T, Tanaka H, Friml J (2011) Clathrin mediates endocytosis and polar distribution of PIN auxin transporters in *Arabidopsis* Plant Cell 23:1920-1931 doi:10.1105/tpc.111.083030
- Klein M, Papenbrock J (2004) The multi-protein family of *Arabidopsis* sulphotransferases and their relatives in other plant species J Exp Bot 55:1809-1820
- Kobayashi K, Otegui MS, Krishnakumar S, Mindrinos M, Zambryski P (2007) INCREASED SIZE EXCLUSION LIMIT2 encodes a putative DE VH box RNA

helicase involved in plasmodesmata function during *Arabidopsis* embryogenesis The Plant Cell Online 19:1885-1897

Kosky RG et al. (2002) Somatic embryogenesis of the banana hybrid cultivar FHIA-18 (AAAB) in liquid medium and scaled-up in a bioreactor Plant Cell Tissue Organ Cult 68:21-26

Kotake T, Hojo S, Yamaguchi D, Aohara T, Konishi T, Tsumuraya Y (2007) Properties and physiological functions of UDP-sugar pyrophosphorylase in *Arabidopsis* Biosci, Biotechnol, Biochem 71:761-771

Krajňáková J, Häggman H, Gömöry D (2009) Effect of sucrose concentration, polyethylene glycol and activated charcoal on maturation and regeneration of *Abies cephalonica* somatic embryos Plant Cell, Tissue and Organ Culture (PCTOC) 96:251-262

Kubeš M, Drážná N, Konrádová H, Lipavská H (2014) Robust carbohydrate dynamics based on sucrose resynthesis in developing Norway spruce somatic embryos at variable sugar supply In Vitro Cellular & Developmental Biology-Plant 50:45-57

Kürsteiner O, Dupuis I, Kuhlemeier C (2003) The pyruvate decarboxylase1 gene of *Arabidopsis* is required during anoxia but not other environmental stresses Plant Physiol 132:968-978

Lakshmanan P, Geijskes RJ, Aitken KS, Grof CLP, Bonnett GD, Smith GR (2005) Sugarcane biotechnology: the challenges and opportunities In Vitro Cellular & Developmental Biology-Plant 41:345-363 doi:10.1079/ivp2005643

Lakshmanan P, Geijskes RJ, Wang L, Elliott A, Grof CPL, Berding N, Smith GR (2006) Developmental and hormonal regulation of direct shoot organogenesis and somatic embryogenesis in sugarcane (*Saccharum* spp. interspecific hybrids) leaf culture Plant Cell Rep 25:1007-1015 doi:10.1007/s00299-006-0154-1

Lalli PM et al. (2013) Baseline resolution of isomers by traveling wave ion mobility mass spectrometry: investigating the effects of polarizable drift gases and ionic charge distribution J Mass Spectrom 48:989-997 doi:10.1002/jms.3245

Lao J et al. (2015) Proteome profile of the endomembrane of developing coleoptiles from switchgrass (*Panicum virgatum*) Proteomics doi:10.1002/pmic.201400487

Latkowska M, Kvaalen H, Appelgren M (2000) Genotype dependent blue and red light inhibition of the proliferation of the embryogenic tissue of *Norway spruce* In Vitro Cell Dev Biol Plant 36:57-60

Leterrier M, Barroso J, Palma J, Corpas F (2012) Cytosolic NADP-isocitrate dehydrogenase in *Arabidopsis* leaves and roots Biol Plant 56:705-710

Li GZ, Vissers JP, Silva JC, Golick D, Gorenstein MV, Geromanos SJ (2009) Database searching and accounting of multiplexed precursor and product ion spectra from the data independent analysis of simple and complex peptide mixtures Proteomics 9:1696-1719

Li T, Fan H, Li Z, Wei J, Cai Y, Lin Y (2013) Effect of different light quality on DNA methylation variation for brown cotton (*Gossypium hirsutum*) Afr J Biotechnol 10:6220-6226

Lin BL, Wang JS, Liu HC, Chen RW, Meyer Y, Barakat A, Delseny M (2001) Genomic analysis of the Hsp70 superfamily in *Arabidopsis thaliana* Cell Stress Chaperones 6:201-208

Lin Y, Li J, Li B, He T, Chun Z (2011) Effects of light quality on growth and development of protocorm-like bodies of *Dendrobium officinale* in vitro Plant Cell, Tissue and Organ Culture (PCTOC) 105:329-335

Linder P, Owttrim GW (2009) Plant RNA helicases: linking aberrant and silencing RNA Trends Plant Sci 14:344-352

Lippert D et al. (2005) Proteome analysis of early somatic embryogenesis in *Picea glauca* Proteomics 5:461-473 doi:10.1002/pmic.200400986

- Litterer LA, Plaisance KL, Schnurr JA, Storey KK, Jung HJG, Gronwald JW, Somers DA (2006) Biosynthesis of UDP-glucuronic acid in developing soybean embryos: possible role of UDP-sugar pyrophosphorylase *Physiol Plant* 128:200-211
- Liu H, Liu B, Zhao C, Pepper M, Lin C (2011) The action mechanisms of plant cryptochromes *Trends Plant Sci* 16:684-691 doi:10.1016/j.tplants.2011.09.002
- Lu C-C, Currah L, Peffley EB (1989) Somatic embryogenesis and plant regeneration in diploid *Allium fistulosum* × *A. cepa* F1 hybrid onions *Plant Cell Rep* 7:696-700
- Luan S (2009) The CBL–CIPK network in plant calcium signaling *Trends Plant Sci* 14:37-42
- Luge T, Kube M, Freiwald A, Meierhofer D, Seemüller E, Sauer S (2014) Transcriptomics assisted proteomic analysis of *Nicotiana occidentalis* infected by *Candidatus Phytoplasma mali* strain AT *Proteomics* 14:1882-1889
- Mahdavi-Darvari F, Noor NM, Ismanizan I (2014) Epigenetic regulation and gene markers as signals of early somatic embryogenesis *Plant Cell Tiss Org Cult*:1-16
- Mahdavi-Darvari F, Noor NM, Ismanizan I (2015) Epigenetic regulation and gene markers as signals of early somatic embryogenesis *Plant Cell Tissue Organ Cult* 120:407-422
- Malik MR, Wang F, Dirpaul JM, Zhou N, Polowick PL, Ferrie AM, Krochko JE (2007) Transcript profiling and identification of molecular markers for early microspore embryogenesis in *Brassica napus* *Plant Physiol* 144:134-154
- Mallón R, Covelo P, Vieitez AM (2012) Improving secondary embryogenesis in *Quercus robur*: application of temporary immersion for mass propagation *Trees* 26:731-741
- Marsoni M, Bracale M, Espen L, Prinsi B, Negri AS, Vannini C (2008) Proteomic analysis of somatic embryogenesis in *Vitis vinifera* *Plant Cell Rep* 27:347-356 doi:10.1007/s00299-007-0438-0

- Martinelli L, Scienza A, Villa P, Deponti P, Gianazza E (1993) Enzyme markers for somatic embryogenesis in *Vitis* J Plant Physiol 141:476-481
- Martzivanou M, Hampp R (2003) Hyper-gravity effects on the *Arabidopsis* transcriptome Physiol Plant 118:221-231
- Massa GD, Kim H-H, Wheeler RM, Mitchell CA (2008) Plant productivity in response to LED lighting HortScience 43:1951-1956
- Matsumura T, Tabayashi N, Kamagata Y, Souma C, Saruyama H (2002) Wheat catalase expressed in transgenic rice can improve tolerance against low temperature stress Physiol Plant 116:317-327
- Matunis MJ, Coutavas E, Blobel G (1996) A novel ubiquitin-like modification modulates the partitioning of the Ran-GTPase-activating protein RanGAP1 between the cytosol and the nuclear pore complex J Cell Biol 135:1457-1470
- Mc Alister B, Finnie J, Watt M, Blakeway F (2005) Use of the temporary immersion bioreactor system (RITA®) for production of commercial Eucalyptus clones in Mondi Forests (SA). In: Liquid Culture Systems for in vitro Plant Propagation. Springer, pp 425-442
- Mengxi L, Zhigang X, Yang Y, Yijie F (2011) Effects of different spectral lights on *Oncidium* PLBs induction, proliferation, and plant regeneration Plant Cell Tissue Organ Cult 106:1-10
- Merkle SA, Montello PM, Xia X, Upchurch BL, Smith DR (2006) Light quality treatments enhance somatic seedling production in three southern pine species Tree Physiol 26:187-194
- Metz AM, Timmer RT, Browning KS (1992) Sequences for two cDNAs encoding *Arabidopsis thaliana* eukaryotic protein synthesis initiation factor 4A Gene 120:313-314
- Mhamdi A, Queval G, Chaouch S, Vanderauwera S, Van Breusegem F, Noctor G (2010) Catalase function in plants: a focus on *Arabidopsis* mutants as stress-mimic models J Exp Bot 61:4197-4220

Michler CH, Lineberger RD (1987) Effects of light on somatic embryo development and abscisic levels in carrot suspension cultures Plant Cell Tissue Organ Cult 11:189-207

Ming R et al. (1998) Detailed alignment of *Saccharum* and *Sorghum* chromosomes: comparative organization of closely related diploid and polyploid genomes Genetics 150:1663-1682

Moon H-K, Lee H, Paek K-Y, Park S-Y (2015) Osmotic stress and strong 2, 4-D shock stimulate somatic-to-embryogenic transition in *Kalopanax septemlobus* (Thunb.) Koidz Acta Physiologiae Plantarum 37:1-9

Mordhorst AP, Toonen MAJ, deVries SC (1997) Plant embryogenesis Crit Rev Plant Sci 16:535-576 doi:10.1080/713608156

Mordocco AM, Brumbley JA, Lakshmanan P (2009) Development of a temporary immersion system (RITA®) for mass production of sugarcane (*Saccharum* spp. interspecific hybrids) In Vitro Cellular & Developmental Biology-Plant 45:450-457

Morrow R, Bula R, Tibbitts T (1989) Light emitting diodes as a photosynthetic irradiance source for plants ASGSB Bull 3:60

Muneer S, Kim EJ, Park JS, Lee JH (2014) Influence of green, red and blue light emitting diodes on multiprotein complex proteins and photosynthetic activity under different light intensities in lettuce leaves (*Lactuca sativa* L.) Int J Mol Sci 15:4657-4670 doi:10.3390/ijms15034657

Murad AM, Souza GH, Garcia JS, Rech EL (2011) Detection and expression analysis of recombinant proteins in plant-derived complex mixtures using nanoUPLC-MSE Journal of separation science 34:2618-2630

Murashige T, Skoog F (1962) A revised medium for rapid growth and bio assays with tobacco tissue cultures Physiol Plant 15:473-497 doi:10.1111/j.1399-3054.1962.tb08052.x

Murch SJ, Liu C, Romero RM, Saxena PK (2004) In vitro culture and temporary immersion bioreactor production of *Crescentia cujete* Plant Cell Tiss Org Cult 78:63-68

Müssig C (2005) Brassinosteroid-Promoted Growth Plant Biol 7:110-117

Nhut DT et al. (2015) Light-emitting diodes and their potential in callus growth, plantlet development and saponin accumulation during somatic embryogenesis of *Panax vietnamensis* Ha et Grushv Biotechnology & Biotechnological Equipment 29:299-308

Nieves N, Segura-Nieto M, Blanco MA, Sanchez M, Gonzalez A, Gonzalez JL, Castillo R (2003) Biochemical characterization of embryogenic and non-embryogenic calluses of sugarcane In Vitro Cellular & Developmental Biology-Plant 39:343-345 doi:10.1079/ivp2002391

Otvos K et al. (2005) Nitric oxide is required for, and promotes auxin-mediated activation of, cell division and embryogenic cell formation but does not influence cell cycle progression in alfalfa cell cultures Plant J 43:849-860 doi:10.1111/j.1365-313X.2005.02494.x

Park S-Y, Yeung EC, Paek K-Y (2010) Endoreduplication in phalaenopsis is affected by light quality from light-emitting diodes during somatic embryogenesis Plant Biotechnol Rep 4:303-309

Patnaik D, Khurana P (2001) Germins and germin like proteins: an overview Indian J Exp Biol 39:191-200

Peterman TK, Ohol YM, McReynolds LJ, Luna EJ (2004) Patellin1, a novel Sec14-like protein, localizes to the cell plate and binds phosphoinositides Plant Physiol 136:3080-3094

Petrak J et al. (2008) Deja vu in proteomics. A hit parade of repeatedly identified differentially expressed proteins Proteomics 8:1744-1749

Poon S, Heath RL, Clarke AE (2012) A chimeric arabinogalactan protein promotes somatic embryogenesis in cotton cell culture Plant Physiol 160:684-695

- Prouse MB, Campbell MM (2012) The interaction between MYB proteins and their target DNA binding sites Biochimica et Biophysica Acta (BBA)-Gene Regulatory Mechanisms 1819:67-77
- Qi Y, Yamauchi Y, Ling J, Kawano N, Li D, Tanaka K (2005) The submergence-induced gene OsCTP in rice (*Oryza sativa L.*) is similar to Escherichia coli cation transport protein ChaC Plant Sci 168:15-22
- Ragauskas AJ et al. (2006) The path forward for biofuels and biomaterials Science 311:484-489
- Raghavan V (2004) Role of 2, 4-dichlorophenoxyacetic acid (2, 4-D) in somatic embryogenesis on cultured zygotic embryos of *Arabidopsis*: cell expansion, cell cycling, and morphogenesis during continuous exposure of embryos to 2, 4-D Am J Bot 91:1743-1756
- Ravanel S, Cherest H, Jabrin S, Grunwald D, Surdin-Kerjan Y, Douce R, Rébeillé F (2001) Tetrahydrofolate biosynthesis in plants: molecular and functional characterization of dihydrofolate synthetase and three isoforms of folylpolyglutamate synthetase in *Arabidopsis thaliana* Proceedings of the National Academy of Sciences 98:15360-15365
- Ravilious GE, Jez JM (2012) Nucleotide binding site communication in *Arabidopsis thaliana* adenosine 5'-phosphosulfate kinase J Biol Chem 287:30385-30394
- Reis RS, Vale EdM, Heringer AS, Santa-Catarina C, Silveira V (2016) Putrescine induces somatic embryo development and proteomic changes in embryogenic callus of sugarcane J Proteom 130:170-179 doi:10.1016/j.jprot.2015.09.029
- Rose A, Meier I (2004) Scaffolds, levers, rods and springs: diverse cellular functions of long coiled-coil proteins Cellular and Molecular Life Sciences CMLS 61:1996-2009
- Rose AB, Casselman AL, Last RL (1992) A phosphoribosylanthranilate transferase gene is defective in blue fluorescent *Arabidopsis thaliana* tryptophan mutants Plant Physiol 100:582-592

- Ruotolo BT, Giles K, Campuzano I, Sandercock AM, Bateman RH, Robinson CV (2005) Evidence for macromolecular protein rings in the absence of bulk water Science 310:1658-1661
- Santiago J, Henzler C, Hothorn M (2013) Molecular mechanism for plant steroid receptor activation by somatic embryogenesis co-receptor kinases Science 341:889-892
- Santos D, Fevereiro P (2002) Loss of DNA methylation affects somatic embryogenesis in *Medicago truncatula* Plant Cell Tissue Organ Cult 70:155-161
- Saze H, Tsugane K, Kanno T, Nishimura T (2012) DNA methylation in plants: relationship to small RNAs and histone modifications, and functions in transposon inactivation Plant Cell Physiol 53:766-784 doi:10.1093/pcp/pcs008
- Schluter H, Apweiler R, Holzhutter H, Jungblut PR (2009) Finding one's way in proteomics: a protein species nomenclature Chemistry Central Journal 3:11
- Sghaier-Hammami B, Jorrín-Novo JV, Gargouri-Bouzid R, Drira N (2010) Abscisic acid and sucrose increase the protein content in date palm somatic embryos, causing changes in 2-DE profile Phytochemistry 71:1223-1236
- Shikanai T, Müller-Moulé P, Munekage Y, Niyogi KK, Pilon M (2003) PAA1, a P-type ATPase of Arabidopsis, functions in copper transport in chloroplasts The Plant Cell Online 15:1333-1346
- Shimizu-Sato S, Huq E, Tepperman JM, Quail PH (2002) A light-switchable gene promoter system Nat Biotechnol 20:1041-1044 doi:10.1038/nbt734
- Shimizu T et al. (2008) Effects of a bile acid elicitor, cholic acid, on the biosynthesis of diterpenoid phytoalexins in suspension-cultured rice cells Phytochemistry 69:973-981
- Silva JC et al. (2005) Quantitative proteomic analysis by accurate mass retention time pairs Anal Chem 77:2187-2200

- Silva JC, Gorenstein MV, Li G-Z, Vissers JP, Geromanos SJ (2006) Absolute quantification of proteins by LCMSE a virtue of parallel MS acquisition Molecular & Cellular Proteomics 5:144-156
- Silveira V, Santa-Catarina C, Tun NN, Scherer GFE, Handro W, Guerra MP, Floh EIS (2006) Polyamine effects on the endogenous polyamine contents, nitric oxide release, growth and differentiation of embryogenic suspension cultures of *Araucaria angustifolia* (Bert.) O. Ktze Plant Sci 171:91-98 doi:10.1016/j.plantsci.2006.02.015
- Silveira V, Vita AM, Macedo AF, Dias MFR, Floh EIS, Santa-Catarina C (2013) Morphological and polyamine content changes in embryogenic and non-embryogenic callus of sugarcane Plant Cell Tiss Org Cult 114:351-364 doi:10.1007/s11240-013-0330-2
- Smeekens S, Ma J, Hanson J, Rolland F (2010) Sugar signals and molecular networks controlling plant growth Current opinion in plant biology 13:273-278
- Smulders MJM, de Klerk GJ (2010) Epigenetics in plant tissue culture Plant Growth Regul 63:137-146 doi:10.1007/s10725-010-9531-4
- Smulders MJM, Klerk GJ (2011) Epigenetics in plant tissue culture Plant Growth Regulation 63:137-146 doi:10.1007/s10725-010-9531-4
- Snyman SJ, Meyer GM, Koch AC, Banasiak M, Watt MP (2011) Applications of in vitro culture systems for commercial sugarcane production and improvement In Vitro Cellular & Developmental Biology-Plant 47:234-249 doi:10.1007/s11627-011-9354-7
- Steinmacher DA, Clement CR, Guerra MP (2007) Somatic embryogenesis from immature peach palm inflorescence explants: towards development of an efficient protocol Plant Cell Tiss Org Cult 89:15-22
- Steinmacher DA, Saare-Surminski K, Lieberei R (2012) Arabinogalactan proteins and the extracellular matrix surface network during peach palm somatic embryogenesis Physiol Plant 146:336-349

- Su YH, Su YX, Liu YG, Zhang XS (2013) Abscisic acid is required for somatic embryo initiation through mediating spatial auxin response in *Arabidopsis* Plant Growth Regul 69:167-176
- Sugiharto B et al. (2002) Identification and characterization of a gene encoding drought-inducible protein localizing in the bundle sheath cell of sugarcane Plant and cell physiology 43:350-354
- Tatra GS, Miranda J, Chinnappa CC, Reid DM (2000) Effect of light quality and 5-azacytidine on genomic methylation and stem elongation in two ecotypes of *Stellaria longipes* Physiol Plant 109:313-321
- Tatsis EC, O'Connor SE (2016) New developments in engineering plant metabolic pathways Curr Opin Biotechnol 42:126-132
- Tautorus TE, Fowke LC, Dunstan DI (1991) Somatic embryogenesis in conifers Canadian Journal of Botany-Revue Canadienne De Botanique 69:1873-1899
- Thomas TD (2008) The role of activated charcoal in plant tissue culture Biotechnol Adv 26:618-631 doi:10.1016/j.biotechadv.2008.08.003
- Thomas TL (1993) Gene expression during plant embryogenesis and germination: an overview The Plant Cell 5:1401
- Tsuwamoto R, Fukuoka H, Takahata Y (2007) Identification and characterization of genes expressed in early embryogenesis from microspores of *Brassica napus* Planta 225:641-652
- Tzin V, Malitsky S, Zvi MMB, Bedair M, Sumner L, Aharoni A, Galili G (2012) Expression of a bacterial feedback-insensitive 3-deoxy-d-arabino-heptulosonate 7-phosphate synthase of the shikimate pathway in *Arabidopsis* elucidates potential metabolic bottlenecks between primary and secondary metabolism New Phytol 194:430-439
- USDA (2012) Sugar: world production supply and distribution. United States Department of Agriculture (USDA). <http://www.fas.usda.gov/psdonline/circulars/sugar.pdf>. Accessed 20/05/2013

Vale EdM et al. (2014) Comparative proteomic analysis of somatic embryos maturation in *Carica papaya* L. *Proteome Science*

Verdeil J-L, Alemanno L, Niemenak N, Tranbarger TJ (2007) Pluripotent versus totipotent plant stem cells: dependence versus autonomy? *Trends Plant Sci* 12:245-252 doi:10.1016/j.tplants.2007.04.002

Vierstra RD (1993) Protein degradation in plants *Annu Rev Plant Biol* 44:385-410

Waclawovsky AJ, Sato PM, Lembke CG, Moore PH, Souza GM (2010) Sugarcane for bioenergy production: an assessment of yield and regulation of sucrose content *Plant Biotechnol J* 8:263-276 doi:10.1111/j.1467-7652.2009.00491.x

Washburn MP, Wolters D, Yates JR (2001) Large-scale analysis of the yeast proteome by multidimensional protein identification technology *Nat Biotechnol* 19:242-247

Winkel-Shirley B (2002) Biosynthesis of flavonoids and effects of stress *Curr Opin Plant Biol* 5:218-223

Wise MJ (2003) LEAping to conclusions: a computational reanalysis of late embryogenesis abundant proteins and their possible roles *BMC Bioinformatics* 4:52

Wu C, Siems WF, Klasmeier J, Hill HH (2000) Separation of isomeric peptides using electrospray ionization/high-resolution ion mobility spectrometry *Anal Chem* 72:391-395

Yu Y-Q, Gilar M, Lee PJ, Bouvier ES, Gebler JC (2003) Enzyme-friendly, mass spectrometry-compatible surfactant for in-solution enzymatic digestion of proteins *Anal Chem* 75:6023-6028

Zhang J et al. (2011) Targeted mining of drought stress-responsive genes from EST resources in *Cleistogenes songorica* *J Plant Physiol* 168:1844-1851

Zhang J, Ma H, Chen S, Ji M, Perl A, Kovacs L, Chen S (2009) Stress response proteins' differential expression in embryogenic and non-embryogenic callus of

Vitis vinifera L. cv. Cabernet Sauvignon - a proteomic approach Plant Sci 177:103-113 doi:<http://dx.doi.org/10.1016/j.plantsci.2009.04.003>

Zhang Z, Pang X, Xuewu D, Ji Z, Jiang Y (2005) Role of peroxidase in anthocyanin degradation in litchi fruit pericarp Food Chem 90:47-52

Zhou S, Wei S, Boone B, Levy S (2007) Microarray analysis of genes affected by salt stress in tomato African Journal of Environmental Science and Technology 1:014-026

Zhu L-H, Li X-Y, Welander M (2005) Optimisation of growing conditions for the apple rootstock M26 grown in RITA containers using temporary immersion principle. In: Liquid Culture Systems for in vitro Plant Propagation. Springer, pp 253-261

APPENDICES

APPENDICE A

Table S1. Co-expressed proteins identified in the embryogenic and non-embryogenic sugarcane cultures submitted to maturation treatments.

SUCEST accession	Description	Peptide count	Confidence score	Highest mean condition	Lowest mean condition	E-0	NE-0	E-21	NE-21
SCEZAD1078B05	curcin precursor	1	3.9787	NE-0	E-0	10.25848	13622.64	34.16956	137.015
SCJFST1010G02	capp1_sachy	11	77.9309	NE-0	NE-21	8348.267	19232.39	9256.739	359.7991
SCACSD1017D11	clone 205-like isoform 1	17	152.9226	E-0	NE-21	8234.341	7809.416	700.9264	201.4516
SCCCCL4014A08	geranylgeranyl pyrophosphate synthase 4	4	20.7251	E-0	NE-21	8534.896	2470.607	959.5335	109.0277
SCCCCL3005C05.b	embryo-specific protein	13	141.2254	E-21	NE-21	2066.585	132.5363	73345.13	7.288948
SCJLLR1101G05	hmgi y protein	2	10.4044	NE-0	NE-21	340.7214	3706.119	1699.157	210.8935
SCEPRZ1008D03	fen11_sorbi	4	27.7696	NE-0	NE-21	1706.446	12984.94	2431.46	893.5078
SCQGFL3053H05	Iz-nbs-lrr class rga	2	9.8136	NE-0	E-0	93.04693	4901.694	170.659	359.549
SCACHR1041H05	cyclic phosphodiesterase	3	19.7656	NE-0	NE-21	2139.018	3541.926	3345.375	339.5296
SCCCRZ1001H06	co-chaperone protein sba1	6	64.0411	NE-0	NE-21	19605.58	48914.92	16330.74	4786.291
SCSBFL1101H09.b	integral membrane single c2 domain protein	5	33.0867	E-21	NE-21	12021.12	6676.68	45850.57	660.4339
SCCCCL3002E04.b	trehalose-phosphate synthase	22	121.5711	E-0	NE-21	9493.06	1060.605	4030.1	106.3465
SCSGHR1066E06	aspr2 protein	23	147.6478	E-0	NE-21	9149.26	3882.674	6048.93	410.2096
SCCCLR1069D07	guanylate binding protein	10	52.0733	NE-0	NE-21	2752.892	4093.555	1298.486	469.5092
SCQSST1038D08	sec12-like protein 2	3	16.7043	NE-0	E-21	464.894	3901.299	246.8576	478.6646
SCJFRT2055E11.b	beta-expansin 1a precursor	19	127.8494	NE-0	E-21	7773.25	52332.28	4657.187	6564.604
SCVPLR2019F03	ASF sf2-like pre-mRNA splicing factor srp32	7	47.9284	NE-0	NE-21	1536.824	4504.274	2525.114	571.4726
SCCCRZ2C04F02	amidase family expressed	14	85.3448	NE-0	E-0	6258.07	73499	7947.87	9652.354
SCCCHR1002G07	gpi-anchored protein	9	66.7657	E-0	NE-21	44154.71	10450.31	33538.33	1372.436
SCEZLB1007F05	clpb3_orysj	26	153.2617	NE-0	E-0	9259.183	73881.34	17871.11	9921.871
SCQGHR1013D03	conserved oligomeric golgi complex subunit 5-like	6	34.8339	E-0	NE-21	22699.32	3663.37	1371.498	529.2136
SCEQLB1066E08	loc100284659 precursor	4	26.3181	NE-0	NE-21	606.9579	1692.314	885.4945	252.5909
SCSGST1072D03	calreticulin precursor	19	122.667	NE-0	NE-21	4049.291	25884.97	10858	4047.466
SCJFLR1017A04	heat- and acid-stable phosphoprotein	2	21.9397	E-21	NE-21	5373.2	1135.684	5951.419	183.0112
SCAGSD1039H04	anthranilate N-benzoyltransferase protein 1	8	44.6412	NE-0	NE-21	2725.669	5881.267	2081.17	971.665
SCEZRZ1015B08	phg1a protein	7	31.9824	E-0	E-21	5399.204	4235.963	257.7837	699.885
SCCCRT1003G09	isoform 1	10	62.8079	E-21	NE-21	20111.49	12259.47	31147.98	2061.882
SCCCRT1001G11	lipid transfer protein	15	116.9914	NE-0	E-0	10859.78	257523.7	25568.72	43430.11
SCJFLR1074H09	nhp2-like protein 1	11	81.4932	E-0	NE-21	108098.6	18676.75	26903.21	3389.828
SCEZLB1009D02	u2 small nuclear ribonucleoprotein a	15	98.1446	NE-0	NE-21	34323.76	95823.74	60557.71	18442.41
SCCCCL3003B01.b	cbs domain protein	25	284.1879	E-21	NE-21	233909.2	169165	296230.9	33223.86
SCJFRT1012F01	protein-I-isoaspartate O-methyltransferase-like...	5	28.1116	E-21	NE-21	3393.302	5690.942	7655.616	1138.87

Table S1 cont.

SUCEST accession	Description	Peptide count	Confidence score	Highest mean condition	Lowest mean condition	E-0	NE-0	E-21	NE-21
SCJLRT1015F05	osmotin-like protein precursor	22	256.641	E-0	NE-21	91860.46	29323.84	52880.13	6145.986
SCJLLR1104H07	phytocyanin-related protein pn14	2	12.5023	NE-0	NE-21	4109.405	4405.142	2401.979	944.3243
SCCCAM2003E05	pirin-like protein	4	21.3422	E-0	NE-21	3865.225	724.1863	1579.028	160.8459
SCMCRT2089E02	pdc1_maize	18	159.9512	E-0	NE-21	21547.95	16655.42	12178.37	3739.72
SCEQRT2029D07	gh34_orysj	2	11.7119	NE-0	NE-21	3544.695	5166.808	2315.291	1169.686
SCSGFL1078A05	phosphopantothenate--cysteine ligase	6	37.6406	NE-0	NE-21	5093.587	10312.33	3254.986	2350.502
SCCCCL3001B10.b	b chain semi-active e176q mutant of rice a plant...	21	122.9118	E-0	NE-21	3371.559	1728.38	1108.885	403.5121
SCSFFL4082E10	ninja4_maize	1	8.6336	E-21	NE-21	1678.457	4011.469	4376.204	949.1452
SCSBFL1043A02	pro-resilin precursor	10	62.24	E-21	NE-21	10608.7	704.6884	44374.02	167.8921
SCBFRZ2045E10	tpr domain containing protein	22	180.3759	E-0	NE-21	37738.6	16845.21	26775.9	4097.186
SCAGLR1043F02	70kda heat shock protein	59	566.1407	NE-0	E-21	4346.079	23436.34	2679.956	5870.194
SCEQRT2028H08	phosphate chloroplast expressed	11	84.1807	E-0	NE-21	8438.567	1055.179	3173.679	270.2784
SCBGRT3074G12	loc100284334 precursor	20	185.3751	NE-0	E-21	8581.919	736176.5	4897.184	188638.7
SCEQRT1028C10	spo76 protein	13	80.2677	E-0	NE-21	9605.116	8445.394	4620.278	2175.576
SCRURT2005G02	indole-3-glycerol phosphate chloroplastic-like...	6	36.94	NE-0	NE-21	14135.53	14321.38	5682.16	3824.566
SCBFRZ2050A05	af384033_1 hd2 type histone deacetylase hda106	7	49.4199	E-0	NE-21	12772.42	4948.467	7429.606	1339.628
SCCCCRZ2001E10	dna-directed rna polymerase ii	46	275.2676	NE-0	NE-21	26701.7	37556.64	25187.14	10167.4
SCCCLR1001G12	gdp dissociation inhibitor	14	106.7583	NE-0	E-21	2354.357	9572.733	1681.266	2678.543
SCSGAD1006C03	biotin synthase-like	10	63.0486	E-0	NE-21	84580.25	39993.52	40727.37	11197.23
SCJFRZ2025D08	hsc70-interacting protein	26	211.5694	NE-0	NE-21	16493.02	49180.13	30251.18	13901.53
SCBFLR1026G11	fatty acid biosynthesis1	12	81.2758	E-0	NE-21	15541.13	3123.664	10036.26	902.6691
SCEZHR1087D09	mapeg family expressed	5	54.4549	NE-0	E-21	10406.66	33158.59	7158.302	9605.61
SCCCCL3080H04.b	glycine-rich rna-binding protein 2	48	350.4326	E-21	NE-21	92617.99	114120.1	154965.6	33302.84
SCEZLB1010A08	pseudouridine synthase 1	8	39.6867	E-0	NE-21	20770.94	4165.265	20038.1	1221.344
SCQSRT2031H06	late embryogenesis abundant protein group 3...	45	376.3579	E-21	NE-21	177221.4	27030.12	234399.9	8022.879
SCCCRT1001H12	root cap protein 2 precursor	11	93.8942	E-0	E-21	38817.4	33340.49	8497.131	9948.497
SCACLR1126F12	lea1_orysj	10	79.8727	E-0	NE-21	43667.15	4966.897	43497.36	1497.096
SCBFRZ2016F05	unknown [Zea mays]	172	1491.7787	NE-0	NE-21	661380.3	935162.7	665131.9	283858.6
SCAGLR1043H10	apobec1 complementation factor-like	18	137.4153	E-0	NE-21	20713.91	15950.42	13396.39	4931.739
SCCCSD2C04B03	loc100284192 precursor	7	43.415	NE-0	NE-21	21994.73	38170.73	15912.63	11811.97
SCQSRT2036C02	translocon-associated protein beta containing...	10	79.2186	E-21	NE-21	14024.08	19707.78	28219.55	6146.433
SCCCLR1079A08	membrane steroid-binding protein 1	20	151.2625	E-21	NE-21	14975.57	14667.98	37465.62	4597.427
SCSGRT2063H01	tpa: class iii peroxidase 64 precursor	105	1017.829	NE-0	NE-21	479424.8	1356623	444147.7	430163.2
SCJLRZ1023B07	minichromosomal maintenance factor	57	353.9359	E-0	NE-21	40521.7	39564.19	35830.82	12636.96

Table S1 cont.

SUCEST accession	Description	Peptide count	Confidence score	Highest mean condition	Lowest mean condition	E-0	NE-0	E-21	NE-21
SCCCAM1C04B04	10 kda expressed	10	97.7551	NE-0	NE-21	17838.81	21316.56	15230.41	7011.072
SCRFLR2037C07	ac092172_32 activator-like transposable element	2	10.8622	E-0	NE-21	3569.356	2389.852	1391.673	787.8611
SCCCLR1C04B11	selenoprotein o	26	152.3315	E-0	NE-21	29454.99	15766.57	13607.03	5198.808
SCCCCL3140F04	proliferating cell nuclear antigen	27	247.3734	NE-0	NE-21	15967.64	39562.86	20641.73	13130.94
SCACST3159D04	inosine-5 monophosphate dehydrogenase 2	4	24.2281	NE-0	E-0	1882.933	7943.754	2326.698	2638.164
SCRLFL4102C08	minichromosome maintenance deficient protein 5	29	186.5796	E-0	NE-21	26021.58	7954.051	14852.67	2645.203
SCCCCL2001B11.b	xip1_wheat	14	117.1312	NE-0	E-21	253.2493	11644.13	118.5275	3876.128
SCCCLR1070C10	af384035_1 nucleosome chromatin assembly...	17	125.4361	NE-0	E-21	58289.69	71809.95	22926.27	24254.25
SCEZRT2023B09	ac018727_1 ubiquinone oxidoreductase subunit	4	21.492	E-21	NE-21	1388.139	1926.904	2702.305	652.5547
SCEZRZ1014E01	nucleotide pyrophosphatase phosphodiesterase...	21	121.9374	NE-0	E-21	6471.613	24193.68	4606.337	8312.028
SCEZRZ3098F04	bronze-2 protein	8	52.3352	NE-0	NE-21	10240.39	19472.9	10080.76	6706.954
SCEQLR1093H04	polyadenylate-binding protein2	11	86.1342	E-21	NE-21	14654	18816.27	32509.32	6643.371
SCEQRT2026A06	bright-associated protein p12 precursor	2	21.7547	NE-0	NE-21	3505.567	6742.9	2908.875	2383.467
SCJFRZ2026B04	gmp synthase	5	40.199	NE-0	E-0	2453.387	20444.29	4106.639	7244.688
SCEQLR1007A06	profilin-2	7	70.4517	NE-0	E-21	32190.84	50948.42	11465.8	18067.61
SCEQLR1050A01	kda proline-rich protein	11	72.4064	E-0	NE-21	68751.97	9868.948	42586.63	3515.349
SCEPCL6019C06	c3h14_orysj	7	43.5165	E-0	NE-21	2305.464	187.1959	680.2542	66.68867
SCJFRZ1006A12	ac077693_26 pyruvate kinase	17	112.1933	E-21	NE-21	2319.575	1870.484	3806.124	667.2333
SCCCCL3001E12.b	arabinogalactan protein	15	99.1966	NE-0	NE-21	17637.34	42757.71	34845.07	15313.77
SCVPAM2065H07	uracil phosphoribosyltransferase	7	40.6418	E-0	NE-21	6171.491	3828.115	4410.603	1379.854
SCCCLR1070C03	ef hand family expressed	16	108.3608	E-0	E-21	29997.77	25269.17	8682.702	9301.994
SCCCRZ1C01A05	nls receptor	22	156.4408	E-21	NE-21	39921.35	18789.3	48691.69	6985.96
SCBGLR1002H03	prefoldin subunit 3	33	268.1885	E-21	NE-21	27090.14	28534.46	45107.43	10781.71
SCCCLR2002F10	histidine triad nucleotide binding protein	21	169.6583	NE-0	NE-21	33954.6	51995.42	26408.3	19702.24
SCEZHR1048F05	3-hydroxyisobutyryl-coenzyme a hydrolase	23	160.228	NE-0	NE-21	31381.12	51275.9	27912.75	19434.1
SCJLRZ1024H10	myosin-like protein	23	154.1587	NE-0	NE-21	12377.58	17318.26	9766.813	6605.962
SCCCCCL3120C04	superoxide dismutase 2	3	17.253	E-0	NE-21	3161.909	1950.595	1517.485	746.9981
SCJLRT1019E04	early fruit mrna	19	105.023	E-0	NE-21	7732.982	3505.157	4971.766	1344.603
SCCCST1001B03	rvvb-like 2	13	77.7325	E-21	E-0	1878.077	5972.429	13335.03	2324.254
SCJLLR2013G12	fusca homolog	15	85.1998	NE-0	E-21	13609.49	22565.26	6222.655	8856.839
SCCCLR1066F11	gamm1 protein	16	97.8087	E-0	NE-21	11825.14	11379.9	7520.187	4483.329
SCJLRZ1027D12	methylthioribosE-0-phosphate isomerase	5	42.4532	E-0	NE-21	37593.42	14877.64	33784.29	5875.188
SCRLCL6030A07	acyl carrier protein 3	27	243.7388	NE-0	E-21	54251.96	127953.3	29482.91	50534.39
SCCCCL4012D10	polypyrimidine tract-binding protein homolog...	9	49.0548	E-0	NE-21	11850.44	1754.976	6229.037	698.445

Table S1 cont.

SUCEST accession	Description	Peptide count	Confidence score	Highest mean condition	Lowest mean condition	E-0	NE-0	E-21	NE-21
SCCCCL5071F02	anionic peroxidase	37	375.2503	E-0	NE-21	695185.7	300182.6	560647.3	120625.8
SCQSL3038A12	nuclear transport factor 2	125	752.1508	E-21	NE-21	158210.2	56319.1	201196.1	23549.18
SCCCLR1C07H02	calmodulin	22	192.2242	E-0	NE-21	155405.9	121929.5	87987.89	51479.43
SCQGLR2010A04	tubulin alpha-3 chain	118	1183.5289	E-21	NE-21	96449.7	71487.64	110280.8	30669
SCMCRT3082C04	rickettsia 17 kda surface antigen family protein	4	41.4123	E-0	NE-21	19627.27	14559.83	14262.45	6272.105
SCJLRT1013H07	electron transfer flavoprotein beta-subunit	14	101.8223	E-0	NE-21	29026.61	16117.72	12190.46	6959.043
SCACLR2014A07	threonyl-tRNA synthetase	39	219.2549	E-0	NE-21	27243.44	15978.9	24832.23	6934.326
SCQSRT1035E10	phosphoserine aminotransferase	30	265.2805	NE-0	E-0	45810.18	130091.8	51935.27	56653.01
SCSFBS1106D06	NADP-dependent oxidoreductase p2	93	585.0908	NE-0	E-0	51182.41	125772.4	74921.01	54815.18
SCCCLR1072C07	vesicle tethering family expressed	16	109.8345	E-21	NE-21	4660.377	5967.63	7867.335	2619.233
SCSFRT2072E08	tbc1 domain family member 13-like	2	10.6299	E-0	NE-21	3026.915	2007.471	2188.935	884.346
SCJLLR1107G01	auxin-induced protein pcnt115	77	578.9254	E-0	NE-21	172096.8	117381	169095.1	52138.42
SCCCLB1021C06	adhesion regulating molecule conserved region...	8	62.9888	E-0	E-21	15207.54	9514.027	3550.521	4229.058
SCCCCL4015B08	skp1-like protein 1a	22	170.9967	E-21	NE-21	36501.18	16967.66	65200.61	7602.448
SCJLAM1061C04	diaminopimelate decarboxylase	37	259.7618	E-0	NE-21	75135.35	48813.05	41469.9	22111.24
SCEPRZ1016A01	nucleolar protein expressed	56	383.7019	E-0	NE-21	81335.09	74701.6	60340.3	34373.37
SCEPRZ1008C01	acyl-peptide hydrolase-like	14	93.2828	E-0	NE-21	44983.17	34311.9	27391.09	15857.23
SCCCLR1C02B03	beta 5 subunit of 20s proteasome	47	363.7959	E-21	NE-21	33825.91	45105.92	69495.13	20936.55
SCCCRZ1002F11	beta-tubulin r2242	57	587.7045	E-0	NE-21	74278.85	71154.07	47624.72	33177.55
SCACST3159D04	inosine-5-monophosphate dehydrogenase 2	18	148.4253	NE-0	NE-21	25164.12	33977.62	24968.15	15987.78
SCCCLB1025C04	nascent polypeptide-associated complex alpha...	17	146.7821	E-0	NE-21	130729.3	100740.1	74112.93	47564.47
SCCCRZ2C04C08	prostaglandin e synthase 3	5	41.8054	E-0	NE-21	36751.34	16756.93	27338.45	7996.927
SCCCCRL4017D10	ranbp1 domain containing protein	25	133.1254	E-0	NE-21	22850.61	10176.12	7463.292	4930.13
SCRFLR1034A04	sec13-related protein	15	95.6432	E-21	NE-21	60757.39	54676.09	81266.4	26532.86
SCCCRT2001A06	quinone oxidoreductase	16	137.456	E-21	NE-21	13029.31	9713.393	19095.86	4732.964
SCCCLR1072B04	glyceraldehyde 3-phosphate dehydrogenase	51	665.9893	E-0	NE-21	770775.4	518275.4	663792.3	252634.1
SCCCCL1002F12.b	enoyl-acp reductase	32	236.894	NE-0	NE-21	71584.47	86746.15	81690.61	42496.99
SCSGRT2064D05	phd finger protein	8	39.8759	NE-0	NE-21	2888.132	3499.87	3039.767	1735.115
SCBFLR1046F09	bah domain containing protein	7	42.5079	E-21	NE-21	1265.306	311.4779	3171.289	154.9217
SCJFRT1008G12	somatic embryogenesis related protein	15	89.0304	NE-0	NE-21	22208.38	26163.01	24385.94	13041.2
SCCCLR1070B12	plasma membrane H+-ATPase	48	302.2677	E-21	NE-21	26546.45	31342.83	53515.99	15646.09
SCBFRZ2017F08	pantothenate kinase 4	28	167.9045	E-0	E-21	27162.13	26163.18	6883.14	13114.91
SCCCCL2001F11.b	clc1_orysj ame: full=clathrin light chain 1	9	53.2832	E-21	NE-21	5855.767	2453.989	7414.976	1231.822
SCCCLR1078D11	sorting nexin 1	21	115.3347	NE-0	E-0	2751.052	8326.759	3991.44	4192.45

Table S1 cont.

SUCEST accession	Description	Peptide count	Confidence score	Highest mean condition	Lowest mean condition	E-0	NE-0	E-21	NE-21
SCEZRZ3101F09	formate dehydrogenase	20	174.4554	E-21	NE-21	73161.97	38089.35	100938.5	19220.87
SCMCLR1125D12	116 kda u5 small nuclear ribonucleoprotein...	15	116.2499	NE-0	E-21	16955.85	31854.59	12511.69	16208.19
SCCCRZ2C03A09	5-methyltetrahydropteroyltriglutamate...	94	810.5021	NE-0	E-21	293238.9	457924.3	221567.8	233482.2
SCCCRT3001A02	chitinase b	28	295.0208	E-0	NE-21	273470	173355.2	212346	88600.41
SCJFRZ1007F04	nadph--cytochrome p450 reductase-like	2	8.8185	NE-0	E-21	2736.054	5843.504	2344.567	2989.69
SCVPRT2081E09	endo -beta-glucanase 2-like	39	261.6547	NE-0	E-21	62792.95	73869.21	28859.34	37804.78
SCCCRT1004A10	pre-mrna-splicing factor syf1-like	68	444.4595	E-21	NE-21	43103.42	31157.54	56412.76	15970.89
SCSGHR1069E04.b	trehalose-6-phosphate synthase 2	36	224.2937	E-0	NE-21	31125.3	13526.22	16347.45	6948.419
SCEZFL5090B07	glycosyltransferase [Saccharum officinarum]	9	52.9845	E-0	NE-21	10425.95	4539.957	4857.533	2334.337
SCCCLR1048G01	asparaginyl-trna cytoplasmic 3	51	357.4129	E-0	NE-21	65650.15	46798.07	49548.2	24114.26
SCSBAD1087E01	aminoimidazolecarboximide ribonucleotide...	15	93.4449	E-0	NE-21	19893.84	5411.426	12979.9	2797.844
SCCCCL3080A03	ago4a_orysj ame: full=protein argonaute 4a...	19	96.6411	E-0	E-21	19268.61	11949.65	1192.382	6190.217
SCCCLR2004G08	20 kda chloroplastic-like	26	180.2457	E-21	NE-21	33033.14	37050.59	41056.15	19197.54
SCJFRZ1007F10	es43 protein	8	51.1088	E-0	NE-21	5967.87	742.8884	4304.821	385.2131
SCCCCL6005E02	ornithine--oxo-acid aminotransferase	22	138.9313	E-21	NE-21	11669.21	17553.08	18791.48	9105.552
SCCCST3006H01	asparate aminotransferase	6	30.4836	NE-0	E-21	4783.492	14881.43	3698.923	7721.678
SCQGLR1041F04	n-alpha-acetyltransferase auxiliary subunit	5	27.4206	NE-0	E-21	3801.054	41138.45	2796.419	21447.35
SCQGLR1062G12	ac026815_7 rna binding protein	8	45.5295	E-21	NE-21	20049.11	12235.34	24078.52	6393.833
SCUTLR1058B03	atp-dependent rna helicase ddx23	180	1121.7103	NE-0	NE-21	86808.51	117642.8	104460	61830.14
SCCCLR1048C04	ftsh8_orysj	9	63.4664	NE-0	E-21	2959.241	3328.018	649.5664	1757.965
SCSFSD1066D11.b	kh domain containing protein	39	261.8801	E-21	NE-21	20699.47	27736.84	35455.16	14699.91
SCQGHR1013H09	sucrose cleavage	174	1550.9992	NE-0	E-0	456706.9	1250714	517858.5	668383.1
SCCCCCL3140F07	plasminogen activator inhibitor 1 rna-binding...	34	241.139	E-21	NE-21	28525.99	6686.977	30684.71	3585.271
SCQSLR1018E09	nucleosome chromatin assembly factor group a	64	510.2717	E-21	NE-21	193137.7	147671.3	271009.1	79275.14
SCCCCL3001B04.b	prolyl-trna synthetase -like	35	264.7046	NE-0	E-21	58016.27	122779.3	41448.39	65924.91
SCCCRZ2001A04	2-hydroxy-3-oxopropionate reductase	19	106.7992	E-0	NE-21	19029.83	10211.36	18397.93	5498.327
SCCCLR2C03F11	annexin p33	95	765.9604	NE-0	NE-21	169923	259366.2	198689.3	140256.1
SCEZAD1081B12	leucyl-trna synthetase	43	265.4449	NE-0	E-21	50110.91	80105.01	24452.83	43410.34
SCCCRZ2001C11	usp family protein	32	259.1192	E-21	NE-21	61343.17	52697.75	133927.5	28634.61
SCJFRZ3C01G05	lysosomal alpha-mannosidase-like	14	75.6865	NE-0	NE-21	8075.897	11701.38	9044.214	6380.334
SCAGLR1043H07	carrier protein	22	143.2347	NE-0	E-0	1018.081	13790.63	1812.751	7525.776
SCCCLR2002D08	translocon tic40	12	67.0322	E-21	NE-21	7433.326	1630.517	7591.528	890.002
SCSGFL1078A06.b	endoplasmic precursor	86	678.8232	E-21	NE-21	182447.8	177120.2	188442.4	96714.32
SCCCCL7C02A04	cupin family expressed	16	160.3824	E-21	NE-21	113367.5	3069.773	243333	1684.903

Table S1 cont.

SUCEST accession	Description	Peptide count	Confidence score	Highest mean condition	Lowest mean condition	E-0	NE-0	E-21	NE-21
SCCCLB1024G12	glucosidase 2 subunit beta-like isoform 1	4	20.6856	E-0	E-21	6336.318	5499.077	1859.324	3032.711
SCCCLR2001F05	delta-1-pyrroline-5-carboxylate synthetase	37	233.9558	NE-0	E-0	22056.56	42155.74	25802.42	23283.83
SCSGFL5C07C07	replication licensing factor mcm7 homologue	64	393.213	E-21	NE-21	56902.78	51006.17	60840.62	28401.23
SCCCLB1004D05	nadh-cytochrome b5 reductase-like protein	30	236.5468	NE-0	NE-21	45656.56	67372.69	38693.61	37599.27
SCBFLR1083H11	rae1-like protein	12	80.1728	NE-0	E-21	3672.048	18514.62	1924.544	10334.28
SCJLLR1107E04	snrk1-interacting protein 1	16	113.3718	E-21	NE-21	16859.42	9986.667	26116.58	5589.197
SCCCCL3004H02.b	proliferation-associated protein 2g4	23	177.0052	NE-0	E-21	12233.23	50275.86	11581.64	28215.31
SCACLR2007C03	guanine nucleotide-binding protein beta subunit...	34	336.4325	NE-0	NE-21	189353.7	275623.8	168088.9	154703
SCCCLR2C02D02	macrophage migration inhibitory factor	7	67.7377	E-21	NE-21	36436.77	21238.68	72445	11958.45
SCJLRT2049G08	copa3_orysj ame: full=coatomer subunit alpha-3	43	280.1992	E-21	NE-21	158485.4	30481.7	182556.2	17215.88
SCQSST1035B11	calreticulin-3 precursor	5	23.8042	NE-0	E-21	362.8173	12433.49	314.0735	7023.24
SCCCRZ1004G02	acetylornithine deacetylase	34	252.0388	E-0	NE-21	78344.28	47826.29	60535.73	27049.28
SCEPRZ1009B12	triosephosphate cytosolic	79	815.0929	E-21	NE-21	1032059	1010360	1046807	573461.8
SCEZLB1007F07	arginyl-tRNA synthetase	34	222.2821	NE-0	E-21	39850.79	96330.06	17782.52	54921.04
SCEQAM2039A03	monocopper oxidase-like protein sku5-like	16	101.2518	NE-0	E-21	16407.23	18547.62	10493.52	10621.8
SCCCCL4009B07	villin-2-like isoform 1	13	71.4903	NE-0	E-0	3632.479	11624.74	5027.946	6673.302
SCSGLR1081B03	reticulon-4-interacting protein 1	11	78.3725	E-21	NE-21	13010.34	9173.099	17908.92	5279.217
SCAGLR1043D06	methyl binding domain106	33	327.3972	E-21	NE-21	126800.5	77970.33	219334.1	45015.41
SCJLLR1011H01	msi type nucleosome chromatin assembly factor c	11	57.765	E-0	E-21	11621.21	9131.821	5100.079	5319.851
SCEZHR1084E11	peroxidase 1 precursor	196	1500.1908	NE-0	E-21	214332.2	762890.7	196183.6	445562.3
SCVPFL1134D05	riboflavin biosynthesis protein riba	5	34.3912	NE-0	E-0	1306.805	4532.236	1815.342	2651.968
SCCCRT2C04H02	enolase 1	64	715.8054	NE-0	E-21	501699.8	896197.1	496830.8	525112.2
SCCCRT1004F06	aminotransferase y4ub	27	161.2251	E-0	NE-21	109953.2	28780.2	45769.83	16907.45
SCRFLR2034H11	heterogeneous nuclear ribonucleoprotein a3...	51	361.9446	NE-0	NE-21	59956.61	64495.27	62233.24	38095.87
SCCCLR2004H11	t-complex protein 1 theta chain	247	1796.2058	NE-0	NE-21	367881.4	437040.1	301286.9	258472.7
SCBGLB2072H09	cw-type zinc finger family expressed	3	12.2557	E-21	NE-21	827.7621	383.8954	2321.253	227.5287
SCRFLR1034B02	dead-box atp-dependent rna helicase 56-like	69	539.1461	E-0	NE-21	127907.6	69445.71	106213.7	41218.56
SCQSSB1059F03	ribose-5-phosphate isomerase	13	94.1233	NE-0	E-21	11375.72	18843.33	1980.486	11203.3
SCCCCC5071D04	tonoplast intrinsic protein	1	8.0538	E-21	NE-21	2071.329	153.1161	11229.84	91.78444
SCJFRZ2027B01	amp-binding protein	30	207.5364	NE-0	E-21	10054.19	48292.36	7906.608	29095.54
SCRLLR1059F06	mucin-like protein	6	39.1242	NE-0	E-21	4584.2	6730.207	1703.159	4077.27
SCBFRT3093E07	leucoanthocyanidin dioxygenase 1	8	53.157	NE-0	NE-21	23543.82	34670.29	34361.15	21052.83
SCCCCL4003A03	tetratricopeptide repeat protein 1-like	17	105.7923	NE-0	E-21	3359.192	7391.617	1726.573	4501.017
SCVPRZ2038H03	proteasome alpha subunit	273	2233.0416	NE-0	NE-21	586563.6	907677.7	611121.1	558296.9

Table S1 cont.

SUCEST accession	Description	Peptide count	Confidence score	Highest mean condition	Lowest mean condition	E-0	NE-0	E-21	NE-21
SCACFL5027E11	pyruvate kinase isozyme chloroplast precursor	299	2363.9015	NE-0	NE-21	719697	1035781	656631.2	642341.6
SCJFSB1012F11	phospholipase d alpha 1	64	475.6482	NE-0	E-0	115868.5	354727	146014.1	222421.1
SCSFAD1068F07	beta-hexosaminidase beta chain precursor	3	27.0589	E-0	NE-21	10407.07	8224.332	9023.819	5172.37
SCJFRZ2026E06	pura1_sorbi	11	90.9944	NE-0	E-21	27358.06	39704.79	16044.91	25037.24
SCRLRZ3042G05	calmodulin-binding protein	11	66.7211	E-21	NE-21	4193.471	3806.943	12318.58	2400.631
SCCCLR1066A08	rh2 protein	25	199.6764	E-21	NE-21	394868.4	62804.44	686279.4	39640.3
SCAGRT2041G07	dihydrolipoamide s-acetyltransferase	55	368.609	NE-0	E-0	51565.38	109660.9	72459.27	69421.21
SCVPLR1028E03	pci domain containing protein	47	360.5509	NE-0	E-21	79730.7	108209.5	41642.19	68596.62
SCEQRT2090H11	transducin wd-40 repeat	63	403.7021	E-0	NE-21	65479.68	49014.09	54293.91	31103.67
SCCCSB1002A08	outer mitochondrial membrane protein porin	71	579.0222	E-21	NE-21	110848.2	114230.8	143874.5	72741
SCCCCL5002C02	isopenicillin n epimerase	13	90.5812	E-0	NE-21	5782.331	883.2609	2924.96	564.0289
SCACLR1036F01	alpha-l-fucosidase 2-like	10	62.5603	E-21	NE-21	7214.004	3971.947	8211.804	2543.701
SCCCCL5004D04	cinnamoyl reductase-like 2a	33	256.4894	E-0	NE-21	72557.91	64074.58	60028.31	41213.78
SCSFRT2069D09	pyrophosphate-dependent phosphofructokinase...	66	520.8001	NE-0	NE-21	102853.9	122198.1	93271.21	78676.03
SCEPLB1043H10	rRNA 2'-o-methyltransferase fibrillarin 1-like	11	90.88	E-21	NE-21	200664.5	23208.57	276916.8	14947.77
SCCCCL4009H11	af236369_1 prohibitin	21	198.4113	E-21	NE-21	108187.7	49983.28	130494.3	32217.84
SCSGHR1071C01	sumo-activating enzyme subunit 2-like	20	125.5071	E-21	NE-21	39974.71	19053.49	48161.15	12304.71
SCCCCL6002B05	nitrilase 2	10	83.8845	E-0	NE-21	53769.3	22726.34	20925.3	14835.75
SCQGST1034A08	14-3-3-like protein	100	1000.6875	NE-0	E-21	714481.4	1481639	709083.7	967775.7
SCCCCL3001A01	2-hydroxyacyl- lyase-like	8	64.4219	NE-0	E-0	4161.339	10026.22	7259.066	6554.907
SCEPSB1128E09	nad-dependent malic enzyme 62 kda...	44	268.799	NE-0	E-21	36905.19	61815.89	25756.22	40439.55
SCVPCL6046A06	seed maturation protein pm41	17	116.4626	E-21	NE-21	27935.78	13183.74	52056.28	8659.311
SCQSRT1035C02	dna-binding protein	54	353.1174	NE-0	NE-21	108387	131469.5	98393.24	86721.19
SCRLAM1013H08	u5 small nuclear ribonucleoprotein component	34	205.9656	NE-0	E-0	28909.73	57914.67	38128.38	38460.22
SCEQLB1065B12	fk506-binding protein 2-1 precursor	10	61.412	E-21	NE-21	17904.27	9733.813	22668.5	6490.266
SCMCLR1123B01	fasciclin-like arabinogalactan protein 10...	26	185.5833	E-0	NE-21	39403.8	16558.53	30468.35	11071.8
SCJFRZ2027B03	nadph-thioredoxin reductase	8	55.989	NE-0	E-0	2054.639	12256.54	5035.935	8281.633
SCEPRZ1010H09	dynamin-related protein 1a	35	205.1526	E-21	NE-21	62602.3	60227.79	66463.19	40847.37
SCACSB1038A04	rhicadhesin receptor precursor	11	138.4831	NE-0	E-21	116855	447323.7	77191.99	303575.4
SCEQLB1066D03	syntaxin 72	12	77.3964	E-21	NE-21	22997.97	20547.07	27027.96	14004.1
SCEQRT1026G11	leucine aminopeptidase	77	686.4492	E-21	NE-21	164992.3	174897.2	177630.1	119770.9
SCEQAM1035F11	calcium ion binding	10	64.6461	E-0	NE-21	14615.28	2805.966	13825.92	1926.642
SCRLFL4028D02	Na+ H+ antiporter	3	17.7953	NE-0	E-0	10111.08	80009.23	19986.98	54939.98
SCCCCL3002B06.b	isochorismate synthase 1	28	229.2697	E-21	NE-21	104275	67205.01	127662.5	46157.56

Table S1 cont.

SUCEST accession	Description	Peptide count	Confidence score	Highest mean condition	Lowest mean condition	E-0	NE-0	E-21	NE-21
SCQGSB1144A01	PREDICTED: uncharacterized protein...	32	185.4905	E-21	NE-21	12051.74	9310.524	20785.99	6417.587
SCCCCL4011E04	pairing protein meu13-like	4	23.1364	E-0	NE-21	1388.743	344.6668	909.4002	237.9263
SCUTHR1065A04	nucleic acid binding protein	60	352.7818	E-0	NE-21	40129.63	20315.44	24435.38	14107.74
SCBGAM1092H06	carboxypeptidase d	13	121.1111	E-21	NE-21	10577.64	12100.08	24351.72	8408.027
SCEQRT1025H04	heat-shock protein 101	36	207.1056	E-21	NE-21	5652.596	2414.997	6680.752	1687.738
SCBFRZ2017C11	per1_maize	15	131.0551	E-0	NE-21	15548.62	10426.71	12847.17	7289.34
SCCCFL3002F10	dna replication licensing factor expressed	132	791.317	E-0	NE-21	170456	68698.14	160615.6	48085.72
SCEQRT2092A09	peroxisomal targeting signal 1 receptor	57	363.565	NE-0	E-0	42391.23	152763	49291.21	106989.9
SCJLLR1033F07	2-cys peroxiredoxin bas1	17	144.5669	E-0	NE-21	95273.67	87182.54	89350.56	61068.46
SCRLLR1016F07	alpha- galacturonosyltransferase 1-like	72	585.3258	NE-0	E-0	103343.5	325892.2	135569.6	228666
SCCCLR1C01E07	histidinol-phosphate aminotransferase	7	46.9907	NE-0	E-21	5289.503	5866.128	3954.729	4143.786
SCBGRH1061F05	phosphoribosylamine--glycine ligase	14	97.2493	NE-0	E-21	22293.84	58495.7	20677.24	41365.1
SCCCLR2001D01	histone h4	128	1083.4304	E-0	NE-21	753854.4	393670.1	634370.3	278821.5
SCQGLR1086B12	stress responsive protein	20	134.116	NE-0	NE-21	5882.284	6563.433	4950.185	4649.453
SCEZLB1012H08	actin-like protein 6a	16	91.8375	E-0	NE-21	17344.37	7081.566	10237.87	5077.334
SCVPRZ2041G12	indole-3-acetic acid-amido synthetase	56	397.5192	E-0	NE-21	143433.7	42131.11	55305.94	30211.17
SCCCLR2003G06	thaumatin-like cytokinin-binding expressed	20	150.1229	NE-0	E-0	49037.01	75202.2	71884.94	54048.66
SCACHR1036C12	hypersensitive-induced response protein	39	246.3901	E-21	NE-21	39537.28	42816.8	48480.11	30835.02
SCRCLAM1012D07	iq calmodulin-binding motif family protein	18	128.2619	NE-0	E-0	33574.67	69188.61	46288.84	49901.46
SCEQRT1033B09	2-oxoglutarate e1 subunit	30	221.0685	NE-0	E-21	17409.72	26735.4	11512.32	19347.83
SCSGAM1095C10	prs4_orysj	32	261.372	E-0	NE-21	74892.45	43254.84	66431.65	31363.46
SCACLR2029H09	xylogen protein 1	11	108.9826	E-0	NE-21	107769.1	51824.15	98386.1	37737.26
SCRURT2008D11	glycosyl hydrolase family 3 n terminal domain...	77	543.3879	NE-0	E-0	41165.65	116845.4	56625.39	85102.8
SCJFST1012D03	mannosylglycoprotein endo-beta-mannosidase...	11	55.7308	NE-0	E-21	431.8701	9243.849	211.3116	6743.537
SCCCLR2002B03	dynamin-like protein	2	18.0477	E-21	E-0	866.8606	1827.795	3889.421	1340.13
SCJFRT1012A02	oep24_orysi	14	85.5001	E-0	E-21	46041.86	21283.05	4751.748	15610.14
SCRFFL5039B12	ankyrin protein	30	181.3596	E-0	NE-21	52934.78	44062.91	48696.31	32464.8
SCQSLR1061C03	small nuclear ribonucleoprotein e-like	31	231.1935	NE-0	E-0	37800.26	66301.91	47839.37	48883.83
SCMCLR1053H06	lysyl-tRNA synthetase	22	162.262	NE-0	E-0	14696.43	44147.86	37540.87	32608.06
SCCCLR2001E04	huntingtin-interacting protein k-like	9	88.5859	NE-0	E-21	98325.29	225374.2	52908.66	167026.4
SCCCLB1004H08	adenosine kinase	25	244.7617	NE-0	E-0	95256.16	173290.5	101767	128862.4
SCCCCCL4011E03	toc75_orysj	23	128.3332	E-0	NE-21	20962.34	10499.95	16564.13	7828.337
SCQSLR1061B01	fibroblast growth factor 2-interacting factor	22	123.2497	NE-0	E-0	19052.43	32498.6	21985.39	24289.97
SCJLLR1054A06	1-aminocyclopropane-0-carboxylate oxidase 1	22	157.5474	NE-0	E-21	33000.39	126846.2	15696.77	94853.14

Table S1 cont.

SUCEST accession	Description	Peptide count	Confidence score	Highest mean condition	Lowest mean condition	E-0	NE-0	E-21	NE-21
SCMCCL6053E09	tryptophan synthase beta-subunit	12	87.0141	NE-0	E-21	6731.032	19031.68	6367.3	14236.97
SCQGLB1027C07	vip3 protein	10	69.5008	E-21	NE-21	32876.58	23823.74	35648.45	17941.93
SCCCLR1C01G03	adp-ribosylation expressed	34	225.708	E-21	NE-21	88074.64	68799.58	95959.3	51831.39
SCJLRT1016A04	plastid-lipid-associated protein 2	5	28.0025	E-0	NE-21	3018.852	2266.618	2269.277	1708.314
SCRFAM2071E02	glucan endo- -beta-glucosidase precursor	29	174.1288	E-21	E-0	25478.32	42177.08	86602.12	31828.41
SCBGLF4053G08	phosphoenolpyruvate carboxylase	165	1208.1647	E-0	NE-21	382090.9	195893.1	344223.7	148349.5
SCCCRZ2002H06	aspartic proteinase oryzasin-1 precursor	41	336.1406	NE-0	E-21	114097.8	122595.8	81073.1	94389.26
SCCCLB1002D05	loc100286338 precursor	12	84.6403	E-0	NE-21	16799.22	13064.34	13944.44	10062.5
SCVPLR2027C10	tcp1 cpn60 chaperonin family protein	51	376.2577	E-0	NE-21	128967	97807.57	115546.2	75929.36
SCSFLR2009H09	cytosolic chaperonin delta-subunit	144	1169.3742	NE-0	E-21	200616.2	265758.5	200316.4	206345.3
SCSGLR1045G11	cml7_orysj	17	131.4453	E-0	NE-21	26557.11	12359.01	17553.04	9633.523
SCRFAD1117F03	eukaryotic translation initiation factor 2 beta...	494	3429.5305	NE-0	NE-21	510099.4	524077.4	422520.6	410523.6
SCCCLB1023G10	armadillo beta-catenin-like repeat family protein	17	112.9474	E-0	NE-21	11340.03	2149.754	4585.333	1686.436
SCQGST3123C08	pectin methylesterase	3	16.4109	NE-0	E-21	331.1384	722.1381	190.716	569.3307
SCJLLR1054F05	dnak-type molecular chaperone	111	1063.5405	NE-0	E-0	190782.3	354332.4	206237.2	279669.8
SCCCLB1001H09	methyl-binding domain protein mbd11	46	311.7707	E-0	NE-21	81090.59	59041.97	48025.76	46623.55
SCCCST1006A11	glycine dehydrogenase	19	108.9144	E-21	NE-21	20298	9888.559	24266.31	7823.209
SCCCLR1C02F07	inositol-3-phosphate synthase	26	205.9797	E-21	NE-21	26338.82	2543.435	63197.93	2028.232
SCCCCCL3002A02.b	chloride intracellular channel 6	23	250.8429	E-0	NE-21	189823	90946.06	152418.9	72602.59
SCCCCCL5003C11	glutathione s-transferase 4	216	1804.5944	NE-0	E-21	1048644	1076003	726802.7	861353.4
SCUTSD2028F03	glyceraldehyde-3-phosphate partial	99	1106.989	E-21	E-0	795085.4	1005330	1274650	807328.3
SCSGAM1094A08	ribonucleotide reductase	25	147.9039	E-21	NE-21	8595.877	5199.716	11917.39	4187.315
SCCCLR1C04F06	diphosphomevalonate decarboxylase	8	50.6094	E-21	NE-21	4090.957	854.0574	15357.31	688.1318
SCCCCRZ1003F10	c2 domain containing protein	24	167.6721	NE-0	E-0	57512.21	89918.59	68861.01	72546.75
SCPRRT3026E05	aspartyl-tRNA synthetase	31	207.9798	E-21	NE-21	66556.89	75390.55	78503.35	61126.05
SCACLR1057G08	activator of 90 kDa heat shock protein ATPase	23	169.4497	NE-0	E-21	27748.06	59881.27	16104.42	48567.3
SCSFRT2072C08	ml domain protein	6	49.6795	NE-0	E-0	12901.25	79734.26	13170.21	64924.73
SCEZRZ1012F05	methylenetetrahydrofolate expressed	30	201.373	E-0	E-21	34282.9	25586.16	20658.54	20868.39
SCCCCL7038G03	methionyl-tRNA synthetase	34	226.1558	NE-0	NE-21	37944.78	39824.95	38791.98	32502.11
SCEZRZ1014D09	coatmer beta subunit (beta-coat protein)...	32	190.1765	E-21	NE-21	11773.07	12392.53	15811.08	10119.93
SCCCLR1024C10	endothelial differentiation-related factor 1	3	37.3708	E-21	E-0	2180.491	4481.767	10267.46	3674.765
SCUTSD2025B07	elongation factor 1-alpha	286	2666.7892	E-21	NE-21	1633347	1724345	1753848	1414859
SCRURT2011B01	2-dehydro-3-deoxyphosphooctonate expressed	15	93.936	NE-0	E-21	17454.58	32275.36	17217.97	26491.88
SCCCCL3080C05	aspartyl expressed	14	84.7793	NE-0	NE-21	6924.249	8368.89	7207.115	6869.8

Table S1 cont.

SUCEST accession	Description	Peptide count	Confidence score	Highest mean condition	Lowest mean condition	E-0	NE-0	E-21	NE-21
SCBFLR1083E03	nucleoside diphosphate kinase i	31	275.33	E-21	E-0	121169.7	147116.7	168235.8	121283.5
SCCCFL4092E06	pyrophosphate-fructose 6-phosphate...	58	467.9343	NE-0	E-21	339588.9	518421.1	199443.6	427696
SCCCFL1001E01	loc100283433 precursor	10	52.9694	E-0	NE-21	3312.04	1924.839	3205.94	1588.821
SCEQLR1050F11	hypothetical protein SORBIDRAFT_03g004340...	1945	12700.9317	NE-0	E-21	2054525	2462972	1988846	2035515
SCCCLR2003A04	allene oxide cyclase 4	23	168.2744	NE-0	E-21	10284.17	13434.27	2940.445	11118.03
SCCCCL4017C01	syh_orysj	15	77.4613	NE-0	E-21	8457.308	10406.76	4846.561	8665.216
SCQGLR1019E07	e3 ubiquitin-protein ligase upl1-like	19	108.2425	NE-0	E-0	6700.948	35902.79	6728.296	29900.07
SCVPLR2019B03	polygalacturonase inhibitor 1 precursor	16	123.5409	NE-0	E-0	24223.89	43446.67	30967.68	36182.95
SCEQRT1028A02	gme2_orysj	23	178.988	NE-0	E-0	1736.575	31515.72	3887.324	26248.75
SCRFA1026D04	ran gtpase activating protein	48	298.9883	E-0	E-21	52795.85	28585.23	20838.83	23908.47
SCJLFL1053D04	nodal modulator 1-like	15	83.6124	E-0	E-21	8017.094	7347.709	6063.324	6145.961
SCCCLR1C03G09	chalcone flavanone isomerase1	4	23.3373	NE-0	E-0	29.7517	1388.701	33.13002	1162.936
P00330	ADH1_YEAST Alcohol dehydrogenase 1...	25	218.6479	E-21	NE-21	54015.14	42137.33	374341	35565.13
SCQSAM2101B07	splicing arginine serine-rich 7	95	661.8774	E-0	NE-21	116706.1	110511.7	110693.7	93791.5
SCCCRT2002B07	tRNA- expressed	7	35.1372	E-21	NE-21	2426.741	249.3176	3223.02	212.0904
SCMCRZ3065B07	xylulose kinase	18	99.4766	NE-0	E-0	1970.062	16202.37	6282.198	13827.22
SCVPFL3040H07	salt tolerance expressed	33	317.0089	E-0	NE-21	251460.1	240998.8	222168.7	205695.5
SCVPCL6041E09	leukotriene a-4 hydrolase	30	255.7269	E-0	NE-21	89128.81	34980.55	72535.73	29935.91
SCSFFL3093H05	sister-chromatid cohesion protein	12	73.0126	E-0	NE-21	8699.827	1313.395	5002.368	1125.531
SCVPRZ2038C12	polyubiquitin 14	26	227.1644	E-0	NE-21	44891.4	26439.86	33323.55	22667.63
SCRFR13057C02	translational initiation factor eif-4a	115	1039.4061	NE-0	E-21	248597.1	286578.9	228670.3	245809.3
SCCCST2004E07	gras family transcription factor containing...	10	63.4382	E-0	E-21	6601.26	1391.955	609.9562	1193.942
SCCCLR1024G01	low quality protein: alanyl-tRNA synthetase-like	106	699.4997	E-0	NE-21	97401.23	85609.82	85387.54	73604.27
SCCCLR2001H06	transcriptional coactivator-like	17	91.7628	E-21	NE-21	6933.847	3443.456	13172.12	2960.566
SCRFLR1012E03	isopentenyl pyrophosphate:dimethylallyl...	4	23.4073	E-0	NE-21	1893.905	701.8276	1202.537	603.7318
SCCCLR1C01A11	tyrosyl-tRNA synthetase	16	118.6678	NE-0	E-0	16635.2	28118.55	25462.83	24199.02
SCVPLB1015B03	fructose-bisphosphate aldolase	105	1061.5568	NE-0	E-0	870112.8	1353397	1225315	1165637
SCSGRT2062E10	transformer-sr ribonucleoprotein	5	29.6866	E-21	NE-21	1767.69	670.431	2956.072	578.0975
SCVPC16041A03	cysteinyl-tRNA expressed	10	68.0316	E-21	NE-21	2621.543	1407.225	8597.425	1222.321
SCEPCL6018F02	glycyl-tRNA synthetase	75	478.2277	E-0	NE-21	88030.32	86624.65	85253.16	75263.2
SCBGLR1117A05	ran-binding protein 1	22	230.7805	E-21	NE-21	59761.54	34275.68	60293.37	29812.93
SCRFR13060F01	actin-depolymerizing factor 3	15	121.8193	E-21	NE-21	23773.79	5996.99	33279.94	5233.604
SCAGLR1021D02	ubiquitin-conjugating enzyme e2 n	49	396.7887	E-21	NE-21	145520.4	65868.3	191691.8	57760.24
SCEPAM1015B01	tryptophanyl-tRNA synthetase	22	134.1992	E-0	NE-21	39691.26	18554.88	26792.28	16328.06

Table S1 cont.

SUCEST accession	Description	Peptide count	Confidence score	Highest mean condition	Lowest mean condition	E-0	NE-0	E-21	NE-21
SCCCLR1024C11	stromal 70 kda heat shock-related protein	52	365.3031	E-0	NE-21	96371.73	56035.74	75716.72	49324.29
SCCCRZ1001D04	cytoplasmic 2	56	446.465	E-0	NE-21	249919.9	134091.5	188013.3	118191.9
SCACAM1072H07	gcn5-related n- expressed	7	51.2557	NE-0	E-0	3330.35	4730.989	3565.234	4171.443
SCCCCL3120B01	fructokinase-2	42	443.8685	NE-0	E-0	245682.9	463442	359332.8	408938
SCCCCL4011G05	rna-binding protein luc7-like 2	78	454.437	E-0	NE-21	37891.93	19107.31	36265.27	16878.27
SCJFL3019C04	pmm_orysj	9	78.0818	NE-0	E-21	2572.568	11685.43	2452.054	10335.83
SCCCLR1024D03	malate cytoplasmic	108	1109.0054	E-21	NE-21	719765.7	730947.7	868406.8	648927.4
SCVPRZ2042F09	glutaminyl-tRNA synthetase	27	161.3599	NE-0	E-21	12400.99	15329.59	9947.018	13628.95
SCUTLR1058E05	spermidine synthase 1	19	127.7186	NE-0	E-0	14944.81	23201.39	20277.16	20656.27
SCRFSB1020B02	serine threonine-protein phosphatase 6...	175	1248.6378	NE-0	E-21	341905.6	379557.6	333791.4	338606.6
SCSFAD1123C03	6-phosphofructokinase chloroplastic-like	39	238.8922	E-0	E-21	75016.63	20911.21	4763.05	18774.96
SCCCLR1C01E08	rna recognition motif -containing protein	196	1247.7788	NE-0	E-21	242328.6	275123.2	232412	248022.6
SCQSHR1022C01	beta- partial	18	111.7126	NE-0	E-21	3687.016	69496.47	176.5582	62758.76
SCJFRT1009B01	patatin t5 precursor	17	132.0317	NE-0	E-0	7983.405	136596.3	16331.03	123497.9
SCCCRZ1004G05	chaperonin 60 beta precursor	199	1640.3547	NE-0	NE-21	322240	323297.6	299951.1	292477.3
SCMCAM1101A10	karyopherin-beta 3 variant	9	65.0093	E-0	E-21	15636.45	8341.553	4196.399	7559.728
SCAGLR2033E02	clc2_orysj	4	26.605	NE-0	E-21	106.9704	5419.096	19.69416	4915.32
SCCCLR1C06E11	oxidative-stress responsive	3	20.2947	NE-0	E-21	3943.804	4151.246	3269.793	3765.798
SCBFBSB1046C09	nuclear-pore anchor-like	27	154.6113	E-21	E-0	7647.63	23130.41	30347.07	21021.24
SCVPLR2005H09	3-oxoacyl-synthase i	28	219.4778	E-21	E-0	16984.86	24437.36	26258.63	22212.33
SCJFRT1007A07	short chain alcohol	6	49.7768	NE-0	E-21	15377.02	42823.59	11274.35	38972.53
SCSBFL5014H12	lipoxygenase 2	8	46.8468	E-21	E-0	531.2384	2376.585	2902.554	2168.075
SCBFRZ2016H11	ribophorin ii precursor	25	175.5667	NE-0	E-0	22407.37	57584.27	23840.1	52576.43
SCCCCCL6004H07	beta-galactosidase expressed	16	106.4066	E-0	E-21	4709.118	2706.784	615.7299	2475.56
SCCCLR1048H09	catalase cata	67	668.8414	E-21	NE-21	178035.9	95822.58	325197.2	87673.27
SCCCRZ2C04F03	thioredoxin-dependent peroxidase	12	116.8022	E-21	NE-21	32589.29	15966.42	35880.11	14617.86
SCACRZ3036C09	act domain containing protein	12	71.5636	E-21	E-0	3620.28	13367.08	13706.72	12239.88
SCMCST1051A04	tripeptidyl peptidase ii	23	135.7629	E-0	E-21	28470.11	27600.57	22641.71	25366.68
SCVPRZ2043F04	atp synthase gamma chain	180	1492.9312	E-21	NE-21	710958.2	579632.2	874379	532859.5
SCCCLR1070F12	calnexin precursor	45	358.3521	E-21	NE-21	135344.4	139828.1	178953.2	128959.2
SCRLSD1012E03	probable ubiquitin ribosomal protein s27a fusion...	226	1576.8175	E-21	NE-21	234070.2	167346	246005.2	154865.4
SCCCFL5061H09	dihydrolipoyl dehydrogenase mitochondrial-like	80	645.8615	NE-0	E-0	89077.59	126891	105539.8	117759.4
SCSGLR1045D11	glutaryl- dehydrogenase	8	45.0578	E-21	NE-21	6520.363	5822.297	8689.453	5406.487
SCBFRT1069C12	wd-repeat domain phosphoinositide-interacting...	4	17.709	E-0	NE-21	4251.437	672.3406	2690.154	624.9944

Table S1 cont.

SUCEST accession	Description	Peptide count	Confidence score	Highest mean condition	Lowest mean condition	E-0	NE-0	E-21	NE-21
SCCCST1002H09	pi starvation-induced protein	6	46.1816	E-0	NE-21	4110.506	3117.959	3892.471	2909.314
SCCCRT2001A05	heme oxygenasE-0	10	56.6951	NE-0	E-21	6236.536	6243.141	4731.32	5863.327
SCVPLB1015D09	vip1 protein	21	159.6792	E-21	NE-21	35136.33	24987.25	47390.15	23485.42
SCCCCL6004A10	succinyl- ligase beta-chain ligase beta-chain	73	622.0395	E-21	NE-21	200257.6	163278.7	209832	154238.3
SCCCCL3001A05	acoc_orysj	83	768.8705	E-21	NE-21	382800.1	194173.1	396829.5	184156.7
P00489	PYGM_RABIT Glycogen phosphorylase...	40	250.9546	NE-0	E-21	55047.29	80009.64	42201.15	76109.81
SCMCRT2103C07	acidic leucine-rich nuclear phosphoprotein 32...	25	214.9496	E-0	NE-21	30444.34	15093.86	21931.63	14378.68
SCEZLR1052F04	mitochondrial atp synthase precursor	348	2614.9436	E-21	NE-21	477559.5	475156.8	564870	452741.6
SCCCCL4007E05	diphosphate-fructose-6-phosphate...	29	186.7013	E-21	NE-21	5047.84	1229.181	5479.865	1178.199
SCBGFL5077B05	sap domain containing expressed	36	212.062	NE-0	E-0	30134.77	55889.39	30600.65	53681.94
SCCCRZ2004B10	3-isopropylmalate dehydrogenase	56	433.1876	E-21	E-0	74361.05	94099.22	107285.5	90406.2
SCSGAM2105D01	ubiquitin-activating enzyme e1 expressed	99	733.3053	NE-0	E-21	163905	235930.1	162598.9	226733.9
SCEQLR1091D05	60s ribosomal protein l5-1	413	3353.6115	NE-0	E-21	616271.9	1305998	576340.7	1257170
SCQSLB1052H09	ubiquitin 11	224	1440.2458	E-0	NE-21	226826.8	120700.9	205361	116594.1
SCQSRT2034F02	proline iminopeptidase-like	25	154.2862	E-0	NE-21	28462.36	14980.24	19199.36	14489.87
SCSBFL5015D06	snf1-related protein kinase regulatory subunit...	16	87.3172	E-0	E-21	4813.092	3883.842	2456.041	3765.678
SCCCCL3120F12	rh40_orysj	36	219.1224	E-0	NE-21	23847.74	10600.99	22310.53	10351.01
SCRFHR1007E11	cop9 signalosome complex subunit 6a	56	371.1732	E-0	NE-21	37362.75	20016.46	32685.37	19563.76
SCCCAM2C08A07	senescence-associated protein dh	7	37.8831	E-0	E-21	2890.548	2502.012	2203.827	2454.084
SCCCCCL4008A08	loc100282868 precursor	12	77.1027	E-0	NE-21	12800.81	3146.509	5709.609	3092.195
SCBGST3105A03	glyoxylate reductase	1	8.7718	NE-0	E-21	404.5068	14346.22	328.7608	14160.24
SCJLRZ1027C05	dna-damage inducible protein	14	110.6966	NE-0	E-21	11443.65	18147.02	10588.12	18015.29
SCCCCL3002A09.b	alanine aminotransferase	80	678.0574	NE-0	E-0	202204.6	505406	203762.3	502113.9
SCACCL6010C02	bifunctional aspartokinase homoserine...	85	487.475	NE-0	E-21	65739.17	86571.58	47541	86020.39
SCJLLR1105C04	nadp-specific isocitrate dehydrogenase	57	502.0314	NE-0	E-0	92510.06	112355.3	109416.8	111713.7
SCCCCRZ2002F04	clh1_orysj	60	465.982	NE-0	E-21	100014.8	124453.4	76329.71	123804.9
SCJLRT1020A08	aglu_orysj	42	295.2149	NE-0	E-0	19244.59	150781.1	21605.46	150497.3
SCJFLR2035A04	rnase h domain-containing protein	4	21.6426	E-0	NE-21	1167.399	144.9018	435.074	144.6489
SCCCLB1025F10	secondary cell wall-related glycosyltransferase...	7	37.07	E-0	NE-21	2680.56	412.7753	1629.088	412.4008
SCEQRT1025E03	cysteine proteinase inhibitor	162	1195.8613	NE-21	E-0	275449.6	440534.2	396208.1	440547.3
SCEPLR1051C09	multidomain cystatin	16	147.907	E-21	NE-0	61441.32	28034.2	63438.25	28044.22
SCSGFL1078C02	phytanoyl- dioxygenase domain-containing...	9	62.8412	E-0	NE-0	41729.73	9043.181	38538.06	9084.32
SCMCST1054G01	3-mercaptopyruvate sulfurtransferase-like...	12	67.7397	E-21	NE-0	12314.11	10662.4	12490.04	10729.29
SCEQRZ3089H09	metal ion binding protein	4	17.6808	NE-21	E-0	1701.247	15213.95	1875.499	15425.23

Table S1 cont.

SUCEST accession	Description	Peptide count	Confidence score	Highest mean condition	Lowest mean condition	E-0	NE-0	E-21	NE-21
SCUTSD1085B08	adenine nucleotide translocator	52	409.9623	E-0	NE-0	66774.71	25403.42	63463.33	25854.91
SCJFRT1007H07	af271894_1 lipoxygenase	38	207.7176	NE-21	E-0	10665.81	15031.55	11843.78	15299.31
SCSGRZ3061H04	cycloartenol-c-24-methyltransferase 1	10	59.9545	NE-21	E-21	32710.04	33930.2	16234.64	34635.37
SCAGLR1021H11	nadh-ubiquinone oxidoreductase 13 kda-b subunit	118	810.5534	E-21	NE-0	175022.7	133216.1	201999.6	135991.9
SCQGLR1041H04	aquaporin pip2-1	21	170.9123	E-0	NE-0	75480.15	18161.01	55717.89	18546.79
SCQSLB2055F11.b	bri1-kd interacting protein 103	25	161.8403	E-21	NE-0	10050.31	5301.024	12324.36	5430.382
SCRFL4004D05	udp-glucuronic acid decarboxylase	22	128.2554	NE-21	E-0	18707.44	125930.8	22839.65	129314.4
SCRFLR1055E09	alpha-soluble nsf attachment protein	39	270.6368	E-0	NE-0	25086.5	15128.36	21985.48	15580.72
SCJFLR1073D03	gsa_orysj	18	114.6194	E-21	NE-0	8252.239	7086.912	8553.328	7314.693
SCUTLR1015G05	auxin-independent growth promoter	5	26.843	E-0	E-21	4183.449	1356.207	202.1771	1400.345
SCMCSD1059B05	argininosuccinate synthase	67	469.7506	E-21	NE-0	148344.2	70118.19	221706.7	72638.41
SCEPLR1030A02	stress-related protein	21	121.325	E-0	NE-0	61506.73	7803.571	23249.67	8108.076
SCJLLB2077A12	heat shock protein 90	621	5280.6091	E-0	NE-0	1404223	1068935	1344565	1110969
SCQSRT2033A11	ras gtpase-activating protein-binding protein 1-like	8	53.3578	E-0	E-21	4432.478	3189.202	2604.93	3316.552
SCAGLB1070D03	protein disulfide isomerase	575	4019.7566	E-21	E-0	999001.7	1135185	1487718	1182717
SCEPFL3082H10	copper chaperone	17	157.652	E-21	NE-0	77342.9	54884.27	107173.7	57199.94
SCRUFL1118G01.b	ago4b_orysj	27	163.1605	E-21	NE-0	25806.41	25803.79	28345.79	26929.96
SCCCRT2002G04	tktc_maize	38	303.029	NE-21	E-21	45643.09	100909.8	34290.13	105367.1
SCCCRT2001H08	ap-1 complex subunit gamma-1	8	47.958	NE-21	E-21	3217.953	8204.493	658.4614	8605.073
SCEPLR1030H09	dynamin like protein 2a	12	67.3017	NE-21	E-0	5427.083	8373.557	7318.93	8808.275
SCCCLR1048A06	super-oxide dismutase	20	206.7179	NE-21	E-0	90410.08	151270.2	105994.7	159308.8
SCEPLR1051C05	cystathionine gamma-synthase	12	83.6517	NE-21	E-21	2814.152	4085.836	2192.489	4303.821
SCCCLR1072B10	26s proteasome non-atpase regulatory subunit 6	405	3093.8801	E-21	NE-0	713145.1	540558.8	1154515	574143.5
SCCCHR1001E04	class iv family protein	37	302.5096	NE-21	E-21	153727	153717	88550.83	163478.4
SCEQHR1079G09	haloacid dehalogenase-like hydrolase...	23	132.6663	NE-21	E-0	26123.77	48774.03	34577.33	51891.08
SCEQLB2020F06	mitochondrial-processing peptidase beta subunit	105	834.0594	NE-21	E-0	170107.4	287188.9	299087.2	306005.5
SCJLFL1053H07	bsl2_orysj	2	9.1788	NE-21	E-21	1347.884	2990.377	597.0121	3189.799
SCEPAM1015E11	rubisco subunit binding-protein beta subunit	13	75.852	E-0	NE-0	31271.86	1463.795	6771.609	1562.146
SCAGLR1043G11	40s ribosomal protein s3	394	3253.4612	NE-21	E-0	734524.5	1140312	920593.8	1233218
SCCCRZ2C01E11	ill1_orysj	11	91.9757	E-21	NE-0	15609.7	4696.915	22657.71	5089.189
SCCCLR2C03H03	at5g19150 t24g5_50	26	165.4289	NE-21	E-21	22707.2	23268.44	10471.95	25241.56
SCBGLR1096H12	propionyl- carboxylase beta chain	17	118.9826	E-0	NE-0	35097.72	11590.03	21252.65	12687.71
SCEQRT2027H04	dolichyl-diphosphooligosaccharide--protein...	29	173.5003	E-21	NE-0	10693.52	9345.925	14919.41	10233.88
SCACAM1070F09	ima1b_orysj	25	196.6967	NE-21	E-21	26262.97	30810.96	21914.93	34095.46

Table S1 cont.

SUCEST accession	Description	Peptide count	Confidence score	Highest mean condition	Lowest mean condition	E-0	NE-0	E-21	NE-21
SCCCCL3004C10.b	transaminase transferring nitrogenous groups	29	202.3379	E-21	E-0	9621.908	20176.19	28526.65	22420.29
SCVPRT2073B10	glyoxysomal fatty acid beta-oxidation...	56	387.5833	E-21	NE-0	68268.35	41793.45	103147.6	46585.84
SCSGRT2066A01	fumarylacetoacetate hydrolase	21	158.0197	E-21	NE-0	33086.21	19053.84	39659.45	21258.4
SCCCCL4014B10	presequence protease chloroplastic mitochondrial...	28	174.8154	E-21	NE-0	20054.32	10205.61	107555.1	11455.01
SCJFRT2059E04	puromycin-sensitive aminopeptidase isoform 1	25	170.3212	NE-21	E-21	38388.13	35881.97	32707.55	40376.22
SCCCCRZ1004H06	glutaredoxin subgroup i	24	183.4941	E-0	NE-0	51039.19	14299.07	41353.84	16127.11
SCQGST1033G06	cob22_orysj	17	100.4087	NE-21	E-21	3673.939	21220.27	1573.117	24160.69
SCRFAM1025D12	valyl trna synthetase	19	129.4339	E-21	E-0	8378.943	9528.301	11991.85	10854.33
SCUTFL1062H05	ubiquitin-like protein	23	215.7332	E-21	NE-0	12598.82	3215.468	31146.56	3677.824
SCCCCRZ2C03E03	wound stress protein precursor	7	43.3138	E-0	NE-0	10780.18	2555.116	9962.961	2937.639
SCEZAM2059G02	thioredoxin-like 1	12	79.0355	E-0	NE-0	12951.78	6472.717	10242.02	7473.954
SCCCCL4001H04	coatomer subunit delta	58	377.3979	E-0	NE-0	64114.69	24244.12	32083.11	28091.67
SCQSRT1035G12	universal stress protein family expressed	8	51.7592	E-21	NE-0	2424.146	1185.589	4750.498	1374.017
SCQSST3116B04	qltg3-1	6	48.0942	E-21	NE-0	9187.646	7121.796	39501.46	8270.209
SCBGRT1047D12	hxk3_orysj	12	70.3645	NE-21	E-21	44664.15	46667.32	31618.61	54268.7
SCEQRT1028A07	lactate dehydrogenase	6	35.1814	NE-21	E-21	2032.269	6471.751	1904.016	7536.504
SCCCCL3001F05	ru large subunit-binding protein subunit beta	118	953.4877	NE-21	E-21	188671.4	180628.2	176587.5	211816.9
SCJFRZ2033E06	stomatin-like protein 2	34	214.2932	E-0	NE-0	47319.8	22415.5	40269.05	26298.93
SCMCCL6050B01	branched-chain-amino-acid aminotransferase	23	154.3267	E-21	NE-0	45488.53	10861.08	47427.96	12747.03
SCCCCL7001C09	suppressor enhancer of lin-12 protein 9 precursor	26	192.1813	NE-21	E-0	15255.58	27529.94	17062.81	32376.29
SCCCCRZ1003A10	cell division cycle protein expressed	153	1261.2591	NE-21	E-0	332895.1	420749.2	337471	494924.8
SCVPRZ2042B04	protease candidate1	100	635.5616	E-0	NE-0	147217.5	96500.64	108618.3	113881.1
SCVPRZ2043H12	methionine synthase protein	44	332.3212	E-21	NE-0	31496.72	10282.8	34402.68	12135.85
SCCCCRZ1003E07	moco containing protein	7	49.4682	E-0	NE-0	1340.946	461.4353	995.2368	550.8515
SCVPLR1049C03	methylmalonate semi-aldehyde dehydrogenase	39	286.8357	E-0	NE-0	86217.27	43079.56	71486.13	51461.55
SCJFRT1007A12	ethylene receptor	6	34.2764	E-21	NE-0	1297.331	350.6846	2686.527	419.5365
SCBFRT1069A05	mrna capping c-terminal domain containing...	24	149.8674	E-0	NE-0	26037.84	18122.24	19213.34	21719.97
SCCCLR1024D02	atp-citrate expressed	62	466.261	NE-21	E-21	72774.39	77207	63597.36	92545.76
SCMCRZ3067G02	atypical receptor-like kinase mark precursor	30	170.0077	E-0	NE-0	27493.07	8792.677	19344.25	10554.63
SCMCLR1010F10	fip1 motif family expressed	3	17.2944	NE-21	E-21	553.0657	3785.652	351.7943	4546.825
SCMCST1050A01	nucleoporin nup43	11	68.013	E-21	NE-0	16260.2	3460.165	17239.78	4163.922
SCCCST1002C11	loc100281207 precursor	4	24.8516	NE-21	E-21	3068.106	5953.97	2565.706	7172.015
SCEPCL6019A06	prolyl endopeptidase	21	150.5659	NE-21	E-21	28167.73	28859.55	15860.29	34820.55
SCJFRT2055F03.b	succinate dehydrogenase flavoprotein precursor	81	630.6849	NE-21	NE-0	166367.5	151404.4	160946.9	183652.2

Table S1 cont.

SUCEST accession	Description	Peptide count	Confidence score	Highest mean condition	Lowest mean condition	E-0	NE-0	E-21	NE-21
SCJLRT2049D05	heme-binding protein 2	14	145.3774	E-0	NE-0	138552.9	10760.01	88564.24	13095.66
SCEPAM1051A02	predicted protein [Hordeum vulgare subsp. vulgare]	11	57.3682	NE-21	E-0	2537.247	7613.048	5394.041	9300.845
SCAGLR2011G10	ob-fold nucleic acid binding domain containing...	16	147.7353	E-0	NE-0	43497.08	19099.52	33001.49	23379.74
SCCCLR1001F10	fact complex subunit spt16	21	123.9478	E-0	NE-0	12100.22	3265.551	7170.555	4004.201
SCCCRZ1002D03	pinin sdk mema protein conserved region...	5	23.8042	E-0	E-21	1970.916	1067.075	401.0014	1311.418
SCBFRZ2016E05	zinc finger transcription factor zfp30	40	238.4418	E-21	NE-0	12706.34	11528.82	39464.63	14181.21
SCCCCL4004A04	ras-related protein rab-2-a	105	700.8236	E-0	NE-0	44214.92	29537.13	39707.29	36366.14
SCBGRH1058B11	pp2ac-2 - phosphatase 2a isoform 2 belonging...	14	88.7217	E-0	E-21	2415.739	1400.939	795.6635	1725.677
SCJFST1011D09	dag protein	14	86.0034	NE-21	E-21	40059.28	52431.24	39722.88	65260.43
SCRFLR1012E06	scrk1_maize	32	335.8111	NE-21	NE-0	205384.2	200720.9	208936.4	249934.2
SCRURT2005F02	bowman-birk serine protease inhibitor precursor	9	74.2667	NE-21	E-21	12867.06	113296.5	11053.55	141584
SCEPAM2055H02	legumin-like protein	13	94.475	E-21	NE-0	42608	18363.68	59377.46	23071.9
SCCCLR2001B02	carbamoyl-phosphate synthase small chain	21	146.7265	NE-21	E-0	8297.006	11364.45	8601.214	14298.93
SCCCRZ1001B12	rhamnose biosynthetic enzyme expressed	17	97.925	NE-21	E-0	1579.386	3469.244	2805.366	4369.419
SCJLRZ1024A04	af465643_1 lipoxygenase	79	547.9581	NE-21	E-21	79446.95	121314.6	62498.72	153402
SCEQLR1029D10	acetyl-coenzyme a carboxylase	11	52.8785	NE-21	E-21	2890.338	8286.234	1604.966	10517.6
SCCCCL3001F10	ribosomal protein component of cytosolic...	22	191.6009	NE-21	E-21	480.7644	1539.105	318.8181	1955.506
SCEPAM1015F11	n-acetyl-gamma-glutamyl-phosphate reductase	28	176.3599	E-21	NE-0	34731.71	10999.42	39366.14	13986.46
SCCCLR2002G03	inorganic pyrophosphatase	55	372.5985	NE-21	E-21	25592.12	53542.32	24884.91	68423.48
SCCCCL3001C07.b	alpha tubulin	72	669.6514	E-21	NE-0	128890.9	80791.83	130596.8	103345
SCEPSB1135E11	vacuolar atp synthase subunit g	302	2115.1985	E-21	NE-0	317051.7	315335.8	419811.4	404419.2
SCRUSB1063D08	aminoacylasE-0 precursor	16	90.2429	E-0	E-21	16088.28	10051.54	8655.785	12898.89
SCVPFL3047F02.b	purple acid phosphatase precursor	29	203.5377	E-0	NE-0	49988.84	30447.57	47708.35	39203.73
SCRFLR1034D01	p68 rna helicase	19	119.8216	E-0	NE-0	13917.87	10146.25	13258.77	13104.54
SCCCLR1C01B06	dj-1 family protein	8	61.6831	NE-21	E-0	5287.953	10774.77	7079.429	14004.85
SCAGRT3047C03	peptidyl- cis-trans isomerase	127	991.8356	NE-21	E-0	404455.7	609752.3	559338	796457.8
SCSGHR1066E03	cold shock protein-1	10	104.5509	E-0	NE-0	15271.17	5570.054	7749.754	7300.073
SCCCHR1002H03	6-phosphogluconate decarboxylating	50	412.7844	E-21	E-0	42308.74	51196.06	80027.77	67374.03
SCRLLR1038E03	---NA---	389	2459.316	E-21	NE-0	343523.5	168499.4	374987.1	221767.9
SCEZLR1031A11	acetyl- cytosolic 1	34	212.4588	E-21	E-0	21700.13	23520.74	61964.22	31014
SCJFRZ1006H10	threonine synthase	21	144.9893	NE-21	NE-0	16518.85	13470.36	14217.22	17766.35
SCSGLR1045G02	rh9_orysj	10	54.8735	E-0	E-21	7853.337	4078.961	2357.435	5382.759
SCMCRT2107G02	aspartate-semialdehyde dehydrogenase	12	103.813	E-21	NE-0	25829.11	20631.46	30040.75	27257.55
SCUTSD1024F06	3-ketoacyl- thiolase peroxisomal precursor	26	238.7143	E-21	NE-0	108690.2	37748.4	113640.9	50057.1

Table S1 cont.

SUCEST accession	Description	Peptide count	Confidence score	Highest mean condition	Lowest mean condition	E-0	NE-0	E-21	NE-21
SCCCCL5002H02	globulin-1 s allele precursor	20	265.8498	E-21	NE-0	82181.6	21216.6	457292.2	28227.8
SCQSRT1034D04	transmembrane 9 superfamily protein member 4	18	112.6511	NE-21	E-0	380.4992	14427.35	921.0051	19546.78
SCJFRZ2027G04	phenylalanyl-tRNA synthetase beta chain	35	201.2606	NE-21	E-0	34885.21	54565.86	52370.81	73952.76
SCJFRT1009E03	maize insect resistance1 precursor	8	66.0039	NE-21	E-0	384.4646	15976.62	745.5031	21687.91
SCCCLR1C01H06	topoisomerase-like protein	19	116.4818	E-21	NE-0	22874.32	5583.625	46788.92	7584.866
SCRLFL4025A02	af458962_1 cdc5 protein	17	89.5041	E-0	NE-0	5145.047	1434.214	2650.658	1953.87
SCQGLR1062D04	udp-glucose pyrophosphorylase	115	1016.7641	NE-21	E-21	377805.3	491240.9	360357.4	669449
SCCCCL4011B08	2-isopropylmalate synthase b	80	659.0114	E-0	NE-0	212387.4	122253.9	189894.7	166916.3
SCQSRT1034D03	loc100282597 precursor	13	80.1427	NE-21	E-21	8765.896	12396.74	4276.14	16949.74
SCCCCL3080H09.b	glutamate dehydrogenase	49	310.2596	NE-21	E-0	34070.8	46302.3	42390.75	63347.22
SCSGAM2105G02	mar binding protein	5	29.3544	E-0	NE-0	4918.739	230.5194	1825.902	316.1165
SCCCRT2004D04	alcohol dehydrogenase 1	89	861.8701	NE-21	E-0	315919.3	715396.4	369319.1	984478.7
SCCCRT2001B05	aminolevulinic acid dehydratase	26	171.1902	E-21	NE-0	14924.84	8168.829	22587.5	11284.3
SCJFL4098H05	tip120 protein	40	248.1536	NE-21	E-21	28672.93	27495.89	24687.29	37989.71
SCUTLR2023D11	aldehyde dehydrogenase family 7 member a1	38	255.0943	E-0	NE-0	60259.48	35711.93	53284.55	49467.38
SCEQLR1050G04	dihydrodipicolinate synthase 2	14	80.496	E-0	NE-0	7433.244	3244.413	5212.532	4545.602
SCCCRZ1003A11	glutamine synthetase	51	457.7516	NE-21	E-0	94232.76	274729.8	146333.6	385881.8
SCBGLR1023B04	udp-sulfoquinovose synthase	16	92.6635	E-0	NE-0	16530.31	8614.156	13320.13	12104.48
SCCCCCL3001H07	f-box ankyrin repeat protein skip35-like	21	122.3541	NE-21	E-0	12609.29	18044.71	15741.29	25522.43
SCQSLR1018B02	chromosome region maintenance protein	15	102.5908	NE-21	E-0	3056.833	6784.304	3963.241	9616.037
SCCCRZ2003A07	aminopeptidase m	87	598.4648	NE-21	E-21	110617.9	97053.93	92684.49	137589.4
SCSBSD2058B02	aldose 1-epimerase	19	121.8085	NE-21	E-0	4892.929	26869.36	7885.853	38130.83
SCRFRZ3059F04	uridine monophosphate synthase	19	118.7684	E-21	NE-0	28360.23	12215.18	30418.28	17342.09
SCJLRZ1019A04	calcium-dependent protein kinase sk5-like	45	280.2227	E-0	NE-0	29661.68	7439.057	12142.09	10590.72
SCCCRZ1001C05	phosphoglycerate kinase	97	849.4121	NE-21	E-0	309307.2	379834.6	355789.9	541411
SCBGLR1027E10	3-hydroxyisobutyryl- hydrolase-like protein...	7	44.4597	E-0	NE-0	6697.5	1751.861	2999.477	2503.341
SCCCST1002D07	glyoxalase i	26	204.2009	NE-21	E-0	101601.4	194117.3	121108.3	277624.3
SCJLLR1033A07	hydroxyacylglutathione hydrolase	30	204.0219	E-0	NE-0	95237.97	65068.47	93782.52	93321.25
SCJFRZ2010G03	r40c1 protein - rice	31	372.5379	NE-21	E-0	224111.3	302982.3	276490.4	436147.7
SCCCLR1C01C08	chloroplast outer envelope 86-like protein	50	306.1569	E-0	NE-0	45060.27	16676.13	25635.49	24010.59
SCVPRT2075E07	c-1-tetrahydrofolate cytoplasmic	11	69.6575	E-0	NE-0	26721.03	3533.091	20813.83	5097.71
SCCCCCL3002F02.b	betaine aldehyde dehydrogenase	34	282.924	E-21	NE-0	57725.95	43964.56	68680.09	63525.59
SCEQRT1029D09	glucose-6-phosphate isomerase	133	905.1306	NE-21	E-0	105731	138714.9	109463	200525.1
SCRLFL1004D11	dihydroxy-acid dehydratase	36	349.203	E-0	NE-0	104953.3	63244.99	101291.8	92142.34

Table S1 cont.

SUCEST accession	Description	Peptide count	Confidence score	Highest mean condition	Lowest mean condition	E-0	NE-0	E-21	NE-21
SCQGLR1019B02	ferredoxin-sulfite reductase precursor	28	197.9992	E-0	E-21	61646.55	33767.91	32806.94	49253.7
SCEPAM2053F09	cyclase dehydrase family protein	17	133.167	E-21	NE-0	17463.18	6281.617	21660.67	9210.173
SCJFRZ2031F10	acetyltransferase 1-like	8	51.5425	NE-21	E-0	10369.8	13683.24	10371.67	20121.15
SCEPCL6021H04	cytochrome b5	120	991.5899	NE-21	NE-0	236304.3	183604.4	243752.6	270263.5
SCCCLR1C05E01	signal recognition particle 9 kda protein	20	121.976	NE-21	E-0	8539.665	25458.94	10901.45	37540.98
SCCCLR1076E03	brassinosteroid biosynthesis-like protein	36	215.9217	NE-21	E-21	20966.05	16219.72	10917.65	24003.16
SCVPLR1028C10	ornithine carbamoyltransferase	25	177.9965	NE-21	E-21	17607.61	21077.51	14434.94	31295.4
SCJLLR1054H06	pur alpha-1	14	80.6289	E-0	NE-0	18506.65	7837.401	12761.71	11744.34
SCCCCL3001C03	citrate synthase mitochondrial expressed	61	461.2317	NE-21	NE-0	159397.4	126388	141184.1	189466.9
SCCCCL4003G01	serine-threonine kinase receptor-associated protein	19	100.2133	E-0	NE-0	12959.93	5153.485	11203.1	7725.854
SCJFRZ1007H03	aspartate kinase-homoserine dehydrogenase	121	956.9267	NE-21	E-0	215527.3	235045.6	305899.5	352380.5
SCBFLR1083D11	seryl-tRNA synthetase	34	201.9085	NE-21	NE-0	17802.41	14209.1	17716.95	21429.02
SCCCRT1002A01	importin alpha-2 subunit	19	113.4126	NE-21	E-21	11646.02	20079.64	8296.315	30368.05
SCJFRT2057F01	subtilisin-like proteinase	17	97.3431	NE-21	E-21	7817.369	22807.2	7589.001	34792.62
SCRFLT3058D06	rh52b_orysj	40	271.0959	E-0	NE-0	16649.44	3018.379	7659.141	4622.378
SCMCLR1123A03	vhs and gat domain protein	13	67.8877	NE-21	E-0	1776.447	2640.003	2114.112	4050.854
SCJFST1015G05	dnaj protein	17	98.3281	E-0	NE-0	5239.415	1964.189	4459.301	3016.247
SCJFRZ2025F03	farnesylcysteine lyase-like	5	28.287	E-0	NE-0	4885.708	2515.415	3799.67	3869.415
SCAGHR1016D09	acetolactate small	20	154.4059	NE-21	E-21	19396.47	29239.07	8721.339	45499.67
SCRFLR2034B06	at-hook protein 1	16	95.2811	NE-21	NE-0	7342.632	4754.321	5388.878	7467.916
SCSGRT2066B08	rh52c_orysj	15	106.8476	NE-21	E-0	1309.541	14114.26	2112.538	22183.35
SCJFRZ2032H05	tubulin-specific chaperone a	9	64.93	E-21	NE-0	12034.44	6456.251	18514.77	10166.81
SCCCLR2C02F10	alpha chain complex of hsp90 n-terminal and sgt1 cs...	30	346.3485	NE-21	E-21	21972.75	48010.27	17560.82	75629.67
SCEZLR1031E10	translationally-controlled tumor protein	12	125.9446	NE-21	E-21	44786.28	44482.63	31590.9	70360.5
SCAGRT2039A02	asparagine synthetase	24	142.802	E-21	NE-0	12988.34	6238.179	24271.43	9899.098
SCCCFL6001G05	auxin response factor 7a	20	108.7202	E-21	NE-0	4536.967	3130.943	5188.852	4981.613
SCJFST1015F01	glycoside family 28 precursor	9	50.6523	NE-21	E-0	565.7834	1951.493	2085.221	3119.36
SCSGAM2076D04	actin [Brassica napus var. napus]	42	399.5254	NE-21	E-0	8028.612	10639.38	13549.69	17096.08
SCEPFL4175E04	gtp-binding protein	111	855.4305	NE-21	NE-0	109429.6	108118.5	156686.3	173767.6
SCSFFL3090D03	h2b1_wheat	11	108.8972	NE-21	E-0	1488.735	5637.372	2421.792	9085.678
SCJFRZ3C03A07.b	d-amino acid oxidase	6	33.1243	NE-21	E-21	6096.713	5715.711	2498.878	9245.482
SCCCLR1004G11	transcription factor apf1	152	989.8626	E-0	NE-0	181263.2	78276.84	174570.2	126622.9
SCCCLR2003A05	cullin- expressed	8	40.1554	NE-21	E-21	3191.496	5004.104	1576.257	8096.117
SCEQRT2094H09	receptor-mediated endocytosis 1 isoform i	8	45.8398	NE-21	E-0	453.6316	749.1057	667.2405	1213.935

Table S1 cont.

SUCEST accession	Description	Peptide count	Confidence score	Highest mean condition	Lowest mean condition	E-0	NE-0	E-21	NE-21
SCSFRT2068B02	receptor-like kinase	17	104.9318	E-21	NE-0	4131.051	1774.282	5107.771	2897.995
SCJFLR1074A06	pdi-like protein	40	330.8388	E-0	NE-0	183540.1	107895.2	157599.2	177371.3
SCCCCL3120E12	at1g05520 t25n20_16	13	70.7751	NE-21	E-21	2705.186	11726.74	1518.933	19324.37
SCEZRZ1013F01	cullin-1-like isoform 1	33	198.0795	NE-21	E-0	7829.818	25037.35	15623.14	41650.58
SCJFRZ2005G03	swib mdm2 domain containing protein	19	147.6731	E-21	NE-0	22951.72	4222.274	26844.58	7029.609
SCVPLR1049A01	smc3 protein	42	225.6356	NE-21	E-21	12048.24	11200.47	10280.78	18665.82
SCCCLR1070A12	dihydrolipoyllysine-residue succinyltransferase...	37	257.8554	E-21	NE-0	96013.11	34774.6	100769.1	58054.22
SCCCCL4011H03	ribulose-phosphate 3-epimerase	6	44.5961	NE-21	E-21	9744.957	13348.71	9176.036	22435.05
SCJLLR1011F03	ketol-acid chloroplastic-like	54	440.086	NE-21	E-0	171108.5	223383.2	188328.1	375617.3
SCCCCRZ2002H11	pentatricopeptide repeat-containing protein...	50	296.6477	NE-21	E-0	15523.22	15804.1	20478.14	26739.4
SCCCCHR1004H09	choline-phosphate cytidylyltransferase b	5	29.7236	E-21	NE-0	1667.216	1123.523	2645.953	1904.696
SCCCAM1001G03	beta-ketoacyl-acp synthase	9	48.2706	NE-21	NE-0	4649.644	3224.028	4142.611	5506.579
SCRLLR1109C03	arginine serine-rich splicing factor	14	79.1207	E-21	NE-0	11569.13	2052.711	12240.41	3509.128
SCQGLR1086B07	selenium binding protein	19	127.7782	E-21	NE-0	7698.515	3268.772	44171.77	5606.784
SCUTST3090E03	unknow protein	11	55.1742	E-21	NE-0	3098.405	2604.365	4829.062	4506.125
SCQSRT1036D03	pathogenesis-related protein 1	19	157.4153	NE-21	E-21	8623.274	40430.5	6541.682	70516.4
SCCCCL3002C07.b	amy3c_orysj	22	221.7233	E-0	NE-0	118016.9	7184.268	66777.42	12595.85
SCVPLR2027B06	ubiquitin-associated ts-n domain-containing	12	81.2512	NE-21	E-21	15910.05	12810.09	1541.389	22560.89
SCQSRT2036A12	monodehydroascorbate reductase	53	423.8478	NE-21	E-0	87285.34	94612.6	112541	167025.4
SCCCRZ1001E09	uncharacterized protein LOC100191561 [Zea mays]	329	2248.5165	E-0	NE-0	228858.8	110777.8	225016.6	195636.9
SCCCLR1C04E01	wheat adenosylhomocysteinase-like protein	39	441.5666	NE-21	NE-0	217368.5	180554.2	283080.5	321103.5
SCBFSB1049C11	cgep_orysj	8	39.862	NE-21	E-0	2957.885	4772.647	4667.987	8504.882
SCRLLR1059B07	like protein	15	110.2418	E-0	NE-0	6800.722	2304.057	6486.117	4120.669
SCCCLR1001B11	pyridoxin biosynthesis protein er1	12	96.5465	NE-21	E-0	19475.31	37711.94	34624.76	67730.24
SCCCCCL3001B09.b	aconitate hydratase 1	106	793.2703	NE-21	E-0	125324.8	147981.7	145864.5	267525.8
SCCCLR1022D04	mdhg_orysj	10	76.2918	E-0	NE-0	8740.465	2769.662	5426.668	5007.454
SCJLRT1014A07	ac090882_14 dehydratase deaminase	5	23.1247	NE-21	NE-0	1062.78	745.2839	960.77	1348.763
SCRLRT3033C05	gibberellin 20 oxidase 2	28	171.3414	NE-21	E-21	4072.503	26679.31	3579.308	48492.59
SCJLLR1107G02	late-embryogenesis-abundant protein	8	60.6813	E-0	NE-0	33245.43	6074.199	19980.44	11049.53
SCCCCL1001A02	translocase of chloroplast 34	15	90.3312	E-0	NE-0	11396.76	5444.552	10983.96	9912.481
SCCCCL7037A10	loc100282411 precursor	27	247.3887	NE-21	E-21	69744.79	105846	58123.57	193589.7
SCUTFL3075D02	thioredoxin domain-containing protein 9	88	665.9546	NE-21	E-0	177307	190994.5	214851.4	351326.9
SCRFLR2034A07	ma3 domain-containing protein	33	272.9223	E-0	NE-0	76354.49	28008.09	50187.56	51823.68
SCQSRT2034G08	alpha-galactosidase expressed	26	173.2528	NE-21	E-21	5217.268	65524.54	3819.028	121285.9

Table S1 cont.

SUCEST accession	Description	Peptide count	Confidence score	Highest mean condition	Lowest mean condition	E-0	NE-0	E-21	NE-21
SCEZAM2059G08	ppwp domain containing protein	4	24.4405	E-0	NE-0	7140.614	268.4423	811.5248	502.5144
SCMCRZ3068H09	s-adenosylmethionine synthetase 1	19	151.1013	NE-21	E-0	1848.258	12281.99	2505.215	23113.9
SCEQLR1091F06	sorbitol dehydrogenase	30	284.4472	E-21	NE-0	116466	31413.24	167142.1	59651.2
SCCCLR1C05F08	fumarate hydratase chloroplastic-like	19	129.2365	E-0	NE-0	21137.66	7143.467	18879.05	13640.97
SCJLRT1014F08	progesterone 5-beta-	9	62.509	NE-21	E-0	5806.666	6867.778	11005.56	13304.04
SCACRZ3109E01	xaa-pro aminopeptidase 1	25	163.0807	NE-21	E-0	9572.21	10963.84	11514.54	21308.39
SCUTLR2023H05	r40g2 protein	23	221.494	NE-21	E-0	7703.439	17602.11	31186.44	34541.32
SCACLR2007H10	va0d_orysj	8	51.4652	NE-21	E-21	2989.956	15511.95	428.9026	31064
SCCCCL4013H06	coproporphyrinogen iii oxidase	19	135.6832	NE-21	E-21	24151.03	27019.77	20355.45	54416.96
SCSBRZ3117C09	clpc1_orysj	55	352.4594	E-21	NE-0	20172.2	7061.096	41075.3	14877.87
SCRULB1060C09	cathepsin b-like	17	133.737	NE-21	E-21	25132.57	46530.27	21095.82	99015.48
SCCCLR1C07C11	fiber protein fb15	4	40.9095	NE-21	E-21	2800.244	2967.319	2411.688	6325.932
SCCCLR1065E09	3-dehydroquinate synthase	19	127.9345	NE-21	E-21	8311.268	18401.9	5941.92	39236.58
SCQGLR1019B10	ac077693_3 eukaryotic initiation factor subunit	19	142.0314	E-21	NE-0	15553.62	2005.269	19065.23	4283.104
SCEQRT2095D10	gdp-mannose -epimerase 1	40	298.3393	E-21	NE-0	15608.31	12066.73	32949.84	25947.64
SCCCCL4007F09	adenylosuccinate lyase	30	218.9687	NE-21	E-21	13769.58	27693.02	10373.83	59589.14
SCCCLR1065D04	beta-cyanoalanine synthase	5	33.438	NE-21	E-0	238.4804	1076.118	2069.228	2324.78
SCSGFL1083E06	imidazole glycerol phosphate synthase chloroplast...	11	66.4856	E-21	NE-0	7257.865	2535.442	13968.84	5483.522
SCEZLB1010A09	anamorsin homolog	8	43.5762	E-0	NE-0	7638.322	623.2277	5106.552	1356.134
SCMCAM2084F10.b	cigr1_orysj	5	24.9975	NE-21	E-0	808.4208	2573.248	2240.177	5613.158
SCCCCCL4014E03	set domain-containing protein set104	30	178.5288	E-0	NE-0	42396.89	2853.61	12535.67	6252.984
SCMCLB2081E11	dna-dependent atpase snf2h	9	47.0861	NE-21	E-21	1990.877	3774.249	938.3026	8276.813
SCEZLR1031A02	fructose tagatose bisphosphate aldolase	7	43.4762	NE-21	E-0	418.9709	4383.906	708.6348	9623.53
SCBFRZ2045G10	metallopeptidase family m24 containing expressed	16	83.8374	E-0	NE-0	2438.725	981.3237	1103.247	2157.212
SCCCCCL3004C07.b	regulatory protein viviparous-1 protein viviparous-1	8	47.7295	NE-21	E-21	165.2351	3122.073	47.47746	6865.82
SCSGFL5C03H04	chromatin complex subunit a101	12	71.9779	NE-21	NE-0	7285.664	6351.098	6355.65	14070.68
SCSGFL4C03C08	disease resistance response protein 206	12	73.8497	NE-21	E-21	25347.95	34295.6	17178.97	76056.39
SCJFRT1058F10	ferredoxin--nadp root isozyme	22	154.9769	E-21	NE-0	24374.23	8857.359	53189.86	19739.95
SCCCLB1026C11	transposon pong sub-class	52	357.4911	NE-21	E-21	44137.82	28791.7	21797.05	64203.66
SCCCRZ1001F01	chaperone dna j2	43	280.9767	E-0	NE-0	29354.22	11709.75	16493.7	26273.05
SCEPSB1130D06	retrotransposon line subclass	20	136.3313	E-21	NE-0	9178.465	2803.421	12814.13	6381.456
SCBGSD2049D08	cdpk-related protein kinase	3	12.1363	NE-21	E-21	439.6682	1438.646	344.0187	3310.968
SCBFBSB1048E08	ent domain containing protein	9	57.0652	E-0	NE-0	3670.505	190.4852	2541.492	441.2616
SCCCRZ2C01A04	cinnamoyl- reductase	12	71.6016	E-21	NE-0	8586.397	2441.43	10656.51	5661.807

Table S1 cont.

SUCEST accession	Description	Peptide count	Confidence score	Highest mean condition	Lowest mean condition	E-0	NE-0	E-21	NE-21
SCSGFL1083D09	snrnp core sm protein sm-x5-like protein	6	74.7124	NE-21	E-0	4443.626	14633.8	4782.347	34153.27
SCACLR1036C04	pp2a regulatory subunit tap46	15	86.4801	E-0	NE-0	6397.695	1251.437	4439.526	2941.933
SCJLST1022F12	n-ethylmaleimide sensitive fusion protein	9	51.3135	NE-21	E-0	2923.719	11565.36	2961.371	27516.53
SCJLRT1020E04	urate oxidase	6	41.8733	NE-21	E-0	3425.733	4887.648	3776.72	11703.28
SCEPLB1041A06	stad5_orysj	8	46.189	NE-21	NE-0	1267.809	667.0424	1534.473	1602.916
SCACSB1036C04	rvubl1 protein	28	178.2026	NE-21	NE-0	24827.43	10252.01	21015.22	24903.52
SCACLR1036A01	h aca ribonucleoprotein complex subunit 2	7	45.3146	E-0	NE-0	16144.75	1691.947	4487.39	4182.239
SCEQAD1018G06	ramosa 1 enhancer locus 2	29	215.6709	NE-21	NE-0	24081.56	17986.74	25146.16	44636.39
SCJFRZ2025G05	chorismate mutase	28	174.8319	NE-21	E-21	19001.09	12094.21	4606.621	30110.01
SCSFAM1077D01	oxidoreductase [Zea mays]	4	21.5302	NE-21	E-21	755.3486	501.6291	82.62142	1262.165
SCCCRZ1004B05	topless-related protein 1-like	26	161.7293	NE-21	NE-0	8829.038	8449.516	15381.7	21321.71
SCJLLR1033G07	uba ubx kda protein	15	84.003	NE-21	NE-0	2268.045	1346.015	1875.489	3430.943
SCJFFL1C04C08.b	3-n-debenzoyl-2-deoxytaxol n-benzoyltransferase	23	146.1507	NE-21	E-0	7354.013	10140.09	9263.287	26259.26
SCSGLR1045A03	shikimate dehydrogenase1	30	190.7724	E-0	NE-0	71224.86	14565.08	24695.19	37887.26
SCVPCL6046C06	Os04g0543900 [Oryza sativa Japonica Group]	3	17.7088	NE-21	E-21	1220.615	1415.225	100.06	3682.269
SCEZAM2059G06	ribosome recycling factor	17	89.349	E-0	E-21	17052.58	3938.213	3538.494	10269.45
SCEZRZ1012D01	rh37_orysj	29	190.8626	NE-21	NE-0	5115.331	3066.284	3948.095	8013.377
SCCCCL4015F12	xylanase inhibitor	43	421.2061	NE-21	E-21	139803	259774.9	82399.06	678950.7
SCRFAD1116E01	stem-specific protein tsjt1	34	276.8097	E-0	NE-0	84224.95	23838.91	77818	62404.23
SCMCLV1031F09	invertase inhibitor-like	8	70.4384	NE-21	E-0	2163.731	27038.84	2723.95	71024.12
SCEPLB1043E09	rab gdp dissociation inhibitor alpha	25	163.8801	E-21	NE-0	3423.373	2676.743	7295.997	7032.843
SCEZLR1031B05	spfh domain band 7 family	6	34.6506	NE-21	NE-0	4345.645	2976.264	4382.28	7867.49
SCSGST1072B08	cytosol aminopeptidase	16	136.9601	E-21	NE-0	612.8977	389.3293	3859.101	1030.659
SCEPAM1015E02	d-3-phosphoglycerate dehydrogenase	31	294.4057	NE-21	NE-0	326750.2	187075.4	221275.1	498447.3
SCEQRT1030G05	ribose-phosphate pyrophosphokinase 4	14	118.0301	NE-21	NE-0	26046.48	23973.2	27841.22	64399.63
SCCCRT1002E01	stad1_orysj	8	46.97	NE-21	E-0	3903.905	6875.601	5962.644	18702.35
SCJLST1027A10	thiamine thiazole synthase chloroplastic precursor	9	56.0639	NE-21	E-21	3055.331	7117.093	2284.071	19424.24
SCCCCL4017B10	iws1 c-terminus family protein	4	20.8175	NE-21	E-0	489.9689	1540.352	1315.218	4221.65
SCMCCL6051B09	u3 small nucleolar rna-associated protein 25-like	5	24.9419	NE-21	E-21	11521.38	17671.76	1595.531	48995.25
SCJLRZ1027G11	in2-1 protein	9	69.8633	E-21	NE-0	12129.4	5725.117	23303.72	16061.56
SCCCCCL7C03F06	isocitrate dehydrogenase	32	244.3969	E-0	NE-0	24403	6220.061	21570.44	17485.25
SCJFRT1010G02	dynamin-2b-like isoform 1	7	33.0535	E-21	NE-0	6015.886	5999.79	18203.75	16942.4
SCCCCCL4001H11	bgl15_orysj	15	101.3812	E-21	NE-0	3822.912	2200.807	6484.751	6230.069
SCVPRT2083C04	cue domain containing expressed	3	15.2139	E-21	NE-0	5441.777	1082.909	8172.5	3077.681

Table S1 cont.

SUCEST accession	Description	Peptide count	Confidence score	Highest mean condition	Lowest mean condition	E-0	NE-0	E-21	NE-21
SCJLLR1101A05	dcp1-like decapping family protein	7	42.4029	NE-21	E-0	3716.453	5634.838	10559.9	16257.66
SCQSRT2034D09	carbonyl reductase 1	20	148.2089	E-0	NE-0	29878.96	1672.689	23122.39	4949.219
SCCCCL3002B11.b	alpha-amylase isozyme 3d precursor	23	236.2604	E-0	NE-0	154504.3	3261.995	136655.4	9655.833
SCBGS2053C08	abscisic stress ripening protein 2	12	85.7047	NE-21	E-21	5120.264	13486.04	1755.259	39963.07
SCJFAD1012C08	translation elongation factor 1	52	373.8943	NE-21	NE-0	11383.29	4404.694	6885.204	13070.62
SCEPRZ1011H03	pyrroline 5-carboxylate reductase	11	73.9084	NE-21	E-0	3735.677	8580.364	4876.706	25741.32
SCJLAM1062B12	nadph-dependent reductase a1-a	6	30.0011	E-0	NE-0	22699.37	3426.701	20360.12	10341.15
SCCCLB1004B02	atpase subunit 1	11	105.8416	E-21	NE-0	109311.1	29210.41	128329.5	88829.27
SCEPRZ1008B12	macronuclear development protein	12	89.8305	NE-21	E-21	2573.052	2932.062	2338.488	8922.866
SCVPRZ2037B11	dihydropyrimidine dehydrogenase	19	159.4111	E-21	NE-0	24026.93	14750.75	60567.56	45059.51
SCBGLR1113H05	farnesyl pyrophosphate synthetase	12	91.2445	NE-21	E-21	824.645	5621.449	422.5236	17235.47
SCSBAD1085A06	xylose isomerase	35	332.9796	E-0	NE-0	142849	39521.35	112764.8	123477.2
SCEQRZ3024B12	microtubule-associated protein	28	160.1693	E-21	NE-0	10088.79	1760.422	26434.63	5549.039
SCVPCL6061A06	plastid adp-glucose pyrophosphorylase large...	10	55.5052	E-21	NE-0	11303.03	988.4725	20576.22	3144.502
SCCCLR1070G05	mtbc_sorbi	28	201.1421	E-21	NE-0	28878.75	11935.25	140519.2	37973.03
SCQSRT3051B10	methylthioribose kinase	10	62.65	E-21	NE-0	2112.438	698.3932	2270.266	2229.916
SCCCCRZ1003G02	pp1 pp2a phosphatases pleiotropic regulator prl1	5	26.3387	NE-21	NE-0	1118.624	918.0021	1635.127	2971.032
SCCCCL4017A06	beta-glucosidase 31-like isoform 1	3	15.2858	NE-21	NE-0	1678.982	1297.473	1329.622	4281.552
SCMCZRZ3064B09	hemoglobin 2	14	121.1966	NE-21	E-0	5347.02	22358.1	9900.894	73895.37
SCCCRT1002F07	pma1_orysj	63	445.3845	NE-21	NE-0	59287.03	25766.8	42766.4	89763.74
SCRFLF4025E09	ribokinase-like isoform 1	9	54.8817	NE-21	NE-0	4690.264	3783.085	6364.6	13283.89
SCCCRT1002C11	nicalin precursor	17	96.7543	NE-21	E-21	8836.812	4928.647	2762.683	17734.92
SCJFRT1008E10	af486280_1 cytosolic 6-phosphogluconate...	24	193.7775	NE-21	E-0	5332.047	6743.223	8151.91	25499.17
SCVPLR2027G04	peptidase family m48 containing protein	4	22.5992	NE-21	NE-0	1267.189	924.762	3063.853	3541.028
SCBFAD1094E08.b	nadph dependent glutamate synthase	85	604.6363	NE-21	E-21	46421.4	53149.13	34266.18	204104.5
SCCCCL4002C03	letm1 and ef-hand domain-containing protein...	24	147.6087	NE-21	NE-0	13628.69	9902.282	16796.81	38696.67
SCSGST3118A01.b	caffeic acid 3-o-methyltransferase	20	137.8339	NE-21	E-21	15412.92	7276.696	5117.86	28601.06
SCVPRT2078B04	myosin heavy chain-like protein	6	29.1347	E-21	NE-0	1552.039	484.2082	2948.918	1925.027
SCSBRZ2020D09	caffeooyl- o-methyltransferase-like	16	100.8831	NE-21	E-0	2891.371	18228.43	3587.817	74177.19
SCEQLR1092H02	oleosin 18 kda	13	134.5861	E-21	NE-0	18608.38	339.0747	120747	1386.569
SCCCCL3001A01.b	2-hydroxyphytanoyl- lyase	14	88.0419	NE-21	E-0	2777.797	11868.02	3355.886	48582.47
SCEQRT1024E12	phenylalanine ammonia-lyase	56	360.1322	NE-21	E-21	5448.114	27334.54	4022.891	113240.5
SCQQLR1086C06	kelch motif family protein	29	198.6539	NE-21	NE-0	14730.27	7704.591	10289.36	32421.39
SCCCCL5071H05	isovaleryl- dehydrogenase	28	200.6749	NE-21	NE-0	24172.15	5958.669	12368.21	25300.65

Table S1 cont.

SUCEST accession	Description	Peptide count	Confidence score	Highest mean condition	Lowest mean condition	E-0	NE-0	E-21	NE-21
SCCCRZ2001C09	golgin candidate 5-like	8	46.3676	NE-21	E-0	151.301	820.8344	167.0511	3498.631
SCCCLR1067H01	mitogen activated protein kinase 20-1	8	39.9389	NE-21	NE-0	2999.45	1033.968	2987.816	4652.819
SCACAD1037G05	substrate binding domain containing expressed	12	81.5268	NE-21	E-0	607.6821	5441.159	4157.033	24868.29
SCVPRT2075C09	c4-specific pyruvate orthophosphate dikinase	30	187.1215	NE-21	NE-0	45520.3	39157.38	55884.2	185790.6
SCAGLR2026C06	4-methyl-5-(b-hydroxyethyl)-thiazol monophosphate...	21	168.0412	NE-21	NE-0	16074.89	12031.5	16133.93	57486.78
SCRLLR1038A10	transaldolase 2	48	422.1533	NE-21	NE-0	71264.32	47654.31	54510.37	229310.3
SCBFLR1083H09	pathogen induced protein 2-4	4	32.8852	NE-21	E-0	2478.073	5277.258	3309.175	25524.87
SCCCLR1001H04	ubiquinol-cytochrome c reductase complex 14 kda...	22	177.0342	E-21	NE-0	14481.66	1877.655	19385.14	9144.241
SCEZRZ1016A05	casp c	3	13.9554	NE-21	NE-0	1141.956	327.5088	645.2625	1655.038
SCCCRT1003D07	b12d protein	3	23.2545	E-21	NE-0	93.18415	59.18682	1913.174	313.7282
SCQGLR2032B05	dehydrogenase reductase sdr family member 2	6	31.7552	E-0	NE-0	9104.99	135.0033	6257.349	719.0342
SCQSLR1090A06	casein kinase ii alpha subunit	10	70.769	NE-21	E-0	3015.455	12954.44	3373.671	71110.41
SCRUFL1111F06.b	phospho-2-dehydro-3-deoxyheptonate aldolase 1	9	43.6486	NE-21	E-0	564.6521	3012.684	1143.641	16561.47
SCCCLR1070A11	surfactant protein b containing protein	7	52.1495	NE-21	E-0	1176.12	3191.471	3484.528	18842.92
SCEZHR1087B05	homeobox-leucine zipper protein hox25-like	1	5.2492	E-21	NE-0	2049.79	305.1361	2468.555	1919.442
SCAGAD1076F02	ac074282_20 o-deacetylba	3	13.8464	E-21	NE-0	2330.606	339.5244	3268.893	2222.181
SCCCCL7038F03	chloroplastic group iia intron splicing facilitator...	3	15.0471	NE-21	E-0	748.9879	1384.657	873.7133	9446.71
SCBFFL5072F08	kinase interacting protein 1	4	18.5957	E-21	E-0	11.68252	92.78824	1394.916	644.0767
SCRLAM2050F05	domain containing expressed	7	42.2633	NE-21	E-21	498.2039	124.8057	111.0818	890.1537
SCCCCL7C03C05	af467541_1 aldehyde dehydrogenase mis1	20	158.9494	NE-21	NE-0	31671.77	6804.664	48792.25	48851.5
SCJFRT1008A03.b	wd repeat-containing protein 61-like	19	119.7596	NE-21	NE-0	73034.95	14837.62	26925.31	117662
SCACST3159E08	ferredoxin--nitrite reductase	10	53.0397	NE-21	E-0	2700.26	3154.465	3290.24	25180.65
SCBFRZ2047H07	receptor protein kinase clavata1 precursor	17	105.8308	NE-21	E-0	2476.152	7856.113	5605.902	63509.9
SCCCCCL3080G02.b	nucellin-like aspartic protease	6	49.306	NE-21	E-0	657.4146	1739.987	667.3672	14590.29
SCBGLR1095E10	blue copper protein precursor	6	33.2082	NE-21	E-0	3.966386	1374.824	24.96262	11616.93
SCAGLR1043B02	ap-2 complex subunit um	9	44.1013	NE-21	E-21	641.3112	1667.972	630.1002	14883.17
SCCCRZ2C04C12	inosine triphosphate pyrophosphatase	3	22.7064	E-21	NE-0	1794.463	112.9193	2557.42	1111.249
SCJFAD1011E09	argenate dehydrogenase isoform 2	4	23.0113	NE-21	E-0	38.8445	950.0637	96.9687	11675.79
SCCCLR1C04H07	fas-associated factor 1-like protein	7	34.7869	NE-21	NE-0	534.1301	399.9501	714.0567	5350.828
SCCCRZ2001F12	aluminum-induced protein	12	67.4665	E-21	NE-0	23395.65	2410.174	35225.23	32503.22
SCPRLB2030E07	mitogen-activated protein kinase-like	8	44.1889	NE-21	NE-0	620.0231	402.8649	889.1058	5829.69
SCAGLR1043H01	porphobilinogen deaminase	10	72.3999	NE-21	NE-0	1676.533	798.4983	2264.919	12047.12
SCCCLB1003B08	5-enolpyruylshikimate-3-phosphate partial	5	39.0088	NE-21	E-21	330.2331	490.2632	204.7612	7580.013
SCCCLB1003D11	exosome component 10-like	2	10.5547	NE-21	NE-0	3448.666	227.7669	3358.809	4598.659

Table S1 cont.

SUCEST accession	Description	Peptide count	Confidence score	Highest mean condition	Lowest mean condition	E-0	NE-0	E-21	NE-21
SCBGLR1082E04	diphosphonucleotide phosphatase1	6	35.0161	NE-21	NE-0	1526.339	377.1985	1391.945	7690.57
SCCCST3002H10	cysteine-type endopeptidase ubiquitin thiolesterase	8	36.5644	NE-21	E-0	13.73474	83.81224	92.6475	1710.596
SCAGFL8010F12	isco subunit binding-protein beta subunit	28	192.5824	NE-21	NE-0	1942.145	1389.551	2318.338	31924.4
SCCCCL7037E09	germin-like protein subfamily 1 member 17...	3	25.9475	E-0	NE-0	4731.655	126.189	388.9264	3606.88
SCSGFL4035A04	nefa-interacting nuclear protein	4	21.8265	NE-21	NE-0	921.2072	38.8317	608.9068	1187.849
SCEQLR1007C02	adapter-related protein complex 1 beta 1 expressed	6	30.9711	NE-21	NE-0	1493.91	37.99793	1658.479	1954.023

a) Confidence scores are calculated by ProteinLynxGlobalServer (PLGS). They are indicated from biological repeat 1–3.

Table S2. Non-exclusive proteins identified in the embryogenic and non-embryogenic sugarcane callus submitted to maturation treatments.

SUCEST accession	Description	Peptide count	Confidence score	Highest mean condition	Lowest mean condition	E-0	NE-0	E-21	NE-21
E-0 and E-21 co-expressed proteins									
SCCCCL7C05H06	af377694_1globulin 1	3	31.3073	E-21	NE-0	119422.8	-	158714.7	-
SCRFLB1054G09	hgd_orysj	4	24.7468	E-21	NE-0	1078.17	-	24681.04	-
SCRUHR1074B04	bet v i allergen	4	23.4893	E-21	NE-0	546.4049	-	11045.67	-
SCSBRZ3124G06	mutator protein	2	9.921	E-21	NE-21	2366.436	-	11039.03	-
SCACCL6008G06	moc31_maize	1	4.6752	E-21	NE-0	14.22238	-	4936.53	-
SCCCLB1021E06	granule bound starch synthase iiia precursor	5	33.8698	E-0	NE-0	96629.06	-	4618.632	-
SCSFAM1075G06	nucleotide-binding protein 1	4	29.1558	E-21	NE-21	780.8832	-	4586.045	-
SCAGSD1041H08	cleavage and polyadenylation specificity factor 5	5	29.7977	E-21	NE-21	772.5915	-	4284.757	-
SCQSRZ3037C07	spl15_orysj	2	15.4379	E-21	NE-21	2730.865	-	3168.567	-
SCBFRT1068E01	ac093180_11 abc transporter	3	16.8625	E-21	NE-21	528.3885	-	2881.488	-
SCCCLR1048F06	phospholipid transfer protein 1	11	96.2497	E-21	NE-21	2200.105	-	2827.642	-
SCEZLB1005D03	tld family expressed	1	8.5722	E-21	NE-0	1310.173	-	2819.915	-
SCMCAM2081A09	cepp protein	1	5.3661	E-0	NE-21	6466.554	-	2717.662	-
SCMCCL6055G06	math domain containing protein	1	5.1637	E-21	NE-0	389.9162	-	2667.703	-
SCJLAM1062A05	gp protein	16	122.8607	E-0	NE-0	3032.642	-	1789.144	-
SCJLRZ1027C02	truncated xa1-like protein	4	23.7848	E-21	NE-21	1016.923	-	1630.003	-
SCQGLR2025G12	nitrate-induced noi protein	1	6.0061	E-0	NE-21	1732.745	-	1483.335	-
SCCCRZ2C02B02	adaptor protein kanadapin	3	20.4898	E-21	NE-21	510.75	-	1453.147	-
SCJFLR1074D04	6pgl4_orysi short=6pgl 4 flags: precursor	2	10.5112	E-21	NE-0	788.3677	-	1400.964	-
SCCCLR1048A07	af083327_1101 kda heat shock protein	3	24.7449	E-21	NE-21	991.7542	-	1327.934	-
SCCCLR1048B09	alpha-expansin 5	3	19.7897	E-21	NE-0	220.1973	-	1176.967	-
SCEZFL5091D09	adaptin n terminal region family protein	5	36.2095	E-21	NE-0	601.8373	-	1167.83	-
SCJFLR1013B09	endonuclease exonuclease phosphatase family...	8	42.4942	E-0	NE-21	1296.781	-	963.8132	-
SCRLAM1007E03	ydg sra domain containing expressed	3	18.68	E-0	NE-21	1320.854	-	910.6222	-
SCVPHR1090G07	enhancer of rudimentary	1	6.9601	E-21	NE-21	228.3095	-	871.0664	-
SCCCLR1001F08	photosystem i reaction center subunit iii	2	10.3432	E-0	NE-0	3278.126	-	866.8843	-
SCVPAM2068D11	uridylylate kinase	3	19.0962	E-21	NE-0	410.3214	-	775.2716	-
SCQSST1037G12	cdk5rap3-like protein	6	29.3875	E-0	NE-21	913.9618	-	769.7857	-
SCMCFL5005E07	fertilization-independent endosperm protein	2	8.8596	E-21	NE-21	253.6779	-	765.5348	-
SCBFSD1038G02	steroid 22-alpha-hydroxylase protein	2	9.3773	E-21	NE-21	686.902	-	707.3843	-
SCACCL6010B02	wrky transcription factor 4	6	29.7225	E-21	NE-21	540.7644	-	662.4369	-
SCBGFL4053H08	ligatin (hepatocellular carcinoma-associated...)	7	38.545	E-0	NE-0	2231.231	-	655.6858	-

Table S2 cont.

SUCEST accession	Description	Peptide count	Confidence score	Highest mean condition	Lowest mean condition	E-0	NE-0	E-21	NE-21
SCSGFL4031D04	duf246 domain-containing protein at1g04910-like	1	5.287	NE-21	NE-0	573.3003	-	637.9043	-
SCEZRZ1015H08	trehalose expressed	1	5.315	E-21	NE-21	533.8582	-	549.0573	-
SCEQRT2093F11	L-ascorbate peroxidase chloroplastic-like isoform1	2	13.1473	E-0	NE-0	2194.198	-	483.5013	-
SCCCLR1001A08	negatively light-regulated protein	3	17.8638	E-21	NE-21	46.65051	-	457.9018	-
SCJFRT1005C01	3-hydroxybutyryl- dehydrogenase	2	11.6597	NE-21	NE-0	394.6509	-	433.4855	-
SCCCLR1080F11	cycloartenol synthase	6	31.1505	E-0	NE-21	960.6443	-	432.5893	-
SCEQRT2094F10	scar-like protein 2-like	2	9.0117	E-21	NE-0	99.73954	-	376.0142	-
SCRLAD1040A04	ac104428_17 glutathione reductase	1	5.8039	E-21	NE-21	217.0267	-	310.4601	-
SCEPLB1042B03	heavy-metal-associated domain-containing...	1	5.5208	E-21	NE-21	276.6267	-	310.2851	-
SCSFRT2071G10	ubiquitin-specific protease	9	56.174	E-21	NE-0	226.8296	-	302.0132	-
SCRUFL1019B10.b	ac090713_15 peroxidase	4	22.7776	E-0	NE-21	285.5838	-	281.931	-
SCUTAM2010B06	formin-like protein 16-like	1	5.7904	E-21	NE-0	105.768	-	253.9452	-
SCUTST3086D12	erebp-like protein	2	11.1536	E-0	NE-21	339.3342	-	233.7392	-
SCQSRT1036B03	lysine-ketoglutarate reductase saccharopine...	3	15.7737	E-21	NE-0	110.9464	-	232.8247	-
SCEZLB1014A01	saccharopine dehydrogenase	2	10.128	E-21	NE-21	153.6449	-	230.0149	-
SCBGR3071C03	syntaxin-related protein nt-syr1	2	10.7001	E-0	NE-0	367.1587	-	193.2725	-
SCRFST1041F07	map kinase activating	2	11.3203	E-0	NE-0	218.3869	-	187.3048	-
SCAGCL6016A03	exocyst complex component expressed	5	31.305	E-0	NE-21	10537.88	-	186.0253	-
SCJFRT2056F09	tousled-like kinase 2	2	14.894	E-0	NE-21	149.2125	-	126.2326	-
SCRFRT3056B06	fye zinc finger family protein	4	20.6945	E-0	NE-21	371.9014	-	122.9216	-
SCCCLB1003E11	sapk3_orysi	11	52.6467	E-21	NE-21	56.86367	-	121.2291	-
SCJFHR1034E06	histidyl-tRNA synthetase	2	10.605	E-0	NE-0	452.5816	-	115.9657	-
SCEQRT2095F07	chitin-inducible gibberellin-responsive protein...	2	15.2063	E-21	NE-21	31.31632	-	110.4365	-
SCEZLR1052A09	vamp-like protein ykt62	4	21.126	NE-21	NE-0	44.02738	-	95.08381	-
SCEZRZ3049D03	xylosyltransferase oxt	2	11.4949	E-0	NE-21	230.1275	-	73.95792	-
SCJFLR1073H12	delta 1-pyrroline-5-carboxylate synthetase	7	38.2654	E-0	NE-21	874.9202	-	34.03878	-
SCEQRT1025A05	ferritin- chloroplastic	24	224.1018	E-0	NE-0	15105.71	-	10379.16	-
SCBFAM2023E05	cohesin-like protein	10	63.4802	E-21	NE-0	6482.564	-	15126.45	-
SCJFRZ2005H03	cleft lip and palate transmembrane protein 1...	7	34.4338	E-21	NE-0	7186.469	-	19755.17	-
SCCCCL3080B02.b	r-interacting factor1	15	98.6392	E-21	NE-21	8046.608	-	11324.67	-
SCBFRZ2019H02	p-loop containing nucleoside triphosphate...	3	21.2021	E-21	NE-0	742.373	-	13313.98	-
SCRLFL1005H09	adenylyl cyclase-like	4	19.2341	E-21	NE-0	5322.507	-	13257.39	-
SCBFLR1026E05	vata_maize	43	346.9665	E-21	NE-21	10230.56	-	12893.73	-

Table S2 cont.

SUCEST accession	Description	Peptide count	Confidence score	Highest mean condition	Lowest mean condition	E-0	NE-0	E-21	NE-21
				NE-21	NE-21			NE-0	NE-21
SCJFRT2053C06	bola-like protein	3	26.6587 E-21	NE-21	173.096	-	9946.539	-	
SCQSAM2099E03	Os12g0109600 [Oryza sativa Japonica Group]	6	36.8272 E-21	NE-21	5754.243	-	8522.741	-	
SCJLRT1023H02	growth regulator	5	28.8823 E-0	NE-21	12022.32	-	7059.053	-	
SCAGFL8010G09	skip interacting protein 18	11	63.4319 E-0	NE-0	8648.712	-	7036.335	-	
SCEQAM1040A04	cyclopropane fatty acid synthase	7	41.6012 E-21	NE-0	3967.459	-	6886.839	-	
SCEQRT1030A09	aba stimulation map kinase	7	46.1654 E-0	NE-0	7529.452	-	6850.633	-	
SCCCCL3080B09.b	gh32_orysj	3	22.2683 E-0	NE-21	6827.306	-	6181.195	-	
SCAGLR1021D07	acetoxyhydroxyacid synthase	15	80.9393 E-0	NE-21	11078.04	-	6132.397	-	
SCJFLR1073H05	ac079935_17 pyridoxamine 5-phosphate oxidase	4	21.6584 E-21	NE-0	5675.852	-	5739.901	-	
SCCCLR1076G12	act7_orysi	32	312.9281 E-21	NE-0	557.3014	-	5345.201	-	
SCAGRT2042G05	npl4 family protein	9	65.6475 E-0	NE-0	11086.45	-	5336.08	-	
SCQSAM2100C06	nudix hydrolase 13	7	43.6333 E-0	NE-21	4643.253	-	4577.331	-	
SCEQRT1031A11	27k vesicle-associated membrane protein....	4	28.9022 E-21	NE-21	171.2609	-	4475.963	-	
SCCCLR1024B12	molybdenum cofactor biosynthesis protein	4	27.2865 E-21	NE-0	2027.243	-	4111.339	-	
SCCCRZ2001B06	gtpase sar1	12	88.6145 E-21	NE-21	2112.971	-	3289.907	-	
SCSGRT2062D07	loc100280824 precursor	6	48.4203 E-0	NE-21	5919.34	-	3465.834	-	
SCRFAM1025D09	sad1 unc-84-like protein 2	5	32.0012 NE-21	NE-0	1586.699	-	2522.812	-	
SCJLLR2020C02	pumilio-family rna-binding domain-containing...	3	22.6798 E-0	NE-21	2628.643	-	2451.743	-	
SCJFRZ2015B02	myb family	4	15.8657 E-21	NE-21	6.333296	-	2695.924	-	
SCEZLR1009F04	triose phosphate phosphate non-green precursor	3	25.0663 E-0	NE-21	38914.99	-	3058.252	-	
SCJLFL4186E12	tocopherol cyclase	2	10.8585 NE-0	E-21	2663.302	-	1489.258	-	
SCJFRZ3C07F11	amine expressed	1	6.7596 E-21	NE-0	535.4959	-	1433.951	-	
SCAGAM2126D12	peptide-n4-(n-acetyl-beta-glucosaminyl)asparagine	3	15.8159 E-21	NE-21	1227.892	-	1383.561	-	
SCEZRZ3127F12	phi-1 precursor	7	57.2496 E-21	NE-0	465.9253	-	1652.396	-	
SCSBRZ3125G04	mechanosensitive ion channel domain-containing	3	27.1658 E-21	NE-21	1357.818	-	1592.713	-	
SCSBHR1052D02	12-oxo-phytodienoic acid reductase	2	10.2798 NE-0	E-21	3174.634	-	1868.285	-	
SCSGAD1009D06	Os04g0136700 [Oryza sativa Japonica Group]	4	21.5311 E-21	NE-0	865.6683	-	1900.441	-	
SCQSST1038H12	non-green plastid inner envelope membrane protein	4	24.2926 E-21	NE-0	146.9131	-	2139.624	-	
SCQSRT2036H09	glycylpeptide n-tetradecanoyltransferase 1	3	24.1167 E-21	NE-21	1865.422	-	2122.651	-	
SCCCRT1001F11	decussate protein	3	16.2406 E-21	NE-21	1300.464	-	1923.162	-	
SCJLRT1006F02	ngg1 interacting factor 3 like 1 binding protein 1...	3	16.5657 E-0	NE-21	2297.967	-	1908.425	-	
SCCCCL3004A05.b	ac079890_16 myb-related protein	1	6.0122 E-0	NE-21	1950.133	-	1279.045	-	
SCVPLR2027B10	sm protein f	4	24.4947 E-21	NE-0	1128.436	-	1247.712	-	

Table S2 cont.

SUCEST accession	Description	Peptide count	Confidence score	Highest mean condition	Lowest mean condition	E-0	NE-0	E-21	NE-21
				NE-21	NE-0	1247.681	-	1172.476	-
SCRFLR1012H01	24 kda seed maturation protein	2	15.5171	E-21	NE-21	544.5423	-	1247.681	-
SCRFLR1034A06	upf0172 protein at5g55940-like	5	27.047	E-0	NE-0	1396.791	-	1172.476	-
SCCCRT1003F05	proline-rich cell wall	5	25.4011	E-21	NE-0	420.9564	-	660.702	-
SCSGFL4194F09	ocs-element binding factor	2	12.7575	E-21	NE-21	233.7876	-	658.6958	-
SCSGLR1045F12	r11_orysj ame: full=60s ribosomal protein l11	12	95.7492	E-0	NE-21	1263.722	-	1056.037	-
SCMCRT3084G08	lactoylglutathione lyase	8	53.6044	E-0	NE-21	1125.058	-	1007.641	-
SCSFAM1074E12	abc-type transport system involved in resistance...	6	40.9388	NE-21	NE-0	443.3123	-	989.4016	-
SCCCHR1003D08	swim domain-containing protein	2	9.7118	E-21	NE-0	388.4356	-	906.4819	-
SCVPRT3090B11	uvrb uvrc motif family protein	3	13.8908	E-0	NE-0	995.5613	-	959.5507	-
SCSBAD1052A06	fk506 binding protein	1	4.6229	E-0	NE-0	872.1036	-	846.172	-
SCCCLB1004F04	flowering time control protein isoform -4	4	26.8101	NE-0	E-0	453.2016	-	774.7984	-
SCACLR2007D05	phloem-specific lectin	1	6.3101	E-0	NE-0	1029.3	-	767.7769	-
SCVPRZ2038G11	aaa-type atpase family expressed	4	21.5782	E-21	NE-21	717.8112	-	737.1259	-
SCUTAM2088B01	switch sucrose nonfermenting 3c	2	9.8033	E-0	NE-0	1291.087	-	726.099	-
SCAGLR1021H04	upf0510 protein inm02-like	4	19.9272	NE-21	E-0	405.801	-	719.3362	-
SCCCRT1002A11	neutral alpha-glucosidase ab expressed	8	47.791	E-21	NE-21	537.7151	-	671.4131	-
SCEZRZ1013A06	senescence-inducible chloroplast stay-green protein	3	21.0673	NE-0	NE-21	393.2263	-	549.1498	-
SCBGSB1026A09	bgl01_orysj	1	5.2736	E-21	NE-21	310.0842	-	535.8566	-
SCJFRT1010D08	5-azacytidine resistance expressed	2	10.9678	NE-21	E-0	148.9985	-	521.9716	-
SCBFRZ2046C02	dual specificity protein phosphatase 4	2	10.8165	E-0	NE-21	1012.094	-	499.8202	-
SCJLLR1104B01	p8mtcp1	2	16.2956	NE-0	E-0	249.1479	-	498.3417	-
SCBGLB2012C11	polygalacturonase-1 non-catalytic beta subunit...	2	9.8858	E-0	NE-21	310.1021	-	125.2583	-
SCEQRT2098A06	phytochrome and flowering time protein 1	5	30.1907	E-0	NE-21	731.7702	-	349.6319	-
SCQSLR1090C03	embryogenic callus protein 98b	1	5.3158	E-0	NE-21	834.3746	-	347.4189	-
SCRLAM1007C02	af272758_1kinesin heavy chain	5	21.9783	E-0	NE-0	1038.233	-	434.9498	-
SCUTAD1032A02	bzip transcription factor	3	18.2784	E-0	NE-21	1190.952	-	429.0899	-
SCCCRT1002B01	homocysteine s-methyltransferase 3	4	17.9407	E-0	NE-0	390.5908	-	339.2392	-
SCQGST1030G10	gebp transcription factor	3	18.7071	E-21	NE-21	126.6987	-	363.2258	-
SCRFLR1012F06	sec61 alpha form 2	3	12.0126	NE-21	E-0	298.3154	-	359.4085	-
SCEQRT1028B04	gck-like kinase mik	2	8.8674	E-21	NE-21	123.7242	-	383.7148	-
SCAGAM2124H09	parp1_maize ame: full=poly synthase 1	3	16.1601	E-0	NE-21	412.5143	-	326.4693	-
SCEZLR1031B12	rh27_orysj	5	24.0521	E-0	NE-21	3984.795	-	207.3643	-
SCCCRT1001D03	leaf senescence related	1	4.7681	E-21	NE-21	182.0567	-	312.8176	-

Table S2 cont.

SUCEST accession	Description	Peptide count	Confidence score	Highest mean condition	Lowest mean condition	E-0	NE-0	E-21	NE-21
				NE-0	E-21			NE-21	NE-21
SCJLHR1027G02	anthocyanin biosynthetic gene regulator pac1	2	16.477 E-21	NE-0	169.2787	-	312.3001	-	-
SCQGLB2042B09	wall-associated kinase 3 precursor	1	6.1102 NE-21	E-0	149.3308	-	311.7912	-	-
SCRFL1005D09	clv1 receptor kinase-like protein	1	5.2744 NE-21	E-0	47.30683	-	311.2656	-	-
SCACCL6007G01	centromeric protein	1	4.7387 E-0	NE-21	384.9289	-	294.6766	-	-
SCCCLR1C07B06	gamma-glutamyl hydrolase precursor	8	40.7686 E-21	NE-21	209.1849	-	285.2517	-	-
SCUTAM2086B11	high light protein	1	6.247 NE-0	E-21	487.2497	-	282.281	-	-
SCCCLR1048C10	carbon-nitrogen family expressed	11	57.2693 NE-0	E-21	163.7967	-	140.0126	-	-
SCRFLR1012H03	ferritin 1a	14	137.6533 NE-21	E-21	251.712	-	75.44348	-	-
SCCCCL3080E01	loc100282003 precursor	1	7.0442 NE-0	E-21	162.3203	-	73.05045	-	-
SCEPAM1017F02	adenylate kinase	4	24.3173 E-0	NE-21	639.6828	-	61.40506	-	-
SCRURL1042H01	molecular chaperone	2	8.7704 E-0	NE-0	831.6082	-	60.60552	-	-
SCCCRZ1001H10	af466201_7small heat shock-like protein	1	4.9336 E-0	E-21	1060.256	78.8719	-	-	-
SCBGSB1027G09	psag protein	4	16.5154 E-0	E-21	3559.846	86.76414	-	-	-
SCCCLR1067B10	sec14 cytosolic factor	3	20.1895 E-0	NE-21	923.3768	306.7306	-	-	-
SCRURT2009H10	bsd domain containing protein	3	20.2821 E-0	NE-21	130.4291	18.79472	-	-	-
SCBGLR1116G01	cml13_orysj	1	9.7526 E-0	NE-21	1876.712	340.4877	-	-	-
SCEQRT1030C03	potassium transporter	4	24.4503 E-0	E-21	674.8477	221.9122	-	-	-
SCQGLR1086F03	ssxt protein	3	18.813 E-0	NE-21	3981.076	90.89605	-	-	-
SCEZAM1080D04	kinase-like protein	1	5.2168 NE-0	NE-21	50.21461	1875.201	-	-	-
SCEZRZ3053H07	latex-abundant protein	3	14.388 NE-0	E-21	67.75435	118.516	-	-	-
SCMCFL5006A05	cap protein	2	11.2477 NE-0	NE-21	14.42866	1048.996	-	-	-
SCBFAD1048G12	c3h27_orysj	1	4.1728 E-0	NE-21	5317.621	130.6885	-	-	-
SCCCRT3004D06	sex determination protein tasselseed 2	2	13.1896 E-21	NE-0	1738.776	158.5947	-	-	-
SCEQRT1028D11	carnitine racemase catalytic racemase catalytic	5	29.541 NE-21	E-0	2304.128	2669.127	-	-	-
SCEPAM2015B05	af311223_1c2h2 zinc-finger protein	3	21.9422 NE-21	E-0	2536.517	4734.287	-	-	-
SCQGLR2025F03	loc100285096 precursor	1	5.2321 NE-0	E-0	729.1455	29637.08	-	-	-
SCAGCL6016A11	insulin-degrading enzyme-like	1	4.0948 E-21	NE-21	399.7043	340.9489	-	-	-
SCEZRZ1013F08	diacylglycerol kinase	2	17.5291 NE-21	E-0	524.8941	1434.854	-	-	-
SCJLLR1011E05	plus-3 domain containing expressed	2	9.5705 NE-0	E-0	159.9445	542.0793	-	-	-
SCEPLR1030D10	developmentally-regulated gtp-binding protein 1	7	36.4096 NE-0	NE-21	3005.882	10652.65	-	-	-
SCJFRZ2007A04	bet1 sft1-related snare	3	22.2033 E-0	NE-21	1207.948	98.89431	-	-	-
SCSBFL1043F07	phosphatase 2a regulatory a subunit	10	68.0643 NE-0	E-21	23.6132	471.5577	-	-	-
SCCCCL3120D03	gst6 protein	4	24.7338 E-0	NE-21	2868.377	2797.104	-	-	-

Table S2 cont.

SUCEST accession	Description	Peptide count	Confidence score	Highest mean condition	Lowest mean condition	E-0	NE-0	E-21	NE-21
SCJFRT1012D11	poly(adp-ribose) polymerase	3	16.4694	E-0	NE-21	2721.516	373.1395	-	-
SCSBFL4013A07	geminivirus rep-interacting motor	2	10.2771	E-0	NE-21	1915.896	162.7622	-	-
SCACSD2017E01	chch domain containing protein	2	17.9928	E-0	NE-0	4313.055	750.5825	-	-
SCVPLB1020E02	zf-hd homeobox protein	4	22.5077	NE-0	E-21	522.1445	851.797	-	-
SCBGLR1099D07	zinc-binding protein	4	27.9748	E-0	NE-21	1740.814	1029.407	-	-
SCCCCL3005F05.b	vernification independence 4	1	7.5398	NE-21	E-21	916.0861	1292.813	-	-
SCJFRZ2025H09	glutaredoxin i	3	20.9448	E-0	NE-21	476.186	91.56269	-	-
SCEPRT2044F09	bgal6_orysj	2	11.4444	E-0	NE-0	774.9935	109.3112	-	-
SCCCLR1C08E10	receptor-type tyrosine-protein phosphatase s	3	15.2273	NE-0	E-21	97.08772	105.9372	-	-
SCJLRT2052B09	caleosin related protein	4	27.0221	E-0	NE-21	671.067	130.4102	-	-
SCVPRZ2041D10	ring-h2 finger protein	2	10.7752	E-0	E-21	10576.95	9128.581	-	-
SCRLAM1013H01	beta-alanine synthase	6	34.3283	E-0	NE-0	4207.603	201.0223	-	-
SCCCFL8001G12	arsenical pump-driving atpase	2	15.8619	E-0	NE-21	723.257	494.4283	-	-
SCEPLB1042D02	nac2 protein	6	30.7981	E-0	E-21	8396.966	2049.159	-	-
SCEQRT2099E04	glucosyl transferase	6	28.072	NE-21	E-21	244.8818	65.25165	-	-
SCMCAM2084F02	hexokinase 5	2	10.7125	E-21	NE-0	429.4005	241.5855	-	-
SCEQRT2030H10	auxin-inducible protein	1	4.7787	NE-0	E-0	16.37097	1051.223	-	-
E-0 and NE-21 co-expressed proteins									
SCRFAM1025C02	b3 domain-containing protein os03g0619600-like	1	5.8706	NE-21	E-21	30.48963	-	-	2405.302
SCMCSB1111D02	rhamnogalacturonate lyase-like	4	23.5721	NE-21	E-21	139.3517	-	-	4415.754
SCVPFL3044D11	monoglyceride lipase-like	2	11.0007	NE-0	E-21	59.00658	-	-	2199.115
SCVPLR2012H05	tonneau expressed	5	31.7575	E-0	E-21	877.7539	-	-	61.80625
SCEQLR1007G09	single-strand binding protein	3	15.3955	E-21	NE-0	98.16094	-	-	432.9607
SCEQRT2026E04	glo3_orysj	5	42.2544	NE-21	NE-0	89.19105	-	-	11860.73
SCEPLB1043G04	cytokinin-o-glucosyltransferase 2	1	5.4354	NE-21	NE-0	97.89129	-	-	974.5534
SCSGRT2063D10	silencing gene b101	6	36.7001	E-21	NE-0	720.8007	-	-	1096.76
SCCCCL6001A04	dehydrin 11	4	34.0289	E-21	NE-0	42463.02	-	-	87.53858
SCRFLB1055D11	mir-interacting saposin-like protein precursor	4	21.8278	NE-0	E-21	2799.262	-	-	2233.506
SCSGRT2066E06	basic helix-loop-helix family protein	2	10.0949	E-0	NE-0	588.7743	-	-	71.62245
SCQSRT2033B03	single myb histone 1	2	7.7643	E-0	NE-0	181.9722	-	-	63.4017
SCBFST3133F03	rab1 small gtp-binding protein	4	31.0843	NE-0	E-21	62.57188	-	-	82.56396
E-21 and NE-21 co-expressed proteins									
SCQSRT2032G07	atp-binding cassette sub-family e member expressed	7	43.7112	NE-21	E-0	-	-	1542.181	1826.774

Table S2 cont.

SUCEST accession	Description	Peptide count	Confidence score	Highest mean condition	Lowest mean condition	E-0	NE-0	E-21	NE-21
SCACLR2007G05	remorin-like isoform 1	5	25.2142	E-21	NE-0	-	-	676.0972	165.2924
SCRFFL1025G01	formate--tetrahydrofolate ligase-like	6	33.8444	E-21	E-0	-	-	2190.808	149.0613
NE-0 and NE-21 co-expressed proteins									
SCCCCL2001A04.b	xylem serine proteinase 1 precursor	4	18.2139	NE-0	E-0	-	597.346	-	206.8833
SCCCRZ1C01C03	nonsense-mediated mrna decay protein 3	5	29.6395	NE-0	E-21	-	1646.653	-	1602.347
SCCCLR1048A10	60 ribosomal protein l14	10	85.762	NE-0	E-21	-	1702.804	-	1659.839
SCRLSB1042H02	ribonucleoside-diphosphate reductase	2	8.389	NE-21	E-21	-	200.1354	-	3142.556
SCJLRT1006C03	acc synthase	3	13.296	E-0	NE-21	-	687.4143	-	236.6315
SCEQRT2026F02	smc2 protein	3	18.836	NE-21	E-21	-	294.1504	-	2249.753
NE-0 and E-21 co-expressed proteins									
SCUTST3129G12	gdp-l-fucose synthase 1	5	35.2344	E-21	NE-21	-	294.6131	5158.496	-
SCCCLR2003G12	brefeldin a-inhibited guanine nucleotide-exchange...	1	5.5506	E-21	E-0	-	1277.32	1493.317	-
SCMCRT2104E04	glycerophosphodiester phosphodiesterase	3	15.7586	NE-0	E-0	-	4236.655	608.6302	-
SCSGFL4C06C03	dna-damage-repair toleration protein	3	15.7275	NE-0	E-0	-	2462.8	51.25466	-
E-0, E-21 and NE-21 co-expressed proteins									
SCVPRT2080F11	3-methyl-2-oxobutanoate hydroxymethyltransferase	6	33.6337	E-21	NE-0	1761.78	-	3010.027	77.1727
SCCCC7C02A05	peroxin pex14	5	25.1365	E-21	NE-0	711.2938	-	1223.035	393.6839
SCCCC4C01F06	atp12 atpase	4	20.3682	NE-21	NE-0	1319.603	-	990.3515	1986.301
SCSFST3076G09	luminal binding protein	13	118.626	E-0	NE-0	1116.049	-	929.9285	33.81498
SCJLRT1018D04	roothairless 1	3	15.4031	E-21	NE-0	155.162	-	837.2004	27.37189
SCVPFL1072G12	gamma-tubulin complex component 3 homolog	1	6.2997	E-21	NE-0	247.4116	-	606.4626	51.91938
SCCCC7C02F04	dpe1_orysj	5	24.3169	E-0	NE-0	903.6117	-	8.754731	74.74067
SCCCLR1024C05	nonspecific lipid-transfer protein 3 precursor	2	15.8891	NE-21	E-21	118.4203	-	72.65892	4332.72
SCQSRZ3037B01.b	minor isoform	7	77.7615	NE-21	E-0	54.97563	-	58.2645	7694.211
SCSBST3101G12	multiple c2 and transmembrane domain-containing...	1	4.8189	NE-21	E-21	95.43805	-	90.65438	2987.049
SCRURT2012B06	lysine ketoglutarate reductase saccharopine...	6	30.5248	E-0	E-21	5117.682	-	84.28483	3192.181
SCEPAM1016H05	early-responsive to dehydration stress protein	2	10.7201	NE-21	NE-0	47.06252	-	32.82346	520.6783
SCCCLR1C07E12	ccr4-not transcription complex subunit 7	1	9.7556	NE-21	E-21	55.3322	-	25.6008	22310.87
SCJFRZ2013G11	metk4_horvu	8	94.0577	NE-21	E-21	449.8119	-	19.97597	4465.023
SCBFAM2023E02	homoserine kinase	1	7.7797	E-21	NE-0	315.0325	-	2099.533	68.76865
SCCCRT2004D12	snare domain containing protein	6	44.2215	E-21	NE-0	813.9506	-	1904.813	1455.977
SCBGLR1119F12	gldh1_orysj	9	65.5153	NE-21	NE-0	510.0832	-	1883.551	4230.875
SCCCLR1024G08	catalytic acting on nadh or nadph	14	75.3387	NE-21	NE-0	1446.179	-	1857.036	24559.93

Table S2 cont.

SUCEST accession	Description	Peptide count	Confidence score	Highest mean condition	Lowest mean condition	E-0	NE-0	E-21	NE-21
				NE-0	NE-21			E-21	NE-21
SCJLFL4097H07.b	2-keto-3-deoxy-l-rhamnonate aldolase-like	2	11.9587 E-21	NE-0	989.9905	-	1719.915	422.434	
SCRUFL4020G01	inositol monophosphatase 3	3	24.4356 E-0	NE-0	7733.469	-	1845.878	483.18	
SCCCCL5071H07	calcyclin-binding protein	5	27.0673 NE-21	NE-0	2158.102	-	2957.128	3568.668	
SCJLFL3015D04	degp1	3	23.4407 E-21	NE-0	3428.293	-	14991.13	571.4653	
SCCCCL3002C12.b	reticulon-like protein b2-like isoform 1	3	33.9967 E-21	NE-0	11528.89	-	11664.51	3517.665	
SCCCRT3010C11	amidohydrolase family protein	4	25.2055 E-21	NE-21	5278.618	-	12061.74	244.8793	
SCSBSD1033E10	per1_sorbi	9	75.9006 E-21	NE-0	1820.812	-	21628.64	396.7859	
SCRLLB2032D09	flower-specific gamma-thionin precursor	3	44.0915 E-21	NE-0	4384.83	-	32454.95	276.7213	
SCRFLR2037D07	nad h-dependent oxidoreductase	7	57.5961 E-0	NE-21	12629.37	-	7182.559	387.2621	
SCMCAM2084B09	flavonoid 3 -hydroxylase	12	66.6351 NE-0	NE-21	6115.678	-	6081.802	5103.755	
SCCCAM2001F04	auxin-repressed kda protein	5	43.6788 E-21	NE-0	3923.346	-	4153.277	839.3202	
SCCCAM2001F04	ubiquinone biosynthesis protein coq9	2	19.0502 E-21	NE-0	1360.777	-	3196.04	1724.915	
SCEZAM2031E09	dut_orysj	7	58.5372 E-0	NE-0	5109.524	-	3718.156	110.7801	
SCVPF3045D08	hemoglobin-like protein	3	15.8265 E-21	NE-21	1968.437	-	4875.157	820.0707	
SCCCLR1C03B10	Os01g0663800 [Oryza sativa Japonica Group]	8	55.7002 E-21	NE-0	2286.275	-	5511.444	119.9844	
SCVPLR2005B12	mct-1 like pua rna binding-domain containing...	8	53.3802 E-0	NE-0	10515.2	-	5749.859	3731.864	
SCACCL6007H09	fd vi	9	57.4914 E-0	E-21	25061.01	-	2265.134	5722.617	
SCVPAM2067E05	fmn binding protein	1	10.4592 E-0	NE-0	5503.53	-	2128.56	1258.772	
SCACLR1036G09	sucrose-phosphate synthase	3	15.2631 E-21	E-0	135.9911	-	1025.502	387.0763	
SCEQRT1031B11	acyl-coenzyme a oxidase 2	15	83.2302 E-0	E-21	6411.549	-	1175.045	3626.623	
SCJFST1015B05	altered response to gravity	2	14.9227 E-0	NE-21	1284.938	-	1199.719	871.6458	
SCJLRT2051F02	utp--glucose-1-phosphate uridylyltransferase-like	16	132.9731 NE-21	NE-0	2319.989	-	1194.516	8818.51	
SCJLRZ1024F09	phosphoribosyl pyrophosphate synthase	2	10.3874 E-21	E-0	368.6241	-	648.1967	416.075	
SCRFSD2022E02	apospory-associated protein c	8	53.3628 E-0	NE-0	1518.211	-	1309.02	863.6151	
SCSGAM1096C06	insulinase containing expressed	4	19.8139 E-21	NE-0	299.3052	-	533.0246	430.57	
SCJFRZ2032C10	dek protein	6	37.214 NE-21	NE-0	794.4643	-	292.9086	8476.367	
SCUTLR1037C03	loc100282421 precursor	3	18.2353 NE-21	E-0	87.07206	-	200.8873	5265.112	
SCVPLR2005B02	thylakoid luminal kda chloroplast precursor	3	15.259 NE-0	E-21	216.7141	-	198.5861	2526.918	
SCQSLB2054E09	gnat family protein	4	19.5209 E-0	NE-21	567.4801	-	340.4747	155.1932	
SCMCSSB1107H02	resistance protein rga2	2	9.8558 NE-21	E-0	40.10382	-	339.8106	47435.72	
SCEQLB1063H10	iaa21_orysj	1	5.1469 NE-21	E-0	142.9205	-	476.9637	1163.111	
SCEPLR1051C10	ef-hand containing protein	3	17.535 E-21	NE-0	197.5069	-	443.8401	290.0542	

Table S2 cont.

SUCEST accession	Description	Peptide count	Confidence score	Highest mean condition	Lowest mean condition	E-0	NE-0	E-21	NE-21
				E-0	NE-0				
SCQSAD1059D02	kinesin heavy chain	9	41.5309	NE-21	NE-0	681.9785	-	442.3909	1943.035
E-0, NE-0 and E-21 co-expressed proteins									
SCCCAM2004E12	plastidic phosphate translocator-like protein1	4	18.1097	E-0	NE-21	15774.13	3858.449	2912.492	-
SCBGST3104H11	23 kda polypeptide of photosystem ii	1	5.6361	E-0	NE-21	1051.793	355.9346	336.227	-
SCEZFL5087C02	double strand break repair protein	3	16.8577	E-21	NE-21	316.7647	9.06048	463.3046	-
SCCCRZ2002B03	hydroxyproline-rich glycoprotein 1	9	73.8111	E-0	NE-21	64.28073	62.18255	40.53833	-
SCCCRZ1C01D10	unnamed protein product [Oryza sativa Japonica...]	7	42.653	E-0	E-21	7134.456	265.2607	53.59017	-
SCEZLR1031G01	udp-arabinose 4-epimerase 2	5	27.6552	E-0	E-21	76735.26	153.3325	12.05067	-
SCACLB1048B09	alpha-mannosidase calcium ion binding protein	2	10.4472	NE-21	E-21	43.69594	82.67582	11.41805	-
SCACAD1037F10	exb18_orysj	4	23.7802	NE-0	E-21	138.148	8018.908	9.093619	-
SCAGLR1021H06	vignain precursor	8	61.456	NE-0	E-21	394.2885	7305.515	230.2136	-
SCVPAM1055E12	selt selw selh selenoprotein domain containing...	7	35.527	E-0	NE-21	802.3868	72.00119	284.8517	-
SCSGFL1081H07	sad1-unc84-like protein	7	33.3651	NE-0	E-21	191.0601	3428.673	128.8825	-
SCQGAM1049G02	starch branching enzyme interacting protein-1	8	47.7523	NE-0	E-21	2151.239	7902.248	306.6329	-
SCUTST3092C06	epoxide hydrolase 2-like	8	47.2257	E-0	E-21	35158.14	2694.353	333.6142	-
SCQGST1034H10	will die slowly expressed	4	26.6666	E-0	E-21	1839.576	558.5942	418.769	-
SCUTRZ3106H10	formylglycineamide ribotide amidotransferase	10	68.5696	NE-0	E-21	744.0202	2344.876	470.7005	-
SCCCCCL3140E08	phosphoribosylformylglycinamidine cyclo-...	4	31.6582	NE-0	E-21	1560.223	6223.431	429.5291	-
SCJFHR1031E10	50s ribosomal protein l12-1	9	46.5522	NE-0	E-0	71.22124	938.3691	718.7987	-
SCRUAD1132B11	methylcytosine binding domain protein	1	4.5156	NE-21	E-0	82.76021	583.608	103.9999	-
SCSGRT2065E10	loc100282067 precursor	3	19.9744	NE-0	NE-21	326.6184	5893.124	590.3282	-
SCRLAD1044E07	l-galactose dehydrogenase	1	6.8887	E-0	NE-21	766.9356	464.3744	588.204	-
SCRFAM2131E11	phytoene synthase	2	9.4491	NE-21	NE-0	732.2367	388.723	541.5807	-
SCACLR2029D05	loc100285305 precursor	3	21.7758	NE-21	E-0	109.2857	2573.115	534.3879	-
SCJLLR1105H10	mp703_orysj	2	8.1709	NE-0	E-0	501.2447	3640.307	517.0848	-
SCQGLB1039F03	nodulation receptor kinase	3	14.6472	E-0	NE-21	2000.654	1341.734	514.0626	-
SCCCRZ1001A11	sec20 family protein	3	20.8764	NE-0	NE-21	1395.914	22902.74	931.6277	-
SCEZLR1009E04	eyes absent-like protein	4	27.4525	E-21	NE-0	876.1701	15.54965	1176.04	-
SCRFAM2128E12	sl-tps p	3	16.8636	E-21	NE-0	96.65735	20.90383	1133.738	-
SCQGAM1048E11	ac079936_18 retroelement	5	23.422	E-0	E-21	4672.923	2253.799	1000.622	-
SCCCRZ1001C07	hap5 subunit of hap complex	4	32.5117	NE-0	NE-21	1610.378	2849.615	623.6084	-
SCPIRT3022D04	ac091238_14 cytosolic trna-ala synthetase	13	86.5601	NE-21	E-0	135.0246	1074.185	953.3261	-
SCCCCCL4013E03	Oryza sativa unknown protein AAP03423...	6	31.5819	E-21	E-0	125.188	551.5151	815.3719	-

Table S2 cont.

SUCEST accession	Description	Peptide count	Confidence score	Highest mean condition	Lowest mean condition	E-0	NE-0	E-21	NE-21
SCMCST1055F01	proliferating-cell nucleolar	5	23.4391	NE-0	NE-21	963.3151	1050.656	777.4044	-
SCQSLB1051H10	agenet domain containing expressed	4	21.5879	NE-0	NE-21	1477.208	1634.64	755.4896	-
SCRFLR1012H05	act1_orysj	27	306.9723	NE-0	E-21	936.2848	2328.022	645.0663	-
SCJLRT3077C07	sec1 family transport protein sly1-like	7	36.2007	E-0	NE-21	1144.292	258.3949	640.4691	-
SCJLRT2049H04	chorimate mutase	2	9.5971	NE-21	E-0	1255.577	3891.668	1382.872	-
SCCCCRZ1003H11	mitochondria fission 1 protein	6	34.1163	E-0	E-21	1315.439	1109.502	806.429	-
SCUTLR1058B12	thymidylate kinase	7	39.7275	NE-0	E-0	946.7576	1520.814	1311.927	-
SCJFRT1008C02	retinol dehydrogenase 14	5	27.1081	NE-0	E-0	1706.215	6877.955	2033.654	-
SCEQRT1030C08	translin [Zea mays]	3	17.6202	E-21	NE-21	993.7517	398.1878	1981.164	-
SCBFRT1064C08	iron ascorbate-dependent oxidoreductase	10	76.1614	NE-0	E-0	1030.091	23383.08	1955.328	-
SCQGLR1019E12	fha domain containing protein	2	9.7062	E-0	NE-21	3641.748	1805.511	1925.347	-
SCEPRZ3045G05	leucine-rich repeat receptor protein kinase exs	14	79.1813	NE-21	NE-0	1589.139	319.3423	1745.326	-
SCCCST1006G04	translin-associated protein x-like isoform 1	9	64.0795	E-21	NE-0	1355.846	521.3984	1848.783	-
SCQSRT2035A05	infection-related protein	4	37.0237	NE-21	E-0	1199.147	2145.877	1839.595	-
SCSFRT2072E04	4-hydroxyphenylpyruvate dioxygenase	1	6.5948	E-21	NE-0	1581.854	823.1841	1665.959	-
SCCCAM2001A07	pht42_orysj	1	4.5075	NE-0	NE-21	655.922	4298.64	1649.644	-
SCCCCL2001A02.b	pepper esterase	8	45.1032	NE-0	E-21	2370.735	10389.39	1526.71	-
SCEZRT3070D05	mdr-like abc transporter	4	21.1741	E-0	E-21	3428.655	2065.567	1465.477	-
SCVPCL6046A05	copg1_orysj	16	87.7479	NE-21	E-21	1632.75	2256.318	1430.982	-
SCVPRZ2038A09	cob21_orysj	6	37.3246	E-0	E-21	7837.044	6688.87	3020.179	-
SCQSRT2033C03	ethanol tolerance protein geko1	3	20.3816	E-21	E-0	123.2549	125.1517	2919.365	-
SCCCCRZ2001D05	pre-mrna branch site p14-like protein	3	28.6008	E-21	NE-0	2384.574	320.6915	2794.994	-
SCEPLB1044D11	plant-specific domain tigr01615 family protein	4	32.9506	E-0	E-21	8932.957	3606.297	2734.669	-
SCCCRT1001G02	versicolorin reductase	6	33.2725	E-0	NE-21	5907.252	764.9383	3040.588	-
SCCCCL4001D12	cyanate hydratase	2	21.9722	E-0	NE-0	3520.175	1230.268	2658.649	-
SCCCST3144G03	metal-dependent hydrolase-like protein	8	63.2076	NE-21	NE-0	2905.149	584.8807	2551.911	-
SCCCCRZ2004A04	Os07g0150500 [Oryza sativa Japonica Group]	5	23.9921	E-21	NE-21	1907.725	1059.21	2480.417	-
SCRUAD1132E05	phytosulfokine receptor precursor	2	9.2182	E-21	NE-21	2615.969	1287.666	3403.838	-
SCQGFL4079G07	wd-40 repeat protein	7	47.1281	E-21	NE-21	1953.717	105.6473	3127.854	-
SCRLRT3035G03	ubiquitin c-terminal hydrolase	9	54.4231	NE-0	NE-21	2755.972	31065.53	3119.615	-
SCCCCL3120G05.b	structure-specific recognition protein 1	5	25.8091	E-0	NE-21	4740.21	3887.497	3107.151	-
SCEZHR1084H04	pollen-specific protein like	4	38.15	E-0	NE-21	11533.86	3937.401	5343.229	-
SCQSRT2036A02	pp2ac-3 - phosphatase 2a isoform 3 belonging...	10	66.2043	NE-21	E-0	4669.505	6230.793	5340.275	-

Table S2 cont.

SUCEST accession	Description	Peptide count	Confidence score	Highest mean condition	Lowest mean condition	E-0	NE-0	E-21	NE-21
SCEZLB1007D07	polyphenol oxidase	3	15.5869	E-21	NE-0	3012.103	792.4447	4794.5	-
SCEPAM2057G04	dpod1_orysj ame: full=dna polymerase delta...	2	10.6328	E-0	E-21	14747.64	6864.06	5015.448	-
SCVPLC6042B11	salt-induced map kinase 1	11	64.2107	E-21	NE-21	1729.685	1026.303	4405.632	-
SCJLLR1104B12	erwinia induced protein 1	1	7.5513	E-0	NE-21	8923.51	1944.728	3978.774	-
SCEZSB1090C11	temperature-induced lipocalin-1	7	42.0165	E-0	NE-0	5708.457	602.8452	3955.759	-
SCBGSB1027H10	soul heme-binding	4	24.11	E-21	NE-0	2771.342	1243.865	3942.296	-
SCRFRZ3058E08	external nadh-ubiquinone oxidoreductase...	6	34.4928	E-21	E-0	2153.085	2430.45	3784.615	-
SCRLLR1111B02	sam domain family protein	10	64.7544	E-0	NE-21	5544.678	3792.77	3784.12	-
SCCCRT3009E06	pre-mrna-processing atp-dependent rna helicase...	10	58.0686	E-0	NE-0	6508.331	1039.53	3767.172	-
SCCCCRZ1004B02	ribonuclease h-related protein	7	42.8958	E-0	NE-21	4946.254	2343.388	3660.463	-
SCRUSB1064E09	cysp2_maize ame: full=cysteine proteinase 2 flags...	6	47.9438	NE-0	E-21	7898.981	17869.75	6812.689	-
SCCCCRZ1002G03	act3_orysj ame: full=actin-3	33	344.3913	E-0	NE-21	8766.081	7300.621	6500.15	-
SCUTRZ3102C06	phi-1-like phosphate-induced protein	5	30.6385	E-21	NE-21	255.0773	18.28845	6448.763	-
SCRFRZ3057C09	peptidoglycan-binding domain-containing	3	22.375	E-0	NE-21	16684.2	2302.737	6431.682	-
SCEQLR1050H09	drep4 protein	4	24.9143	NE-0	E-0	182.6463	9108.036	5844.083	-
SCEZLB1005C03	tankyrase 1	6	33.3212	E-21	NE-0	374.6888	122.7598	5577.494	-
SCEZLR1009H06	af215854_1hexose partial	2	15.3778	E-21	NE-0	2358.403	55.32743	6867.49	-
SCRFLB2059H06	adp-glucose pyrophosphorylase small subunit	22	144.9706	E-0	NE-21	10311.04	5065.598	7510.95	-
SCJLLR1108E06	carbonic anhydrase	7	49.5694	NE-0	E-21	12322.08	131555	7607.723	-
SCCCCL3001E04.b	non- nadp-malic enzyme	8	49.1138	E-0	NE-0	11231.75	3670.582	7800.023	-
SCEPAM1108G11	quaking isoform 5-like	2	9.7339	NE-0	NE-21	4615.568	19602.34	8171.536	-
SCCCLR1077A10	glutamyl-tRNA cytoplasmic	9	57.1029	E-21	NE-0	1859.967	222.5148	8164.008	-
SCCCCL4012E07	s-glutathione dehydrogenase class iii alcohol...	14	109.5344	E-21	NE-21	6561.471	1333.066	8389.695	-
SCBGAM1090F06	soluble inorganic pyrophosphatase	11	82.1282	E-0	NE-21	15369.3	11799.69	8360.348	-
SCJFST1010F06	nadph adrenodoxin oxidoreductase	16	89.2106	E-0	NE-21	13603.5	380.2137	10603.94	-
SCSBFL1039B03	dead h (asp-glu-ala-asn his) box polypeptide 8...	2	11.1072	NE-0	NE-21	14624.58	23514.9	9636.499	-
SCJFLR1073E04	strictosidine synthase precursor	16	121.4546	NE-0	NE-21	4691.139	23539.87	9543.327	-
SCCCCL7038E07	importin-beta n-terminal domain containing...	10	69.512	E-0	NE-21	23223.14	10652.52	12029.34	-
SCAGLR1043A01	yt521-b-like family protein	4	29.1814	E-21	NE-21	12968.8	25011.41	37673.99	-
SCCCCL4012H11	abc transporter f family member 3-like	4	18.6233	E-21	NE-0	1944.476	440.4467	21238.46	-
SCCCLR2004H12	ago1b_orysj	29	169.1564	E-21	NE-21	9155.702	902.4522	23064.23	-
SCEQRZ3093C12	ubiquitin-fold modifier 1 precursor	3	24.4975	E-21	NE-21	2807.161	110.4378	16938.21	-
SCJFHR1C04H10.b	importin-alpha re-exporter	6	42.7684	E-21	NE-21	6458.499	11190.28	15183.97	-

Table S2 cont.

SUCEST accession	Description	Peptide count	Confidence score	Highest mean condition	Lowest mean condition	E-0	NE-0	E-21	NE-21
				NE-0	NE-21				
SCJLFL4100F04	ferredoxin- chloroplastic-like	4	35.6062	E-0	NE-0	29156.78	2232.372	15992.6	-
SCQGLB1039E05	er6 protein	6	53.6673	E-0	NE-0	12890.14	3735.439	10923.46	-
SCSGAD1005H05	cullin 3	10	47.4942	E-21	NE-21	11670.8	2460.572	12344.64	-
SCEPAM1019D01	nap16kda protein	3	40.3968	E-21	NE-21	2428.835	817.1337	11219.64	-
SCCCCL4015D08	e chain localization of the small subunit ribosomal...	14	112.8181	E-0	NE-0	15671.35	11459.66	15235.81	-
E-0, NE-0 and NE-21 co-expressed proteins									
SCCCLB1001B05	chitin elicitor-binding	4	21.6771	NE-21	E-21	420.8737	6033.358	-	10116.82
SCJLFL1049E05	clathrin-adaptor medium chain apm 4	10	58.9873	NE-0	E-0	78.62876	7125.762	-	6009.186
SCSBSB1053C11	acc1_orysj ame: full=acetyl- carboxylase 1 includes	1	4.3334	NE-21	E-0	114.3596	4268.581	-	4733.753
SCQSLR1040B10	palmitoyl-protein thioesterase 1 precursor	3	15.9526	E-21	E-0	344.386	422.7714	-	540.4591
SCBFLB2091F04	flavonol sulfotransferase-like	3	19.7916	E-21	NE-21	1166.721	517.0104	-	182.0259
SCQSRT1035D12	permatin precursor	4	26.0562	NE-0	E-0	137.1969	4886.809	-	380.3357
SCCCCL4003D04	isoleucyl-tRNA cytoplasmic-like	12	67.6126	NE-0	E-0	4248.496	32897.05	-	23400.72
SCVPCL6042C08	1-deoxy-d-xylulose 5-phosphate reductoisomerase	9	60.6001	E-21	NE-0	34304.79	4007.443	-	5205.608
SCJFRZ2013G10	structural maintenance of chromosomes protein6...	14	73.1554	NE-21	E-0	1278.765	4152.011	-	9250.292
SCCCLR1C02A06	glo5_orysj	3	17.5293	NE-21	NE-0	481.1488	151.9026	-	824.6285
SCSBAM1086G07	zll phn homologous protein	8	41.2647	E-0	NE-0	541.8879	282.5288	-	412.4079
SCCCLR1066H03	hydrogen-transporting ATP rotational mechanism	5	29.2021	NE-21	E-21	10412.86	18186.37	-	18335.99
SCCCCL4010H07	mitotic checkpoint protein bub3	3	14.8223	NE-21	NE-0	1585.449	408.9103	-	2086.659
SCQSLB1052F09	10-deacetylbaicatin iii 10-o-acetyltransferase	6	34.3282	E-0	NE-0	4607.275	1854.447	-	2368.631
SCCCLR1C05G11	ring3 protein	4	18.9807	NE-0	E-21	3324.157	9430.254	-	9051.915
SCCCLR1024B04	vesicle-associated membrane protein 727	8	52.2444	NE-0	E-21	868.2298	2932.157	-	1219.637
SCCCLR1069D05	actin- expressed	36	386.7377	NE-21	NE-0	1786.629	1131.222	-	1820.509
SCEPLR1030A12	inner envelope membrane protein	4	28.3519	NE-0	E-21	1697.231	4256.233	-	2214.452
SCSFAM1075C07	inositol-tetrakisphosphate 1-kinase 1	5	26.5442	NE-21	E-21	3592.448	5124.949	-	9023.039
SCQSRT1037E09	nifu-like protein mitochondrial-like	4	23.2077	NE-21	E-21	958.711	3212.499	-	3763.386
SCJFRT1059E08	pto kinase interactor 1	11	70.7686	E-0	NE-21	5630.7	4074.264	-	1143.92
SCQGLR1062G06	ferredoxin-dependent glutamate chloroplast...	4	21.421	NE-21	E-21	257.6783	1181.762	-	6378.519
SCRFFL4009A01	pp2ac-5 - phosphatase 2a isoform 5 belonging...	19	117.212	NE-21	NE-0	1315.987	177.3273	-	2251.268
SCCCCL4009H01	trans-cinnamate 4-monooxygenase	4	18.8515	E-0	E-21	993.84	590.7497	-	703.3816
SCEQRT1026G06	phosphoglucomutase chloroplast	8	60.2844	NE-21	E-21	7917.716	4436.402	-	8722.87
SCACAD1037A09	proton translocating pyrophosphatase	21	141.4369	NE-21	E-21	1212.704	830.4915	-	3702.382
SCCCCL4002G01	ctp synthase	2	11.6762	NE-0	NE-21	1133.711	1938.844	-	68.32218

Table S2 cont.

SUCEST accession	Description	Peptide count	Confidence score	Highest mean condition	Lowest mean condition			E-0	NE-0	E-21	NE-21
				E-21	6436.806	4318.837	-				
SCCCLR2C02D12	chlorophyll a b-binding apoprotein cp26 precursor	1	5.5556	E-0	E-21	6436.806	4318.837	-	1835.235		
SCCCLR1022C06	aci-reductone dioxygenase-like protein	8	48.9687	E-0	E-21	11585.7	5988.313	-	3129.438		
SCEQRT1033E11	2-nitropropane dioxygenase-like protein	5	23.5674	NE-21	E-21	69.12966	2547.253	-	3060.996		
SCEPRT2043A01	mannitol dehydrogenase	11	56.5515	NE-0	E-21	935.5621	2827.667	-	198.7454		
SCACFL5027G07	ac079179_18 retroelement	1	6.3214	NE-0	E-21	743.9192	10095.22	-	6153.512		
SCCCRT2002D03	type-1 pathogenesis-related protein	2	13.8263	NE-21	NE-0	924.5275	62.41272	-	4775.178		
SCACAM2043E01	phenazine biosynthesis protein	4	22.8644	E-0	E-21	9559.566	2208.471	-	723.995		
SCRFLR2037A10	type 1 membrane	6	38.65	NE-21	E-21	448.33	514.1831	-	24574.63		
SCCCCL4002F09	snf2 transcription factor	5	24.8291	NE-0	E-21	1099.163	2222.095	-	1174.269		
SCCCRT2C09A10	phosphoglucose isomerase	10	79.4738	NE-0	E-21	198.1708	954.03	-	614.9566		
SCQSRT2033E01	nicotinate phosphoribosyltransferase-like protein	5	29.3151	NE-21	E-21	72.96752	1114.423	-	4862.998		
NE-0, E-21 and NE-21 co-expressed proteins											
SCJFAD1010G05.b	alpha-l-arabinofuranosidase c-terminus family...	1	6.4773	NE-0	E-0	-	3298.045	120.2074	2617.588		
SCQSLR1061D05	ac068923_15 pre-mrna splicing factor	3	16.5192	E-21	NE-0	-	69.07862	1514.217	733.1552		
SCSGLR1025F04	galactose kinase	2	10.6786	E-21	E-0	-	4065.088	5396.657	898.1771		
SCQGST3154G02	nfyb4_orysj	3	16.6891	E-0	NE-21	-	561.5512	479.0187	65.23303		
SCQGLR2032A01	copine i-like	1	3.486	NE-0	E-0	-	8299.828	435.3948	6873.041		

a) Confidence scores are calculated by ProteinLynxGlobalServer (PLGS). They are indicated from biological repeat 1–3.

APPENDICE B

Table S1. Unchanged proteins (1,094) identified in the embryogenic sugarcane callus submitted to W_mB_dR_fR (LED lamps mixture of W= White; _mB= Medium Blue; _dR= Deep Red; _fR= Far Red) in relation fluorescent lamp (control) on day 28 of maturation treatment. Proteins abundance were considered unchanged when the log₂ of the fold change was between -1.2 and 1.2.

Accession	Peptide count	Confidence score ^a	Log ₂ of fold change ^b	Description	Total Ion Counts Control	Total Ion Counts W _m B _d R _f R
SCACAD1036F01	10	65,5058	0,5378	mitochondrial aldehyde dehydrogenase aldh2a	11203,7	16265,21
SCACLB1046D04	4	26,9433	0,2234	cysteine protease 1 precursor	10149,18	8693,316
SCACLR1036B11	17	182,5052	0,4667	60s acidic ribosomal protein p0	316477,3	437367,8
SCACLR1036E10	6	35,0352	0,4109	acyl- synthetase long-chain family member 3	27726,44	36863,65
SCACLR1057E10	6	40,1497	0,0076	nadh-ubiquinone oxidoreductase b18 subunit	11071,52	11013,55
SCACLR1057G05	6	40,0624	0,0464	glutaryl- dehydrogenase	5455,184	5282,37
SCACLR1057G08	16	113,9096	0,2514	activator of 90 kda heat shock protein atpase	23932,97	28489,31
SCACLR1126F12	5	31,0643	0,7334	lea1_orysj ame: full=late embryogenesis abundant protein 1	38441,58	23121,58
SCACLR1127B10	5	41,4664	0,5677	40s ribosomal protein s21-like	21822,89	32344,34
SCACLR1127E10	5	38,268	0,1623	nadh-ubiquinone oxidoreductase kda subunit	14541,55	12994,55
SCACLR1127F07	16	169,0722	0,0584	elongation factor 1-beta	55529,79	57825,24
SCACLR1130B08	3	19,2767	0,0023	40s ribosomal protein s25-1	13021,24	13000,13
SCACLR2007C03	21	175,4795	0,5393	guanine nucleotide-binding protein beta subunit-like protein	172262,4	250336,4
SCACLR2007D12	9	67,5134	0,6159	proteasome subunit beta type 1	5451,858	8355,235
SCACLR2022D05	12	82,4126	0,4035	transaldolase 2	25119,3	33226,24
SCACLR2029B08	3	20,5803	0,5006	cata3_maize ame: full=catalase isozyme 3	4610,265	3258,55
SCACLR2029H09	5	48,4581	0,1481	xylogen protein 1	43970,45	48722,62
SCACRZ3109B10	3	16,8518	0,1084	imidazole glycerol phosphate synthase chloroplast expressed	10741,78	11580,11
SCACSB1037G08	7	82,0766	0,2696	fructose-bisphosphate aldolase cytoplasmic isozyme	114934,7	138555,2
SCACSB1117E06	1	5,2637	0,1536	hypothetical protein SORBIDRAFT_01g008740 [Sorghum bicolor]	10459,96	11634,9
SCACSB1123D05	2	12,3484	0,3212	importin-alpha re-exporter	5890,085	7359,079
SCACSD1017D11	15	140,3604	0,0697	clone 205-like isoform 1	17154,69	18003,57
SCACST3159D04	9	54,3458	0,0791	inosine-5-monophosphate dehydrogenase 2	11822,29	12488,38
SCAGAM2126E02	6	35,5688	0,0082	rna recognition motif family expressed	24484,63	24624,03
SCAGFL1087C05	2	11,4547	0,4676	elongation factor tu	3536,727	4890,674
SCAGLB1069A07	12	77,5169	0,2498	peroxisomal fatty acid beta-oxidation multifunctional protein	19666,55	23383,92
SCAGLB1070D03	18	116,3804	0,0584	protein disulfide isomerase	49895,45	51956,11
SCAGLB1071C03	5	36,0738	0,6432	peroxisomal multifunctional enzyme type 2	5252,594	8203,59
SCAGLB1071F12	8	56,8196	0,1931	glutaredoxin subgroup ii	34786,67	30428,36
SCAGLB2046F01	4	34,7912	0,2122	bowman-birk type bran trypsin inhibitor precursor	3916,171	3380,417
SCAGLR1021A12	10	124,4094	0,3229	histone h2a	534352,9	668372,1
SCAGLR1021B05	24	219,9401	0,1605	alpha- glucan protein synthase	7295,764	6527,654

Table S1 cont.

Accession	Peptide count	Confidence score ^a	Log ₂ of fold change ^b	Description	Total Ion Counts Control	Total Ion Counts W _m B _d R _f R
SCAGLR1021F12	25	188,7203	0,2414	argininosuccinate synthase	84884,63	71804,02
SCAGLR1021H05	22	147,3854	0,1262	hypothetical protein SORBIDRAFT_04g025840 [Sorghum bicolor]	25449,71	23317,7
SCAGLR1043C02	14	157,6139	0,3601	apx2 - cytosolic ascorbate peroxidase	3572,36	4585,104
SCAGLR1043D04	35	289,7383	0,2455	vacuolar proton-atpase	18610,28	22062,53
SCAGLR1043E04	8	44,7265	0,2749	cytochrome p450 cyp74a19	7544,968	9128,984
SCAGLR1043E06	24	169,2898	0,1473	phospholipase d alpha 1	81145,02	89867,69
SCAGLR1043G12	19	190,6117	0,7456	cbs domain protein	30390,42	50955,82
SCAGLR1043H07	6	38,1435	0,0079	carrier protein	4537,341	4562,369
SCAGLR2011C01	9	51,9375	0,1669	glycine-rich rna-binding protein 7	5009,708	4462,455
SCAGLR2011D03	9	78,4025	0,0273	hypothetical protein SORBIDRAFT_03g008870 [Sorghum bicolor]	4970,054	5064,841
SCAGLR2011G10	7	51,3983	0,0813	ob-fold nucleic acid binding domain containing protein	21525,9	20345,83
SCAGLR2026C06	19	143,882	0,1585	4-methyl-5(b-hydroxyethyl)-thiazol monophosphate biosynthesis enzyme	56248,04	62779,27
SCAGLR2033A03	13	78,4541	0,8772	suppressor of g2 allele of skp1	18252,07	33525,43
SCAGLR2033A08	2	11,0884	0,4957	hypothetical protein SORBIDRAFT_07g009470 [Sorghum bicolor]	4187,283	2969,773
SCAGLR2033D11	10	67,8085	0,2157	60s ribosomal protein l3	7486,169	8693,509
SCAGLR2033E03	5	56,8688	0,1953	aquaporin pip1-2	64798,79	56594,06
SCAGLR2033E10	5	32,6535	1,0447	probable zinc finger protein - alfalfa	1154,736	2382,109
SCAGLV1043D04	6	51,6119	0,3757	dna-binding protein mnb1b	8064,26	10463,18
SCAGRT2039B01	17	112,18	0,4414	caffein acid 3-o-methyltransferase	14359,46	19498,77
SCAGRT2041G07	18	109,3654	0,0037	dihydrolipoamide s-acetyltransferase	25507,8	25573,47
SCAGRT3050C09	1	5,7289	0,0613	hypothetical protein SORBIDRAFT_08g019230 [Sorghum bicolor]	4019,674	3852,559
SCBFAD1067E10	6	59,6645	0,2764	dnak-type molecular chaperone nthsp70 - common tobacco	1628,173	1344,276
SCBFLR1026B05	19	130,1767	0,4259	transaminase transferring nitrogenous groups	30232,8	40614,94
SCBFLR1026B07	18	128,1848	0,1404	nucleolar protein nop56	59348,89	65415,9
SCBFLR1026E01	10	64,2285	0,5193	60s ribosomal protein l10-3	25339,54	36317,72
SCBFLR1026E02	24	311,1594	0,2710	14-3-3-like protein	30813,99	37182,41
SCBFLR1026E07	25	166,9377	0,8906	coatomer subunit gamma	33264,18	61667,92
SCBFLR1039A11	3	21,3165	0,6653	aak1 protein	244675,1	154277,6
SCBFLR1039C04	2	11,7931	0,2365	exo - beta-glucanase	647,8806	549,9293
SCBFLR1046E09	7	46,9227	0,2026	nonspecific lipid-transfer protein precursor	4348,416	5003,964
SCBFLR1046F11	5	36,5992	0,4872	60s ribosomal protein l18	32707,29	23332,98
SCBFLR1083E01	15	101,3297	0,5792	glycosyl hydrolases family 38 expressed	37771,62	56430,69
SCBFLR1083E03	12	98,7756	0,2269	nucleoside diphosphate kinase i	212790,1	249031,7
SCBFRT1067A07	6	39,0203	0,4871	ras-related protein rab11b	26868,18	37659,3
SCBFRT1068C11	6	49,1527	0,9731	hypothetical protein SORBIDRAFT_02g023480 [Sorghum bicolor]	6150,202	12073,57
SCBFRZ2016A06	3	17,9975	0,7417	hypothetical protein SORBIDRAFT_02g040270 [Sorghum bicolor]	20132,98	33665,62

Table S1 cont.

Accession	Peptide count	Confidence score ^a	Log ₂ of fold change ^b	Description	Total Ion Counts Control	Total Ion Counts W _m B _d R _f R
SCBFRZ2016F04	2	11,4416	0,0908	heterogeneous nuclear ribonucleoprotein r	3375,447	3594,718
SCBFRZ2017C11	10	78,5278	0,1323	per1_maize ame: full=peroxidase 1	5200,451	4744,789
SCBFRZ2017F08	19	140,8857	0,6333	pantothenate kinase 4	85974,45	133357,2
SCBFRZ2019F04	6	55,7554	0,1729	snrnp core sm protein sm-x5-like protein	25053,43	28242,33
SCBFRZ2045D04	14	155,4	0,2380	60s ribosomal protein l9	2654,514	3130,666
SCBFRZ2046E02	1	5,5747	0,8157	dynamin family expressed	1494,326	848,9479
SCBFBSB1045E12.b	8	56,5671	0,1221	nucleic acid binding protein	18418,24	20044,66
SCBFSD1035A08	2	10,7416	0,2065	3-isopropylmalate dehydratase large subunit	1720,087	1490,673
SCBFST3133F03	4	21,8529	0,2450	rab1 small gtp-binding protein	14554,49	12281,49
SCBFST3133G02	6	34,5577	0,4490	uncharacterized protein LOC100216659 precursor [Zea mays]	24943,05	18272
SCBFST3135H08	4	36,808	0,5313	histone h2a	13300,41	19221,74
SCBGFL5077A04	1	6,6013	1,0768	atp gtp binding protein	2049,668	971,7008
SCBGLR1002D03	14	115,8257	0,2935	proteasome subunit beta type 1	35678,1	43727,35
SCBGLR1002F11	11	103,1582	0,1919	alpha 3 subunit of 20s proteasome	13606,74	15542,36
SCBGLR1003B07	14	108,5748	0,5667	gtp-binding protein sar1a	30077,92	44548,59
SCBGLR1003E06	15	103,9418	0,7535	eukaryotic initiation factor 5c cg2922- isoform f	20058,52	33816,4
SCBGLR1003G06	18	124,0388	0,1394	importin beta-like protein	34950,43	31731,51
SCBGLR1023H10	34	280,1802	0,1348	poly -binding protein	216340,1	237533,7
SCBGLR1047C07	2	12,1055	0,4789	hypothetical protein [Zea mays]	6205,226	8648,117
SCBGLR1047D05	10	87,0072	0,2380	nascent polypeptide-associated complex alpha subunit-like protein	26041,76	30712,91
SCBGLR1082E09	12	76,904	0,9028	ras-related protein ric2	33321,58	62299,15
SCBGLR1082H03	7	65,5176	0,6251	vacuolar atp synthase subunit g	1106,739	1706,919
SCBGLR1096E06	1	6,2791	0,4080	inosine-5 -monophosphate expressed	4174,127	5538,361
SCBGLR1096F04	9	82,5334	0,0290	acyl- -binding protein	27039,62	26501,64
SCBGLR1098A04	3	18,1821	0,8872	lsm sm-like protein family member	1695,907	3136,744
SCBGLR1114F09	5	43,6352	0,6494	chitinase iii-like protein	8946,688	14033,44
SCBGLR1115F09	3	18,6524	0,1848	cop9 signalosome complex subunit 6a	6533,456	5747,986
SCBGLR1117C04	9	50,4769	0,3538	aspartyl-tRNA synthetase	19315,69	24683,47
SCBGLR1117C08	6	41,621	0,3917	regulator of ribonuclease activity a	2077,554	1583,584
SCBGLR1119A06	6	46,1673	0,3073	histone h1	11348,08	9171,164
SCBGLR1119H10	3	16,9662	0,1850	60s ribosomal protein l10-3	2834,145	3221,832
SCBGLR1120G03	8	59,5785	0,1524	grf-interacting factor 2	5588,356	5028,082
SCBGRT3071A03	2	10,89	0,1421	pir7b protein	2702,264	2448,724
SCCCAD1003B05	3	16,7561	0,0513	hypothetical protein SORBIDRAFT_06g019700 [Sorghum bicolor]	3043,004	2936,787
SCCCAM1001A05	7	53,318	0,1666	spermidine synthase 1	38815,81	34583,51
SCCCAM1002E04	3	17,1592	0,7178	tumor-related protein	2129,18	3501,864

Table S1 cont.

Accession	Peptide count	Confidence score ^a	Log ₂ of fold change ^b	Description	Total Ion Counts Control	Total Ion Counts W _m B _d R _f R
SCCCAM1002G10	3	18,5644	0,3046	repressor protein	2219,033	2740,609
SCCCAM1002H03	9	59,1508	0,1707	nucleic acid binding protein	7788,849	6919,915
SCCCAM1073A05	2	18,3352	0,1948	hypothetical protein SORBIDRAFT_01g016490 [Sorghum bicolor]	73788,19	64468,91
SCCCAM1C03D11	1	6,0129	1,0443	bowman-birk type trypsin inhibitor precursor	10636,53	21935,79
SCCCAM1C04B04	15	118,1147	0,7040	10 kda expressed	50501,69	82268,89
SCCCCL1002A05.b	11	72,9331	0,9713	ubiquitin carboxyl-terminal hydrolase 6	11565,63	22674,89
SCCCCL1002D10.b	20	159,7779	0,4421	pyruvate dehydrogenase e1 component alpha subunit	111592,4	151611,8
SCCCCL1002F12.b	12	97,9266	0,3266	enoyl-acp reductase	54800,86	68721,51
SCCCCL2001A05.b	6	41,9897	0,3932	nadp-dependent malic enzyme	3949,473	5186,873
SCCCCL2001B02.b	27	240,8609	0,5963	glyceraldehyde-3-phosphate cytosolic	43034,88	65059,66
SCCCCL2001B11.b	5	36,0803	0,1831	xip1_wheat	11608,19	13179,3
SCCCCL3001A02	4	22,8632	0,2070	serine threonine protein kinase	6121,158	5303,057
SCCCCL3001A05	54	492,0561	0,6693	acoc_orysj ame: full= aconitate cytoplasmic short=aconitase	208445	331484,4
SCCCCL3001B04.b	19	148,4716	0,7978	prolyl-trna synthetase -like	57297,25	99605,99
SCCCCL3001B07.b	27	223,8092	0,6631	pyrophosphate-dependent phosphofructokinase alpha subunit	93190,73	147570,7
SCCCCL3001B09.b	34	277,5463	0,3060	aconitate hydratase 1	75949,69	93897,02
SCCCCL3001B10.b	13	77,2563	0,5559	b chain semi-active e176q mutant of rice a plant - glucosidase	17751,19	26096,39
SCCCCL3001B11	6	32,5548	0,1156	methionyl-trna synthetase	75098,49	81362,08
SCCCCL3001C03	31	226,2531	0,2513	citrate synthase mitochondrial expressed	127673,1	151969,4
SCCCCL3001E03.b	6	46,534	0,4558	xylogen protein 1	91052,71	124879
SCCCCL3001F05	24	183,883	0,2874	ru large subunit-binding protein subunit beta	24367,82	29739,72
SCCCCL3001F09	23	236,6274	0,4120	40s ribosomal protein s3	275065,3	365981,5
SCCCCL3001F10.b	52	479,4382	0,0775	phosphoenolpyruvate carboxylase	181375,9	191387,2
SCCCCL3001G01.b	25	228,3908	0,4161	cell division cycle protein expressed	2051,869	2737,767
SCCCCL3001G05.b	20	190,1256	1,0346	dihydroxy-acid dehydratase	107155,2	219515,6
SCCCCL3001G11.b	7	42,3508	0,1612	2-dehydro-3-deoxyphosphooctonate aldolase	12381,39	13845,24
SCCCCL3002A02.b	13	142,1166	1,1582	chloride intracellular channel 6	19176,82	42797,12
SCCCCL3002A04.b	9	83,9732	0,2017	class iii chitinase homologue (hib3h-a)	34263,42	39403,42
SCCCCL3002A09.b	12	79,7388	0,3257	alanine aminotransferase	55402,88	69434,59
SCCCCL3002B11.b	30	341,3646	1,0586	alpha-amylase isozyme 3d precursor	154230,5	321251,4
SCCCCL3002B12.b	23	148,2666	0,3208	hypothetical protein SORBIDRAFT_01g015200 [Sorghum bicolor]	24593,39	19689,49
SCCCCL3002C07.b	16	139,1435	0,5600	amy3c_orysj ame: full=alpha-amylase isozyme 3c	72355,89	106670,3
SCCCCL3002C09.b	9	97,0362	0,2947	glutathione s-transferase gstd2	1397,094	1713,768
SCCCCL3002D01.b	2	10,6466	0,8018	rna-directed dna polymerase (reverse transcriptase)	5993,824	10448,79
SCCCCL3002E11.b	13	132,4912	0,4338	tpa: class iii peroxidase 14 precursor	91905,66	124148,8
SCCCCL3002G03.b	16	109,1883	0,5321	eukaryotic translation initiation factor 3 subunit 6	27330,8	39521,63

Table S1 cont.

Accession	Peptide count	Confidence score ^a	Log ₂ of fold change ^b	Description	Total Ion Counts Control	Total Ion Counts W _m B _d R _f R
SCCCCL3003A08.b	23	149,2772	0,6610	tktc_maize ame: full= chloroplastic short=tk	40137,2	63465,24
SCCCCL3003B02.b	11	98,9434	0,5120	tpa: class iii peroxidase 60 precursor	244272,2	348330
SCCCCL3003D05.b	19	125,7843	0,2008	nadh-ubiquinone oxidoreductase 51 kda subunit	80186,94	92161,18
SCCCCL3003D06.b	20	159,6079	1,0976	ima1b_orysj ame: full=importin subunit alpha-1b	18515,74	39622,8
SCCCCL3003E02.b	11	74,9242	0,5514	ubiquitin thioesterase otubain-like protein	11019,75	16149,75
SCCCCL3003E07.b	15	192,1275	0,4185	chitinase b	455223,3	608423,2
SCCCCL3003F11.b	16	116,4246	0,6679	citrate glyoxysomal precursor	93804,67	149028,1
SCCCCL3004F01.b	29	372,9565	0,6075	elongation factor 1-alpha	278359,7	424103,3
SCCCCL3004H02.b	18	146,023	0,3969	proliferation-associated protein 2g4	60009,65	79013,46
SCCCCL3004H04.b	15	108,494	0,1560	carbonyl reductase 1	34564,55	38512,02
SCCCCL3004H08.b	7	68,5679	0,1816	copper transport protein atox1-like	230021,7	260879,9
SCCCCL3005C07.b	4	22,6097	0,3527	uncharacterized protein LOC100836836 [Brachypodium distachyon]	2629,078	3357,204
SCCCCL3005C12.b	11	73,406	0,2919	protein argonaute 1b-like	3082,935	3774,197
SCCCCL3005E06.b	20	188,6491	0,0481	fructose-bisphosphate aldolase	201845,5	208683,3
SCCCCL3005G07.b	28	202,3878	0,1953	heat shock cognate 90 kda	14995,3	13096,59
SCCCCL3080A02.b	11	66,7005	0,3018	hypothetical protein SORBIDRAFT_09g007880 [Sorghum bicolor]	10625,17	8619,519
SCCCCL3080A03	5	29,7757	0,7699	ago4a_orysj ame: full=protein argonaute 4a short= 4a	7242,786	12350,04
SCCCCL3080B05	31	213,7875	1,0906	26s protease regulatory subunit 6a	12047,3	25656,87
SCCCCL3080C04	10	75,221	0,3375	60s ribosomal protein l6-like isoform 1	55757,33	70452,8
SCCCCL3080C05.b	8	49,3604	1,1784	aspartyl expressed	10872,33	24606,4
SCCCCL3080G07	11	140,6268	0,0069	40s ribosomal protein s27a	7389,803	7354,461
SCCCCL3080H03	6	40,7844	0,3059	glutamate dehydrogenase	13613,07	16828,43
SCCCCL3080H11	22	186,9687	0,8844	catalase isozyme b	50271,03	92797,84
SCCCCL3120A08.b	6	35,26	0,4526	nadp-dependent d-sorbitol-6-phosphate dehydrogenase	3705,025	5070,314
SCCCCL3120A12	14	106,8888	0,8497	hypothetical protein SORBIDRAFT_04g010023 [Sorghum bicolor]	29319,61	52838,18
SCCCCL3120B01	29	329,888	0,4854	fructokinase-2	445613,5	623830
SCCCCL3120C03	33	433,658	0,4262	fructose-bisphosphate aldolase	139259,3	187120,6
SCCCCL3120C03.b	16	157,4486	0,6790	fructose-bisphosphate aldolase	4720,553	7557,862
SCCCCL3120D06	7	47,5624	0,7244	galactose kinase	11563,87	19105,38
SCCCCL3120F01	8	48,2902	0,9023	nadh dependent glutamate synthase	8302,512	15517,56
SCCCCL3120F02	25	172,6087	0,3816	t-complex protein 1 subunit zeta	91320,98	118974,8
SCCCCL3120F07	10	84,3729	0,3388	proteasome subunit beta type 4 precursor	63015,43	79694,37
SCCCCL3120F12	2	10,4268	0,1563	rh40_orysj ame: full=dead-box atp-dependent rna helicase 40	4981,288	5551,387
SCCCCL3120H02	10	68,9108	0,6182	uncharacterized conserved expressed	8414,626	12916,54
SCCCCL3120H06	3	19,3672	0,4480	acyl-coenzyme a oxidase peroxisomal expressed	3000,805	4093,528
SCCCCL3140B12	24	201,5002	0,5470	60s ribosomal protein l4	30143,3	44040,43

Table S1 cont.

Accession	Peptide count	Confidence score ^a	Log ₂ of fold change ^b	Description	Total Ion Counts Control	Total Ion Counts W _m B _d R _f R
SCCCCL3140C10	17	152,3185	0,8272	cysteine synthase precursor	138408,3	245574
SCCCCL3140D12	21	270,5851	0,4941	glycinebetaine proline transporter	3918,995	5519,642
SCCCCL3140F07	7	48,0428	0,1274	plasminogen activator inhibitor 1 rna-binding protein	7257,226	6643,921
SCCCCL3140G05	21	155,328	0,3958	26s proteasome non-atpase regulatory subunit 11	29361,72	38629,87
SCCCCL4001D06	10	83,1592	0,2847	hypothetical protein SORBIDRAFT_10g007690 [Sorghum bicolor]	15400,46	12642,51
SCCCCL4001F08	9	82,4324	0,1089	malate glyoxysomal	55113,41	59436,07
SCCCCL4001H11	10	72,9363	0,2752	bgl15_orysj ame: full=beta-galactosidase 15 short=lactase 15 flags	11934,05	14441,73
SCCCCL4002B05	14	98,3241	0,5123	t-complex protein 1 subunit epsilon	75287,15	107381,9
SCCCCL4002F05	14	113,51	0,0758	actin-depolymerizing factor 3	130273,9	137297,2
SCCCCL4002F06	11	66,7212	0,0262	tryptophan synthase alpha	4196,375	4273,362
SCCCCL4002F09	2	12,9739	0,4572	snf2 transcription factor	4039,873	5546,42
SCCCCL4002F10	8	48,3116	0,1165	splicing factor 3b subunit 1 isoform 1	19049,46	20652,2
SCCCCL4003F09	8	61,2725	1,0269	xytanase inhibitor protein 1 precursor	6537,044	13319,9
SCCCCL4004A04	6	40,2771	0,2692	ras-related protein rab-2-a	9490,661	11437,3
SCCCCL4004C09	9	62,8074	0,2065	hypothetical protein SORBIDRAFT_03g006650 [Sorghum bicolor]	31745,46	36630,71
SCCCCL4004C11	20	215,1837	0,2898	malate dehydrogenase	62723,46	76677,81
SCCCCL4004D02	3	15,8593	1,0250	villin 2	26303,48	12925,77
SCCCCL4004H01	7	96,8599	0,5945	xytanase inhibitor	18445,65	27852,59
SCCCCL4005D12	12	87,3555	0,3274	26s proteasome regulatory subunit	29996,56	37638,06
SCCCCL4006A03	17	118,6686	0,1584	40s ribosomal protein s3a	4737,258	5287,185
SCCCCL4006B06	7	63,4756	0,7275	late embryogenesis abundant protein group 3 variant 1	21122,48	34973
SCCCCL4006C07	26	187,5758	0,7290	26s proteasome regulatory particle triple-a atpase subunit6	26309,29	43607,38
SCCCCL4006D02	9	66,0032	0,1429	dag protein	59760,18	65984,43
SCCCCL4006G06	10	60,5682	0,1778	cysteine protease 1 precursor	19556,29	22120,59
SCCCCL4006H08	23	234,592	0,9822	alcohol dehydrogenase 2	50758,95	100272,8
SCCCCL4007B06	14	126,7916	0,0910	heat shock protein 70	11816,89	11094,34
SCCCCL4007C09	6	95,32	0,0806	histone h2a variant 1	79585,59	84159,03
SCCCCL4007E05	18	114,9066	0,2594	diphosphate-fructose-6-phosphate 1-phosphotransferase	9224,048	11041,32
SCCCCL4007F05	11	82,3711	0,5937	glutathione s-transferase gstu6	12702,93	19170,62
SCCCCL4007G11	12	102,6502	0,2765	late embryogenesis abundant protein group 3 variant 2	51204,34	42273,95
SCCCCL4008F04	3	21,8154	0,2517	40s ribosomal protein s27	92564,79	110210,3
SCCCCL4008F12	12	65,9343	0,4537	valyl tRNA synthetase	48940,37	67024,78
SCCCCL4008H04	9	58,8387	0,5212	peroxidase 27 precursor	12000,81	17223,2
SCCCCL4009G04	8	60,5998	0,4503	hypothetical protein SORBIDRAFT_01g004270 [Sorghum bicolor]	84561,92	115538,7
SCCCCL4009H11	14	132,3353	1,0198	af236369_1 prohibitin	55098,46	111722,9
SCCCCL4011B08	28	255,1247	0,1342	2-isopropylmalate synthase b	67125,09	73666,28

Table S1 cont.

Accession	Peptide count	Confidence score ^a	Log ₂ of fold change ^b	Description	Total Ion Counts Control	Total Ion Counts W _m B _d R _f R
SCCCCL4011D07	8	72,2864	0,0010	glutathione s-transferase	39780,88	39807,52
SCCCCL4011E03	12	74,0186	0,1523	toc75_orysj ame: full=protein chloroplastic	45649,24	50731,53
SCCCCL4011G05	3	18,0614	0,3288	rna-binding protein luc7-like 2	12884,92	10259,15
SCCCCL4011G09	22	229,5787	0,3192	14-3-3-like protein a	4215,803	5259,752
SCCCCL4011H08	34	317,7993	0,4509	pyrophosphate-fructose 6-phosphate 1-phosphotransferase beta subunit	249665,2	341261,3
SCCCCL4012A01	5	30,8003	0,8670	loc100284334 precursor	14913,04	27199,6
SCCCCL4012B03	9	57,6474	1,0134	xaa-pro aminopeptidase 1	11843,97	23909,69
SCCCCL4012E07	10	58,8031	0,7827	s-glutathione dehydrogenase class iii alcohol dehydrogenase	13300,98	22882,09
SCCCCL4013B01	11	110,3833	0,3200	skp1-like protein 1b-like isoform 1	29888,09	37310,34
SCCCCL4013G01	13	115,7211	0,4717	glutathione s-transferase 4	11276,12	15636,96
SCCCCL4013G04	29	230,329	0,3499	heat shock 70 kda protein 4	14451,94	18418,93
SCCCCL4014B10	4	32,8762	0,3837	presequence protease chloroplastic mitochondrial-like isoform 1	62976,08	48270,24
SCCCCL4014C12	5	26,2918	0,2579	hypothetical protein SORBIDRAFT_02g031470 [Sorghum bicolor]	21147,81	25287,58
SCCCCL4014F01	2	20,2094	0,1503	cysteine proteinase inhibitor b precursor	71175,21	78988,35
SCCCCL4014G02	5	32,8132	0,6690	uridine monophosphate synthase	15776,51	25083,8
SCCCCL4014G07	8	57,4481	0,3167	aspartic protease	13438,53	10789,76
SCCCCL4015D05	14	96,0095	0,5226	protein transport protein sec31a-like	92445,03	132805,7
SCCCCL4015F12	12	166,0226	0,8466	xylanase inhibitor	189088,3	340030,5
SCCCCL4015G12	8	46,6154	0,6026	coatomer subunit zeta-1	73286,56	111283,8
SCCCCL4017A09	29	235,2041	0,2396	nadp-specific isocitrate dehydrogenase	37464,98	44233,72
SCCCCL4017E12	13	131,3963	0,4477	hypothetical protein SORBIDRAFT_05g027350 [Sorghum bicolor]	74262,88	101284,4
SCCCCL5002B01	9	54,4068	0,0652	argininosuccinate lyase	65970,32	69018,56
SCCCCL5002D02	9	51,2153	0,1201	atypical receptor-like kinase mark precursor	11309,41	10406,28
SCCCCL5002H02	20	179,5874	0,3697	globulin-1 s allele precursor	306165,2	236957,8
SCCCCL5072E02	6	66,9841	0,1007	14-3-3-like protein	2803,746	2614,635
SCCCCL6001A04	5	59,1076	0,7858	dehydri n 11	100034	58024,05
SCCCCL6002A08	3	27,8991	0,7770	indole-3-acetic acid-amido synthetase	1193,594	2045,279
SCCCCL6004H07	3	19,045	0,9461	beta-galactosidase expressed	4333,084	8348,58
SCCCCL6004H11	7	75,5394	0,0394	alpha amylase	15106,76	15525,38
SCCCCL6005C02	15	108,0009	0,0568	eukaryotic translation initiation factor 2 alpha subunit	70034,25	72845,6
SCCCCL7001H04	13	81,809	0,6912	fasciclin-like arabinogalactan protein 10 precursor	29837,98	48177,51
SCCCCL7037A10	21	161,1671	0,8261	loc100282411 precursor	186884,7	331321,6
SCCCCL7C02A04	12	107,2621	0,3027	cupin family expressed	152073,1	123292
SCCCCL7C03A06	1	7,1393	0,9226	maize protease inhibitor	2105,488	3990,91
SCCCCL7C03C05	12	73,3762	0,1048	af467541_1 aldehyde dehydrogenase mis1	25078,75	26967,95
SCCCCL7C03F06	7	42,5765	0,4316	isocitrate dehydrogenase	6917,879	9330,025

Table S1 cont.

Accession	Peptide count	Confidence score ^a	Log ₂ of fold change ^b	Description	Total Ion Counts Control	Total Ion Counts W _m B _d R _f R
SCCCCL7C05F08	5	31,1258	0,6357	tpa: class iii peroxidase 66	11851,42	18413,17
SCCCFL1003H07	7	45,4353	0,2061	auxin-induced protein pcnt115	23484,05	27091,05
SCCCFL3003H06	20	136,7487	0,1050	isochorismate synthase 1	14422,6	15511,82
SCCCFL5061G09	1	5,8006	0,0132	alcohol dehydrogenase 1	7312,343	7245,503
SCCCFL5061H09	10	61,6134	0,0573	dihydrolipoyl dehydrogenase mitochondrial-like	5535,238	5759,396
SCCCFL6001G05	3	16,8972	0,2216	auxin response factor 7a	2721,199	2333,8
SCCCHR1002F08	12	94,5355	0,4356	prolyl carboxypeptidase like protein precursor	43311,18	58578,87
SCCCHR1002G07	2	12,3929	0,6438	gpi-anchored protein	13568,62	21199,83
SCCCHR1002H03	6	50,7751	0,1723	6-phosphogluconate decarboxylating	33836,73	30027,53
SCCCLB1001H03	9	61,8579	0,2031	unknown [Zea mays]	23042,11	26526,29
SCCCLB1001H09	6	39,2118	0,0096	methyl-binding domain protein mbd111	17512,02	17395,61
SCCCLB1004B02	13	108,0272	0,5930	atpase subunit 1	61815,39	93243,93
SCCCLB1004D05	10	66,3567	0,4905	nadh-cytochrome b5 reductase-like protein	18546,26	26056,78
SCCCLB1004G11	6	47,2633	0,1609	transcription factor apfi	12534,04	14012,63
SCCCLB1004H02	38	348,9157	0,4279	ubiquitin-activating enzyme e1 expressed	151263,9	203493,7
SCCCLB1004H08	22	184,0786	0,3588	adenosine kinase	164770,1	211287,7
SCCCLB1023F09	20	145,7256	0,9908	cathepsin b-like	63436,56	126065,8
SCCCLB1024B10	5	36,701	0,1395	phosphate carrier mitochondrial expressed	9365,195	10315,98
SCCCLB1024B11	7	50,013	0,5372	diaminopimelate decarboxylase	16693,65	24225,84
SCCCLB1025B01	5	44,2154	0,0540	plasminogen activator inhibitor 1 rna-binding protein	4958,622	4776,431
SCCCLB1025B04	11	74,2855	0,0230	vacuolar atp synthase subunit e	40233,71	39596,53
SCCCLR1001G10	14	135,7425	0,7682	-dimethylmalate lyase-like isoform 1	78182,53	133152,4
SCCCLR2004C08	10	125,7188	0,1268	ubiquitin-like protein	11085,68	10152,92
SCCCLR2009F12	2	12,5512	0,3327	hypothetical protein SORBIDRAFT_06g014760 [Sorghum bicolor]	3163,302	3983,738
SCCCLR1001A05	49	469,1676	0,6628	sucrose synthase	123099,9	194881,1
SCCCLR1001A07	9	83,2752	0,0062	glutathione transferase iii	14793,23	14729,38
SCCCLR1001B04	16	145,9194	0,1007	alpha 1 subunit of 20s proteasome	115477,4	107694
SCCCLR1001B07	6	56,0988	0,0051	atp synthase delta chain	87093,53	86786,91
SCCCLR1001B10	17	118,5113	0,0128	splicing factor u2af 65 kda subunit	22337,03	22140,16
SCCCLR1001B11	15	111,3921	0,2805	pyridoxin biosynthesis protein er1	72210,3	87706,2
SCCCLR1001E03	16	117,1108	0,3985	apx4 - peroxisomal ascorbate peroxidase	22374,86	29493,85
SCCCLR1001E06	34	452,9823	0,8204	glyceraldehyde-3-phosphate cytosolic 3	1465882	2588566
SCCCLR1001F04	2	17,9968	0,5322	dhn2-like protein	1320,505	913,1264
SCCCLR1001G06	6	45,8187	0,0357	s-adenosylmethionine synthetase 1	2602,936	2539,383
SCCCLR1001G12	12	82,7948	0,5224	gdp dissociation inhibitor	39349,33	56519,48
SCCCLR1001H04	8	56,2005	0,4775	ubiquinol-cytochrome c reductase complex 14 kda protein	29381,85	40908,31

Table S1 cont.

Accession	Peptide count	Confidence score ^a	Log ₂ of fold change ^b	Description	Total Ion Counts Control	Total Ion Counts W _m B _d R _f R
SCCCLR1022A05	25	156,6872	0,7548	mitochondrial-processing peptidase alpha subunit	53272,94	89890,48
SCCCLR1022A08	15	85,6077	0,0082	hypothetical protein SORBIDRAFT_03g009870 [Sorghum bicolor]	25889,07	26036,61
SCCCLR1022B11	10	81,9573	0,4595	cysteine protease 1 precursor	59803,13	82234,6
SCCCLR1022D02	15	101,2438	0,1812	vacuolar atpase subunit h protein	23178,16	26279,81
SCCCLR1022D04	10	64,5004	0,0898	mdhg_orysj ame: full=malate glyoxysomal flags: precursor	17071,13	18167,18
SCCCLR1022D05	26	316,3372	0,4035	14-3-3-like protein gf14-6	94408,88	124871,8
SCCCLR1022E06	25	164,3177	0,4546	26s proteasome regulatory particle triple-a atpase subunit4	62064,58	85053,05
SCCCLR1022F10	29	227,2227	0,2476	serine hydroxymethyltransferase	39806,79	47259,82
SCCCLR1022H02	3	16,0909	0,4304	hypothetical protein OsJ_12867 [Oryza sativa Japonica Group]	1010,2	749,6273
SCCCLR1022H03	7	55,6015	0,0825	glycine cleavage system h protein 1	63995,43	60438,12
SCCCLR1022H07	6	40,9965	0,4132	cell division control protein 2	20142,58	26823,3
SCCCLR1024A05	16	120,1585	0,4640	transaldolase 2	49507,19	68290,03
SCCCLR1024C05	3	21,5449	0,5279	nonspecific lipid-transfer protein 3 precursor	2260,293	3259,054
SCCCLR1024C10	8	63,0623	0,4038	endothelial differentiation-related factor 1	5027,384	3800,062
SCCCLR1024C11	23	170,4326	0,2995	stromal 70 kda heat shock-related protein	35099,52	43197,35
SCCCLR1024D03	26	300,7315	0,2740	malate cytoplasmic	558878,2	675764,4
SCCCLR1024D12	30	225,4022	0,1096	succinyl- ligase beta-chain	126184,9	136140,4
SCCCLR1024E02	18	128,8936	0,2212	hypothetical protein SORBIDRAFT_07g005510 [Sorghum bicolor]	90705,12	105736,1
SCCCLR1024E10	19	143,4219	0,7702	ketol-acid reductoisomerase	21596,44	36833,48
SCCCLR1024F02	12	98,272	0,1834	dna repair protein rad23	89197,18	101290,4
SCCCLR1024G01	15	99,021	0,2115	low quality protein: alanyl-trna synthetase-like	62284,55	72117,21
SCCCLR1024G02	6	34,9786	0,2862	oxysterol-binding protein	7539,402	9193,72
SCCCLR1024H08	17	121,1514	0,1964	hypothetical protein SORBIDRAFT_08g008400 [Sorghum bicolor]	32729,1	37503,14
SCCCLR1024H09	9	66,5045	0,2597	enoyl-acp reductase	6432,019	5372,559
SCCCLR1048A06	16	164,7736	0,6529	super-oxide dismutase	101290,4	159265,9
SCCCLR1048A09	18	132,8399	0,7034	60s ribosomal protein l5-1	12607,09	20528,59
SCCCLR1048A11	5	32,4564	0,0025	nadh-ubiquinone oxidoreductase 20 kda subunit	16015,08	15986,85
SCCCLR1048B08	10	92,5412	0,8001	triosephosphate isomerase	23279,09	40534,87
SCCCLR1048B12	30	290,65	0,5407	elongation factor 1-gamma 3	58909,93	85693,54
SCCCLR1048C02	15	178,8342	1,0123	histone h2b	12781,7	6336,408
SCCCLR1048C11	2	19,0328	0,1814	loc100285177 precursor	6352,639	5601,967
SCCCLR1048D04	21	250,4847	0,1828	glutathione s-transferase para	267362,4	303470,8
SCCCLR1048D07	11	76,4815	0,5142	phenylalanine ammonia-lyase	10459,2	14938,06
SCCCLR1048E04	5	30,1224	0,5469	phosphoglycerate mutase-like protein	2455,953	3588,008
SCCCLR1048F08	13	110,3992	0,5097	26s proteasome non-atpase regulatory subunit 14	22849,19	32530,96
SCCCLR1048F12	23	273,2755	0,2787	14-3-3-like protein	75475,89	91559,57

Table S1 cont.

Accession	Peptide count	Confidence score ^a	Log ₂ of fold change ^b	Description	Total Ion Counts Control	Total Ion Counts W _m B _d R _f R
SCCCLR1048G01	19	122,4761	0,9002	asparaginyl-trna cytoplasmic 3	55126,71	102881,9
SCCCLR1048G02	24	150,3714	0,8363	leucyl-trna synthetase	18400,48	32854,23
SCCCLR1048G04	33	350,7112	0,4191	protein disulfide isomerase	382883,2	511945,4
SCCCLR1048G11	23	150,7927	0,4751	26s proteasome non-atpase regulatory subunit 3	35658,79	49565,07
SCCCLR1048G12	10	90,4337	0,7192	proteasome subunit beta type 2	77766,59	128028,2
SCCCLR1048H09	22	192,9516	0,2258	catalase cata	181382	212109,9
SCCCLR1065B07	16	137,2072	0,2279	hsc70-interacting protein	76109,27	89133,76
SCCCLR1065C10	2	11,1141	0,0827	phytochrome c	14602,63	15464,38
SCCCLR1065F02	16	118,1625	0,6749	aconitate cytoplasmic	10558,94	16856,9
SCCCLR1065F10	9	74,851	0,4758	ubiquitin-conjugating enzyme spm2	28761,77	39997,51
SCCCLR1065G03	30	204,2524	0,0681	26s protease regulatory subunit 7	55742,05	58437,95
SCCCLR1066A08	19	152,6728	0,4199	rh2 protein	586957,3	438745,6
SCCCLR1066B02	9	74,3588	0,2117	40s ribosomal protein s6	51980,63	60194,98
SCCCLR1066C11	3	22,8925	0,5067	ubiquitin-like protein smt3	6474,875	4557,257
SCCCLR1066E12	5	30,8703	0,1603	unnamed protein product [Oryza sativa Japonica Group]	8023,695	7179,961
SCCCLR1066F05	6	48,4433	0,5196	ferredoxin- chloroplastic precursor	30773,18	21467,03
SCCCLR1066H08	11	140,7916	0,0257	thioredoxin h-type	94677,89	93005,47
SCCCLR1066H09	13	97,9848	0,5657	alcohol dehydrogenase class 3	22024,13	32598,8
SCCCLR1067D05	8	51,593	0,2711	outer mitochondrial membrane protein porin	7998,772	6628,491
SCCCLR1068B06	30	275,7528	0,3956	tubulin beta-6 chain	6000,897	7893,934
SCCCLR1068C05	7	90,384	0,7945	histone 2	2642,131	1523,32
SCCCLR1068D10	46	358,469	0,3301	endoplasmin precursor	101647,5	127780,6
SCCCLR1069A12	20	208,7022	0,8189	60s ribosomal protein l9	13628,82	24042,41
SCCCLR1069B04	27	190,3771	0,4499	glycyl-trna synthetase-like protein dihydrolipoyllysine-residue succinyltransferase component of 2-oxoglutarate dehydrogenase complex	30736,01	41982,47
SCCCLR1070A12	10	73,6994	0,9894	af384035_1 nucleosome chromatin assembly factor a	6485,586	12876,6
SCCCLR1070C10	14	131,5638	0,4001	pyruvate cytosolic isozyme	95590,46	126144,9
SCCCLR1070D04	30	262,3948	0,1957	eukaryotic translation initiation factor 5a2	31423,46	35987,83
SCCCLR1070E06	12	94,3433	0,1009	karyopherin-beta 3 variant	16768,76	17983,05
SCCCLR1070E07	8	54,1311	1,1225	trehalose-6-phosphate synthase 2	5326,252	11596,65
SCCCLR1070E10	16	115,085	0,1011	calnexin precursor	16194,79	17370,67
SCCCLR1070F12	24	191,1077	0,1682	nadh dehydrogenase	62831,51	55918,22
SCCCLR1070H07	14	110,4648	0,4138	atp synthase delta chain	8743,619	11648,13
SCCCLR1072A03	14	90,0257	0,1504	malate dehydrogenase	10367,35	9341,26
SCCCLR1072A12	19	181,5764	0,5738	dna replication licensing factor mcm3 homolog 1	43405,46	64608,23
SCCCLR1072B11	10	65,3171	1,0875		13429,88	28538,96

Table S1 cont.

Accession	Peptide count	Confidence score ^a	Log ₂ of fold change ^b	Description	Total Ion Counts Control	Total Ion Counts W _m B _d R _f R
SCCCLR1072C08	5	31,1849	0,1527	unknown [Zea mays]	16532,75	18378,91
SCCCLR1072C10	10	75,6526	0,3956	ob-fold nucleic acid binding domain containing protein	40712,78	53556,96
SCCCLR1072D06	18	160,7165	0,3523	cysteine synthase1	112655,7	143814,3
SCCCLR1072D09	5	39,5787	0,3872	coatomer subunit epsilon	80137,08	104807,1
SCCCLR1072E04	13	121,5034	0,0819	usp family protein	36767,85	38916,72
SCCCLR1072F05	65	715,0468	0,4365	elongation factor 2	825894,8	1117698
SCCCLR1072G07	37	401,743	0,6576	translational initiation factor eif-4a	72065,35	113680,5
SCCCLR1072G08	6	46,383	0,1327	vacuolar protein sorting 35	6187,5	6783,652
SCCCLR1072G10	4	35,7331	0,0447	60s ribosomal protein l30	15374,24	15858,26
SCCCLR1075B02	7	59,5846	0,5219	ras-related protein ric1	6657,507	9559,274
SCCCLR1075E09	47	545,1356	0,8013	heat shock protein 90	1869,272	3257,473
SCCCLR1075H11	30	309,2869	0,4905	heat shock protein 82	75635,86	53837,3
SCCCLR1076C03	22	159,163	0,3600	ketol-acid chloroplastic-like	72793,96	93427,42
SCCCLR1076D05	2	16,2008	0,2844	nonspecific lipid-transfer protein 3 precursor	10408,42	12676,85
SCCCLR1077B12	22	185,9876	0,0268	pdil2-2 - zea mays protein disulfide isomerase	50028,32	50967,19
SCCCLR1077D09	19	154,5244	1,1746	26s protease regulatory subunit 6b	3942,727	8899,831
SCCCLR1077F04	13	93,809	0,0838	elongation factor tu	16573,1	17564,6
SCCCLR1077G10	3	25,29	0,2312	protein disulfide isomerase-related protein	12471,22	14638,39
SCCCLR1078C01	9	59,2562	0,2618	rna binding protein	12471,77	14953,77
SCCCLR1079B06	29	326,2182	0,4283	cytosolic phosphoglycerate kinase 1	124549,6	167602,7
SCCCLR1079D09	11	84,2264	0,0664	heat shock cognate 70 kda protein 2	17372,69	18191,41
SCCCLR1079D10	19	165,0079	0,5258	monodehydroascorbate reductase	87974,59	126662,9
SCCCLR1079E05	17	126,4407	0,0845	poly -binding protein	29848,45	31648,41
SCCCLR1079F10	4	22,5464	0,0955	chloroplast inner envelope expressed	6120,576	6539,627
SCCCLR1080E07	26	193,5596	0,7729	heat shock 70 kda protein	57962,72	99038,46
SCCCLR1C01A02	19	154,752	0,2612	protein disulfide isomerase7 precursor	25522,67	21295,52
SCCCLR1C01B02	22	228,9752	0,3272	uncharacterized protein LOC100191561 [Zea mays]	5512,209	6915,34
SCCCLR1C01B10	11	70,3266	0,4605	hydroxyacylglutathione hydrolase mitochondrial-like	26240,65	36107,69
SCCCLR1C01C07	7	96,2589	0,1327	40s ribosomal protein s12	22092,53	20150,78
SCCCLR1C01C09	10	102,5026	0,2847	60s ribosomal protein l12	197074,4	240065,5
SCCCLR1C01D02	12	108,8493	1,0939	transcription factor expressed	31250,81	66703,66
SCCCLR1C01D05	32	325,6896	0,6718	heat shock cognate 70 kda expressed	55745,31	88807,24
SCCCLR1C01F03	12	96,6322	0,1533	translational inhibitor protein	56341,03	62657,08
SCCCLR1C01G05	9	71,9881	0,2231	heterogeneous nuclear ribonucleoprotein a3	27560,55	32169,69
SCCCLR1C01H02	13	119,1042	0,4534	peptidyl-prolyl cis-trans isomerase	33840,96	46338,7
SCCCLR1C02A02	12	121,9906	0,4517	eukaryotic translation initiation factor 5a	89702,98	122680

Table S1 cont.

Accession	Peptide count	Confidence score ^a	Log ₂ of fold change ^b	Description	Total Ion Counts Control	Total Ion Counts W _m B _d R _f R
SCCCLR1C02A03	15	110,9654	0,1475	formate dehydrogenase 1	103126,2	114230,5
SCCCLR1C02B03	16	126,0065	0,7284	beta 5 subunit of 20s proteasome	36733,51	60858,36
SCCCLR1C02E07	9	70,4914	0,3050	60s ribosomal protein l22-2	58648,28	72455,67
SCCCLR1C02F04	31	230,1158	0,3751	ma3 domain-containing protein	114844,7	148945,8
SCCCLR1C02F07	24	149,1805	0,0048	inositol-3-phosphate synthase	23522,45	23601,12
SCCCLR1C03B03	11	91,2348	0,3780	ubiquitin-conjugating enzyme e2	17023,98	22123,47
SCCCLR1C03D02	3	19,2071	0,2640	splicing factor u2af 38 kda subunit	4253,291	3542,008
SCCCLR1C03E08	22	157,0164	0,4840	grx_s17 - glutaredoxin subgroup ii	37149,73	51958,57
SCCCLR1C04E01	30	350,568	0,3890	wheat adenosylhomocysteine-like protein	415010,8	543445,3
SCCCLR1C04F06	5	35,7839	0,4470	diphosphomevalonate decarboxylase	10189,94	13891,41
SCCCLR1C04H06	27	191,489	0,6180	26s proteasome non-atpase regulatory subunit 1-like	19302,14	29624,15
SCCCLR1C05A04	6	36,2749	0,6037	hypothetical protein SORBiDRAFT_03g032180 [Sorghum bicolor]	3364,193	5112,183
SCCCLR1C05B06	9	65,8143	0,8050	eukaryotic translation initiation factor 3 subunit 3	8101,362	14154,16
SCCCLR1C05E11	3	23,2995	0,2525	atypical receptor-like kinase mark precursor	6598,799	7861,105
SCCCLR1C05F08	7	46,1517	0,8428	fumarate hydratase chloroplastic-like	6072,377	10891,15
SCCCLR1C05G02	22	180,605	0,3731	3-ketoacyl- thiolase peroxisomal precursor	102283,1	132473,2
SCCCLR1C05G05	14	114,7099	0,6385	60s ribosomal protein l10a-1	23286,49	36249,27
SCCCLR1C05G08	15	129,0588	0,8569	peroxidase atp6a	35213,24	63775,02
SCCCLR1C05H09	6	37,7176	0,1986	60s ribosomal protein l7-1	2594,037	2976,849
SCCCLR1C05H10	5	33,6051	0,3216	retrotransposon protein sine subclass	1545,328	1236,508
SCCCLR1C06A01	4	29,1715	0,3159	splicing factor 3b subunit 3-like	2432,985	3028,56
SCCCLR1C06F07	27	177,4494	0,4020	t-complex protein 1 subunit gamma	69449,56	91767,12
SCCCLR1C07F11	2	11,9848	0,2343	60s ribosomal protein l32	5216,427	4434,42
SCCCLR1C07G05	25	297,585	0,8868	tubulin alpha-1 chain	23204,36	42905,54
SCCCLR1C07H02	14	153,4831	0,1566	calmodulin	2671,641	2977,916
SCCCLR1C10C03	10	73,1774	0,0392	eukaryotic translation initiation factor 3 subunit 1 35kda	8633,764	8871,635
SCCCLR2001A02	4	30,7754	0,0028	protein chloroplastic-like	1088,859	1091,008
SCCCLR2001A06	11	70,6356	0,5467	auxin-induced protein pcnt115	12534,09	18308,77
SCCCLR2001A08	25	280,7021	0,3622	r40c1 protein - rice	72958,15	93780,79
SCCCLR2001B06	3	17,4224	0,1266	serine threonine protein phosphatase expressed	1361,603	1247,224
SCCCLR2001B08	6	64,3023	0,1242	acidic ribosomal protein p2a-2	94865,52	103391,9
SCCCLR2001C05	22	225,3135	0,4193	stem-specific protein tsjt1	8971,197	11996,66
SCCCLR2001D01	10	104,1573	0,0044	histone h4	153695,4	154165
SCCCLR2001E04	5	48,9541	0,5247	huntingtin-interacting protein k-like	124688,6	179379,1
SCCCLR2001E08	17	128,0361	0,6261	hemoglobin 2	30435,38	46974,76
SCCCLR2001F05	7	49,0231	0,1996	delta-1-pyrroline-5-carboxylate synthetase	12469,2	10857,75

Table S1 cont.

Accession	Peptide count	Confidence score ^a	Log ₂ of fold change ^b	Description	Total Ion Counts Control	Total Ion Counts W _m B _d R _f R
SCCCLR2001F07	11	83,9924	0,5776	40s ribosomal protein s20	66802,05	99690,32
SCCCLR2001G04	3	16,0633	0,4281	hypothetical protein SORBIDRAFT_09g022110 [Sorghum bicolor]	982,6124	730,3141
SCCCLR2001G06	19	198,3961	0,4731	peptidyl-prolyl cis-trans isomerase	285361,9	396098
SCCCLR2001H02	11	77,8178	0,1496	ramosa 1 enhancer locus 2	28492,29	31606,31
SCCCLR2001H05	24	284,4948	0,5537	alcohol dehydrogenase 1	86465,21	126918,5
SCCCLR2001H07	16	127,8589	0,0932	chaperonin 21 precursor	38935,95	36499,5
SCCCLR2001H12	14	136,2387	0,4610	mnd1-interacting protein 1-like	50934,64	70113,69
SCCCLR2002B11	9	56,9687	0,4568	dna replication licensing factor mcm3 homolog 1	6839,653	9387,218
SCCCLR2002C01	7	56,0254	0,2019	40s ribosomal protein s9	3908,977	4496,118
SCCCLR2002C10	4	29,4031	0,0725	60s ribosomal protein l19-like protein	7324,56	6965,394
SCCCLR2002D01	2	11,6228	0,0397	u6 srna-associated sm-like protein lsm3	57231,35	55677,33
SCCCLR2002E04	12	96,2474	0,3286	bet v i allergen	10839,29	8631,388
SCCCLR2002E05	15	107,9565	0,7250	60s ribosomal protein l7-2	74045,9	44796,41
SCCCLR2002F10	8	63,5172	0,4594	histidine triad nucleotide binding protein	21136,86	29062,39
SCCCLR2002G02	26	244,0115	0,6633	d-3-phosphoglycerate dehydrogenase	213180,6	337609,6
SCCCLR2002G03	11	71,542	0,5950	inorganic pyrophosphatase	49818,64	75249
SCCCLR2002H12	12	76,7774	0,1580	ran-binding protein 1	36507,88	40734,54
SCCCLR2003G06	9	69,7829	1,0210	thaumatin-like cytokinin-binding expressed	104197,7	51347,27
SCCCLR2003H03	11	82,1914	0,1502	60s ribosomal protein l27a-3	58819,98	65271,83
SCCCLR2004E06	4	23,6839	0,4019	60s ribosomal protein l2	4981,006	6581,081
SCCCLR2004F06	17	192,027	0,0878	peptidyl-prolyl cis-trans isomerase	174022,1	184935,6
SCCCLR2004G08	4	22,9613	0,0312	20 kda chloroplastic-like	3401,976	3329,159
SCCCLR2004H07	10	75,3553	0,0885	uncharacterized protein LOC100383393 [Zea mays]	55994,8	52662,28
SCCCLR2004H11	26	185,9737	0,6116	t-complex protein 1 theta chain	50335,74	76912,29
SCCCLR2004H12	6	37,7826	0,5023	ago1b_orysj ame: full=protein argonaute 1b short= 1b	21761,53	15363,11
SCCCLR2C01D10	4	23,171	0,3893	6-phosphofructokinase 3-like	2845,606	3727,065
SCCCLR2C01F11	13	116,3555	0,4670	40s ribosomal protein s10	51343,48	70969,93
SCCCLR2C01H02	11	96,9435	0,9428	endo- -beta-d-glucanase precursor	16545,89	31805,38
SCCCLR2C01H11	8	43,5105	0,5761	microtubule-associated protein map65-1a	8050,074	12001,51
SCCCLR2C02C11	3	16,9261	0,7825	60s ribosomal protein l38	5543,772	3222,817
SCCCLR2C02D03	34	255,2095	0,5972	ru large subunit-binding protein subunit alpha	69237,58	104738,4
SCCCLR2C02E06	4	32,1907	0,0929	40s ribosomal protein s26	20210,37	21554,88
SCCCLR2C03C06	5	34,507	0,0875	arginine serine-rich splicing factor 2	6002,627	6377,957
SCCCLR2C03G12	5	29,8649	0,3277	40s ribosomal protein s23	5084,906	4051,59
SCCCLR2C03H03	12	77,4078	0,2994	at5g19150 t24g5_50	10647,06	13103,03
SCCCRT1001H04	6	57,6224	0,5762	auxin-induced protein pcnt115	14366,94	21419,18

Table S1 cont.

Accession	Peptide count	Confidence score ^a	Log ₂ of fold change ^b	Description	Total Ion Counts Control	Total Ion Counts W _m B _d R _f R
SCCCRT1002C05	28	259,6688	0,6835	alanine aminotransferase	135421,4	217495,9
SCCCRT1002C11	5	28,3332	0,8184	nicalin precursor	5604,396	9882,754
SCCCRT1002E01	1	5,5781	0,8097	stad1_orysj ame: full=acyl- desaturase chloroplastic	2174,735	1240,721
SCCCRT1002F07	31	221,2411	0,6077	pma1_orysj ame: full=plasma membrane atpase ame: full=proton pump	77955,27	118788,8
SCCCRT1002F10	10	62,1398	0,0118	late-embryogenesis-abundant protein	36896,29	37199,34
SCCCRT1003B03	5	38,5016	0,8651	hypothetical protein SORBIDRAFT_10g003930 [Sorghum bicolor]	9373,75	17074,04
SCCCRT1003F01	20	154,597	0,4267	cytosolic glutathione reductase	69167,3	92972,47
SCCCRT1003G09	9	65,5838	0,4413	isoform 1	8158,354	11077,69
SCCCRT1003H01	11	70,1906	0,4898	aspartate mitochondrial-like	30562,7	42917,19
SCCCRT1004F06	14	102,9431	0,6545	aminotransferase y4ub	9063,962	14266,89
SCCCRT1C05F07	2	17,652	0,6530	u-box domain containing expressed	10623,25	16704,34
SCCCRT2001B05	7	41,4298	0,1034	aminolevulinic acid dehydratase	36926,08	39669,09
SCCCRT2001H11	11	100,7511	0,1330	adp-ribosylation factor	3439,162	3136,241
SCCCRZ1001B08	21	289,1035	0,4865	triosephosphate cytosolic	862055,8	1207788
SCCCRZ1001C05	36	458,3265	0,5062	phosphoglycerate kinase	427981,4	607875,5
SCCCRZ1001D04	42	357,8414	0,2421	cytoplasmic 2	401322,9	474648,3
SCCCRZ1001E01	6	39,0674	0,8725	proteasome subunit alpha type 2	544,5634	297,4379
SCCCRZ1001E04	11	104,9454	0,2844	nascent polypeptide-associated complex alpha subunit-like protein	9456,753	11517,09
SCCCRZ1001H06	10	77,3832	0,2704	co-chaperone protein sba1	138291,3	166802,5
SCCCRZ1002D10	20	146,2028	0,4669	rh52b_orysj ame: full=dead-box atp-dependent rna helicase	32523,15	44950,9
SCCCRZ1002E01	7	39,7079	0,5630	alanine aminotransferase 2	19125,03	28254,52
SCCCRZ1002E05	33	264,8794	0,5171	pyruvate cytosolic isozyme	105405,9	150848,1
SCCCRZ1002E10	9	48,6333	0,5527	mitochondrial rho gtpase 1-like	10927,79	16029,22
SCCCRZ1002F06	40	593,3663	0,3873	unknown [Zea mays]	439852,6	575300,9
SCCCRZ1002G01	43	474,9943	0,1349	dnak-type molecular chaperone hsp70 - rice	113293,6	124402,3
SCCCRZ1002G07	54	565,77	0,6848	sucrose synthase 2	136852,5	219991,5
SCCCRZ1002H03	24	274,4533	0,3716	tubulin alpha-3 chain	16398,57	21216,18
SCCCRZ1003A03	37	286,2766	0,3329	heat shock 70 kda protein	103029,9	129773,7
SCCCRZ1003A05	5	35,0297	0,0795	outer mitochondrial membrane protein porin	9355,576	9885,755
SCCCRZ1003A10	42	353,6064	0,2541	cell division cycle protein expressed	10478,38	12496,47
SCCCRZ1003B04	9	67,4964	0,1739	rna-binding protein nova-1	38978,99	43973,25
SCCCRZ1003F10	13	108,1049	0,0919	c2 domain containing protein	63098,1	59205,15
SCCCRZ1003G07	8	59,3997	0,3245	uridine monophosphate synthase	97792,77	78095,24
SCCCRZ1004B02	6	38,1452	0,2181	ribonuclease h-related protein	34592,4	40237,79
SCCCRZ1004B05	16	97,6464	0,1812	topless-related protein 1-like	18248,28	16094,01
SCCCRZ1004B07	2	11,1812	0,4418	dihydrolipoyl dehydrogenase-like	2260,02	3069,779

Table S1 cont.

Accession	Peptide count	Confidence score ^a	Log ₂ of fold change ^b	Description	Total Ion Counts Control	Total Ion Counts W _m B _d R _f R
SCCCRZ1004C10	3	17,2984	0,4132	rna recognition motif -containing protein	1853,593	2468,304
SCCCRZ1004G02	18	132,8825	0,3238	acetylornithine deacetylase	32218,69	40324,7
SCCCRZ1004G05	23	181,7459	0,2773	chaperonin 60 beta precursor	47548,2	57625,03
SCCCRZ1004H06	12	101,8348	0,2537	glutaredoxin subgroup i	95823,93	114244,2
SCCCRZ1C01A05	23	179,272	0,2901	nls receptor	78262,6	95695,66
SCCCRZ1C01A11	8	44,3031	0,1889	eukaryotic translation initiation factor 2 beta subunit	12759,94	11193,96
SCCCRZ1C01D04	33	242,435	0,0717	t-complex protein 1 subunit beta	70727,5	67296,93
SCCCRZ2001A01	17	161,0504	0,3027	chaperonin	164669,2	203106,1
SCCCRZ2001A04	17	125,81	0,1081	2-hydroxy-3-oxopropionate reductase	136196	146791,5
SCCCRZ2001C01	8	88,7934	0,2054	thioredoxin h-type	22687,97	26159,31
SCCCRZ2001D03	8	46,3782	0,0858	cysp2_maize ame: full=cysteine proteinase 2 flags: precursor	1135,111	1069,587
SCCCRZ2001D05	3	24,062	0,1113	pre-mrna branch site p14-like protein	5242,267	4853,07
SCCCRZ2001D09	9	59,3341	0,0892	substrate binding domain containing expressed	17123,09	16096,29
SCCCRZ2001E10	7	52,8689	0,1268	dna-directed rna polymerase ii	8739,765	9542,944
SCCCRZ2001F03	37	505,4035	0,2669	fructose-bisphosphate aldolase cytoplasmic isozyme	696405,8	837906,8
SCCCRZ2001F07	4	28,9782	0,1810	calmodulin binding protein	750,7937	662,2811
SCCCRZ2001F10	25	227,8276	0,5765	mitochondrial aldehyde dehydrogenase	208714	311249,7
SCCCRZ2001F12	14	88,8447	0,6493	aluminum-induced protein	35461,94	55618,66
SCCCRZ2001G10	12	69,5531	0,1128	set domain protein sdg111	8113,594	7503,136
SCCCRZ2002A07	5	40,6129	0,4734	ras-related protein ric2	5765,711	8005,073
SCCCRZ2002C12	11	86,7163	0,1340	40s ribosomal protein s18	26296,93	28856,3
SCCCRZ2002D07	16	152,1175	0,5349	elongation factor 1-delta 1	158841,5	230137,7
SCCCRZ2002D10	12	78,2616	0,3263	40s ribosomal protein s8	44187,69	55403,62
SCCCRZ2002E03	14	98,6104	1,0739	tpr domain containing protein	15787,1	33232,82
SCCCRZ2002F04	38	302,7926	0,2668	clh1_orysj ame: full=clathrin heavy chain 1	95195,94	114531,4
SCCCRZ2002G01	36	405,309	0,6487	atp synthase beta chain	76457,1	119869,8
SCCCRZ2002G06	9	65,5548	0,9161	hypothetical protein SORBIDRAFT_03g036890 [Sorghum bicolor]	22672	12014,53
SCCCRZ2002H06	18	189,3284	0,2356	aspartic proteininase oryzasin-1 precursor	100692,7	118556
SCCCRZ2003A07	37	259,7828	0,5791	aminopeptidase m	76360,52	114077,3
SCCCRZ2003B05	2	18,1015	0,2649	enzyme of the cupin superfamily	10694,89	8901,095
SCCCRZ2004A06	15	103,035	0,0999	nadp-dependent glyceraldehyde-3-phosphate dehydrogenase	9726,804	9076,26
SCCCRZ2004A11	23	170,4171	0,1760	annexin p33	56080,45	63355,55
SCCCRZ2004B02	4	23,1616	0,4562	drepp4 protein	1253,213	1719,308
SCCCRZ2004B10	14	110,2345	0,1801	3-isopropylmalate dehydrogenase	47524,87	53844,15
SCCCRZ2004D12	5	40,773	0,5377	hypothetical protein SORBIDRAFT_04g021780 [Sorghum bicolor]	900,6818	620,4391
SCCCRZ2004E10	16	132,0568	0,5922	cinnamoyl reductase-like 2a	3277,983	2174,461

Table S1 cont.

Accession	Peptide count	Confidence score ^a	Log ₂ of fold change ^b	Description	Total Ion Counts Control	Total Ion Counts W _m B _d R _f R
SCCCRZ2004H06	8	51,5692	0,5278	hypothetical protein SORBIDRAFT_05g021640 [Sorghum bicolor]	3241,836	4673,771
SCCCRZ2C01F01	10	82,1322	0,0584	glutathione peroxidase	10904,33	11354,56
SCCCRZ2C01H04	15	201,0511	0,1038	ferritin- chloroplastic	14950,24	13912,08
SCCCRZ2C03A09	44	436,8687	0,0683	5-methyltetrahydropteroylglutamate-homocysteine expressed	176699,8	185272,1
SCCCRZ2C03F04	4	23,466	0,8051	protein-l-isoaspartate o-methyltransferase-like isoform 1	7547,359	13187,54
SCCCRZ2C03F07	6	36,1849	0,2814	pto kinase interactor 1	293890,7	357194,2
SCCCRZ2C03H08	9	61,6867	0,7430	hypothetical protein SORBIDRAFT_01g038880 [Sorghum bicolor]	10467,81	6254,357
SCCCRZ2C04B02	17	120,2003	0,4653	proteasome subunit beta type 6 precursor	108251,7	149452
SCCCRZ2C04F03	10	111,6953	0,1217	thioredoxin-dependent peroxidase	44542,55	48462,99
SCCCRZ2C04F06	7	51,6683	0,0409	phi-1-like phosphate-induced protein precursor	2127,679	2068,213
SCCCRZ2C04G04	15	93,8564	0,0081	vacuolar atp synthase subunit c	4776,748	4803,593
SCCCRZ3002G10	10	106,2352	0,4845	tpa: cystatin	62013,64	86765,46
SCCCSD2001B07	2	13,8235	0,0528	mpi	4412,488	4576,86
SCCCST1003B06	4	22,88	0,1449	nonclathrin coat protein zeta2-cop	7302,716	6604,724
SCCCST1007H01	4	26,6184	0,9023	hypothetical protein SORBIDRAFT_06g000580 [Sorghum bicolor]	16940,51	31662,55
SCCCST2001A03	6	65,321	0,4076	unknown [Zea mays]	9490,655	12589,53
SCCCST2002G06	9	60,686	0,0994	protein binding protein	43610,98	46722,39
SCCCST2003C12	24	257,4562	0,1247	alcohol dehydrogenase 1	53337,95	58153,43
SCCCST3006A03	11	117,5342	0,4250	acidic ribosomal protein p2a-2	61059,88	45479,11
SCEPAM1015F11	11	70,2313	0,2182	n-acetyl-gamma-glutamyl-phosphate reductase	24767,78	21291,43
SCEPAM1019D01	4	29,9371	0,1231	nap16kda protein	9470,825	10314,55
SCEPAM1021C06	2	11,8558	0,1026	ribosome-inactivating protein	2814,403	3021,874
SCEPAM1024D04	11	86,7731	0,7197	elongation factor 1-gamma 3	8633,729	5242,44
SCEPAM2011H12	2	11,8696	0,5443	mitochondrial uncoupling protein 3	4077,645	5946,328
SCEPAM2013E06	9	79,8526	0,7869	hypothetical protein SORBIDRAFT_10g008280 [Sorghum bicolor]	11552,99	6695,802
SCEPAM2014H02	5	36,8535	0,7434	inositol monophosphatase 3	6931,398	11603,86
SCEPAM2053F09	5	33,6038	0,2222	cyclase dehydrase family protein	5124,919	5978,46
SCEPAM2053F11	3	17,9485	0,7226	gtp-binding protein erg-like	5025,968	3045,678
SCEPAM2055H02	7	61,7248	0,2651	legumin-like protein	39363,71	47305,32
SCEPCL6018F02	22	137,6285	0,3098	glycyl-tRNA synthetase	32789,04	40642,88
SCEPCL6020A07	11	78,2084	0,0918	gtp-binding protein ptd004	42727,03	40094,03
SCEPFL4179C08	6	70,5223	1,1771	nucleosome chromatin assembly factor group c	47813,02	108112,9
SCEPLB1041G09	16	139,4955	0,3071	proteasome subunit alpha type 1	86882,94	107490,9
SCEPLB1042F08	5	50,5367	0,1099	glutathione transferase iii	1367,947	1476,24
SCEPLB1043H09	4	22,57	0,8130	low quality protein: carbon catabolite repressor protein 4 homolog 3-like	2286,824	1301,668
SCEPLB1043H10	15	126,3558	0,2918	rRNA 2'-o-methyltransferase fibrillarin 1-like	26777,32	32779,28

Table S1 cont.

Accession	Peptide count	Confidence score ^a	Log ₂ of fold change ^b	Description	Total Ion Counts Control	Total Ion Counts W _m B _d R _f R
SCEPLR1008F05	7	70,1509	0,7515	dut_orysj ame: full=deoxyuridine 5'-triphosphate nucleotidohydrolase	3597,32	6056,221
SCEPLR1030F01	11	76,4145	0,4183	nucleosome chromatin assembly factor group a	46558,74	62216,94
SCEPLR1051C09	15	156,5197	0,1834	multidomain cystatin	84919,27	96433,06
SCEPLR1051D01	20	145,6407	0,4793	probable glycerophosphoryl diester phosphodiesterase 2-like	73350,51	102257,3
SCEPLR1051D02	4	26,759	0,0929	prefoldin subunit 1	12203,45	11442,62
SCEPLR1051D05	12	83,2445	0,2901	protein	12199,76	9977,499
SCEPLR1051G01	6	40,8153	0,0227	glycine-rich rna-binding protein 2	34761,13	35313,4
SCEPRT2043A01	1	5,0921	1,0095	mannitol dehydrogenase	836,0038	415,2489
SCEPRT2047G06	2	11,5273	0,1577	low quality protein: respiratory burst oxidase homolog protein b-like	3028,374	3378,197
SCEPRZ1008F11	3	25,0825	0,2246	threonine synthase	6253,499	5351,975
SCEPRZ1008G07	11	96,2081	0,1058	hypothetical protein SORBIDRAFT_04g007950 [Sorghum bicolor]	37655,53	34993,51
SCEPRZ1009A12	15	98,2729	0,0684	calcium-dependent protein isoform 2	44936,28	47117,89
SCEPRZ1009B12	15	140,3181	0,1913	triosephosphate cytosolic	204534,8	233537,7
SCEPRZ1009D06	10	62,6691	0,1268	unknown [Zea mays]	19851,13	18180,85
SCEPRZ1009H12	7	42,6686	0,5357	thioredoxin peroxidase	17998,63	26090,89
SCEPRZ1010A03	26	223,062	0,0412	protein phosphatase 2a structural subunit	32628,4	31709,29
SCEPRZ1010F12	6	36,1001	0,4161	hypothetical protein SORBIDRAFT_01g019710 [Sorghum bicolor]	6006,649	4501,674
SCEPRZ1010G06	24	224,5352	1,0463	unknown [Zea mays]	61217,86	126424,7
SCEPRZ1010H07	21	167,9955	0,1022	mitochondrial f0 atp synthase d chain	42986,21	46142,26
SCEPRZ1011G11	24	167,6605	0,5718	tip120 protein	43653,92	64887,13
SCEPRZ3044B07	2	10,2186	0,5908	serine threonine-protein kinase sapk7	12522,6	18860,65
SCEPRZ3047F05	13	115,4677	0,4141	dihydrolipoamide s-acetyltransferase1	18127,45	24154,16
SCEPRZ3087H07	22	153,7691	0,8744	nadh-ubiquinone oxidoreductase 75 kda subunit	67105,73	123020,5
SCEPSB1128E09	1	5,6853	0,1697	nad-dependent malic enzyme 62 kda mitochondrial-like	1850,289	1644,914
SCEPSD2007C01	1	5,5721	0,1828	glutathione s-transferase gstu6	3918,448	3452,193
SCEPSD2071B08	5	30,4843	0,7325	hypothetical protein SORBIDRAFT_09g001040 [Sorghum bicolor]	2875,684	1730,809
SCEQAD1019F10	2	10,5761	0,1244	swi snf-related matrix-associated actin-dependent regulator of chromatin subfamily a member 3-like 3-like	6492,441	7076,977
SCEQAM1035F11	4	25,7209	0,1113	calcium ion binding	5780,383	6244,159
SCEQAM2039A03	8	50,535	0,8597	monocopper oxidase-like protein sku5-like	12398,19	22498,38
SCEQLF5052H11	3	22,8598	0,8712	ac084406_1 gag-pol polyprotein	6616,299	12102,26
SCEQLB1063E01	14	88,8174	1,0179	60s ribosomal protein l6	16724,96	33867,16
SCEQLB1065A03	24	194,711	0,5695	translational elongation factor ef-	65785,93	97627,38
SCEQLB1065H03	11	66,8381	0,8445	pp2ac-5'- phosphatase 2a isoform 5 belonging to family 2	4040,496	7255,104
SCEQLB1066E08	11	62,0027	0,6836	loc100284659 precursor	36589,59	58767,7
SCEQLB1066F11	2	11,2829	0,2128	hypothetical protein SORBIDRAFT_04g028290 [Sorghum bicolor]	2164,933	2509,029

Table S1 cont.

Accession	Peptide count	Confidence score ^a	Log ₂ of fold change ^b	Description	Total Ion Counts Control	Total Ion Counts W _m B _d R _f R
SCEQLB1067D01	2	10,9441	1,1145	dtdp-4-dehydrorhamnose reductase	10536,78	22814,9
SCEQLB1067D06	32	223,0006	0,5534	chaperonin cpn60-like mitochondrial-like	37535,19	55084,04
SCEQLB1067D10	5	48,1498	1,0469	chitinase	2907,603	6007,553
SCEQLB1067H09	33	277,5801	0,0347	peptidyl-prolyl isomerase	181026,9	176722,2
SCEQLR1007G11	20	130,3301	0,2399	ran gtpase activating protein	48138,36	40765,07
SCEQLR1029D06	8	59,2752	0,7493	nadp-dependent oxidoreductase p1	10673,95	17942,19
SCEQLR1050E07	24	192,6033	0,8078	elongation factor 1-gamma 2	6224,729	10896,93
SCEQLR1050G03	11	89,4408	0,9772	gtp-binding protein sar1a	8193,787	16130,81
SCEQLR1050G05	15	154,4054	0,1600	elongation factor 1-beta	33140,04	29661,4
SCEQLR1091A10	4	31,1649	0,1172	60s ribosomal protein l23a	32845,1	35625,45
SCEQLR1091B01	2	12,8617	0,3010	copper chaperone	16361,87	20157,57
SCEQLR1091B11	7	82,2301	0,5269	40s ribosomal protein s12	7550,014	5240,221
SCEQLR1091D05	17	154,5976	0,1431	60s ribosomal protein l5-1	9392,959	8506,159
SCEQLR1091D11	2	12,2992	1,1127	potassium transporter hak2p	847,3221	391,834
SCEQLR1091F06	20	155,2589	0,7285	sorbitol dehydrogenase	81666,87	135312,8
SCEQLR1091F08	2	10,3272	0,1976	vacuolar atp synthase subunit f	2952,239	3385,605
SCEQLR1092A03	1	5,503	0,5798	metal ion binding protein	6592,313	9853,077
SCEQLR1092B09	4	25,5305	0,3674	kda class i heat shock protein 3	10522,42	13574,55
SCEQLR1092H10	10	78,5553	0,0108	snf1-related protein kinase regulatory subunit gamma-1-like	15669,65	15552,76
SCEQLR1093B12	10	88,4872	0,5445	transposon protein	16504,98	24072,07
SCEQLR1093D05	8	48,6349	0,4397	rickettsia 17 kda surface antigen family protein	38256,82	51888,48
SCEQLR1093F09	23	173,8631	0,7202	glycosyl hydrolase family 3 n terminal domain containing expressed	47034,91	77488,09
SCEQLR1093H04	6	35,9673	0,0680	polyadenylate-binding protein 2	3870,787	4057,5
SCEQRT1024C01	1	5,3045	0,2381	hypothetical protein SORBIDRAFT_07g019350 [Sorghum bicolor]	52495,19	61913,55
SCEQRT1024C07	11	97,1464	0,6961	proton translocating pyrophosphatase	3613,527	5854,211
SCEQRT1024G06	13	107,3825	0,5289	asparagine synthetase	24931,12	35972,04
SCEQRT1025A07	10	73,1632	0,9583	proteasome 26s non-atpase subunit 1	1073,689	552,5839
SCEQRT1025E03	5	41,2031	0,2437	cysteine proteinase inhibitor	37243,75	44097,52
SCEQRT1025F04	8	57,0918	0,2891	hypothetical protein SORBIDRAFT_10g021150 [Sorghum bicolor]	30898,29	37755,15
SCEQRT1025H04	5	28,1029	0,7619	heat-shock protein 101	4734,036	8027,648
SCEQRT1026F09	12	99,6199	0,0147	peroxidase 2 precursor	25357,66	25101,01
SCEQRT1026G06	14	97,8368	0,2786	phosphoglucomutase chloroplast	36561,06	44348,33
SCEQRT1026G11	28	297,4677	0,2091	leucine aminopeptidase	147114,1	170058,3
SCEQRT1028C10	7	43,1195	0,3693	spo76 protein	23715,34	30633,22
SCEQRT1028H09	20	268,7286	0,3671	anionic peroxidase	281898,6	363589,1
SCEQRT1029D09	23	146,4494	0,4420	glucose-6-phosphate isomerase	27324,54	37120,5

Table S1 cont.

Accession	Peptide count	Confidence score ^a	Log ₂ of fold change ^b	Description	Total Ion Counts Control	Total Ion Counts W _m B _d R _f R
SCEQRT1031B11	11	73,0687	0,2882	acyl-coenzyme a oxidase 2	3994,805	3271,392
SCEQRT1031D02	20	250,4855	0,1760	14-3-3-like protein	2072,377	2341,186
SCEQRT1033F03	16	109,6933	0,2786	26s proteasome non-atpase regulatory subunit 6	24926,47	30236,84
SCEQRT1033H09	15	159,459	0,0618	mitochondrial prohibitin complex protein 2	40577,02	42353,36
SCEQRT2029H09	3	19,4861	0,5355	ef hand family expressed	9016,396	13069,21
SCEQRT2030B01	1	6,5162	0,2462	phd finger-like domain-containing protein 5a	1589,487	1340,095
SCEQRT2090H11	2	11,8915	0,2364	transducin wd-40 repeat	13140,68	15480,19
SCEQRT2094D05	6	35,5932	0,3653	uncharacterized protein LOC100382733 [Zea mays]	3016,801	3886,167
SCEQRT2095D10	16	101,623	0,2628	gdp-mannose -epimerase 1	26520,38	31818,45
SCEQRT2096F01	4	30,1219	0,2392	tip120 protein	5206,555	6145,675
SCEQRT2098F10	2	11,0631	0,3323	nucleotide pyrophosphatase phosphodiesterase	27079,15	21507,58
SCEQRT2099G01	22	166,6363	0,2107	probable l-ascorbate peroxidase chloroplastic-like isoform 1	25476,48	22014,28
SCEQRZ3090B12	2	10,7939	0,3158	snare-interacting protein keule	18282,4	22756,3
SCEQRZ3093C12	7	44,8928	0,0757	ubiquitin-fold modifier 1 precursor	21536,1	20435,4
SCEQSD1078D10	2	10,9128	0,0850	subtilisin-chymotrypsin inhibitor ci-1b	2687,905	2534,164
SCEZAM1082G06	6	78,1359	0,3104	histone h2a	885,3494	713,9492
SCEZAM2059G06	3	17,4112	0,2283	ribosome recycling factor	1084,283	1270,21
SCEZFL4044H06	1	5,0723	0,2327	cytochrome p450	37112,81	43609,93
SCEZHR1049B08	16	134,3113	1,1485	alpha- glucan-protein synthase	12571,32	27867,85
SCEZHR1084H04	5	40,612	0,0732	pollen-specific protein like	8648,476	9098,445
SCEZHR1088A07	1	5,876	0,3912	zinc finger (c3hc4-type ring finger) protein family-like	13292,69	17432,66
SCEZLB1005C03	2	11,4733	0,5453	tankyrase 1	11631,36	7970,177
SCEZLB1006A02	3	18,6803	0,2373	hypothetical protein SORBiDRAFT_02g009450 [Sorghum bicolor]	10196,96	12019,64
SCEZLB1006A07	8	50,5604	0,8300	ubiquitin-like 1-activating enzyme e1a	7095,368	12613,55
SCEZLB1006G09	29	257,5196	0,3515	pyruvate cytosolic isozyme	23231,32	29641,21
SCEZLB1007F05	5	27,6142	0,6982	c1pb3_orysj ame: full=chaperone protein mitochondrial	2946,573	4780,858
SCEZLB1007F07	23	152,7789	0,5702	arginyl-trna synthetase	45045,12	66878,44
SCEZLB1008D04	4	16,1075	0,1809	dynamin-related protein 1c	11228,66	12729,12
SCEZLB1008D12	1	5,9436	0,6723	aquaporin tip4-2	2304,832	3673,053
SCEZLB1009B03	1	5,1129	0,7878	eukaryotic peptide chain release factor gtp-binding subunit erf3a-like	3242,114	5597,367
SCEZLB1009D02	12	87,0765	0,3386	u2 small nuclear ribonucleoprotein a	95629,99	120924,4
SCEZLB1009E05	12	91,9008	0,5861	proteasome alpha subunit	22981,25	34498,48
SCEZLB1010A03	8	61,5932	0,0814	spermidine synthase 1	27547,25	29147,17
SCEZLB1010E07	4	36,6663	0,2162	nadh ubiquinone oxidoreductase b22-like subunit	10593,23	9119,121
SCEZLB1012C10	5	42,1342	0,7707	soluble inorganic pyrophosphatase	7502,469	12800,33
SCEZLB1013H04	5	32,6205	0,3829	adenine phosphoribosyltransferase 2	6741,434	8790,646

Table S1 cont.

Accession	Peptide count	Confidence score ^a	Log ₂ of fold change ^b	Description	Total Ion Counts Control	Total Ion Counts W _m B _d R _f R
SCEZLB1014E02	15	175,2799	1,0129	histone	2604,531	1290,698
SCEZLB1014F09	33	277,1097	0,0683	dihydrolipoyl dehydrogenase mitochondrial-like	161363,1	169191,2
SCEZLR1009D05	2	10,543	0,5740	protochlorophyllide reductase a	7036,969	10475,25
SCEZLR1009F04	6	36,9269	0,0970	triose phosphate phosphate non-green precursor	17812,64	16654,06
SCEZLR1031A11	11	71,8466	0,2930	acetyl- cytosolic 1	31858,11	39032,65
SCEZLR1031E02	9	61,1615	0,0189	rna recognition motif family expressed	20807,43	20536,7
SCEZLR1031E10	11	119,3988	0,6024	translationally-controlled tumor protein	135533,6	205770,7
SCEZLR1052C03	14	143,7269	1,1349	sucrose synthase	15263,67	33519,16
SCEZLR1052D02	22	187,1998	0,3091	26s proteasome non-atpase regulatory subunit 11	13719,43	16997,72
SCEZLR1052F04	22	174,4904	0,3537	mitochondrial atp synthase precursor	130381	166601,8
SCEZLR1052F07	26	198,7805	0,2018	protein phosphatase 2a structural subunit	4850,5	5578,908
SCEZRT2019F10	3	17,8927	0,5980	hypothetical protein SORBIDRAFT_10g011530 [Sorghum bicolor]	118493,6	179359,5
SCEZRT2023E09	5	25,5632	0,4358	atpase family aaa domain-containing protein 1	16750,54	22657,36
SCEZRZ1012A01	6	39,2539	0,1382	hypothetical protein SORBIDRAFT_06g013940 [Sorghum bicolor]	9218,715	10145,77
SCEZRZ1012B02	3	21,0752	0,2964	atp gtp binding protein	13130,03	10691,45
SCEZRZ1012B07	9	51,4979	0,2986	plasma membrane h+ atpase	31404,63	25532,69
SCEZRZ1012C04	2	12,5356	0,0255	thioredoxin domain-containing protein 9 homolog	12048,68	12263,36
SCEZRZ1012D01	14	98,8496	0,3995	rh37_orysj ame: full=dead-box atp-dependent rna helicase 37	15594,76	20570,54
SCEZRZ1012H03	9	69,9731	0,0286	hypothetical protein SORBIDRAFT_01g011580 [Sorghum bicolor]	17268,67	16930,22
SCEZRZ1013F01	4	22,1037	0,0386	cullin-1-like isoform 1	1267,407	1301,791
SCEZRZ1013F11	3	16,24	0,2432	rna recognition motif -containing protein	3447,229	4080,164
SCEZRZ1014C04	13	163,7334	1,1526	osmotin-like protein precursor	50063,51	111300,1
SCEZRZ1014E12	1	5,5969	0,0708	alpha-l-fucosidase 2 precursor	6463,915	6789,12
SCEZRZ1014F10	9	53,5451	0,4439	thioredoxin peroxidase 1	34467,28	46884,69
SCEZRZ1015F05	26	206,9667	0,2433	26s proteasome regulatory subunit s2	80161,66	94884,58
SCEZRZ1017B08	11	73,6702	0,2359	gblpa_orysj	96021,63	113077,6
SCEZRZ3015E11	1	6,1464	1,1910	basic endochitinase c precursor	1316,102	3004,865
SCEZRZ3018G06	4	22,6797	0,1704	hypothetical protein SORBIDRAFT_01g004790 [Sorghum bicolor]	12435,01	11049,78
SCEZRZ3019D02	6	47,2364	0,0013	dna damage-inducible protein 1-like	8820,924	8829,133
SCEZRZ3101H02	1	5,5639	0,3407	uncharacterized protein LOC100304272 [Zea mays]	5724,085	7248,819
SCJFFL3C04H03	5	35,1352	0,4518	glycine-rich protein 2b	2593,55	3547,228
SCJFLR1013A09	3	18,1718	0,0369	cysteine proteinase 1 precursor	4109,108	4215,519
SCJFLR1013B03	23	185,1058	1,0205	bisphosphoglycerate-independent phosphoglycerate mutase	76070,25	154315,9
SCJFLR1013C03	15	113,1468	0,6574	atp synthase gamma chain	31809,3	50171,73
SCJFLR1013D03	17	123,6352	0,4905	cop9 signalosome complex subunit 4	16288,11	22884,22
SCJFLR1013D10	4	27,1342	0,4553	hec ndc80p family protein	3340,778	2436,689

Table S1 cont.

Accession	Peptide count	Confidence score ^a	Log ₂ of fold change ^b	Description	Total Ion Counts Control	Total Ion Counts W _m B _d R _f R
SCJFLR1013E04	8	58,3203	0,0218	udp-glucose 6-dehydrogenase	13036,86	13235,1
SCJFLR1013F02	23	262,1691	0,4990	glutamine synthetase	242472	342670,1
SCJFLR1013G09	2	11,4043	0,4617	loc100281836 precursor	306390,6	222484,3
SCJFLR1035A02	2	10,938	0,1341	alkaline neutral invertase	1889,264	2073,362
SCJFLR1035F03	3	18,715	0,8189	hypothetical protein SORBIDRAFT_03g002080 [Sorghum bicolor]	7554,483	13326,37
SCJFLR1073D03	17	104,1539	0,1277	gsa_orysj ame: full=glutamate-1-semialdehyde - chloroplastic short=gsa	11769,66	12859,36
SCJFLR1073E04	13	94,7061	0,4274	strictosidine synthase precursor	22328,92	30028,66
SCJFLR1073H09	39	537,237	0,6230	enolase 1	1053345	1622217
SCJFLR1074A12	16	124,8312	0,3571	outer mitochondrial membrane protein porin	135946,6	174127,6
SCJFLR1074G03	17	153,6358	0,3392	vacuolar proton-atpase	29516,2	23332,26
SCJFRT1005C01	1	5,1112	0,0103	3-hydroxybutyryl- dehydrogenase	403,8199	400,9448
SCJFRT1005D01	5	46,3448	0,4832	d-3-phosphoglycerate dehydrogenase	87410,66	122188,4
SCJFRT1005G01	2	13,6769	0,2966	glycine rich protein	1064,322	866,5183
SCJFRT1007F05	3	16,3722	0,0481	uncharacterized protein LOC100272910 [Zea mays]	12303,54	11899,78
SCJFRT1009E11	3	19,4336	0,2421	lipid binding protein	6670,004	5639,768
SCJFRT1009F06	7	69,1235	0,6348	ef hand family expressed	45699,17	70958,48
SCJFRT1058C05	6	51,2243	1,1223	cytosolic factor-like protein	5375,111	11701,5
SCJFRT1058F10	9	56,5427	0,2937	ferredoxin--nadp root isozyme	10135,98	12424,31
SCJFRT1060F02	10	106,8073	0,1580	histone h3	2240,362	2499,711
SCJFRT1061H04.b	16	121,1339	0,2002	chaperonin cpn60- mitochondrial-like	19425,81	22316,98
SCJFRT2053C06	3	21,4293	0,2693	bola-like protein	4247,571	3524,241
SCJFRT2057C03	7	44,6023	0,2630	aspartyl-tRNA synthetase	49522,49	59427,4
SCJFRT2057H03	15	136,0646	0,9232	salt tolerance expressed	4622,152	2437,426
SCJFRT2059C12	2	11,0151	0,5725	hypothetical protein SORBIDRAFT_06g029020 [Sorghum bicolor]	2605,858	3875,271
SCJFRT2059E04	20	143,1628	0,3638	puromycin-sensitive aminopeptidase isoform 1	52610,27	67698,44
SCJFRZ1005C03	4	22,4392	0,1608	3-n-debenzoyl-2-deoxytaxol n-benzoyltransferase	5376,734	6010,883
SCJFRZ1005C06	3	19,696	0,4126	auxin-induced protein pcnt115-like isoform 1	11083,52	14753,43
SCJFRZ1005F03	1	5,7424	0,1979	cb22_orysj ame: full=chlorophyll a-b binding protein chloroplastic	8213,391	7160,836
SCJFRZ1006E06	25	214,0205	0,7376	beta-tubulin r2242	18790,84	31332,13
SCJFRZ1007A10	14	118,3314	0,5508	betaine aldehyde dehydrogenase	26561,25	38908,43
SCJFRZ1007B07	18	141,9679	0,1037	methyl-binding domain protein mbd115	55607,71	59751,73
SCJFRZ1007F10	3	17,7639	0,7301	es43 protein	1688,004	2800,05
SCJFRZ1007H03	5	28,2882	0,0049	aspartate kinase-homoserine dehydrogenase	35090,13	35210,16
SCJFRZ2005C12	9	77,5703	0,1443	protein z	39035,87	43141,93
SCJFRZ2005G03	7	41,0926	0,3428	swib mdm2 domain containing protein	11271,09	14294,14
SCJFRZ2007H07	5	28,9804	0,1778	nad-dependent malic enzyme 59 kda mitochondrial expressed	13814,66	15626,51

Table S1 cont.

Accession	Peptide count	Confidence score ^a	Log ₂ of fold change ^b	Description	Total Ion Counts Control	Total Ion Counts W _m B _d R _f R
SCJFRZ2011A01	6	37,9829	0,2623	methionyl-tRNA synthetase-like protein	9418,856	11297,07
SCJFRZ2013F11	10	67,3742	0,0140	adenine phosphoribosyltransferase 1	33515,26	33842,08
SCJFRZ2013G10	6	34,3671	0,2908	structural maintenance of chromosomes protein 6-like	4610,039	3768,525
SCJFRZ2014A08	5	69,7219	0,0515	histone	133690,7	129002,2
SCJFRZ2014H04	8	54,2159	0,0714	hypothetical protein SORBIDRAFT_02g029800 [Sorghum bicolor]	27494,33	28888,77
SCJFRZ2015B06	2	15,1803	0,6335	peptidyl-prolyl isomerase fkbp12	4168,931	6467,182
SCJFRZ2025G05	4	24,1055	0,1940	chorismate mutase	1065,93	931,7954
SCJFRZ2025G07	3	24,8441	1,0397	ankyrin repeat domain-containing protein 2	2203,239	4529,392
SCJFRZ2026B09	2	14,1801	0,0220	gibberellin-regulated protein 2 precursor	3849,346	3791,069
SCJFRZ2026G03	7	42,4171	0,6057	atp-dependent clp protease atp-binding subunit -like isoform 1	4636,159	7054,895
SCJFRZ2027F12	13	103,0766	0,6460	probable 26s proteasome non-atpase regulatory subunit 7-like	30761,91	48137,71
SCJFRZ2029D10	10	68,0596	0,2010	pyruvate cytosolic isozyme	15131,34	17393,04
SCJFRZ2031H09	6	48,5922	0,4265	membrane steroid-binding protein 1	10019,53	13465,6
SCJFRZ2032C10	4	31,4508	0,1237	dek protein	22573,21	20718,3
SCJFRZ2032H05	5	41,1922	0,1675	tubulin-specific chaperone a	37017,46	32959,76
SCJFRZ2033D06	3	19,9226	0,7992	glucan endo- -beta-glucosidase a6 precursor	7298,623	12700,67
SCJFRZ2033E06	15	95,5634	0,2440	stomatin-like protein 2	16501,01	19542,28
SCJLAM1062H06	3	16,6989	0,2234	hypothetical protein SORBIDRAFT_04g000775 [Sorghum bicolor]	4794,209	4106,388
SCJLAM2091A04	2	11,6768	0,6482	gibberellin 2-beta-dioxygenase	28761,36	45075,08
SCJLFL3013C05	3	15,8687	0,3605	loc495012 expressed	12919,06	10062,68
SCJLFL3017H10	4	30,2905	0,2483	hypothetical protein SORBIDRAFT_10g022230 [Sorghum bicolor]	1810,033	1523,86
SCJLFL4098H05	4	45,5444	0,5255	tip120 protein	16655,43	23974,88
SCJLHR1027C12	1	5,4144	0,3646	anthranilate synthase component i-1	3892,157	5011,112
SCJLLB2079F03	3	30,9228	0,1856	udp-sugar pyrophosphorylase	1371,888	1560,182
SCJLLR1011B02	10	64,3162	0,0565	hypothetical protein SORBIDRAFT_03g043970 [Sorghum bicolor]	26905,06	27980,57
SCJLLR1011C10	27	258,5326	0,8038	aspartate aminotransferase	79016,51	137935,2
SCJLLR1011E03	61	696,4155	0,6526	heat shock protein 82	43436,29	68284,08
SCJLLR1011F11	18	119,0473	0,8598	hypothetical protein SORBIDRAFT_10g004260 [Sorghum bicolor]	12488,88	22665,12
SCJLLR1011H03	8	53,5242	0,1262	nucleosome chromatin assembly protein	12802,51	11729,87
SCJLLR1033C10	8	64,486	0,7373	dna repair protein rad23	13390,61	22323,13
SCJLLR1033F07	13	109,7031	0,5563	2-cys peroxiredoxin bas1	67664,13	99497,47
SCJLLR1054A06	15	102,4163	0,1472	1-aminocyclopropane-1-carboxylate oxidase 1	21946,27	19816,94
SCJLLR1054C04	12	69,5027	0,3518	transcription factor apfi	19845,2	25325,14
SCJLLR1054C07	21	157,6642	0,8158	mitochondrial-processing peptidase beta subunit	56694,35	99799,82
SCJLLR1054E03	6	56,5918	0,7677	macrophage migration inhibitory factor	36773,1	62607,65
SCJLLR1054F05	34	298,3311	0,3748	dnak-type molecular chaperone	116826,1	151481,7

Table S1 cont.

Accession	Peptide count	Confidence score ^a	Log ₂ of fold change ^b	Description	Total Ion Counts Control	Total Ion Counts W _m B _d R _f R
SCJLLR1054G06	28	206,0485	0,5207	hypothetical protein SORBIDRAFT_07g023850 [Sorghum bicolor]	91058,67	130639,9
SCJLLR1054H06	12	85,1908	0,1905	pur alpha-1	17847,7	15639,59
SCJLLR1101F06	4	70,106	0,6199	histone h2a	9264,838	14238,04
SCJLLR1101G05	5	58,6049	0,2221	hmgi y protein	49046,22	57208,29
SCJLLR1101H08	16	193,3578	0,1027	histone	7982,099	7433,818
SCJLLR1102F09	3	21,1653	0,2650	hypothetical protein SORBIDRAFT_01g015010 [Sorghum bicolor]	4296,112	5162,281
SCJLLR1102G11	8	45,237	0,2281	hypothetical protein SORBIDRAFT_09g022800 [Sorghum bicolor]	4419,243	3772,994
SCJLLR1106F03	6	37,2451	0,3826	20 kda chloroplastic-like	20536,18	26772
SCJLLR1107C01	8	53,3773	0,5199	ubiquinol-cytochrome c reductase complex 14 kda protein	15805,32	22663,25
SCJLLR1107E04	5	28,8323	0,3645	snrk1-interacting protein 1	12468,08	16051,37
SCJLLR1108F04	3	22,6673	0,3509	mitochondrial import receptor subunit tom20	197715,9	155024,2
SCJLRT1006G01	22	307,5923	0,5972	elongation factor 1-alpha	53403,25	80788,39
SCJLRT1013C01	8	50,1601	0,6354	phenylalanine ammonia-lyase	4030,483	2594,606
SCJLRT1014B04	9	88,1902	0,1222	cytochrome b5	39433,6	42919,35
SCJLRT1017E09	12	78,8332	0,7830	cytosolic chaperonin delta-subunit	2733,056	4702,699
SCJLRT1018A03	1	6,5222	0,7291	isocitrate dehydrogenase	2868,74	4755,085
SCJLRT1018H05	12	74,7866	0,0536	protease 2	10082,64	10464,24
SCJLRT1020A08	9	61,5783	0,1609	aglu_orysj ame: full=probable alpha-glucosidase os06g0675700	11705,84	13086,79
SCJLRT1020F06	6	44,705	1,0934	chitinase	1289,826	2752,117
SCJLRT1021D09	10	82,9935	0,7423	glutathione s-transferase 4	12353,7	7384,715
SCJLRT1021E02	3	17,642	0,3101	mitochondrial nadh ubiquinone oxidoreductase 29 kda subunit	1334,281	1076,22
SCJLRT1022G04	10	69,4032	0,3659	glutathione s-transferase zeta class	9994,855	12880,13
SCJLRT1023A07	13	82,9671	0,5840	pyruvate dehydrogenase e1 component subunit beta	12924,71	19373,51
SCJLRT2049D05	11	121,4227	0,0364	heme-binding protein 2	131554,4	134913,4
SCJLRT2049G10.b	3	16,2075	0,3119	von willebrand factor type a domain containing expressed	3416,252	4240,59
SCJLRZ1021C03	20	118,4327	0,8230	ubiquitin isopeptidase t ubiquitin-specific protease-5	65925,68	37264,57
SCJLRZ1023A10	3	17,09	0,5317	saccharopine dehydrogenase	603,1427	417,2192
SCJLRZ1024A01	22	158,4937	0,3895	phosphoenolpyruvate partial	52935,91	69342,59
SCJLRZ1024A04	21	156,5139	0,1066	af465643_1 lipoxygenase	47387,77	51021,96
SCJLRZ1024A09	5	28,9099	0,3265	succinate dehydrogenase iron-protein subunit	19273,79	24169,15
SCJLRZ1024D11	29	201,3581	0,2704	dna-binding protein	93891,13	113246,9
SCJLRZ1024H09	22	203,2919	0,5038	salt tolerance expressed	58023,69	82275,89
SCJLRZ1027C05	12	70,6864	0,7102	dna-damage inducible protein	20122,94	12300,13
SCJLRZ1027F05	22	141,4332	0,0769	transducin wd-40 repeat	35947,86	37916,68
SCJLRZ1027G11	7	46,2853	0,2082	in2-1 protein	21988,2	25401,62
SCJLST1020D12	3	16,6254	0,6449	26s proteasome non-atpase regulatory subunit 9	9321,487	14575,87

Table S1 cont.

Accession	Peptide count	Confidence score ^a	Log ₂ of fold change ^b	Description	Total Ion Counts Control	Total Ion Counts W _m B _d R _f R
SCJLST1025D02	11	110,5912	0,2834	cytosolic phosphoglycerate kinase 1	7082,51	8619,601
SCMCAM1101A10	5	39,5872	0,7042	karyopherin-beta 3 variant	11553,72	18823,31
SCMCAM1105F12	4	21,7425	1,1212	immediate-early fungal elicitor protein	2010,656	4373,726
SCMCAM2084D04	1	5,3899	0,6959	gs3-like protein	5178,16	8388,321
SCMCCL6050B01	11	69,912	0,5152	branched-chain-amino-acid aminotransferase	68221,47	97501,03
SCMCCL6051B10	10	60,7525	0,2664	ribose-5-phosphate isomerase	36652,3	44084,67
SCMCCL6051E03	9	53,1035	0,3432	lysosomal alpha-mannosidase-like	5562,811	7056,764
SCMCCL6054D04	2	11,76	0,0067	mitochondrial glycoprotein	1735,974	1727,931
SCMCCL6059B02	3	24,8998	0,5590	indole-3-acetic acid amido synthetase	2154,68	3174,337
SCMCCL6059C02	8	70,4957	0,2769	protein binding protein	45669,97	55335,09
SCMCFL5008G05	3	25,6582	0,2210	probable indole-3-acetic acid-amido synthetase -like	4795,375	5589,245
SCMCLR1053H06	13	90,1489	0,6426	lysyl-tRNA synthetase	3982,23	6216,734
SCMCLR1123A02	1	11,2462	0,0399	integrin beta-1-binding protein 2	1656,569	1611,362
SCMCLR1123A09	9	75,4406	0,5397	alpha-soluble nsf attachment protein	48071,43	69879,92
SCMCLR1123B01	3	17,5424	0,3999	fasciclin-like arabinogalactan protein 10 precursor	2115,135	2790,659
SCMCRT2087B02	4	35,1817	0,9993	cysteine proteinase inhibitor 8-like	3583,39	7163,456
SCMCRT2087D10	15	98,2353	0,2121	2-isopropylmalate synthase b	11115,05	12875,71
SCMCRT2089A07	12	75,6904	0,1008	probable splicing factor 3a subunit 1-like	26729,36	24925,01
SCMCRT2089E02	13	100,2538	0,2061	pdc1_maize ame: full=pyruvate decarboxylase isozyme 1 short=pdc	25028,61	28871,55
SCMCRT2103C07	11	94,401	0,1748	acidic leucine-rich nuclear phosphoprotein 32 family member a	22012,14	24847,02
SCMCRT2104E09	4	29,6489	0,1616	urease accessory protein ureg	14148,43	15825,69
SCMCRT2105F08	20	135,1815	0,3254	mitochondrial phosphate transporter	5396,323	6761,535
SCMCRT2107G02	8	59,9459	0,7163	aspartate-semialdehyde dehydrogenase	29246,02	48051,37
SCMCRT2108A04	4	28,9225	1,1418	hypothetical protein SORBI_DRAFT_05g023700 [Sorghum bicolor]	6381,791	14081,8
SCMCBS1113A08	2	11,5158	0,7577	peroxidase 52 precursor	1081,601	639,7027
SCMCST1054G01	10	60,9905	0,9740	3-mercaptopyruvate sulfurtransferase-like isoform 2	25043,91	49193,68
SCMCST1055F02	6	43,8937	0,2120	lysyl-tRNA synthetase	12990,51	15046,73
SCQGLB1027C07	8	44,9203	0,3069	vip3 protein	5346,539	6613,918
SCQGLB1028E02	2	11,7177	0,3620	trf33_orysj ame: full=thioredoxin-like 3-3 ame: full=thioredoxin-like 1	1323,393	1700,877
SCQGLB1038F04	6	41,6175	0,4592	acetolactate synthase amino acid binding protein	9916,207	13632,41
SCQGLB1038F11	12	93,7445	0,4569	40S ribosomal protein s19	135695,4	186258,1
SCQGLB1039E05	2	10,9278	0,0269	er6 protein	3442,073	3506,901
SCQGLB1040H06	3	18,1251	0,3723	cell wall integrity protein scw1	23221,42	30058,55
SCQGLR1019A07	14	90,3775	0,2665	carrier protein	40707,65	48967,26
SCQGLR1019B02	21	184,7094	0,1291	ferredoxin-sulfite reductase precursor	145707	159351,6
SCQGLR1019C05	20	138,9329	0,9808	sap domain containing expressed	30076,1	59355,88

Table S1 cont.

Accession	Peptide count	Confidence score ^a	Log ₂ of fold change ^b	Description	Total Ion Counts Control	Total Ion Counts W _m B _d R _f R
SCQGLR1019D06	6	52,4805	0,0337	legumin-like protein	12918,86	12620,73
SCQGLR1019E07	2	18,3119	0,0201	e3 ubiquitin-protein ligase upl1-like	8224,505	8110,901
SCQGLR1041A05	34	241,0077	0,1628	heat shock protein sti	179709,2	201174
SCQGLR1062D04	43	403,5339	0,2567	udp-glucose pyrophosphorylase	445714,3	532500,8
SCQGLR1062E09	12	111,0935	0,3633	26s proteasome non-atpase regulatory subunit 8	74435,81	95749,02
SCQGLR1062E12	14	108,4411	0,3793	glyoxalase i	72462,51	94252,58
SCQGLR1062G12	4	26,8115	0,5353	ac026815_7 rna binding protein	22508,75	32620,87
SCQGLR1085B04	9	56,249	0,5646	pp2ac-2 - phosphatase 2a isoform 2 belonging to family 2	2422,16	1637,76
SCQGLR1085E02	6	70,5373	0,1361	hypothetical protein SORBIDRAFT_04g001720 [Sorghum bicolor]	82611,8	90784,04
SCQGLR1085E12	8	52,984	0,3533	kelch repeat containing protein	4472,605	5713,851
SCQGLR1085G12	6	36,0602	0,1093	nadh-ubiquinone oxidoreductase 24 kda subunit	19979,29	21551,55
SCQGLR1086F03	3	29,7374	0,2635	ssxt protein	2442,935	2035,187
SCQGLR2017B05	4	26,6214	0,7672	uncharacterized protein LOC100382048 [Zea mays]	10507,04	17882,25
SCQGLR2017D02	4	23,2938	0,0227	nadh-ubiquinone oxidoreductase subunit	16860,2	17127,61
SCQGLR2032G10	14	167,3848	0,1150	polyubiquitin 2	44843,13	48562,38
SCQGRT1039H01	4	23,3293	0,9418	tripeptidyl peptidase ii	3101,754	5958,264
SCQGRT1045A10	2	11,0295	1,0849	hypothetical protein SORBIDRAFT_06g017910 [Sorghum bicolor]	1263,026	595,4387
SCQGRT3045B12	3	17,4201	0,4299	armadillo beta-catenin repeat	1969,612	2653,411
SCQGRZ3011G12	6	50,8901	0,0084	ras-related protein rab11a	2459,797	2474,202
SCQGSB1080F09	1	10,1288	0,5447	e3 ubiquitin-protein ligase upl1-like	18651,41	27206,86
SCQGSB1084H07	7	52,9109	1,0730	heat shock protein 83	6084,931	2892,276
SCQGST1032E05	4	28,254	0,2889	transcription initiation factor iib	8590,684	7031,529
SCQGST3154G02	2	11,5709	0,8422	nfyb4_orysj ame: full=nuclear transcription factor y subunit b-4	573,723	1028,573
SCQSAM1032F05	4	33,4968	0,2946	acyl carrier protein	10189,83	8307,518
SCQSAM2101A12	2	25,3482	0,2455	low quality protein: gdsl esterase lipase at5g45910-like	4734,808	3993,964
SCQSF3032E01	1	5,8074	0,3989	boron transporter expressed	3195,677	4213,565
SCQSF3033E01.b	3	19,0009	0,8137	pvr3-like protein	3579,075	6291,175
SCQSLB1049A06	6	52,2217	0,4192	cytochrome c oxidase subunit vb precursor	64557,04	86325,86
SCQSLB1049C04	4	21,5441	0,6952	glutathione s-transferase 6	2682,025	1656,523
SCQSLB1049G04	2	25,9394	0,3745	ml domain protein	72986,62	94622,01
SCQSLR1018D04	9	66,2533	0,6730	proteasome subunit alpha type 2	35445,2	56511,98
SCQSLR1018E09	15	133,1754	0,4138	nucleosome chromatin assembly factor group a	63102,71	84063,01
SCQSLR1018F09	28	203,9658	0,1501	eukaryotic translation initiation factor 3 subunit a	34437,05	38214,13
SCQSLR1061B01	20	147,931	0,2320	fibroblast growth factor 2-interacting factor	25285,8	29696,27
SCQSLR1061E07	24	182,3746	0,4592	glucose-6-phosphate isomerase	41043,57	56424,21
SCQSLR1089E02	7	65,5052	0,1184	hypothetical protein SORBIDRAFT_04g001720 [Sorghum bicolor]	43951,07	40487,95

Table S1 cont.

Accession	Peptide count	Confidence score ^a	Log ₂ of fold change ^b	Description	Total Ion Counts Control	Total Ion Counts W _m B _d R _f R
SCQLR1090G03	18	113,7875	0,3826	aspartate aminotransferase	72021,61	93890,92
SCQSR1034D03	11	87,1498	0,8406	loc100282597 precursor	29359,17	52576,04
SCQSR1035D04	1	6,5125	0,6092	amp-binding protein	8288,651	5433,856
SCQSR1035E09	4	22,3048	0,4285	pleckstrin homology domain family a	5403,086	7271,474
SCQSR1035E10	19	136,1291	0,2441	phosphoserine aminotransferase	76434,61	90528,41
SCQSR1036D03	6	42,1351	0,4822	pathogenesis-related protein 1	2478,038	3461,499
SCQSR1036H06	7	44,9838	0,2438	importin-beta n-terminal domain containing expressed	9859,804	11675,3
SCQSR2032E04	4	33,4375	0,3086	hypothetical protein SORBIDRAFT_04g033720 [Sorghum bicolor]	8050,275	6500,069
SCQSR2033A11	4	23,5027	0,1197	ras gtpase-activating protein-binding protein 1-like	19047,32	20695,06
SCQSR2034F02	4	33,9674	0,7968	proline iminopeptidase-like	3050,237	5298,978
SCQSR2034G08	6	40,744	0,3552	alpha-galactosidase expressed	11394,08	8907,333
SCQSR2035D10	1	5,2514	0,0035	abscisic stress ripening protein 2	3250,317	3242,421
SCQSR2036C02	3	24,6331	0,0837	translocon-associated protein beta containing protein	8124,448	8609,819
SCQSSB1077E06	1	5,5961	0,4751	t-complex protein 1 subunit zeta	14810,39	20586,44
SCRFA1120B10	3	30,3823	0,3618	aspartate-semialdehyde dehydrogenase	44718,47	57464,59
SCRFA1028B07	5	34,0079	1,0266	jmcj domain containing expressed	28446,41	13963,55
SCRFFL1025G01	2	12,0464	0,1607	formate--tetrahydrofolate ligase-like	3080,702	2755,949
SCRFFH1006A10	2	17,0325	0,0503	dna binding protein	3093,553	2987,562
SCRFLB1053B09	10	80,1286	0,4635	cytosolic 6-phosphogluconate dehydrogenase	18349,72	25301,49
SCRFLB1056D04	1	5,9851	0,4833	thioredoxin h-type 5	5149,723	7199,132
SCRFLB1056F07	10	93,8694	0,2954	skp1-like protein 1b-like isoform 1	12090,62	9852,296
SCRFLB1056H05	10	58,109	0,4506	tyrosyl-tRNA synthetase	13730,5	18764,42
SCRFLB2058C04	2	11,8098	0,2340	hypothetical protein SORBIDRAFT_10g005610 [Sorghum bicolor]	29331,02	34495,8
SCRFLR1012B07	20	130,2464	1,0800	succinate dehydrogenase flavoprotein precursor	160935,3	340217,6
SCRFLR1012B11	28	178,3101	0,1603	eukaryotic initiation factor 4f subunit p82-34 (eif- 4f p82-34)	99940,69	111689,5
SCRFLR1012B12	7	58,3586	0,9993	xyloglucan endotransglucosylase hydrolase protein 23 precursor	7957,816	15908,4
SCRFLR1012E06	19	185,2359	0,2438	scrk1_maize ame: full=fructokinase-1 ame: full=1	128327,8	151949,4
SCRFLR1012F02	8	46,9645	0,8337	alpha- glucan-protein synthase	209586,8	373535,5
SCRFLR1012F09	11	109,6534	0,2385	peptidyl-prolyl cis-trans isomerase cyp19-4 precursor	35972,95	42439,31
SCRFLR1012G07	22	164,8446	0,0849	heat shock	54269,17	57557,32
SCRFLR1034A04	7	44,3346	0,0737	sec13-related protein	5857,636	6164,554
SCRFLR1034D03	8	72,2071	0,3675	spliceosome rna helicase bat1	16891,73	21792,27
SCRFLR1034D04	1	6,97	0,6814	fasciclin-like arabinogalactan protein 11-like	11732,21	18815,17
SCRFLR1055E09	10	57,4867	0,3274	alpha-soluble nsf attachment protein	23504,33	29492,62
SCRFLR1055G09	2	13,6197	0,3215	catalytic acting on nadh or nadph	1871,636	2338,773
SCRFLR2034C11	8	58,4969	0,2027	membrane steroid-binding protein 1	26802,42	23289,43

Table S1 cont.

Accession	Peptide count	Confidence score ^a	Log ₂ of fold change ^b	Description	Total Ion Counts Control	Total Ion Counts W _m B _d R _f R
SCRFLR2034F03	3	29,6021	1,1652	small nuclear ribonucleoprotein e-like	10097,54	22645,36
SCRFLR2034F12	6	40,743	0,0132	splicing factor 3a subunit 3-like	13464,96	13342,58
SCRFLR2034H11	13	93,4145	0,3604	heterogeneous nuclear ribonucleoprotein a3 homolog 2-like isoform 1	25224,63	32382,18
SCRFLR2037F07	4	34,8657	0,9228	60s acidic ribosomal protein p3	6326,325	11993,2
SCRFLR2038F04	36	286,7037	0,1093	heat shock 70 kda protein 4	75408,76	81344,56
SCRFRZ3057C09	2	15,0016	0,1019	peptidoglycan-binding domain-containing	8932,086	9585,849
SCRFBSB1024E09	2	18,704	0,0279	hypothetical protein SORBIDRAFT_01g000520 [Sorghum bicolor]	60428,91	59270,78
SCRFS1T042A04	4	21,0781	0,0843	thiamine thiazole synthase chloroplastic precursor	3316,567	3516,15
SCRLLAD1099B04	3	18,558	0,3028	tpa: class iii peroxidase 66	4276,833	5275,591
SCRLLAM1011F07	1	5,4188	0,4786	beta 3 galactosyltransferase precursor	4055,233	5650,714
SCRLLAM1013C01	1	5,8265	0,1143	probable e3 ubiquitin-protein ligase ari8-like	4763,568	5156,203
SCRLLAM1013H08	4	26,8089	0,2411	u5 small nuclear ribonucleoprotein component	14012,7	16561,65
SCRLLCL6031B10	7	53,4049	0,6559	nad-dependent isocitrate dehydrogenase	13216,13	20822,63
SCRLLFL1007A02	5	34,9523	0,5386	adapter-related protein complex 4 epsilon 1 subunit	18444,38	26792,11
SCRLLFL1011G08	13	102,191	0,3442	40s ribosomal protein s17-4	86787,13	110171,3
SCRLLFL1012B10	1	6,3958	0,3315	hypothetical protein SORBIDRAFT_08g019220 [Sorghum bicolor]	33199,51	41775,91
SCRLLFL1013A03	9	72,0777	0,5122	nucleolar protein 56-like	28863,79	41166,39
SCRLLFL1013E09	2	12,5826	0,6180	uncharacterized protein LOC100381735 [Zea mays]	3179,753	4879,976
SCRLLFL8024A07	1	5,8412	0,0542	thi42_sorbi ame: full=thiamine thiazole synthase chloroplastic ame:	11061,78	11485,48
SCRLLFL8053A03	3	19,968	0,0008	mitochondrial glycoprotein	20963,61	20974,72
SCRLLLB2031B03	2	12,8397	0,7013	uncharacterized protein LOC100273566 [Zea mays]	5397,962	8776,821
SCRLLLR1038D01	10	58,6678	0,0670	uracil phosphoribosyltransferase	88052,93	84058,14
SCRLLLR1038G11	23	190,872	0,2503	t-complex protein 1 subunit alpha	29488,19	35074,75
SCRLLLR1059E05	6	41,0251	0,1550	acetyl- cytosolic 2	3519,584	3161,104
SCRLLLR1059E09	1	11,9234	0,0992	sorting nexin-	15984,26	17121,9
SCRLLRZ3039D01	3	24,1746	0,1613	protein serine threonine kinase	6719,434	7514,301
SCRUFL1019B10.b	2	11,6749	0,3285	ac090713_15 peroxidase	288,7235	362,5632
SCRUFL1023C12	10	67,1532	0,1429	beta actin	6177,45	6820,509
SCRUFL3064C04.b	2	18,4167	0,0004	hypothetical protein SORBIDRAFT_08g020780 [Sorghum bicolor]	7001,041	7003,063
SCRUFL3064H09	2	10,8481	0,5452	hypothetical protein SORBIDRAFT_04g034133 [Sorghum bicolor]	16414,13	11248,41
SCRULB1060G01	5	25,842	0,4304	probable methyltransferase pmt15-like	12086,86	16288,14
SCRURT2005F01	12	137,2273	0,2372	chloride intracellular channel 6	24314,88	28659,57
SCRURT2006B10	6	53,4248	0,2674	glucan endo- -beta-glucosidase precursor	6773,15	5627,263
SCRURT2010A08	6	40,8236	0,2895	mitochondrial 2-oxoglutarate malate carrier protein	43442,32	53096,34
SCRURT2010D12	6	39,7401	1,0640	diaminopimelate epimerase	2698,473	5641,745
SCRURT3064F04	13	164,3271	0,3870	apx1 - cytosolic ascorbate peroxidase	411157,5	537646,8

Table S1 cont.

Accession	Peptide count	Confidence score ^a	Log ₂ of fold change ^b	Description	Total Ion Counts Control	Total Ion Counts W _m B _d R _f R
SCSBAD1054C07	2	12,3333	0,3769	uncharacterized plant-specific domain tigr01615 family expressed	6475,168	4986,387
SCSBAD1054F04	4	22,8806	0,0184	hypothetical protein SORBIDRAFT_06g017130 [Sorghum bicolor]	15549,91	15749,43
SCSBAD1083F08	2	12,5001	0,1531	dna repair helicase xpb2-like	14212,82	15804,48
SCSBAD1085F11	2	10,7527	0,4998	atp gtp binding protein	3780,98	2673,857
SCSBAD1128B01	1	5,8245	0,8187	hypothetical protein SORBIDRAFT_04g033720 [Sorghum bicolor]	50477,33	89035,36
SCSBAM1084D01	12	89,9398	0,1602	heat shock protein 70	30849,2	27606,65
SCSBAM1087H08	2	15,7169	0,9835	PREDICTED: HIPL1 protein-like [Brachypodium distachyon]	9179,221	18149,29
SCSBFL1042G04	20	154,1156	1,0457	phosphoenolpyruvate partial	12370,82	25538,31
SCSBFL1101G02.b	6	41,2631	0,0603	chloroplast heat shock protein 70	41788,95	40079,45
SCSBFL5016F07	7	51,8502	0,3961	lactoylglutathione lyase	12084,2	15902
SCSBLB1033E06	9	54,8022	0,3434	pp2ac-3 - phosphatase 2a isoform 3 belonging to family 1	9882,253	12537,8
SCSBRZ3117B05	9	59,8996	0,4050	dihydrolipoyl dehydrogenase mitochondrial-like	4496,843	3396,197
SCSBRZ3117C09	8	51,7788	0,1707	clpc1_orysj ame: full=chaperone protein chloroplastic	20264,68	22810,13
SCSBRZ3118H12	15	99,0688	0,4329	pentatricopeptide repeat-containing protein mitochondrial-like	9698,779	7184,331
SCSBBSB1051B07	2	10,7975	0,6936	myb family protein	1606,802	993,5093
SCSBST3098G08	19	144,1484	0,2657	annexin p35	77887,3	93635,16
SCSFAD1072H05	2	11,5647	0,2063	cyclin delta-3	1465,823	1691,198
SCSFAD1106B08	1	5,6922	0,6455	hypothetical protein SORBIDRAFT_03g008920 [Sorghum bicolor]	3138,091	4908,998
SCSFCL6067A06	1	5,4291	0,5686	ac079179_7 dna2-nam7 helicase family protein	21846,67	32401,19
SCSFCL6068C11	10	127,2901	0,1286	anionic peroxidase	41648,21	45532,44
SCSFCL6068E04	2	12,0876	0,4231	hypothetical protein SORBIDRAFT_04g010023 [Sorghum bicolor]	3572,843	4790,633
SCSFFL4084F01	1	6,5723	0,4098	hypothetical protein SORBIDRAFT_08g016780 [Sorghum bicolor]	11742,14	8838,917
SCSFHR1046G01	4	27,7871	0,0141	fk506-binding protein 2-1 precursor	32077,76	31764,82
SCSFHR1046H08	2	20,6393	0,0912	importin-alpha re-exporter	7069,532	6636,521
SCSFLR2009H09	3	20,1282	0,1982	cytosolic chaperonin delta-subunit	16991,15	19493,77
SCSFLR2009H11	2	11,9936	0,4618	ankyrin repeat domain-containing protein 2	3973,372	5472,483
SCSFRT2070A04	7	45,8218	0,1693	protein lrp16	6230,327	7006,151
SCSFRT2070C07	6	47,81	0,1007	eukaryotic translation initiation factor 3 subunit 12	54273,05	58197,63
SCSFST1064C10	10	90,1181	0,3520	heat shock protein cognate 70	484,7302	618,6938
SCSFST1066G10	2	15,274	0,2831	hypothetical protein SORBIDRAFT_08g018710 [Sorghum bicolor]	3003,044	3654,132
SCSFST3075E04	1	6,042	0,0514	zinc-binding protein	3111,542	3224,394
SCSFST3076G09	7	59,7401	0,1014	luminal binding protein	3797,941	3540,281
SCSFST3078F06	3	16,396	0,1933	ethylene-responsive protein	10049,13	11489,54
SCSGAD1142C08.b	2	11,7377	0,2095	lipoamide dehydrogenase	7104,719	6144,329
SCSGAM1094A08	5	34,9729	0,5739	ribonucleotide reductase	5254,443	7821,211
SCSGAM1095C10	21	164,2947	0,6434	prs4_orysj ame: full=26s protease regulatory subunit 4 homolog	11681,92	18246,71

Table S1 cont.

Accession	Peptide count	Confidence score ^a	Log ₂ of fold change ^b	Description	Total Ion Counts Control	Total Ion Counts W _m B _d R _f R
SCSGFL1081H08	9	67,5399	0,3101	succinyl- ligase alpha-chain 2	20183,23	25022,74
SCSGFL1083E06	5	31,1892	0,1629	imidazole glycerol phosphate synthase chloroplast expressed	14123,85	15812,35
SCSGFL4192C03	1	5,6802	0,7810	uncharacterized protein LOC100501203 [Zea mays]	11183,22	19216
SCSGLR1025G10	15	113,7645	0,4850	malate glyoxysomal	160214,9	224231,6
SCSGLR1045F04	15	108,4667	0,4260	3-isopropylmalate dehydrogenase 2	14875,26	19984,58
SCSGLR1045G02	2	10,5075	0,3535	rh9_orysj ame: full=dead-box atp-dependent rna helicase 9	2113,107	2699,87
SCSGLR1045G11	13	87,6546	0,0008	cml7_orysj ame: full=probable calcium-binding protein cml7	39577,66	39598,43
SCSGLR1084A12	8	84,6665	0,2222	hypothetical protein SORBIDRAFT_01g004270 [Sorghum bicolor]	114975,4	134119,3
SCSGLV1007E08	1	5,5349	0,7107	hypothetical protein SORBIDRAFT_02g039510 [Sorghum bicolor]	6723,429	11003,54
SCSGRT2062D07	11	98,5042	1,0545	loc100280824 precursor	44005,48	91400,25
SCSGRT2062E10	4	27,7702	0,3647	transformer-sr ribonucleoprotein	879,5696	683,0961
SCSGRT2063H01	22	239,1722	0,6130	tpa: class iii peroxidase 64 precursor	424972,2	649985,6
SCSGRT2064G11	3	25,2888	0,8412	hypothetical protein SORBIDRAFT_09g029720 [Sorghum bicolor]	3636,759	6515,238
SCSGRT2066A01	11	94,0393	0,5692	fumarylacetate hydrolase	21083,18	31280,57
SCSGSB1009F10	2	17,8226	1,0613	vesicle-associated membrane protein 725	1182,764	566,7908
SCSGST1072D03	9	54,9365	0,4567	calreticulin precursor	10520,13	14437,98
SCUTAM2005A11	6	51,3622	0,2367	hypothetical protein SORBIDRAFT_01g011580 [Sorghum bicolor]	12122	14283,66
SCUTCL6034D10	8	63,1054	0,4868	hypothetical protein SORBIDRAFT_05g022640 [Sorghum bicolor]	161576,2	115304,8
SCUTFL1064H04	1	5,348	0,2987	hypothetical protein SORBIDRAFT_02g036120 [Sorghum bicolor]	1395,709	1134,702
SCUTHR1063E12	3	23,714	0,5926	peroxidase 52 precursor	18616,98	28074,47
SCUTLR1015G10	10	63,0366	0,4008	clpc1_orysj ame: full=chaperone protein chloroplastic	6392,614	4841,951
SCUTLR1037B10	2	12,7013	0,3587	nadh-ubiquinone oxidoreductase 75 kda subunit	6542,758	5102,466
SCUTLR1037D04	22	230,3384	0,8885	methyl binding domain106	4788,165	8864,1
SCUTLR1037F12	19	165,5809	0,2148	60s ribosomal protein l5-1	3323,075	2863,421
SCUTLR1037G08	2	16,89	0,3075	sbp transcription factor	4640,412	5742,639
SCUTLR1058A12	10	85,2513	0,3964	cytochrome heme protein	23529,62	30970,74
SCUTLR1058B04	8	64,092	0,1746	dihydrolipoyllysine-residue succinyltransferase component of 2-oxoglutarate dehydrogenase complex	23866,73	26937,57
SCUTLR1058G10	10	62,8194	0,5167	ubiquitin-activating enzyme (alternative splicing product)	12610,46	18041,08
SCUTLR2008B03	18	147,591	0,2139	hypothetical protein SORBIDRAFT_09g026550 [Sorghum bicolor]	38047,94	44127,86
SCUTLR2008B04	9	73,7916	0,3222	3-oxoacyl-synthase i	53309,56	66651,65
SCUTLR2023D11	20	188,6942	0,4497	aldehyde dehydrogenase family 7 member a1	160027,8	218558,2
SCUTLR2023H05	14	119,0551	0,0394	r40g2 protein	16412,92	16866,94
SCUTLR2030A01	6	48,2605	0,3451	gpi-anchored protein	42222,76	53632,74
SCUTLR2030A05	18	126,1117	0,1793	importin subunit beta-1-like	51533,38	45509,28
SCUTRZ2024D10	2	10,9362	1,1166	alcohol dehydrogenases	9754,069	21149,96

Table S1 cont.

Accession	Peptide count	Confidence score ^a	Log ₂ of fold change ^b	Description	Total Ion Counts Control	Total Ion Counts W _m B _d R _f R
SCUTSB1031G10	2	17,9461	0,6620	wox11_orysj ame: full=wuschel-related homeobox 11 ame: full= 11	27700,75	43829,13
SCUTSD2025C12	5	38,7722	0,9603	stress responsive protein	2303,064	4481,05
SCUTSD2028F03	13	182,3436	0,0255	glyceraldehyde-3-phosphate partial	51810,55	52734,79
SCUTST3087G12	3	26,1965	0,5006	cytochrome b5	21489,99	30404,56
SCUTST3090A02	1	5,7391	0,3118	nad h-dependent oxidoreductase	18929,14	23496,55
SCUTST3131G03	5	48,4714	0,4744	lipid transfer protein	7044,87	9788,006
SCVPAM1055E12	6	35,63	0,8607	selt selw selh selenoprotein domain containing protein	3680,979	2027,102
SCVPAM1055G01	3	24,8252	1,1582	phosphoglycerate dehydrogenase	1137,233	2538,113
SCVPAM1056A06	2	10,9414	0,0974	kinesin (centromeric protein)-like protein	20090,67	21493,44
SCVPAM1056H10	3	18,0903	0,3443	ethylene-responsive element binding protein 2	4288,864	5444,964
SCVPCL6038A04	4	22,42	0,6766	transposon protein	4067,176	6500,69
SCVPCL6038H06	5	43,4324	0,2284	heterogeneous nuclear ribonucleoprotein a3-like protein 2	20093,74	23541,15
SCVPCL6041A03	2	12,3763	0,9391	cysteinyl-trna expressed	9802,929	18795,01
SCVPCL6041E09	24	202,6415	0,3756	leukotriene a-4 hydrolase	112411,9	145843,8
SCVPCL6042B11	5	33,8125	0,1893	salt-induced map kinase 1	10878,94	12404,67
SCVPCL6042C08	1	5,1402	0,0638	1-deoxy-d-xylulose 5-phosphate reductoisomerase	3905,116	4081,677
SCVPCL6044F01	7	42,6318	0,2205	npl4 family protein	9005,472	10492,7
SCVPLB1015D09	2	12,7367	0,0589	vip1 protein	4742,15	4939,772
SCVPLB1018F09	13	96,272	0,2416	transcription factor btf3	10673,94	9027,775
SCVPLB1020D03	6	36,349	0,5634	peroxidase 12 precursor	4907,187	7251,667
SCVPLB1020F02	30	191,3248	0,6331	copa3_orysj ame: full=coatomer subunit alpha-3	137015,7	212493,4
SCVPLR1028C12	3	18,8998	0,1668	60s ribosomal protein l7a	8181,74	7288,293
SCVPLR1028D03	17	110,7986	0,3686	rna binding protein rp120	29282,88	37806,72
SCVPLR1028E03	22	159,7959	0,5155	pci domain containing protein	31823,99	45491,31
SCVPLR1028G12	34	308,852	0,4246	pdi-like protein	70532,91	94667,4
SCVPLR1049C03	27	192,8708	0,6626	methylmalonate semi-aldehyde dehydrogenase	117864,2	186568,6
SCVPLR1049C09	52	478,5582	0,4154	cell division cycle protein expressed	30288,35	40394,43
SCVPLR1049D12	3	17,6723	0,5459	nuclear matrix constituent protein 1	12638,35	8656,632
SCVPLR1049H03	11	84,6858	0,1854	60s acidic ribosomal protein p2b	39582,57	34808,13
SCVPLR2005E09	7	48,7533	0,0873	40s ribosomal protein s7	41611,85	44207,58
SCVPLR2012B05	2	12,3249	0,0723	heat shock protein binding protein	7376,902	7016,107
SCVPLR2012D11	9	58,552	0,4295	sucrose cleavage	15118,07	20360,16
SCVPLR2012F11	19	124,8836	0,3468	atp-citrate synthase	29723,97	23373,55
SCVPLR2019B03	11	84,759	0,1111	polygalacturonase inhibitor 1 precursor	8076,885	7478,136
SCVPLR2019F01	9	61,5279	0,5089	60s ribosomal protein l11-1	42886,78	61027,66
SCVPLR2019F03	10	75,6018	0,3569	ASF SF2-like pre-mRNA splicing factor srp32	10809,87	13843,83

Table S1 cont.

Accession	Peptide count	Confidence score ^a	Log ₂ of fold change ^b	Description	Total Ion Counts Control	Total Ion Counts W _m B _d R _f R
SCVPLR2027C10	32	231,1958	0,3095	tcp-1 cpn60 chaperonin family protein	68632,19	85053,57
SCVPLR2027D06	2	11,1631	0,2373	amino acid selective channel protein	4369,759	5151,084
SCVPRT2074G02	1	6,1769	0,3825	uncharacterized protein LOC100194208 [Zea mays]	1077,124	1404,15
SCVPRT2075C09	10	57,8564	0,0240	c4-specific pyruvate orthophosphate dikinase	3119,494	3171,714
SCVPRT2075E07	2	13,1893	0,2305	c-1-tetrahydrofolate cytoplasmic	3723,151	4368,13
SCVPRT2075F01	3	18,5155	0,0318	rna-binding protein	7087,225	7245,36
SCVPRT2078D02	32	310,3354	0,4211	chaperonin cpn60- mitochondrial precursor	279459,7	374193,1
SCVPRT2079H06	8	44,7194	0,3390	glucose-6-phosphate dehydrogenase	42182,43	53355,65
SCVPRT2080B07	5	52,02	0,9234	thaumatin-like protein precursor	5587,989	10598,17
SCVPRT2080G03	7	40,432	0,0738	spotted leaf protein 11	9436,569	8966,227
SCVPRT2083C11	3	18,0784	0,8024	hypothetical protein SORBIDRAFT_01g030340 [Sorghum bicolor]	3915,471	2245,105
SCVPRZ2036B04	4	22,0915	0,4459	uncharacterized protein LOC100193116 [Zea mays]	19627,42	14409,33
SCVPRZ2036B07	10	66,4184	0,0656	hypothetical protein SORBIDRAFT_09g018320 [Sorghum bicolor]	7138,826	7470,671
SCVPRZ2037B11	14	123,5277	0,6017	dihydropyrimidine dehydrogenase	51670,28	78407,37
SCVPRZ2037C11	1	5,1904	0,7499	serine threonine-protein kinase bri1-like 2-like	2136,826	3593,445
SCVPRZ2037F03	6	36,3886	0,0623	heterogeneous nuclear ribonucleoprotein 27c	4272,967	4092,251
SCVPRZ2038B12	1	6,3386	0,0385	fb14	12229,25	12559,85
SCVPRZ2041G12	23	158,9016	0,2431	indole-3-acetic acid-amido synthetase	43489,81	51471,93
SCVPRZ2042B04	28	182,2361	0,1840	protease candidate1	57716,57	65566,05
SCVPRZ2043A12	10	88,4412	0,4475	usp family protein	32591,46	44443,56
SCVPST1062F02	2	17,2069	0,1757	fd vi	2571,179	2276,353

^a Confidence scores were calculated by Progenesis QI for proteomics.

^b Proteins were considered unchanged when the log₂ of the fold change was less than 1.2 and greater than -1.2.